THE FEASIBILITY OF MEASURING WATER TRANSPORT THROUGH THE ENTRANCES OF NARRAGANSETT BAY WITH A GEOMAGNETIC ELECTROKINETOGRAPH

by

Michael Hugh Krabach

Title Abstract

MONITORING TIDAL CURRENTS WITH A GEK

THE FEASIBILITY OF MEASURING WATER TRANSPORT THROUGH THE ENTRANCES OF NARRAGANSETT BAY WITH A GEOMAGNETIC ELECTROKINETOGRAPH

BY

MICHAEL HUGH KRABACH

A THESIS SUBMITTED IN PARTIAL FULFILLMENT OF THE REQUIREMENTS FOR THE DEGREE OF

MASTER OF SCIENCE

IN

OCEAN ENGINEERING

UNIVERSITY OF RHODE ISLAND

1972

In presenting this thesis in partial fulfillment of the requirements for a masters degree at the University of Rhode Island I agree that the Library shall make it freely available for inspection. I further agree that permission for extensive copying of this thesis for scholarly purposes may be granted by my major professor or, in his absence, by the Director of Libraries. It is understood that any copying or publication of this thesis for financial gain shall not be allowed without my written permission.

Signature Michael H. Krabach

Date May 18, 1972

ABSTRACT

Many previous researchers have used the principle of electromagnetic induction for tidal flow measurements. In all cases where the electrode system is stationary, the installation has been highly dependent upon the local conditions such as channel geometry, sediment conductivity, tidal flow patterns and electrical interference. It is the common practice to try to calibrate the installation by other types of instrumentation as opposed to a theoretical calibration. All these installations therefore have the problem that the determination of the accuracy of the GEK (geomagnetic electrokinetograph) seems to be limited by the accuracy of any system used to calibrate it.

This study has tried to improve upon the accuracy of a calibration method so that the inaccuracies of this GEK installation can be seen, and the feasibility of using such a method for monitoring tidal flow in Narragansett Bay determined. The calibration method used drifting poles that were optically tracked as they passed through the section of the channel monitored by the GEK. Two calibrations were performed, the longest for 13 hours and the other for 7 hours. The drifting poles were found to be accurate in determining the mean velocity, if the vertical profile of the water velocity approximated a linear function of the depth, and if the length of the poles was near the depth of the channel. The GEK was found to be accurate within 10% of the mass transport if the electrodes are insulated against temperature differences. The greatest difficulty was in determining telluric potentials that caused the tidal signal to drift slightly.

PREFACE

In the past several years the residential and commercial growth around Narragansett Bay has increased to the point where it is visibly evident that as Man's "progress" on land continues, the Bay will suffer. To prevent this destruction of a natural resource (Rhode Island has few), more information about the ecological and physical processes of the Bay and Man's effect upon them, is needed. Much of this is directly or indirectly related to the water movement in the Bay. During the past year there have been many studies examining the tidal currents, especially with pending development of a nuclear power plant just north of the Jamestown Bridge area.

The author feels that an electromagnetic current meter offers advantages that can be combined with other methods of observing currents to provide more accurate knowledge than any one system could by itself.

Therefore, it is the desire of the author to promote the use of the GEK as an engineering tool. With this philosophy, this paper is arranged and presented mainly for the uninitiated. The original study was to determine the feasibility of using the GEK in Narragansett Bay, and this paper tries to present the conclusions with enough practical detail to enable people with different engineering or scientific backgrounds to use the GEK effectively. To do this, the Manuscript Thesis Plan has been used with the bulk of the information presented in the individual appendixes.

The author would like to acknowledge the following people for their assistance on this project.

Professor T. Kowalski for his suggestions and administrative details. Wislon Lamb for his assistance in the laboratory with the electronic instrumentation. Roger Binkerd and Doug Jones for assistance during many operations in the field. Miss Esther Rodriguez at the Weston Observatory, Mass., for the use of valuable geomagnetic records. The Department of Ocean Engineering's boat captain, John Miller, for his long days and good humor while operating with a "nonprofessional" boat crew.

In addition, acknowledgment must be extended to the following organizations for their assistance.

The Graduate School of Oceanography at URI for the use of their GEK electrodes. The U.S. Naval Underwater Systems Center at Newport, Rhode Island for both access to Fort Wetherill and for the use of the cable permit from the U.S. Army Corps of Engineers. The U.S. Navy Fleet Weather Station at Quonset Point for both tidal data and local wind data. The Rhode Island State Highway Department for use of the Jamestown Bridge.

TABLE OF CONTENTS

LIST OF FIGURES

APPENDIXES

LIST OF TABLES

THE FEASIBILITY OF MEASURING WATER TRANSPORT THROUGH THE ENTRANCES OF NARRAGANSETT BAY WITH A GEOMAGNETIC ELECTROKINETOGRAPH

Introduction

As part of an overall program to examine the water movement in Narragansett Bay, Rhode Island (figure 1), a geomagnetic electrokinetograph (GEK) was installed across the West Passage of the Bay. The purpose was to determine the feasibility of using this kind of flow monitoring device in Narragansett Bay for future programs. In conjunction with the installation of a GEK, a method of calibration was to be determined.

The principle that enables the GEK to work has been known since Faraday discussed the principle in 1832. It has only been since 1920 when Young and others made the first installation that the system has been successful to varying degrees.

Wertheim (1954) shows results of the electrical potential between Key West, Florida, and Havana, Cuba during 1952-1953. The results show a verification of the surface slope of the water as an index of the transport in the Florida Straits. This system was not calibrated to any degree of accuracy because of the difficulty of taking direct observations of the transport, and because of the geomagnetic field disturbances which under most conditions, prevented correlation of the instantaneous transport with instantaneous voltage.

Olsson (1955) presents an analysis of data that was recorded near Wellington, New Zeeland for a period of one month. Two sets of

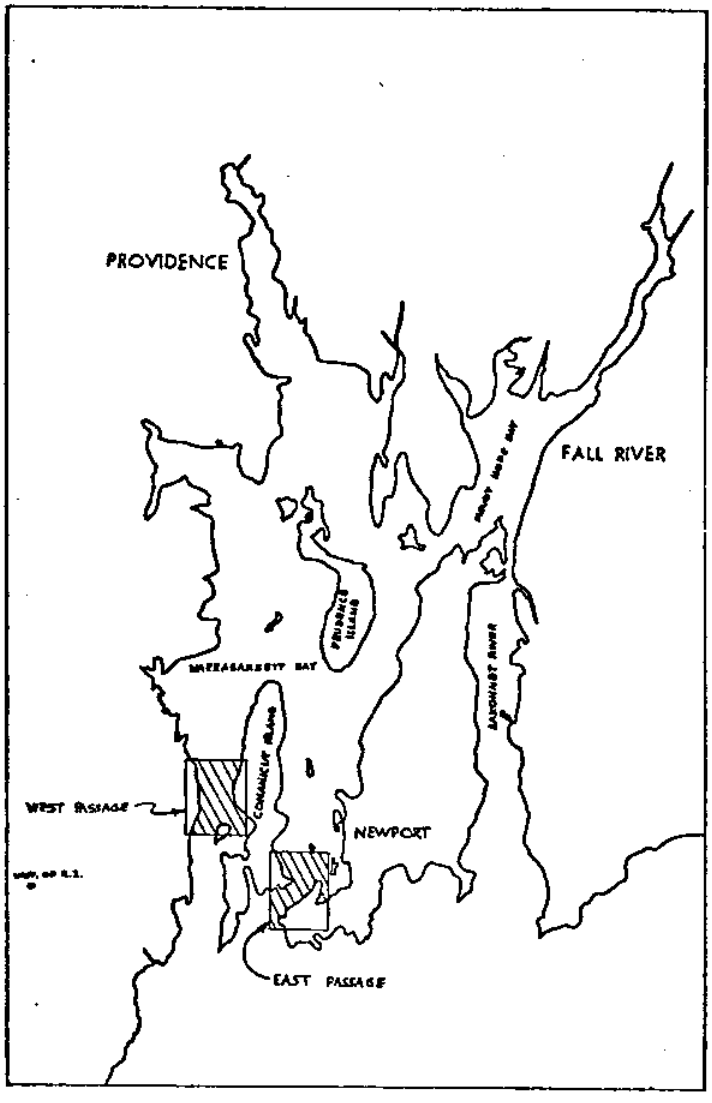

Fig. 1--Map of Narragansett Bay, Rhode Island.

electrodes on land were used to take both the north-south and east-west potential gradients which were compared with the tidal currents in the Cook Strait. In his installation, a problem was caused by the electric tramways about five miles away, which operated on direct current. The direct current influenced the data unpredictably along with geomagnetic storms. Another problem was the lack of comparative data of the actual tidal currents in the strait. Two years later during a hydrographic survey, some observations were

made for one day at each of four stations in Cook Strait. This data was compared with the previous theoretical results, but the accuracy seems to be limited. The theoretical results were based on the assumption that the tidal currents flow in a long uniform channel. For Cook Strait this assumption is not entirely valid. Also, the theory did not apply to cross-channel currents or to any currents near the turn in the Strait.

Morse(1958) used the electromagnetic principle to determine if this method was a practical method for the measurement of transport in small tidal streams. He concluded that in small, deep streams (500 to 1000 feet wide) there was a need for a high standard of control, and that there was no need to be overly concerned with the theoretical solutions because the system will require actual calibration in the field. Data was taken at three locations in the area of the San Juan Islands in the State of Washington. At the Mosquito Pass the field procedures were examined but no actual calibration was performed. In the Wescott-Garrison Bay system the transport was calibrated by comparison with known time-rate of volume changes in the embayments. It was found that a single calibration factor could not be anticipated. Actual direct observations were not taken, but the results of the calibration agreed in general with direct observations taken in another previous study. In the Deception Pass area the velocity measurements were calibrated by comparison with predicted hydraulic current-velocities. The actual velocity distribution was not determined because the location (rock bottom, 150 ft deep) was not suited for anchoring a boat or positioning current meters. The calibration was found to be non-linear and was based on the surface

velocity, not the mean velocity.

Bloom (1964) discusses results from two separate electrode systems used in the Bering Strait. The best installation was operated from 1956-1958 and extended from the eastern shore to a distance of 9.3 km into the strait. The calibration was performed using an acoustic Doppler technique where the volume reverberation is measured as the sonar projector-receiver is rotated 360°. The frequency shift is related to the velocity of the suspended scatter sources in the water which are being carried along by the water. The unit was located 3.7 km from the shore. All independent current-measuring devices that were maintained to provide a check on the calibration were unsuccessful except for two points; these were provided by surface current measurements from a ship during an oceanographic survey.

The calibration shows a displacement from zero that was attributed to the affects of temperature and salinity differences between the electrodes, but this was not entirely verified. The final calibration was with a best fit curve which appears fair except that a one to one correspondence certainly is not shown since there is a considerable amount of scatter in the data points.

Hughes (1969) discusses results of an electromagnetic current system that was installed across three locations in the Irish Sea. The system for cables 001 and 003 were calibrated in terms of water transport by the use of parachute drogues that were followed by a ship and with position fixes taken every 30 minutes with a Decca navigator. Four stations were checked at certain times over a period of two weeks during the calibration. Cable 002 was calibrated the next year by using three ships positioned along the track of the cable and taking simultaneous observations of current velocities at 5 m

and 0.6 of the total depth. The data was analyzed for the tidal harmonic constants and compared with tidal harmonic constants from tidal levels. The agreement was found to be good with respect to the large semi-diurnal constituents. It was also found that the seasonal variation of seawater conductivity had an effect that caused a variation in the cable sensitivity. Other variations from the theoretical predicted values were thought to be caused by the difference in the complicated channel shape as compared to an elliptical shape.

Klein (1970) describes two systems in Netherlands. Both are in areas where the channel bottom conductivity is high. The Ag-AgCl electrodes were placed in the ground in pipes 5 to 10 m deep. This provided stable temperatures and environments for the electrodes. The flow signal included severe magnetic disturbances. A set of perpendicular electrodes place far inland provided compensation signals to eliminate the unwanted disturbances. The Marsdiep system also included heavy DC disturbances due to DC railway traffic. This was eliminated by the use of a compensation signal measured between two points in the region of the railway. Other noise found in the telephone cables used to connect the measuring points was eliminated by filtering.

It appears that the Borndiep system was not calibrated, but it was compared with the water level on tide gauges. The Marsdiep system used a calibration from "simultaneous velocity measurements" performed on a former experimental system in that region. No details were given, but a plot shows very good correlation with the mass transport over a tidal cycle. It was stated that the accuracy of the system is 5 to 10%.

Von Arx (1950) has done the most to investigate the towed GEK for deep ocean work. The reader is referred to this reference for information on this related application of electromagnetic current meters.

Of all these previous systems only the Bering Strait has a long term calibration and it was only done at a specific point on the electrode line. Of the others, only the Marsdiep system appeared to be an accurate calibration, but no details were given about the method that was used. For the installation in Narragansett Bay it was therefore felt that a major effort should be given to the calibration method.

Principle of operation

The basic principle of operation is the fact that a moving conductor in a magnetic field will generate an electromotive force that is described by the relation

$$E = (\bar{V} \times \bar{B}) \cdot \bar{L}$$

where, E = emf in volts

$\bar{V}$ = velocity of the conductor, m/sec

$\bar{B}$ = magnetic flux density, webers/m^2

$\bar{L}$ = length of the conductor, meters

In the case of a GEK, the measured signal across the channel is reduced by electrical losses that are mainly caused by the shunting of the electric current through the channel bottom. Longuet-Higgins and others (1954) show that the measured electrical potential ϕ across a shallow elliptical channel due to the moving sea water can be defined by

$$\phi = \frac{E}{1 + \frac{\rho L}{\rho_1 2D}}$$

where, E = the induced emf

D = depth of the elliptical channel

ρ = the resistivity of the water

ρ_1 = the resistivity of the channel bottom

In the West Passage E = 54.1 mv per knot and ϕ was determined to be 10.65 mv per knot. Even though the channel bed is not a true ellipse, it is shallow (6400 ft wide and equivalent elliptical depth equal to 36 ft), so the solution to the elliptical case can be used for comparative purposes. It was found that the Jamestown Bridge shunted about 68% of the signal and the sediment shunted about 12% of the signal (Krabach, 1972, appendix H).

Installation of the GEK

Because of various conditions the best location to first install the GEK was in the East Passage from the unused Navy comples of Fort Wetherill on Conanicut Island, to the lower part of Fort Adams in Newport, Rhode Island. This is shown in figure 2. This location was suited for cable laying because of dock facilities, but unfortunately, proper submarine cable was not available. Instead a light gage, paired conductor was laid across the East Passage in February of 1971, but it only remained intact for about 10 hours. During this time the GEK was operating and showed that the signal was of sufficient strength to be easily monitored and that telluric potentials were present (Krabach, 1972, appendix A).

Since suitable underwater cable was still not available, it

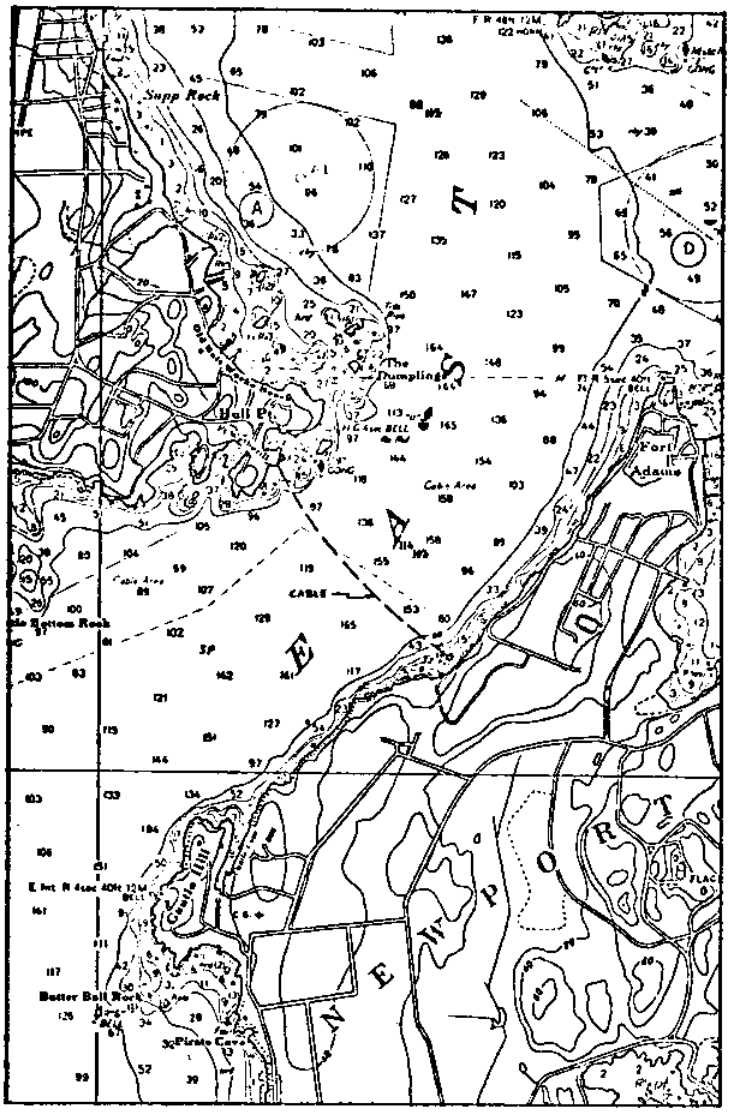

Fig. 2--Detail map of East Passage.

was decided to install the remaining light cable across the Jamestown Bridge over the West Passage shown in figure 3. The GEK was installed and it operated for periods of time from April to Novenber in 1971. It was beset with the usual problems of a prototype installation, but enough good data was obatined to call the operation a success in demonstrating the capabilities of the GEK at this particular location.

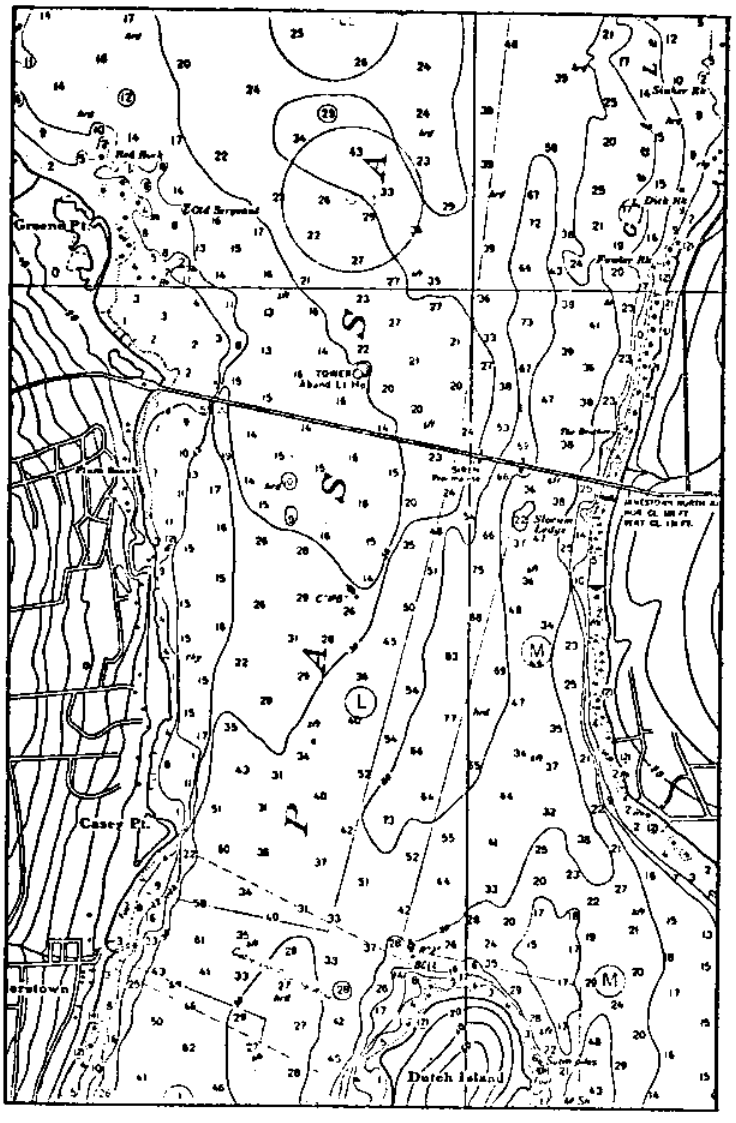

Fig. 3--Detail map of West Passage

Instrumentation

The system consisted of three silver-silver chloride electrodes. one each was installed on each side of the passage and the third was installed in the middle of the passage. The bottom topography of the passage was such that it had a deep half which averaged 40 feet in depth and a shallow half which averaged 18 feet in depth. This was done to study the distribution of the potential across the passage and to try and compare the difference in flow between the two

sides of the passage. The electrodes were encased in plastic holders and protected from outside contamination by a packing of fine glass wool. The whole assembly was encased in a styrofoam block for further protection against marine life, and placed in 4 feet of water off each shore with a lead mooring on each. The center electrode was similar but in 20 feet of water. A complete discription is in appendix B of the reference by Krabach (1972).

The output signal from the electrodes was monitored by a high impedance voltmeter which consisted of a DC operational amplifier with a gain of 100. This signal was then directly recorded on a Rustrak ammeter chart recorder. The recorder operated at a speed of 1/2 or 1 inch per hour and placed a dot on the pressure sensitive paper at the rate of 1 overy 2 seconds. The signal was normally filtered so that the output signal had a time constant of 5 seconds. This eliminated the 60 hz noise from the power cables on the bridgeway. An internal switching circuit operated by a clock, provides for recording the signal across the total passage for 1/2 hour and then recording the deeper half of the passage for the rese of the hour. Manually any two electrodes could be recorded, including monitoring the shallow half of the passage.

The instrument package normally operated on batteries, but could be used on 110 volts AC if it was available. The East Passage used 110 volts while the West Passage system was on battery power all the time.

The input signal from the electrodes consisted of a signal about $\pm$ 10 mv in amplitude that was due to the tidal currents. To this signal, an additional 70 mv that was due to the telluric potential across the passage, was superimposed. To operate at maximum

sensitivity, a bias circuit was included to depress the zero point on the recorder. This enabled the tidal signal to be observed with a maximum degree of clarity. A complete operating guide and circuit description is presented by Krabach (1972) in appendix D.

The wire used across the bridge was military field-phone wire, which was relatively light gage paired conductors having a tensile strength of about 200 lbs. It was found that the wire was susceptible to chaffing due to wind and breakage by people, malicious or otherwise.

Method of calibration

The calibration consisted of observing the tide across the passage at six stations by using drifting poles that were tracked by a telescope. The poles were 1.5 inch hollow aluminum tubes with a buoyant section in the top, and designed to float with a freeboard of 2 feet and a draft that ranged from 10 to 46 feet. These were deployed from a boat across the passage at stations marked on the bridge, and tracked using a WW I battery command telescope (Krabach, 1972, appendix C). This has a reticle grid screen through which the drift rate of the poles could be measured by timing the angular drift across the grid screen. The field of view was parallel to the bridge and measured the same velocity component that the GEK measured. This was V cos 0, where 0 is the angular deviation of the tidal vector from the perpencicular to the bridge. The poles were deployed and recovered on an average of three times every hour for 7 hours one day during neap tides, and three weeks later during spring tides for 13 hours.

This method of tracking the pole velocities proved effective and efficient. A transit would have required the tracking of the poles with a cross hair while with a grid screen the binocular type telescope

could be kept stationary. The telescope was 10 power and was effective in sighting the poles at 6000 feet.

The poles were found to be capable of measuring the mean velocity of the vertical profile of the tides with an accuracy that depended upon the velocity profile approximating a linear function of the depth (Krabach, 1972, appendix C). In this manner the mean velocity was measured to the depth of the poles at each station where a pole was deployed. The mean velocity of the horizontal profile of the tides was determined by averaging the six poles spaced across the passage. Two difficulties are; sometimes the vertical profile is not linear, and because of the variable depth of the channel bottom and the tide height, the poles can not be made to reach as deep as would be desired.

The variation of the vertical profile was shown in the Rome Point Circulation Study (1971) to be different from tidal cycle to tidal cycle. Part of this data is shown in figure 4 for a period of neap tides. During spring tides the variation is not as pronounced and the phase difference between the upper and lower currents is not as noticeable.

The draft of the poles was not the same as the depth of the channel because as seen in figure 3, the depth of the passage varies in a longitudinal direction, plus the normal tidal variation is 3 to 4 feet. Therefore, at times the poles only measured the velocity to 3/4 of the depth of the water. The effect of this is later seen in the comparison of the poles with the GEK.

Telluric potentials

As stated previously, the earth (telluric) potentials affected

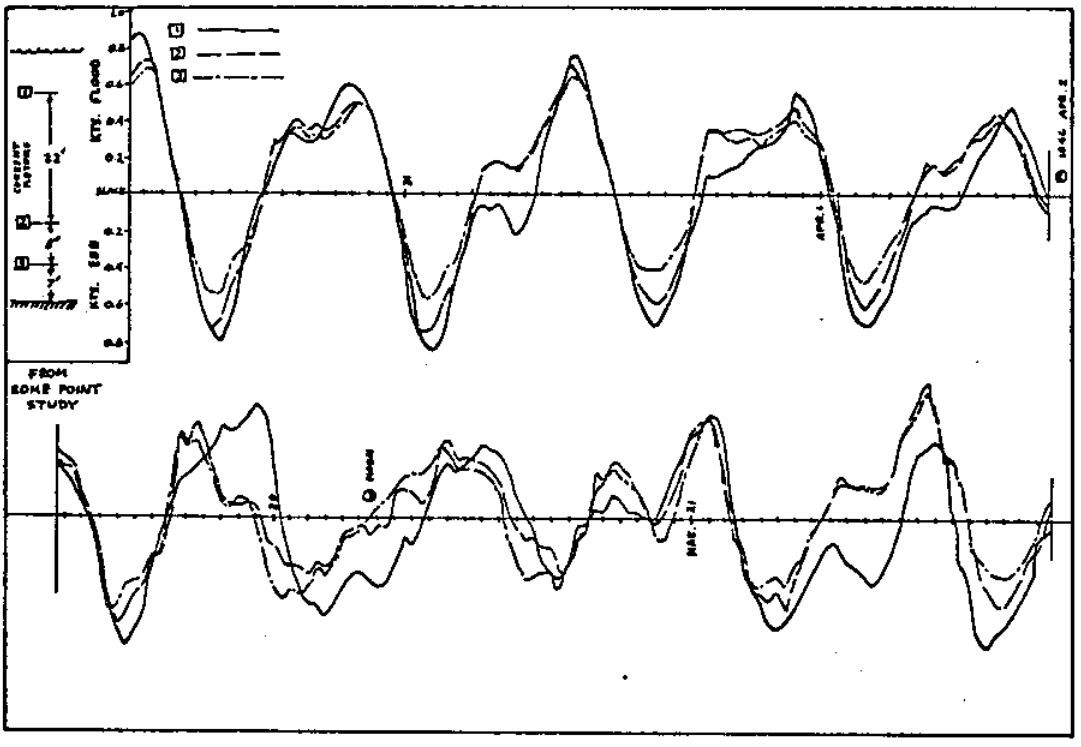

Fig. 4--Vertical profile of tidal velocities during a period of neap tides.

the potential detected between electrode pairs. This signal was fairly stable, but appeared to drift slightly, enough so, that it posed a problem for a permanent calibration of the GEK. In other words, the potential at slack tide drifted and hence, no permanent base line was available for comparing the relative flood and ebb signal strength.

The telluric potential was measured by driving ground rods in the earth up on each shore. It was measured by using a voltage divider and recording a portion of the signal along with the regular electrode signal. The signal was approximately 380 mv across the passage and 530 mv across the passage to the instrumentation area which was about 400 feet up on the shore. The electrodes only recorded about 73 mv of this telluric potential. It was discovered that while the deep half of the passage spanned a telluric potential of 68 mv, the shallow half

only spanned 8 mv. After examining the telluric signal (Krabach, 1972, appendix F), it was found to vary the same amount as the GEK signal. This is what would be expected because it was influenced by the tidal flow, but it prevented any accurate assessment of the telluric potential drift.

Drifting pole results

The GEK operated for a period of two months before some of the equipment was stolen and damaged by vandals. After the system was repaired the GEK was calibrated with the drifting poles on June 17, 1971, during a period of neap tides. Three weeks later on July 8, the system was calibrated again during spring tides. The data from the poles, corrected for wind, is shown in figures 5 and 6.

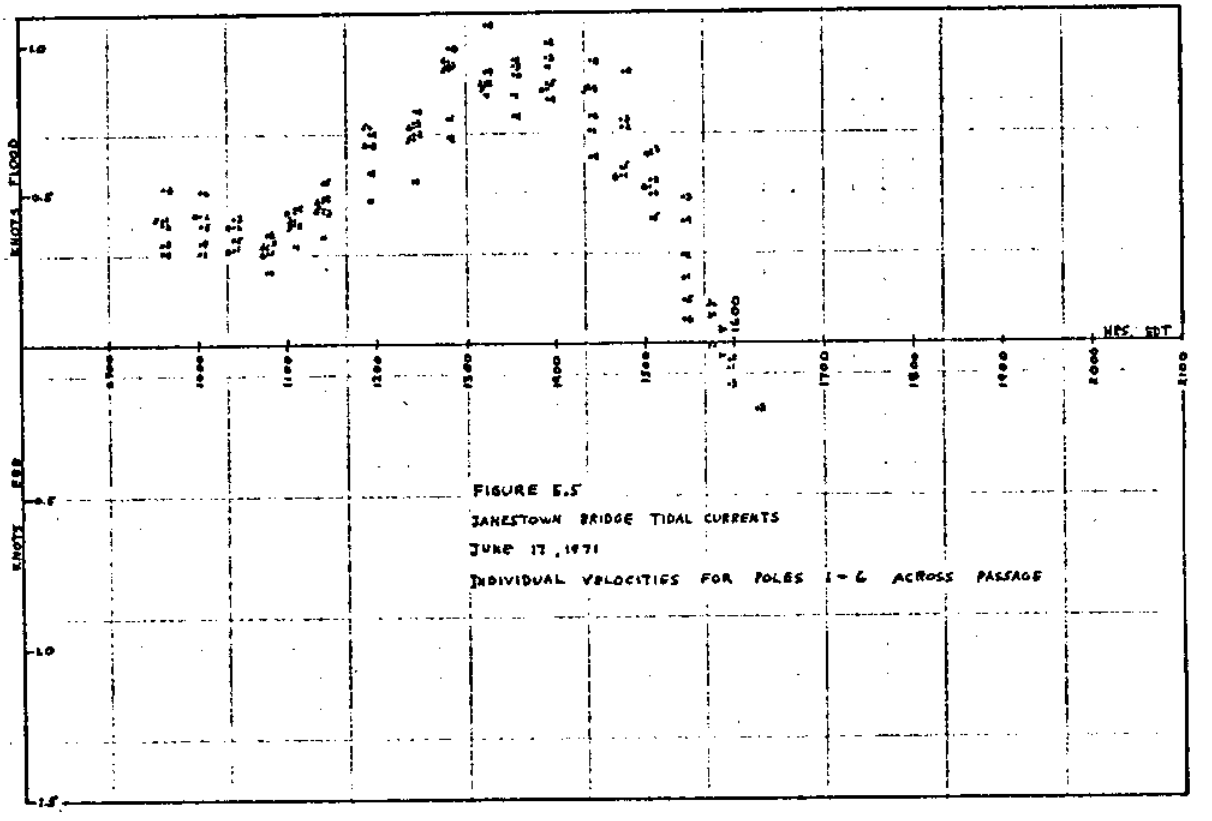

Fig. 5--Jamestown Bridge tidal currents, June 17, 1971; individual velocities for poles 1 thru 6 across the passage.

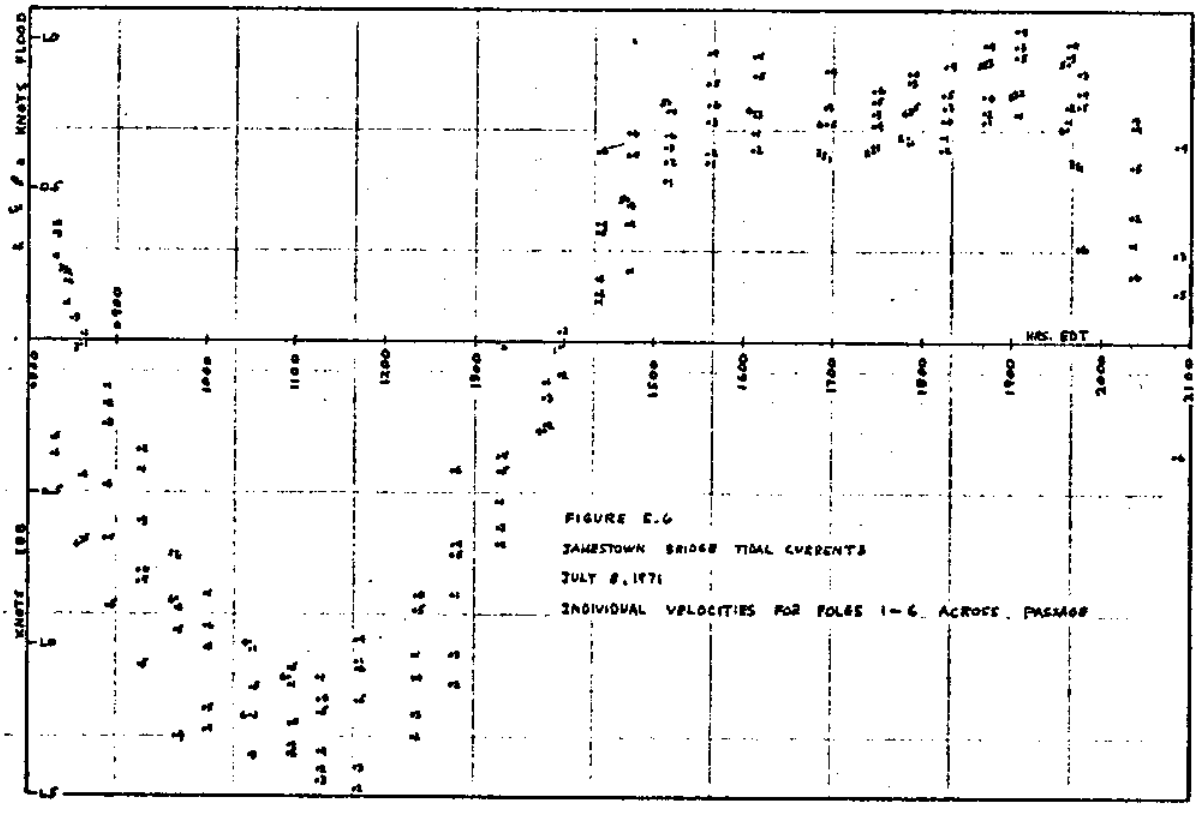

Fig. 6-- Jamestown Bridge tidal currents, July 8, 1971; individual velocities for poles 1 thru 6 across the passage.

The wind was found to influence both the net flow of the water and the drift rate of the poles during calibration. Experimentally the coefficient of drag, C_d, of the wind on the poles was measured and found to be 1.3. Since the wind velocity was not accurately known during the time the test was run, a theoretical C_d of 1.0 was used to correct the pole drift rates. It was determined that the 2 ft of freeboard on the 10 ft poles would cause an excess of deficit drift equal to 0.15 knots in a 10 knot wind. This is a considerable error when the tidal velocities are in the range of zero to one knot maximum. At 0.15 knot tidal velocity this is a 100% error. Details on the wind effects are shown in appendix C of Krabach (1972).

The accuracy of the C_d of 1.3 was not as important as the fact that the pennants, that were attached to the poles for better visibility,

had 37 times less drag. From this it was determined that the freeboard of the poles in future operations should be kept as small as possible and the pennants be relied on for visual tracking.

From examining the pole data (Krabach, 1972, appendix E), the horizontal variation of the tidal velocities was discovered. The particular velocity of any one pole, or section of the passage, can be examined from figures 5 and 6. In general it consisted of the expected lesser velocity nearer the shores of the passage. When the average velocities in the shallow half of the passage were compared against those in the deeper half, a phase difference was discovered. Figures 7 and 8 show this for the two days the GEK was calibrated.

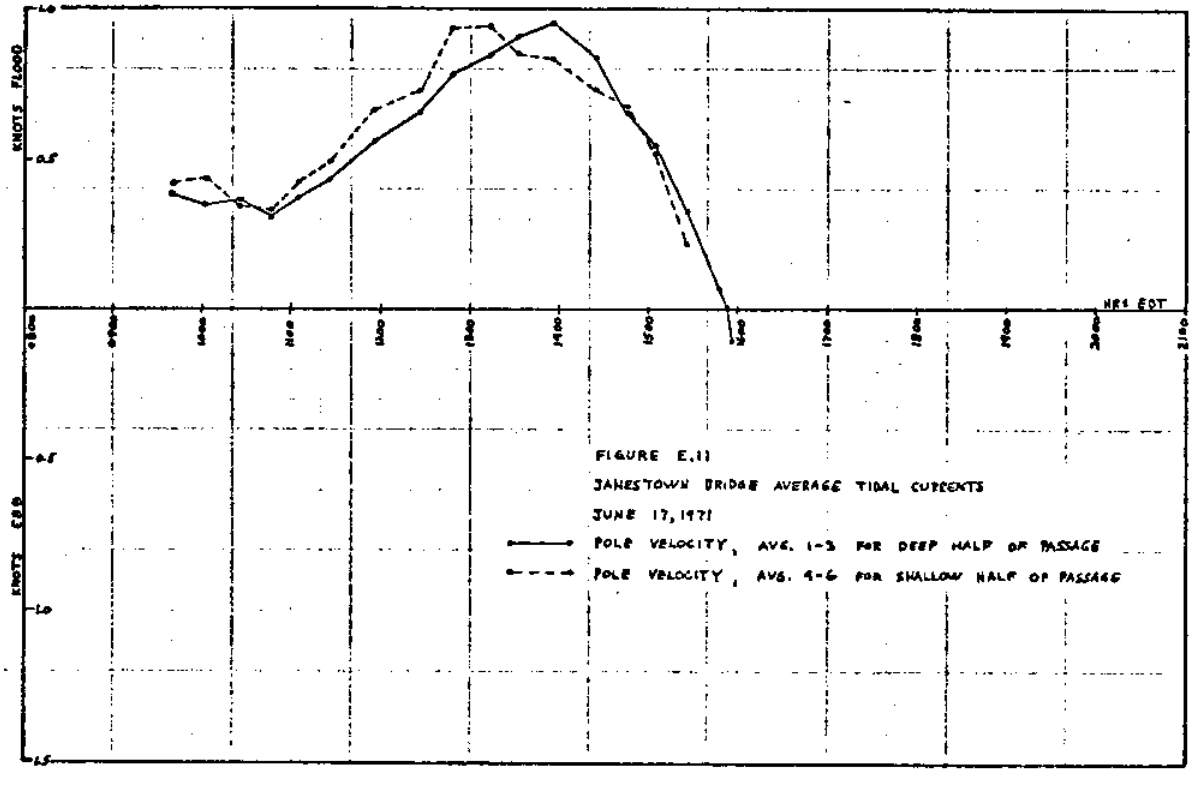

Fig. 7--Jamestown Bridge average tidal currents for shallow and deep half of the passage, June 17, 1971.

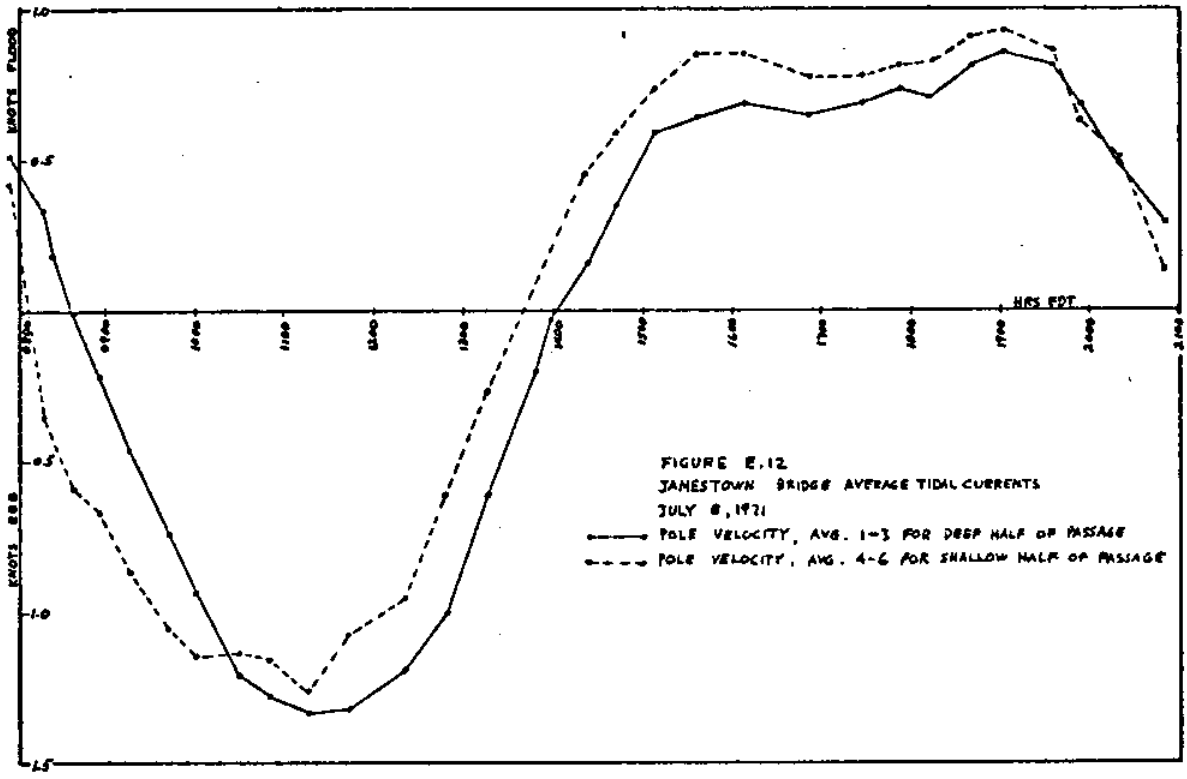

Fig. 8--Jamestown Bridge average tidal currents for shallow and deep half of the passage, July 8, 1971.

The trend is for the tidal velocities in the shallow side to lead the velocities in the deep side by a few minutes to as much as 45 minutes. This also causes the time of slack water to occur sooner in the shallow side. This shows the importance in examining the flow across this area of Narragansett Bay before making firm conclusions about net transport into or out of the Bay.

GEK results

The recordings that were taken during the two calibration days are shown in figure 9. The alternating traces are due to switching between the potential across the total passage ϕ_{AB}, and the potential just over the deep half of the passage ϕ_{CB}. The trace on July 8 was altered because the center scale of the chart was adjusted several

times during the day.

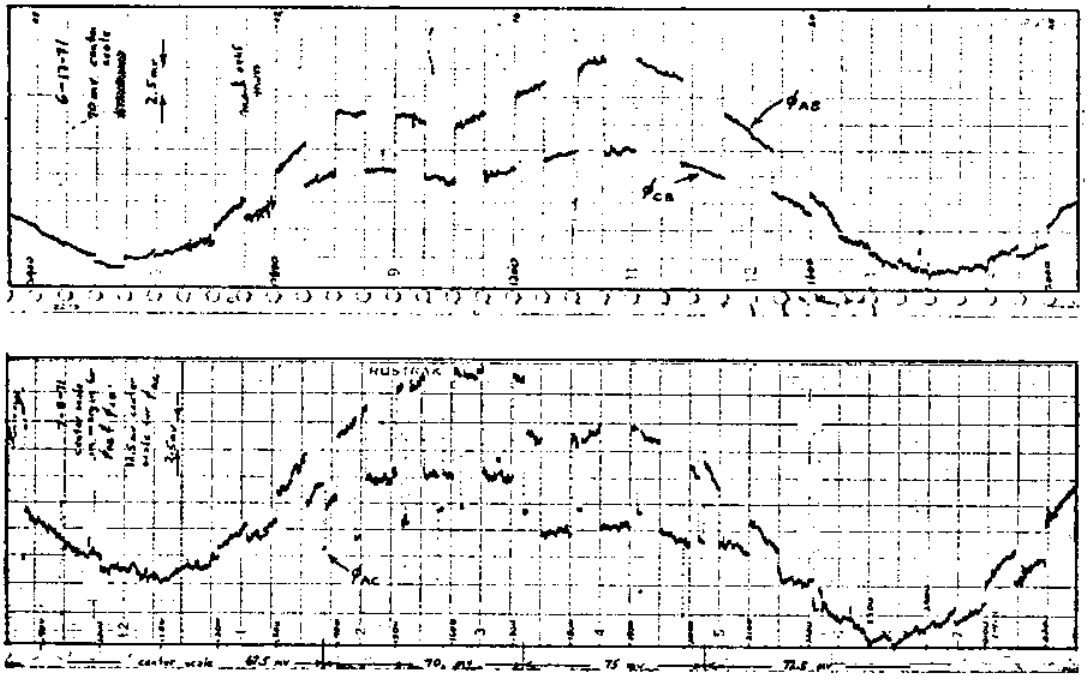

Fig. 9--Original GEK recordings of potentials on June 17, 1971 and July 8, 1971.

The final calibration of the GEK is shown in figures 10 and 11. The method is described in appendix E by Krabach (1972). The most obvious fact is the phase difference between the average velocity of the poles and the corresponding velocity as recorded by the GEK. This is explained by the fact that bottom friction in a tidal estuary causes the water nearer the bottom of the channel to lead the mean velocity of the channel. This is also seen in figure 4 that was taken from a vertical array of current meters about one mile north of the Jamestown Bridge. Since as stated before, the draft of the poles varied in relation to the total depth of the passage, and were at

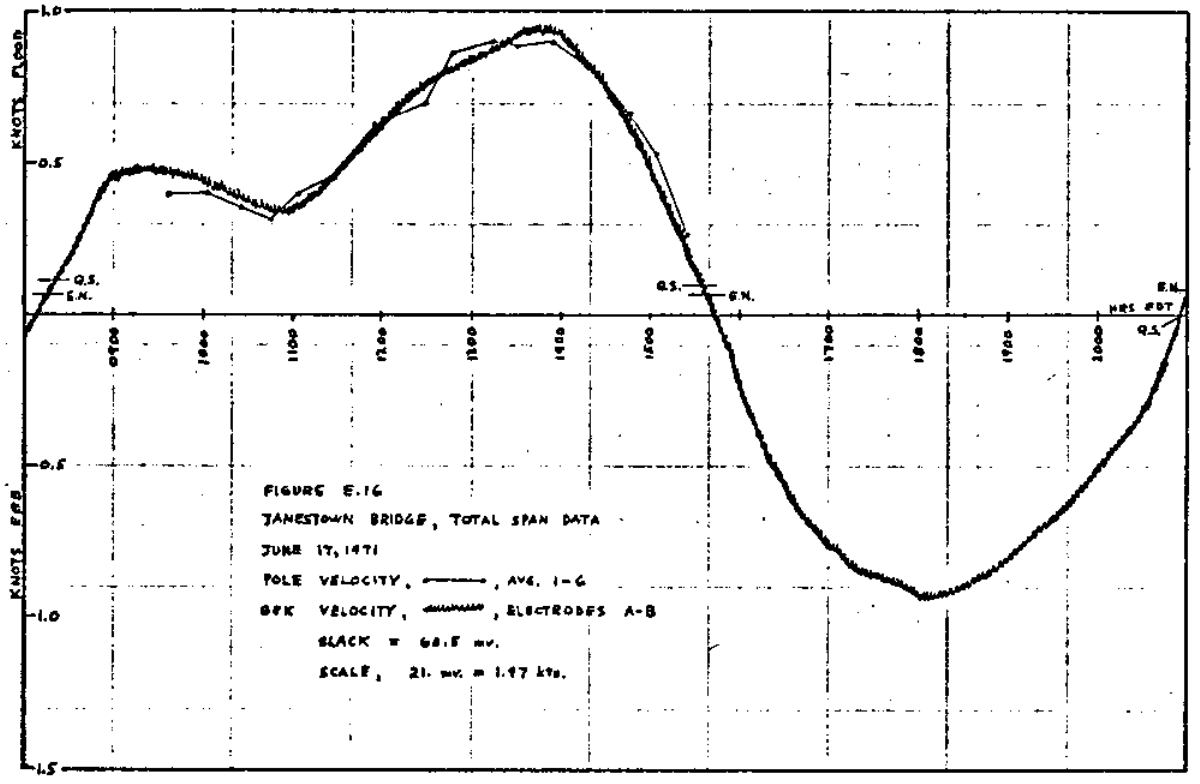

Fig. 10--Jamestown Bridge, total span data, June 17, 1971; comparison of GEK electrodes A-B with average pole velocities 1 thru 6.

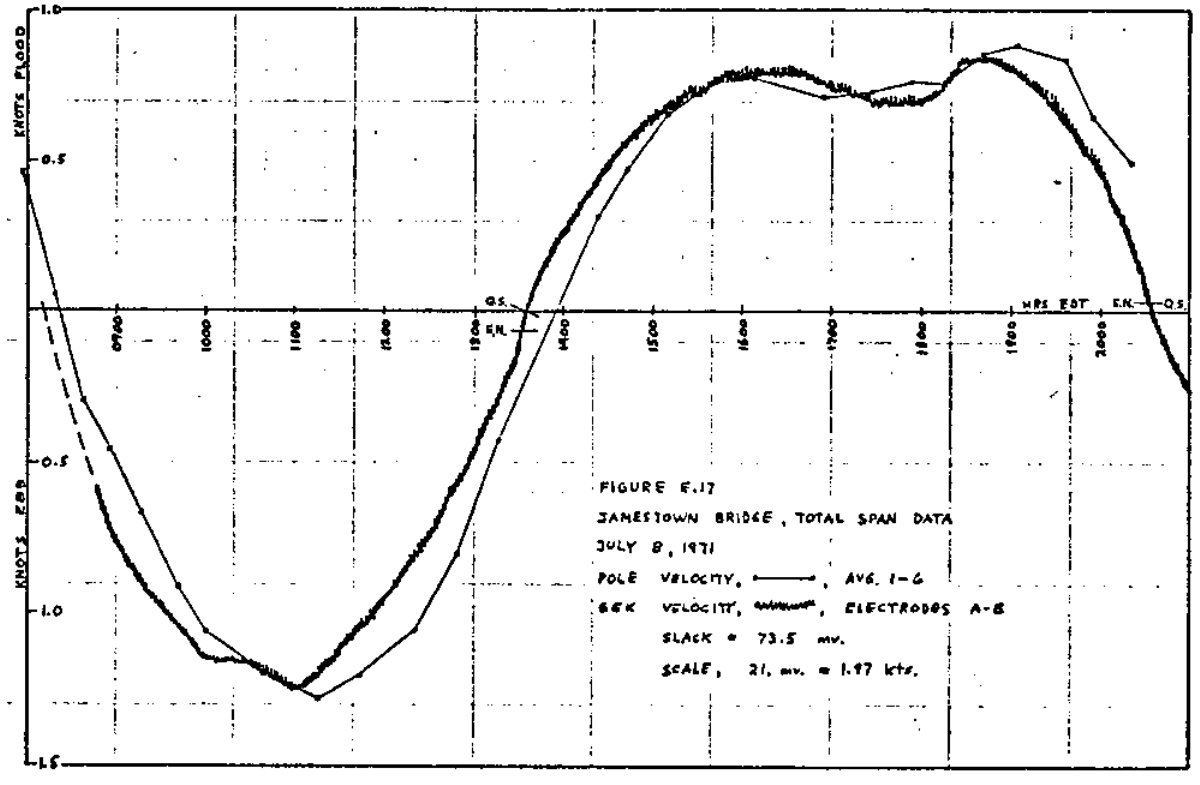

Fig. 11--Jamestown Bridge, total span data, July 8, 1971; comparison of GEK electrodes A-B with average pole velocities 1 thru 6.

times only 3/4 the water depth, the poles would tend to reflect the mean velocity of the upper portion of the water column. The GEK, which would average in the lower portion of the water column, would therefore tend to lead the pole velocities.

This shows the importance of using some means of examining the trend of the vertical profile of the tidal currents while calibrating any future GEK installations. This could be performed with a moored current meter system or by use of the poles themselves. Studies of thise problems were performed by Binkerd (1972).

Quasi-slack analysis

It can be seen in figures 10 and 11 that the slack potential changed between the two calibration dates, from 68.5 mv to 73.5 mv. Even though the calibration of the GEK is the same, 10.65 mv/kt, if the slack potential varies, it prevents using this scale factor on GEK results over a long term basis. If the zero base line, i.e. the slack potential, is unknown, no scaling can be done. To assist in an analysis of this drift of the slack potential, a quasi-slack was devised (Krabach, 1972, appendix F). This is defined as the potential of a base line drawn through adjacent flood and ebb tidal periods, as recorded by the GEK, which divides the cycle into equal flood and ebb areas. In reality it is ignoring any net transport that might occur over any particular tidal cycle. This was done for data over several months. The major cause of the net transport over any tidal cycle is due to the variation in the lunar and solar tidal forces and the effect of the local winds. To make an approximation of the net transport per cycle that occurred during the time intervals of the quasi-slacks, the variation in the average tidal

height over each tidal cycle was determined from tidal data that was recorded at Quonset Point, four miles north of the Jamestown Bridge. This data was used to adjust the quasi-slack potentials, and the resultant curve, the electrode null at slack tide is shown in figure 12. The results still show considerable drift. Some of the variations were found to be related to geomagnetic noise and by extraneous electrical signals that were never fully explained. The times when these variations occurred are also marked on figure 12.

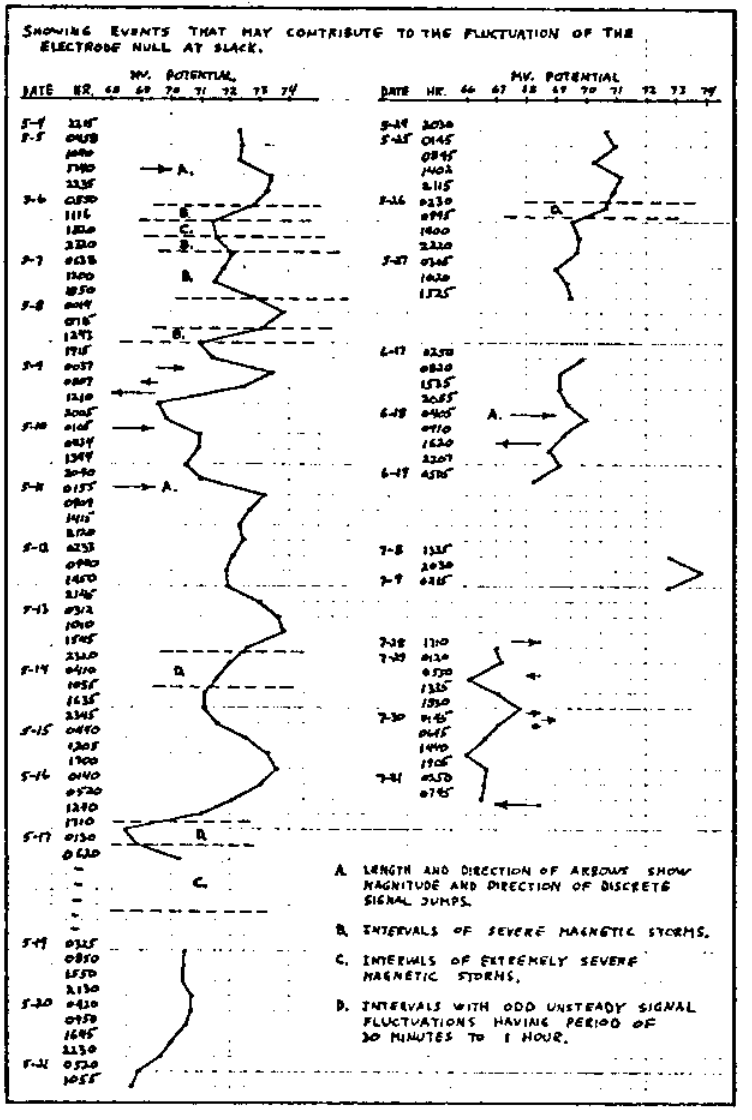

Fig. 12--Showing events that may contribute to the fluctuation of the electrode null at slack.

When the tidal transport for the two calibration days was compared with the respective tidal height change at Quonset Point, it was found that an average of 37% of the flow into and out of the Bay was through the West Passage (Krabach, 1972, appendix F). The bulk of the remaining flow would have had to passed through the East Passage. This was not able to be verified because there was no physical way to measure the actual flow through the East Passage.

Electrothermal variations

The remaining fluctuation of the electrode null is assumed to be caused by the variation in the temperature differential across the passage. This results in a difference in temperature of the GEK electrodes and causes electrothermal potentials which were shown to be equivalent to 0.32 mv/°C. From random sampling of the water near the electrodes, it was found that the temperature differential during the month of June could be around $\pm$ 2° C. This causes an error of $\pm$ 0.64 mv to the actual GEK signal which corresponds to a $\pm$ 0.06 kt velocity error. The mass transport is approximated very well for this passage by the relation,

$$Q = A\int V_m \, dt$$

where, A = the cross sectional area of the passage between the two electrodes

V_m = the average velocity of the poles

If the position of the slack line in figure 10 or 11 is displaced by 0.06 knot, the mass transport error will be around 10%. This value will obviously vary somewhat depending on the tidal cycle. This is about the same magnitude as the net transport that might normally occur, depending of course, upon the local prevailing wind and the particular

phase of the tidal components.

It is felt that in future GEK installations the electrothermal potential can be buffered by the use of an efficient thermal barrier between the electrodes and their surrounding seawater.

The salinity differential across the passage was found to be beffered by the packing in which the electrodes were encased. The resultant time response of the electrochemical action was much longer than a tidal cycle, and therefore the salinity differential across the passage was not a problem. Details of electrochemical and thermal errors are discussed in appendix I of Krabach (1972).

Since the temperature and salinity of the water varied, the resistivity of the water varied during the tidal cycles. Since the resistivity of the sediment and the bridge is relatively constant, the variation in resistivity of the water alters the percentage of current shunted across the passage. A typical change in the resistivity amounted to 1 ohm-cm, which was found to be capable of introducing an additional error of 3% to the GEK signal (Krabach, 1972, appendix H).

Comparison with predicted tidal currents

The local tidal currents are predicted by the Tidal Current Tables (1971) for the channel west of Dutch Island about 1½ miles below the Jamestown Bridge. To check the accuracy of these tables, the times of the quasi-slack were compared against both the slack tide times at Dutch Island and the high-low water times in Newport Harbor (Krabach, 1972, appendix G). Since the quasi-slack times do not necessarily coincide with the true slack it was necessary to determine approximately what the error would be. From an analysis

of the calibrated data it was determined that the quasi-slack time could be in error from the actual mean slack by no more than 10 to 15 minutes. When the predicted slack times were compared to the GEK quasi-slack times the resulting error was found to be on the average about 50 minutes from the Dutch Island data and 30 minutes from the slacks at Newport Harbor. The scatter of the data in both cases was found to encompass a range of an hour.

The time of predicted maximum ebb tide was also compared against the time of maximum ebb of the GEK. This also encompassed an error band of an hour with an average error of 35 minutes.

The time of predicted maximum flood was not compared because the double flood phenomenon in the Bay prevented an accurate determination of the time of maximum flood. Sometimes the GEK would show a steady flood velocity for as long as three hours. Other times it would show the two peak floods.

These results show that the published predicted tides can not be relied on for accurate studies of water movenent in Narragansett Bay. Currently other mathematical models are being developed at the University of Rhode Island with the hope of predicting the current patterns in the Bay with greater accuracy. These models are based on the same tidal components that the Tidal Tables are based on, but by using real time data obtained from measurements in the Bay, the model can be adjusted to better duplicate the water movement in the Bay.

Geomagnetic disturbances

An investigation of the effects the geomagnetic variations had on the GEK signal was performed. The results show that the long term

variation of the Earth's magnetic field can not affect the GEK, but the short term transients such as micropulses and magnetic storms were found to affect the record and account for much of the signal noise on the GEK record (Krabach, 1972, appendix J).

The large induction loop made by the wire across the bridge and the water beneath it, picked up horizontal geomagnetic transients. When individual micropulses were compared with their respective pulses on the GEK, as in figure 13, the effect was found to be 2000 times greater than the theoretical effect.

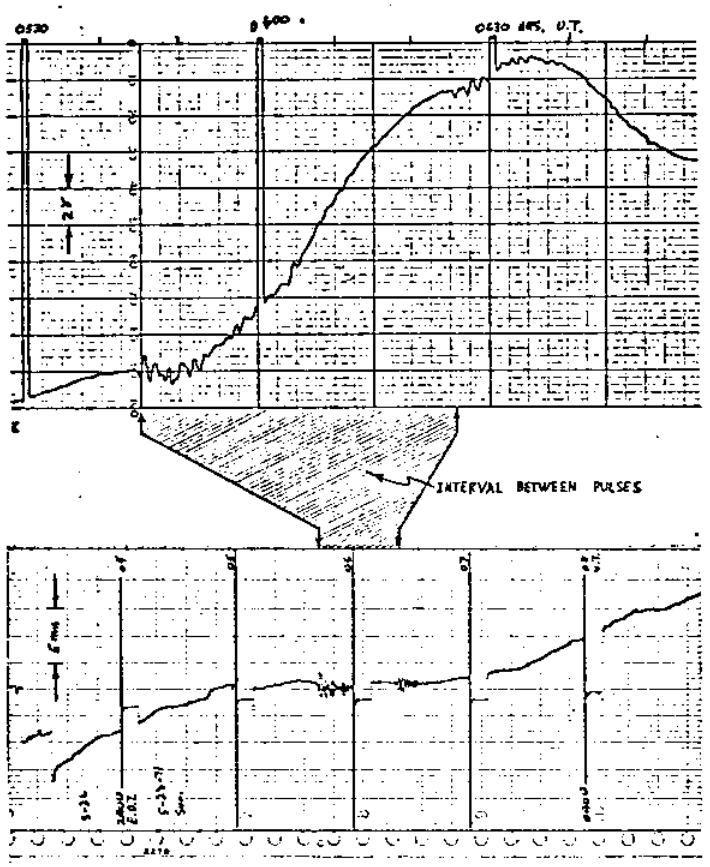

Fig. 13--Comparison between geomagnetic micropulses and pulses on the GEK, May 23, 1971.

These were not as serious as the magnetic storms that caused a much more erratic behavior of the GEK. An example of the effect is shown in figure 14 for a severe geomagnetic storm. Fortunately storms of this magnitude do not occur very often and rarely last for more than a couple of days. By examining all the times when the geomagnetic noise on the GEK was greater than 10% of the maximum GEK signal strength, it was determined that this would occur during 15% of the days throughout a year. Since some of the noise could be averaged, not all this recording time would be lost.

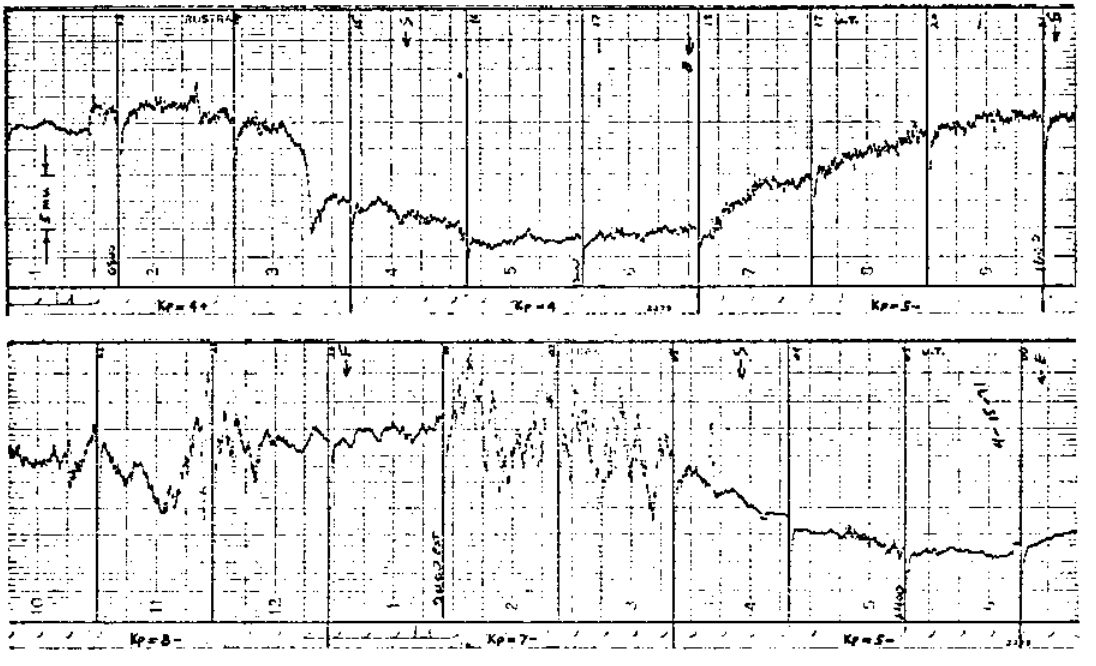

Fig. 14--Example of severe geomagnetic storm as shown by noise on GEK signal, April 14-15, 1971.

Conclusions

The study showed that the tidal cycle was in close agreement with the GEK signal, and that several improvements can be make to make it both more reliable and more accurate. Other studies on the

tidal currents were being made in the same area of the Bay before, during, and after the GEK installation was operating. Comparing the GEK results with other results pointed out that it is doubtful that the GEK alone or any other single method could be successful in monitoring the water movement in the Bay. Individual current meters can be more accurate, but they only measure the velocity at a particular site. The best solution is a careful combination of instrumentation, so as to allow for the advantages and disadvantages of the different instruments on an economical basis.

The strong advantages of the GEK are that the system is capable of continually monitoring the water through a large section of the Bay. It also provides less chance of damage and less chance of maring fouling if installed properly. The system can be relatively inexpensive; the major expense is placing a cable across the area to be monitored. The output is in electrical form and could be easily modified for computer input if a long term installation was built.

The major disadvantage is the signal drift due to the telluric (earth) potentials. The telluric potentials were found in both the East and West Passage, and it is assumed that any area around the Bay would have the problem. Unfortunately, each GEK installation would have to be tried before any evaluation of the drift could be made.

The inaccuracy of the GEK in West Passage was about 20%. This was mainly due to the signal drift. Part of the drift was caused by electrothermal potentials which could be eliminated in future installations by insulating the electrodes in a thermal barrier. In the present GEK the accuracy would have been improved by 10%. Further accuracy is not predictable because this is dependent upon the methods used to calibrate the GEK and the particular location the

GEK is installed.

This study showed that the specific method of the drifting poles could be a very economical and efficient method of observing the water movement in Narragansett Bay, as well as a method of calibrating the GEK.

REFERENCES

Binkerd, R.
1972. A New Application for Pole Floats. Univ. of Rhode Island Dept. of Ocean Engineering, thesis.

Bloom, G. L.
1964. Water Transport and Temperature Measurements in the Eastern Bering Strait, 1953-1958. Jour. of Geophysical Research. vol. 69, no. 16, pp. 3335-3354.

Hughes, Peter
1969. Submarine Cable Measurements of Tidal Currents in the Irish Sea. Limnology and Oceanography. vol. 14, no. 2, pp. 269-278.

Klein, R. E.
1970. The Measurement of Tidal Water Transport in Channels. Coastal Engineering Proceedings, vol. I-III. Sept. 13-18, 1970 at Washington, DC. Pub. by Amer. Soc. of Civil Eng. pp. 1887-1901.

Krabach, M. H.
1972. The Feasibility of Measuring Water Transport through the Entrances of Narragansett Bay with a Geomagnetic Electrokinetograph. Univ. of Rhode Island, Dept. of Ocean Engineering, thesis.

Longuet-Higgins, M. S.; Stern, M. E.; and Stommel, Henry
1954. The Electrical Field Induced by Ocean Currents and Waves, with Applications to the Method of Towed Electrodes. Papers in Physical Oceanography and Meteorology. vol. XIII, no. 1, Cambridge and Woods Hole, Mass.: MIT and WHOI. 37 pp.

Morse, R. M.
1957. The Measurement of Transports and Current Velocities in Tidal Streams by an Electromagnetic Method. Univ. of Washington, thesis. (Also pub. as Univ. of Wash. Dept. of Ocean., Tech. Report 57, 1958)

Olsson, B. H.
1955. The Electrical Effects of Tidal Streams in Cook Strait, New Zeeland. Deep Sea Research. vol. 2, London: Pergamon Press Ltd. pp. 204-212.

Rome Point Circulation Study, Final Report
1971. July 31, 1971. Contract URI-98-20-7057 to Narragansett Electric Co. Prepared at the Univ. of Rhode Island.

Tidal Current Tables
1971. For Atlantic Coast of North America. U.S. Dept. of Commerce, Environmental Science Services Admin., Coast and Geodetic Survey. (Starting 1972, pub. by National Oceanic and Atmospheric Admin., National Ocean Survey, Rockville, Md.)

von Arx, W. S.
1950. An Electromagnetic Method for Measuring the Velocities of Ocean Currents from a Ship Under Way. Papers in Physical Oceanography and Meteorology. vol. XI, no. 3, Cambridge and Woods Hole, Mass.: MIT and WHOI. 62 pp.

Wertheim, G. K.
1954. Studies of the Electric Potential Between Key West, Florida, and Havana, Cuba. Transactions, American Geophysical Union. vol. 35, no. 6, pp. 972-882.

Young, F. B.; Gerrard, H.; and Jevons, W.
1920. On Electrical Disturbances due to Tides and Waves. Phil. Magazine, Ser. 6, vol. 40, pp. 149-159.

APPENDIX A

THE GEK INSTALLATION IN EAST PASSAGE

The East Passage of Narragansett Bay would have been a more suitable location for recording and observing the operation of a GEK than the GEK at the Jamestown Bridge. The project was not a complete success because of the lack of suitable cable that could be laid across the passage. The following is a short history of the first project so that it can serve as a guide if another GEK is installed in the East Passage.

The location of the installation is shown in figure A.1. To install and maintain a cable in Narragansett Bay permission was obtained from:

Department of the Army
New England Division, Corps of Engineers
Waltham, Massachusetts 02154

The request included a preliminary installation plan and the actual locations desired for the cables. The west end of the cable terminated at the unused Fort Wetherill dock just south of Bull Point. A license to use this dock and access to the property was issued through:

Department of the Army
Northern Division
Naval Facilities Engineering Command
Naval Base
Philadelphia, Pennsylvania 19112

This was obtained through the assistance of the Newport Laboratory Naval Underwater Systems Center in Newport, Rhode Island. Access to install and service the east electrode at the Naval Reservation at

Brenton Village was obtained from the Commanding Officer at the U.S. Naval Base at Newport.

The cable laid in February 1971 across the passage was military field-phone wire with the following specifications:

Mil-C-13294 type WD-1/TT
FSN 6145-243-8466
Double twisted conductor
21 AWG, 7 strand (4 Cu, 3 steel)
Polyethylene compound insulation
46 ohms/1000 ft

This wire was weighted with 0.8 lb lead weights every 20 feet to keep the wire from drifting with the tidal currents which reach a maximum average velocity of 1.5 knots. It was hoped that this installation would last at least a week to evaluate the GEK. While laying the wire, one of the conductors was damaged or broken, but the second conductor enabled the GEK signal to be observed for 10 hours. At that time the second conductor became inoperative.

The electrode installations are shown in figure A.2 and consisted of two individual pairs on each side. The recorder could read any two of the four electrodes. This was to provide redundancy if any of the electrodes became inoperative and to provide a method of observing the general drift of the electrode self-potentials. It would have been inconvenient to remove the electrodes for checking them, so it was decided that being able to check the drift of either pair on each side was a fair indication of any gross electrical drift of the across-channel pairs.

The original trace in figure A.3 shows that the signal fluctuated 14 mv with about a 35 mv offset, positive to the west side of the passage.

About 300 feet of the wire was recovered on the west side of the

passage and approximately one bushel of seaweed was found tangled with the wire toward the broken end. This indicates that the drag on the wire and the resulting wire stress could have increased greatly because of the accumulation of seaweed.

The method of calibration was to be photographic tracking of drifting floats and drogues at night. The floats in preliminary tests each had an ACR "Fire Fly Rescue Lite" Xenon flashing light attached to them which puts out a 200,000 peak lumen flash approximately every second. While these Xenon lights are waterproof and well suited for this work it must be realized that they are powered by mercury batteries which tend to have a severely reduced output in cold weather. In one case after an hour of operation during freezing temperatures the flash rate was down to three per minute which made it difficult to locate and recover the floats.

To deploy and recover several floats with drogues a method was devised to allow the drogues to descend quickly to as much as 100 feet and be pulled up rapidly. The "wind sock" type of drogue is much better than the traditional current cross which tends to plane up and lose drag as the vertical current profile becomes more pronounced. Figure A.4 shows the drogues and the floats. The styrofoam floats were waterproofed with irridescent orange paint. The drogues were waterproof nylon cloth which is quick drying, non-rotting in the summer and non-freezing in the winter.

In preliminary tests floats were tracked by using a stationary camera with a time exposure that recorded the path of the flashing Xenon light. An exposure of f/5.6 to f/8 was determined to produce adequate density for recording the flashes of light on film with an ASA of 80. To determine time intervals on the photographic negatives a time

sequence such as 5 minutes exposure, one minute with the lens blocked, another 5 minutes exposure, etc. can be used. To determine the position of the floats there are two methods that could be used. (a) Using two cameras and a time exposure system. The cameras would be spaced far enough apart to enable position determination by triangulation from the photographic plates. (b) Using only one camera with the time exposure system and determining a bearing of the floats with a transit. Since a transit may not have illuminated cross hairs and may have a small light gathering ability for night use, the author recommends the use of an instrument similar to the one described in appendix C. The B.C. telescope does have an illuminated grid and the 43 mm objective lense is satisfactory for night use.

To use flashing lights in navigable waterways at night requires that permission be obtained from:

Commander 1st Coast Guard District (OAN)
J.F. Kennedy Federal Building
Government Center
Boston, Massachusetts 02203

The local Coast Guard Stations should also be notified at the time of starting the night runs.

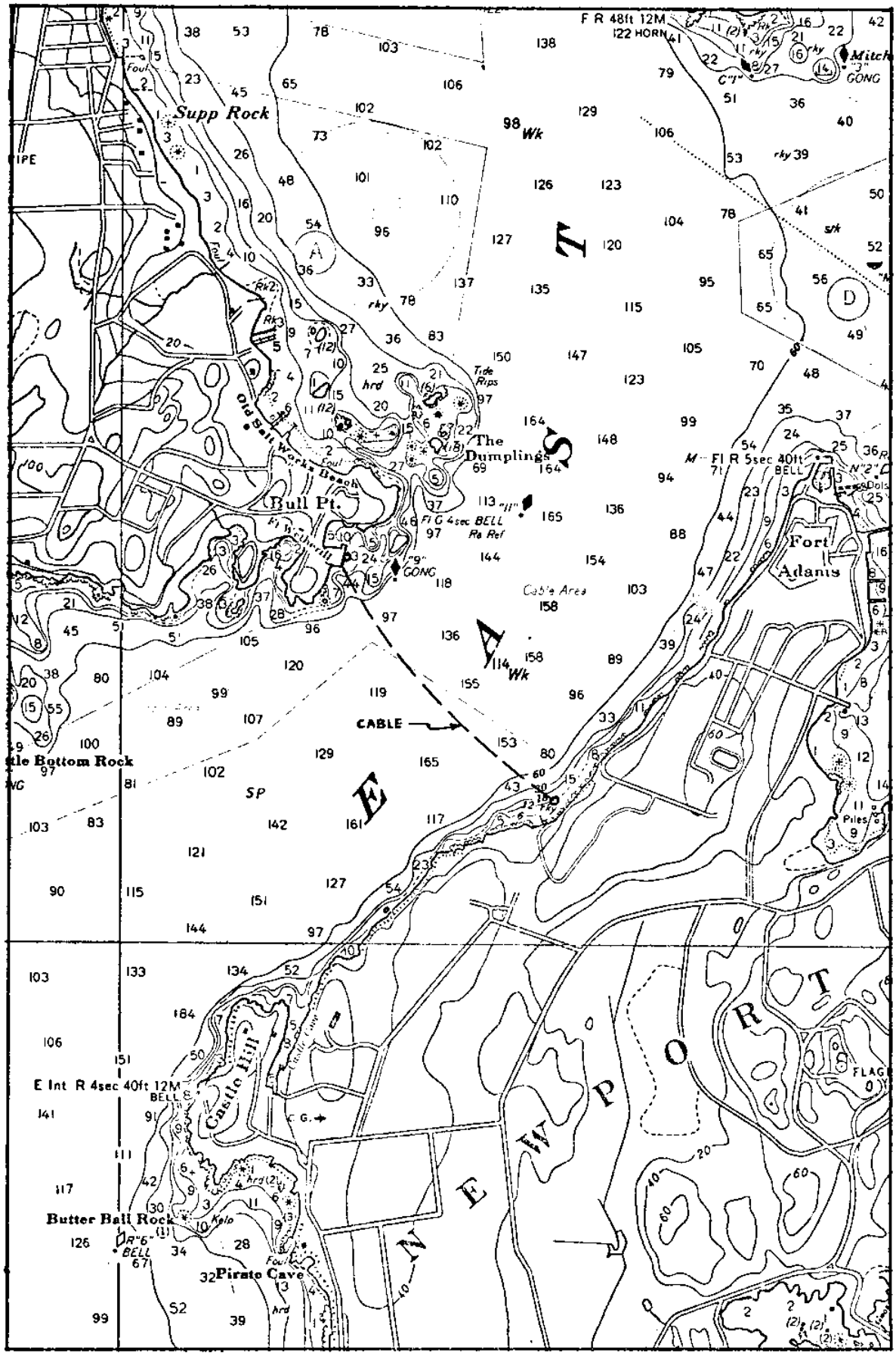

Fig. A.1--Location of GEK installation in East Passage.

EXAMPLE OF CIRCUIT EQUILIBRIUM FOR FOUR ELECTRODES IN LABORATORY. THIS METHOD CAN NOT DETECT DRIFT BETWEEN A-B AND C-D IN SITU, BUT WILL INDICATE IF ANY ONE ELECTRODE IS BEHAVING ERRATICALLY AND ALSO PROVIDE REDUNDANCY FOR SYSTEM.

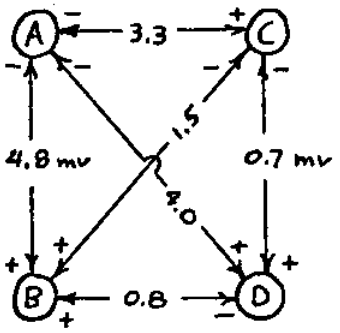

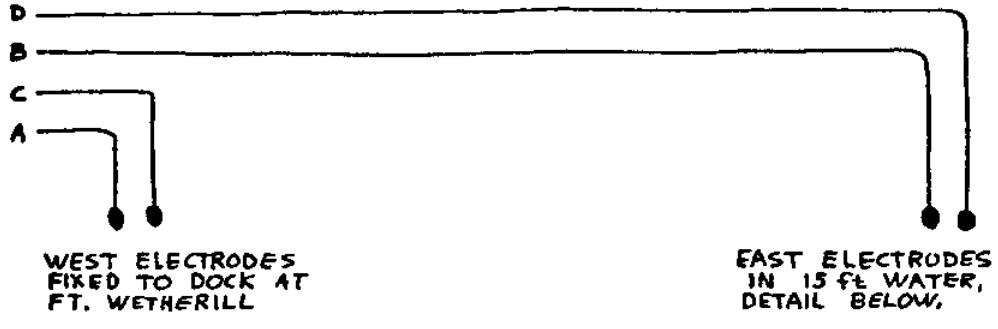

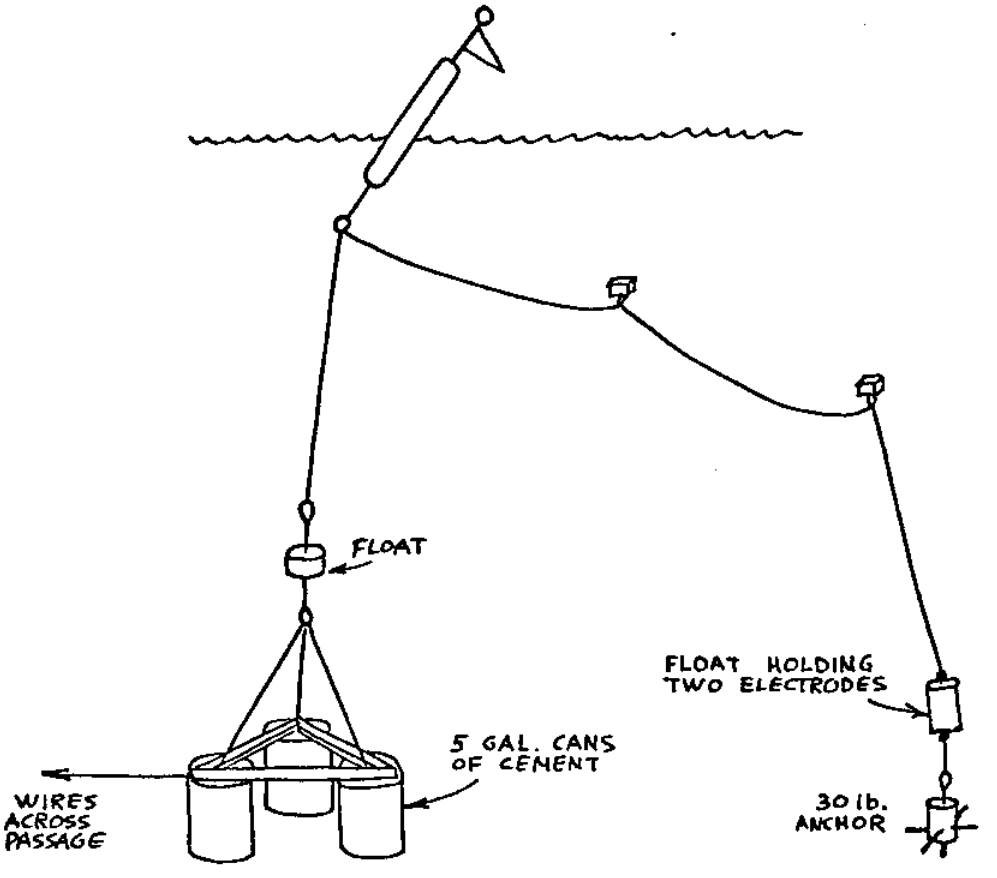

DETAIL OF MOORING SYSTEM FOR EAST ELECTRODES

Fig. A.2--Electrode installations for East Passage.

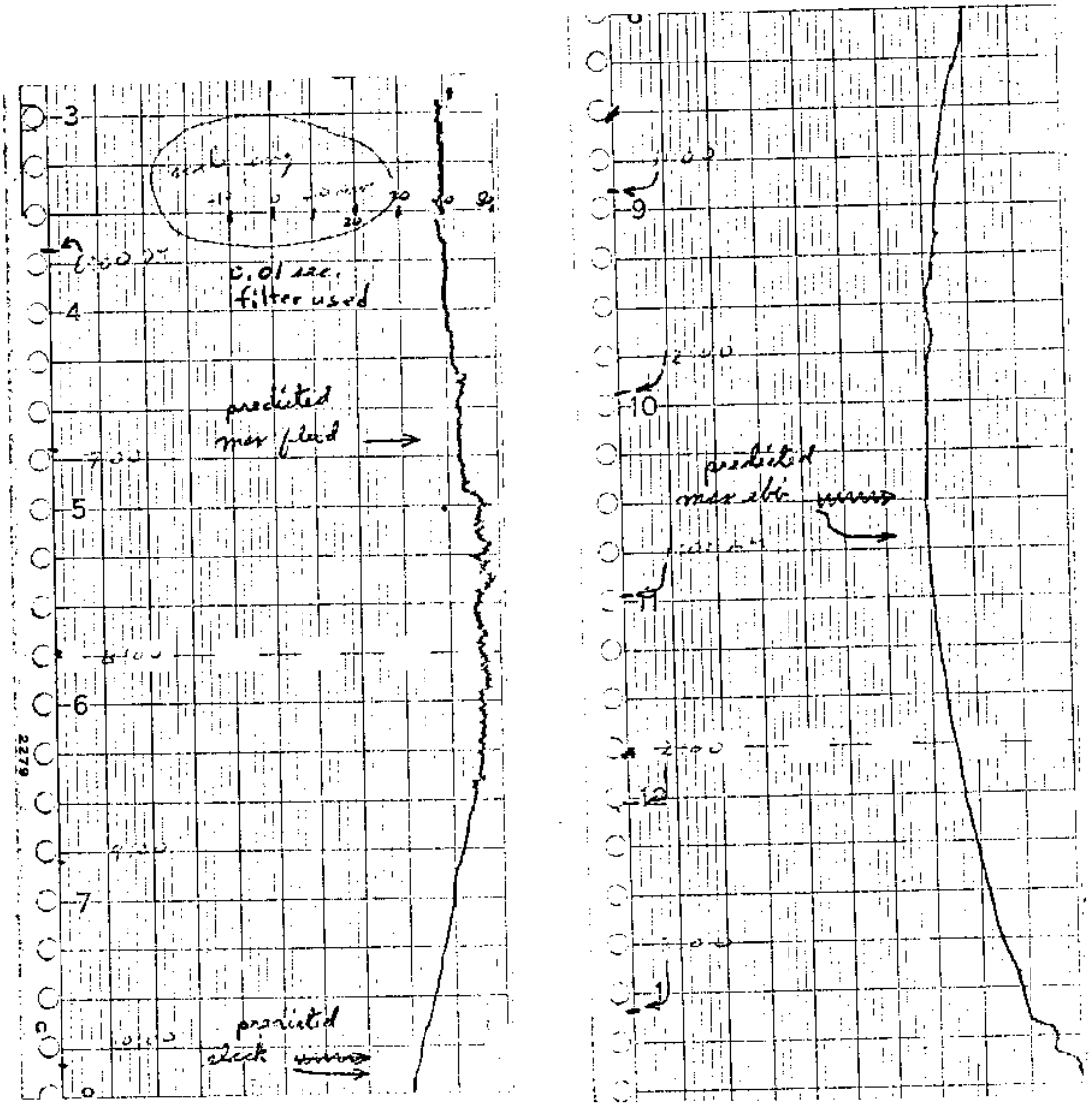

Fig. A.3--GEK recording before becoming inoperative in East Passage.

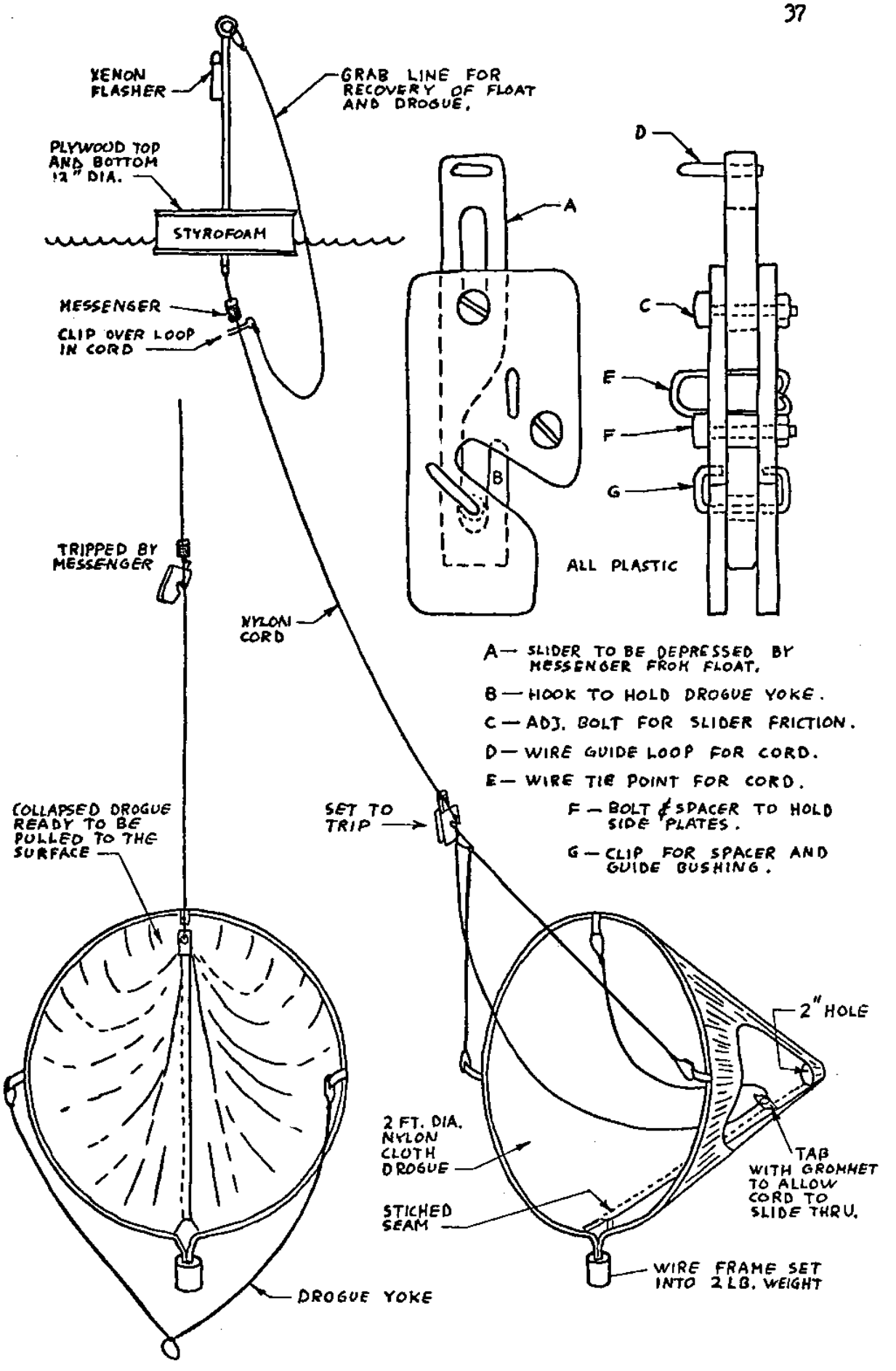

Fig. A.4--Float, drogue and trip device for East Passage.

APPENDIX B

THE WEST PASSAGE GEK INSTALLATION

After the wires in the East Passage had broken and suitable underwater wire was not available in the near future, it was decided to utilize the remaining military field-phone wire across the Jamestown Bridge. Figure B.1 shows the location. Laying it across the bridge would eliminate the possibility of damage to such a light wire which had prevented the sucessful operation in East Passage. Another added advantage was the fact that other studies were being performed in the Bay at and above the bridge for the Rome Point Circulation Study. This made it possible to compare data from different sources to give a better understanding of the tidal currents in that area. This benefited all the people involved.

The tensile strength of the wire is 200 lbs per conductor and it was felt that this was adequate to prevent damage from handling by people who would inadvertently discover the wires. The two twisted conductors were laid across the bridge by taking the wire around the sidewalk railing posts and letting it hang slack between posts under the bridge. In general the installation was very inconspicuous.

While laying the wire across the bridge in the late afternoon an observant person must have noticed the military reel and wire being installed. Since it looked suspicious, the author and an assistnat were apprehended, searched, questioned and subsequently cleared by the State Police. Permission had been obtained to install the wire from

the State Highway Department, but the State Police were inadvertently not notified about the situation before starting.

Electrode assemblies shown in fugure B.2 were lowered from each end of the bridge and placed on the channel bottom. After the large ground potential was discovered across the passage, copper ground rods were installed on each shore and connected to the recorder with the spare conductor over the bridge. When the necessary data was acquired it was decided to install a third electrode at the center of the bridge so as to divide the passage into a deep and shallow section. This electrode was similar to that in figure B.2 except that a 30 lb spiked block of lead was used as the anchor and the electrode was floated in a styrofoam float about 2 feet above the anchor. This was a precaution against crabs and lobsters since the electrode was in deeper water.

On Memorial Day vandals, malicious or otherwise, climbed over the cyclone and barb wired fence that the recording instrumentation had been placed behind. Even though the instruments were covered with dirty cardboard boxes the recorder was discovered and the timer clock was stolen and all the connector plugs on the recorder were disconnected. A new clock was built and the fenced enclosure was braced against further onslaughts with a massive dose of barbed wire.

By the middle of May 1971 the wires down to the electrodes from the bridge had been damaged by people pulling on the wires. To prevent further damage heavy Rural "C" telephone line was installed from the bridge to the electrodes and connected to the bridge railing with a thimble, steel cable and cable clamp. The wire was copperclad steel cable with a tensile strength of 1100 lbs. Since the cable was clamped taut between the railing and the mooring it was almost impossible to

reach through the railing and pull up the 40 lb moorings with the cable. This effectively prevented any more damage to this part of the installation. Through the summer months other small breaks were found and vandalism occurred on Labor Day when 1000 feet of wire was taken from the bridge. The electrodes and moorings proved immovable against fishermen. Over the summer, the east mooring provided several dozen fishing rigs even though the yellow float and wire very conspicuous.

The GEK was operated all during April and May, then for shorter periods throughout the summer. It was again operated during the month of October for another research project. After that, the installation was subsequently removed.

Several of the most significant operational problems besides damage by people should be mentioned. The insulation on the wire across the bridge was not strong enough to prevent chaffing and damage for a long period of time. The Mecca connectors were found to leak several times even though they were greased. Later all the three connectors underwater to the electrodes were covered with splicing tape and sealing compound. Corrosion between the lead moorings and the steel eyebolts was severe and had to be checked. All other hardware lasted very well. The rubber potting compound eventually parted from the PVC tubing used to hold the electrodes, but the inner splice prevented an electrical short to the sea water.

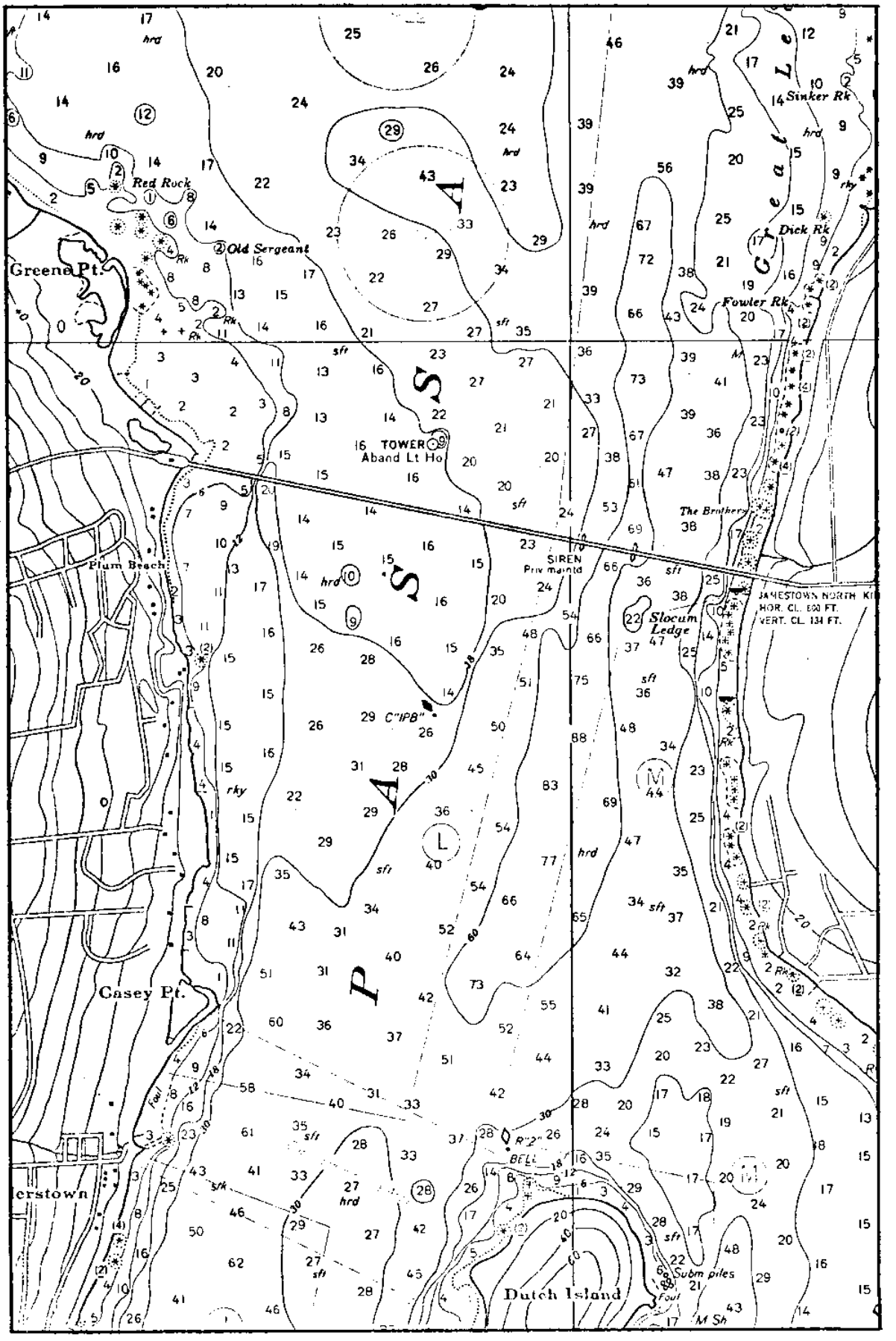

Fig. B.1--Location of GEK installation in West Passage.

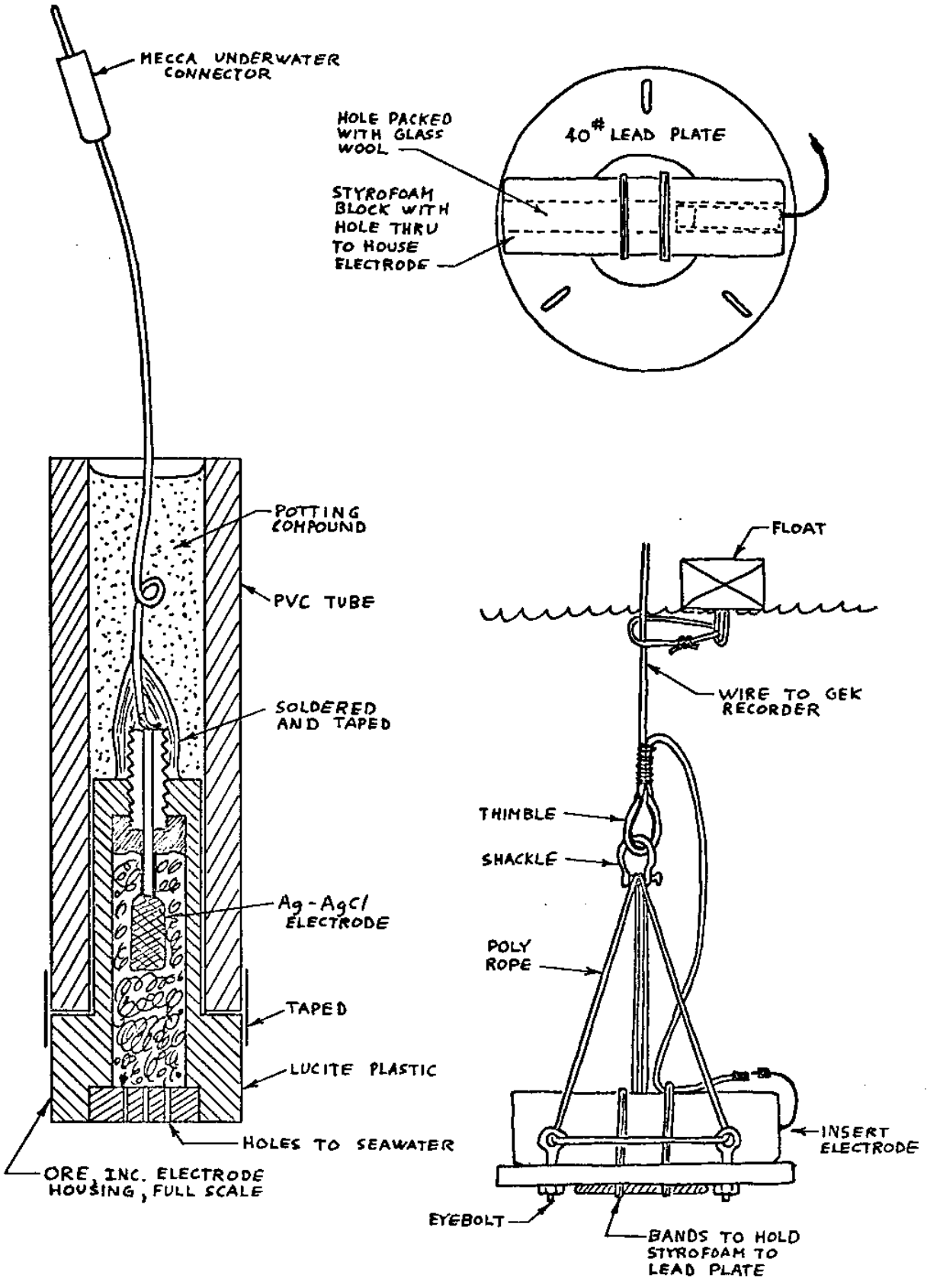

Fig. B.2--Electrode assemblies for GEK installation in West Passage.

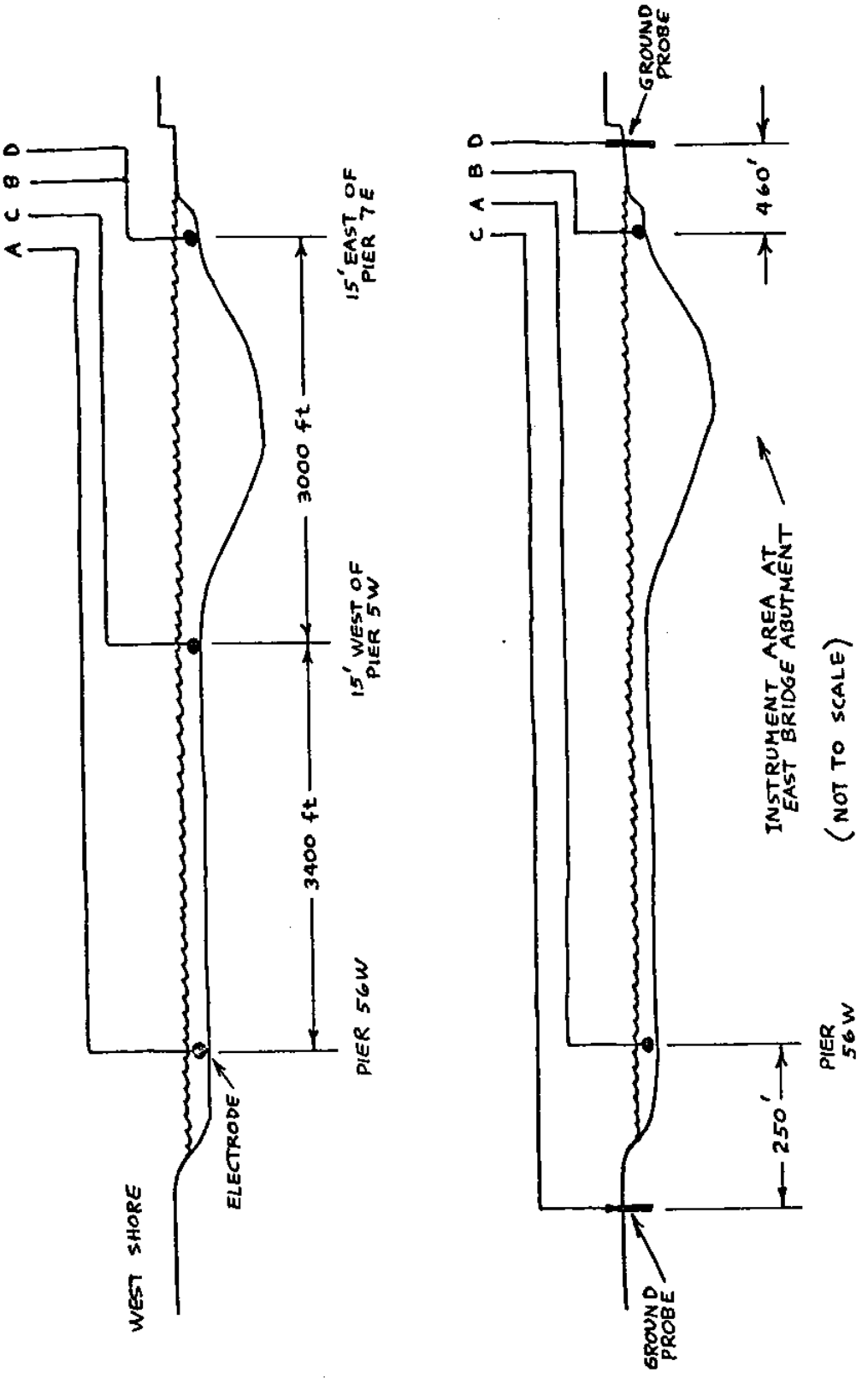

Fig. B.3--Installation of GEK system in West Passage.

APPENDIX C

OBSERVING TIDAL CURRENTS WITH DRIFTING POLES

The use of a floating object to measure the velocity of an ocean current has been practiced for a long time. In the deep oceans and deep channels the sea anchor principle has been used as mentioned previously. For shallower bodies of water and shallow channels, a simple pole weighted on the bottom and showing enough of itself above the water to be observed visually, has been used. The accuracy of this method has been questioned at times. Therefore an examination will be made as to how well the actual water velocity is represented by the pole and how accurately an observer can locate and determine the position of the drifting pole.

Drag on a drifting pole

The velocity of a mass of water may vary as a function of its depth. In this situation the drag on the pole will not be the same over the length of the pole. By definition the drag of an object in a fluid is described by the relation;

$$D = \frac{1}{2} \rho V^2 C_d S$$

where, D = drag
ρ = mass density
V = velocity vector of the object through the fluid
C_d = drag coefficient which is a function of R_e
R_e = Reynolds number, $f(V,D,\nu)$
S = surface area, usually facing the flow, equal to the projected area of the object

Notice that since the drag coefficient is a function of the Reynolds number, the drag is not necessarily proportional to V^2.

When a pole is placed in the water, the drag upon the pole will decrease as the pole accelerates to the speed of the water, at which time the drag force is zero. If the pole has a greater mass density than the water it will experience some drag as the pole adjusts to a change in velocity of the water. The pole will also experience a drag force if the pole velocity does not match the water velocity all along the length of the pole. If the mass of the pole is small, as it is in this case, the only concern is the relative velocity between the water and the pole, along the length of the pole.

Consider how the drag coefficient might vary on the pole. The greatest relative velocity that might be experienced in the Jamestown Bridge area of West Passage is probably no greater than 1 ft/sec (0.6 knot), and the minimum worth considering around 0.01 ft/sec. For a circular cylinder (L/d =∞) in a flow normal to the axis, the drag coefficient is a function of the Reynolds number as shown in figure C.1 from Hoerner (1965).

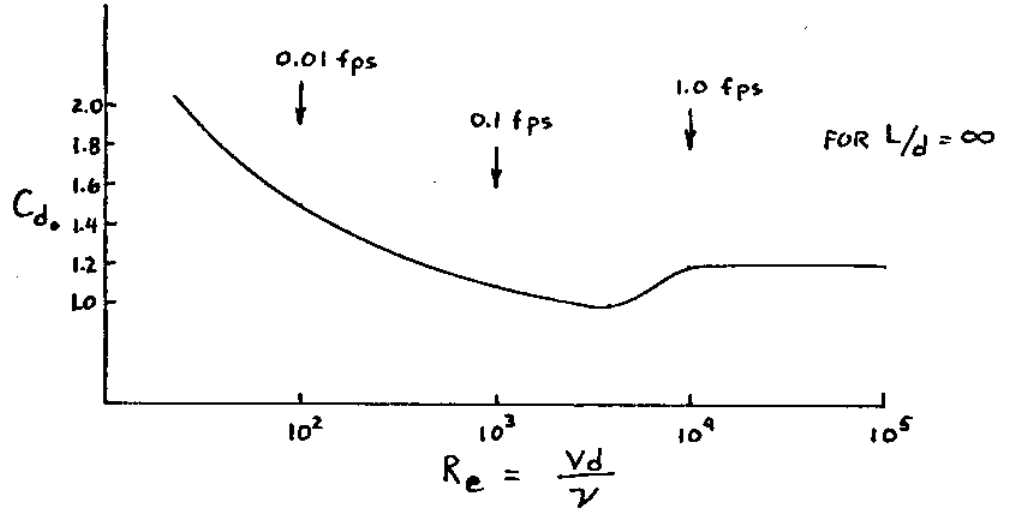

Fig. C.1--Drag coefficient of the circular cylinder in a flow normal to the axis as a function of the Reynolds number.

The fact that the pole has a finite length will not affect the C_d enough to alter this case where for our shortest pole,

$$L/d = 10 \text{ ft}/1.5 \text{ inches} = 80$$

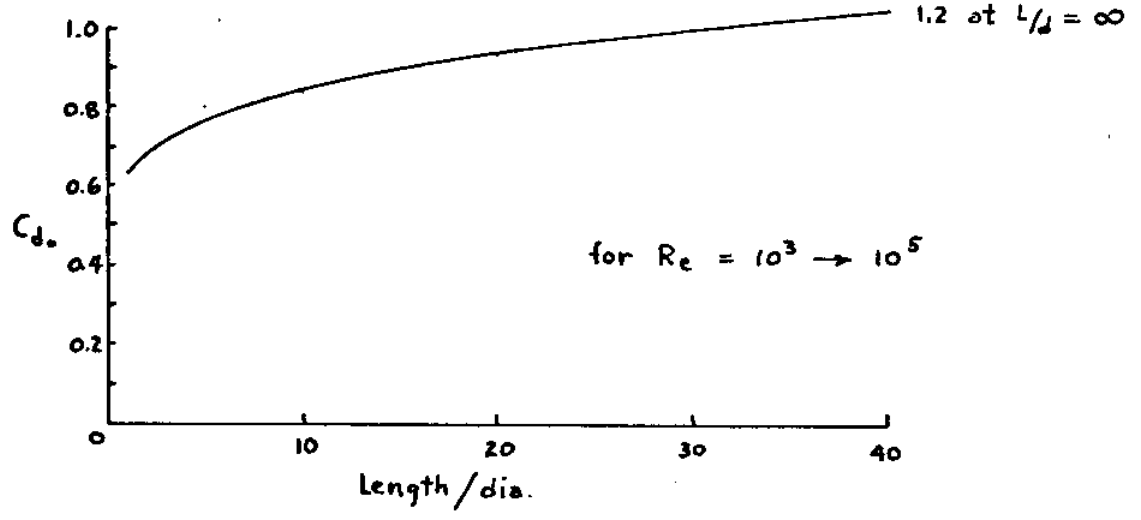

Fig. C.2--Variation of C_d for a circular cylinder as a function of a finite length.

Also it is seen in figure C.3 that if the pole is inclined to the flow as much as 20° the C_d only drops from 1.2 to 1.0.

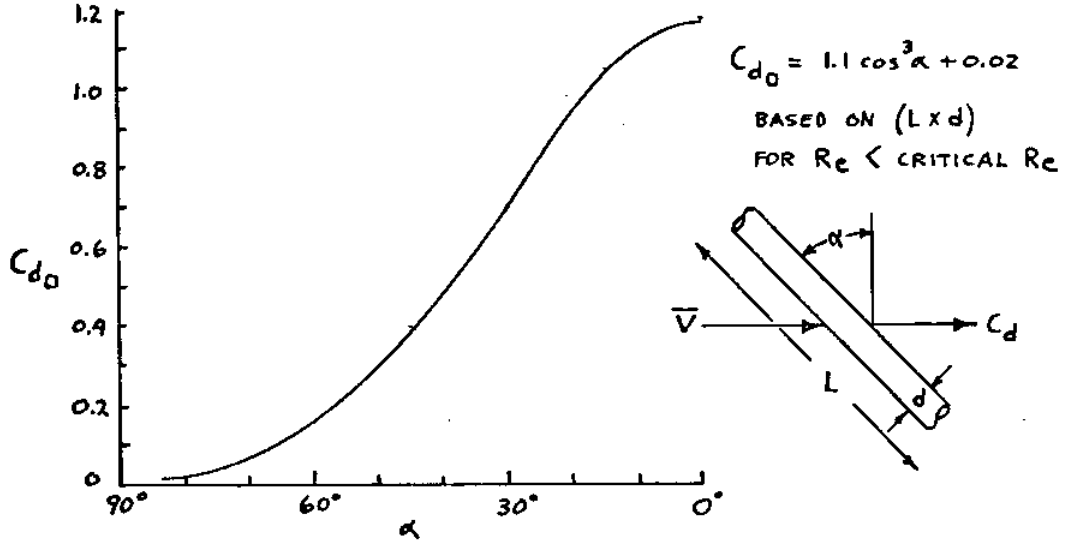

Fig. C.3--Variation of C_d for a circular cylinder as a function of the angle of inclination to the flow.

In this case,

$$R_e = \frac{Vd}{\nu}$$

where, V = velocity, fps
d = dia. of pole, 1.5 in
ν = kinematic viscosity, 1.1×10^{-5} ft^2/sec for seawater at 20^0 C.

For a relative velocity of 1.0 fps and 0.01 fps, the Reynolds numbers are respectively 10^4 and 10^2. These points are marked on the figure C.1 above. From this it is assumed that the C_d is relatively constant with respect to the accuracy of these calculations.

The variation of the vertical velocity profile is shown in figure C.4 for a complete tidal cycle on March 23, 1971, which was approximately three days before a full moon. This shows that the vertical variation can be extreme at times and when figures E.2 and E.3 (Rome Point, 1971) are examined, it is apparent that the variation is not easily predictable.

Three situations are now examined to determine if observed pole velocities will represent the mean water velocities in a channel. Let the water velocity be some function of the depth

$$V = F\left(\frac{z}{h}\right)$$

$$D = \frac{1}{2} \rho V^2 C_d S$$

If , C_d and S are all constants,

$$D \propto V^2$$

The first case is with the velocity a linear function of depth as in the sketch below. The pole reaches an equilibrium velocity when the total drag from water faster than the pole equals the total drag from water slower than the pole. It is easily seen that the mean velocity of the water (for the depth of the pole only) will be equal to the observed pole velocity. This shows the importance of making the

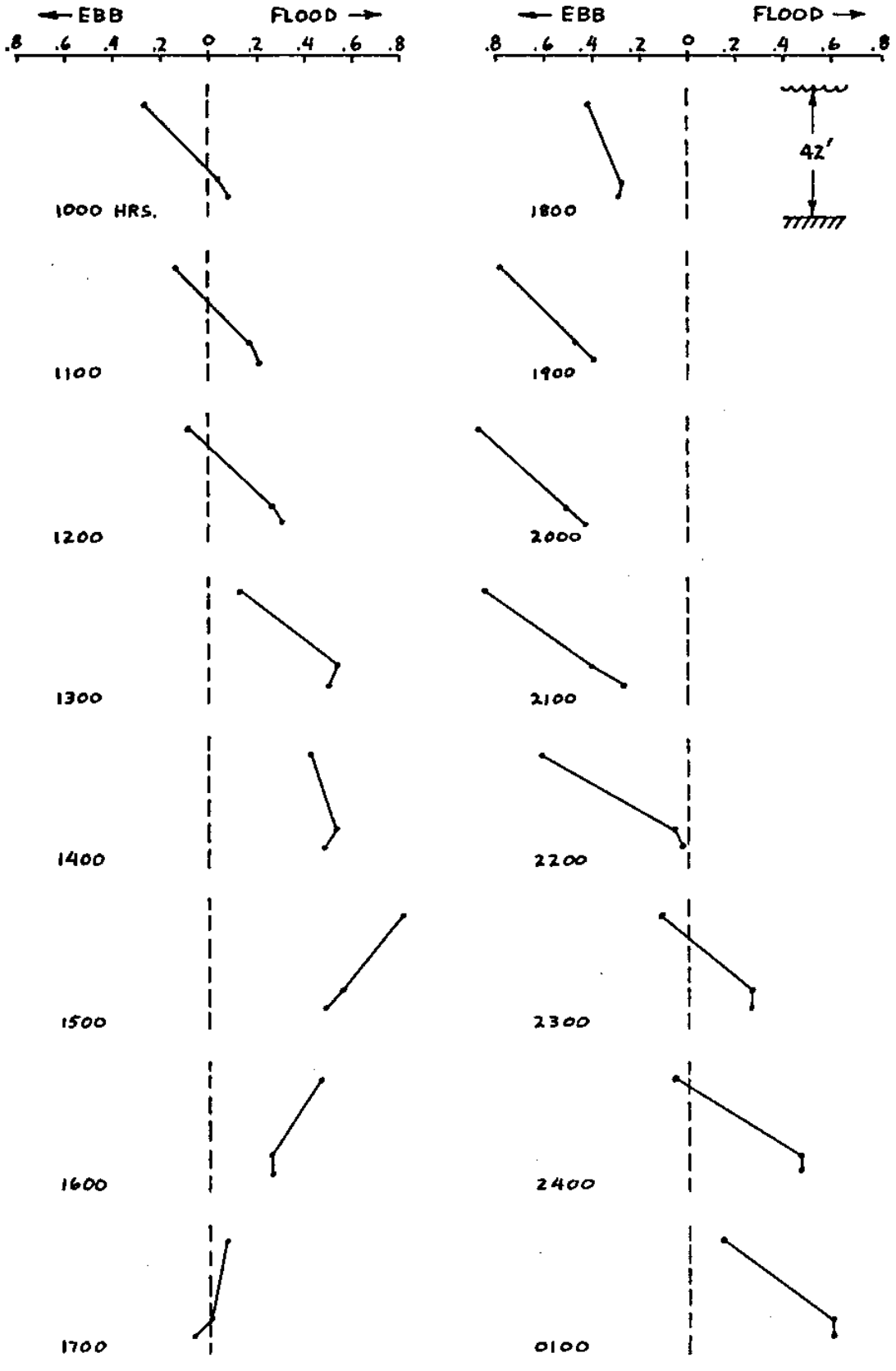

Fig. C.4--Vertical velocity profile (knots) on March 23, 1971 from Rome Point Circulation Study.

pole with a draft equal as near as possible to the depth of the water.

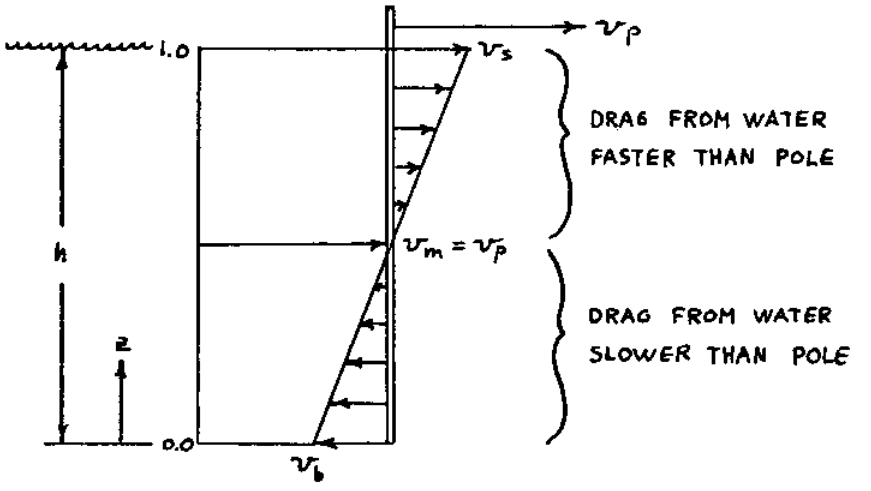

For a second case a velocity profile is examined that is representative of water flowing in a single direction down a channel with bottom friction. (Yen & Wu, 1969)

$$v = v_{SURFACE} \left(\frac{z}{h}\right)^{\frac{1}{7}}$$

Figure C.5 shows this profile on a non-dimensional scale. Referring to the sketch below, at equilibrium

$$\int_0^z D_s \, dz = \int_z^h D_f \, dz$$

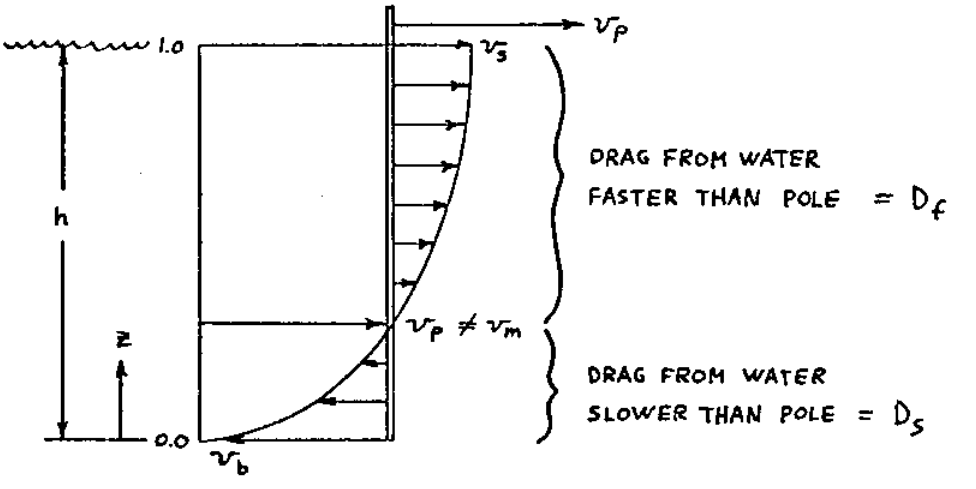

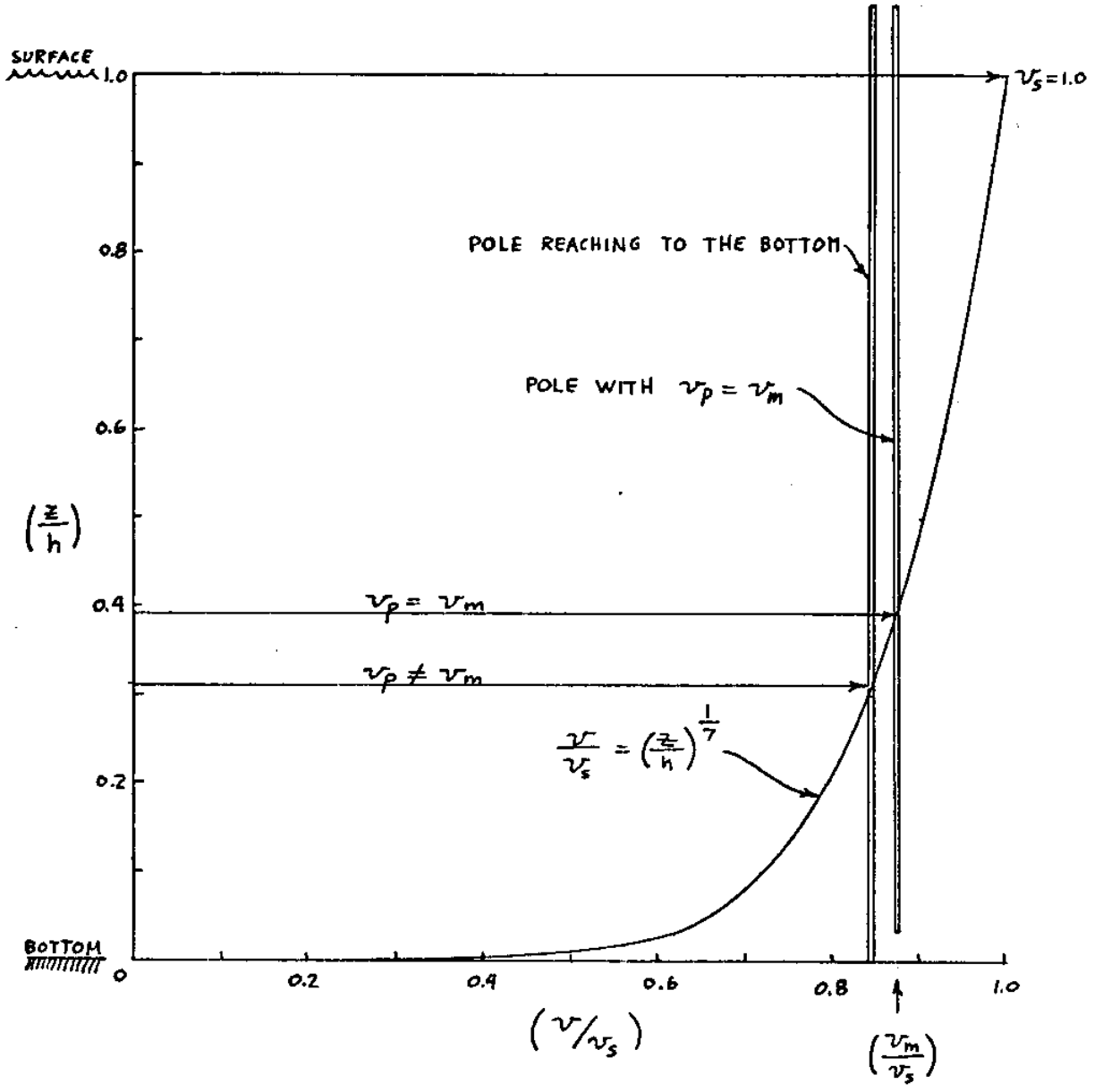

Fig. C.5--Showing velocities of two poles in a stream with a current profile.

For a pole that reaches to the bottom of the channel,

$$D_s = \int_0^{z/h} \left[v_p - v_s \left(\frac{z}{h}\right)^{1/7} \right]^2 d\left(\frac{z}{h}\right)$$

$$D_f = \int_{z/h}^{1.0} \left[v_s \left(\frac{z}{h}\right)^{1/7} - v_p \right]^2 d\left(\frac{z}{h}\right)$$

equating and integrating,

$$\left[2\left(\frac{z}{h}\right)-1\right]\frac{v_p^2}{v_s^2} - \left[2\left(\frac{z}{h}\right)^{8/7}-1\right]\frac{7}{4}\frac{v_p}{v_s} + \left[2\left(\frac{z}{h}\right)^{9/7}-1\right]\frac{7}{9} = 0$$

This equation must be solved by trial and error methods, which give z/h = (0.312). This value is plotted on figure C.5.

For the curve v/v_s, the mean velocity is,

$$\frac{v_m}{v_s} = \frac{\int_0^1 v \, d\left(\frac{z}{h}\right)}{\frac{z}{h}\Big|_0^h} = \frac{\int_0^1 \left(\frac{z}{h}\right)^{1/7} d\left(\frac{z}{h}\right)}{1} = 0.875$$

From this it is seen that the observed pole velocity is less than the mean water velocity.

For this same velocity profile, the length a pole would need to be so that the pole velocity would be equal to the mean water velocity is calculated.

Equating $D_s = D_f$

where, $\frac{v}{v_s} = 0.875$

$$\frac{z}{h} = (0.875)^7 = 0.393$$

$$D_s = \int_{z/h}^{.393} \left[v_p - v_s \left(\frac{z}{h}\right)^{1/7} \right]^2 d\left(\frac{z}{h}\right)$$

$$D_f = \int_{.393}^{1.0} \left[v_s \left(\frac{z}{h}\right)^{1/7} - v_p \right]^2 d\left(\frac{z}{h}\right)$$

equating and integrating,

$$+0.00435 - 0.7777\left(\frac{z}{h}\right)^{9/7} + 1.530\left(\frac{z}{h}\right)^{8/7} - 0.765\left(\frac{z}{h}\right)^{7/7} = 0$$

let $x = \left(\frac{z}{h}\right)^{1/7}$

Solving this by trial and error methods gives x = 0.62.

Therefore (z/h) = 0.0352 and the pole has a draft of 0.965 times the depth of the channel. This length is also shown in figure C.5.

In reality, the pole's draft will be made slightly shorter than the channel depth so as not to drag on the bottom; then the observed velocity will be very close to the actual mean water velocity. It must be restated that this profile is for a non-oscillatory flow of water in a channel. In the situation of a tidal estuary where the bottom friction causes a variable phase difference between the bottom currents and the upper currents, it might not be possible to use drifting poles for observing mean tidal currents, unless a lesser degree of accuracy is acceptable. In many cases it is not economically possible to use more complicated instrumentation. So it is important to be able to judge the merits of a system on more than its accuracy alone.

Basic concepts of drifting poles for West Passage

The poles chosen were thin wall aluminum tubes because they had many advantages over conventional wooden spars.

(a) Light weight for easy handling of long sections on a small boat.

(b) Low cost when used many times.

(c) Will not absorb water so careful depth control is possible.

(d) Constant density per unit length makes it possible to interchange sections and make replacement parts without separate buoyancy adjustments.

(e) Easy to work with and join together.

(f) Round, symmetrical cross section for predictable drag calculations.

(g) No maintenance necessary, except they should not be left in the salt water.

The topography of the channel bottom varied from 16 feet to 65 feet and the shallowest pole draft was 10 feet and the deepest draft was 46 feet. The tubing had enough strength and rigidity to be easily handled up to 48 feet in length. Probably 60 feet would still have been maneuverable.

Two methods of buoyancy were used; an open air bubble trapped in the tube for the shallow draft poles and a sealed air chamber for the deep draft poles. The choice was mainly determined by the convenience of manufacturing for both types. The method of joining the pole sections and plugging the ends is shown in figure C.6.

The pole will float at a level where the buoyant force of the displaced water equals the weight of the pole. Some length of pole must be left above the water for reserve buoyancy and as a means of viewing the drifting pole. The tracking of the poles is discussed later, but it is in general dependent upon the viewing distance and the wave height. Reserve buoyancy is needed only in the case of the open bubble type where it is possible to have the pole submerge and since the air bubble is compressible, continue to sink. The closed air chamber type always retains its full buoyancy, even submerged. In both types, the formula used to determine the required length of the buoyant section is;

$$\left[\begin{array}{l}\text{Upward force from the}\\ \text{buoyancy of the air chamber}\end{array}\right] = \left[\begin{array}{l}\text{Downward force from the}\\ \text{weight of tube submerged +}\\ \text{weight of tube above water +}\\ \text{weight of misc. hardware above}\\ \text{and below the waterline}\end{array}\right]$$

Closed air chamber system

As an example, determine the length of the sealed air chamber for a pole that has a draft of 40 feet and a freeboard of 2 feet. Since each tube section is 12 feet long, at least four sections with three

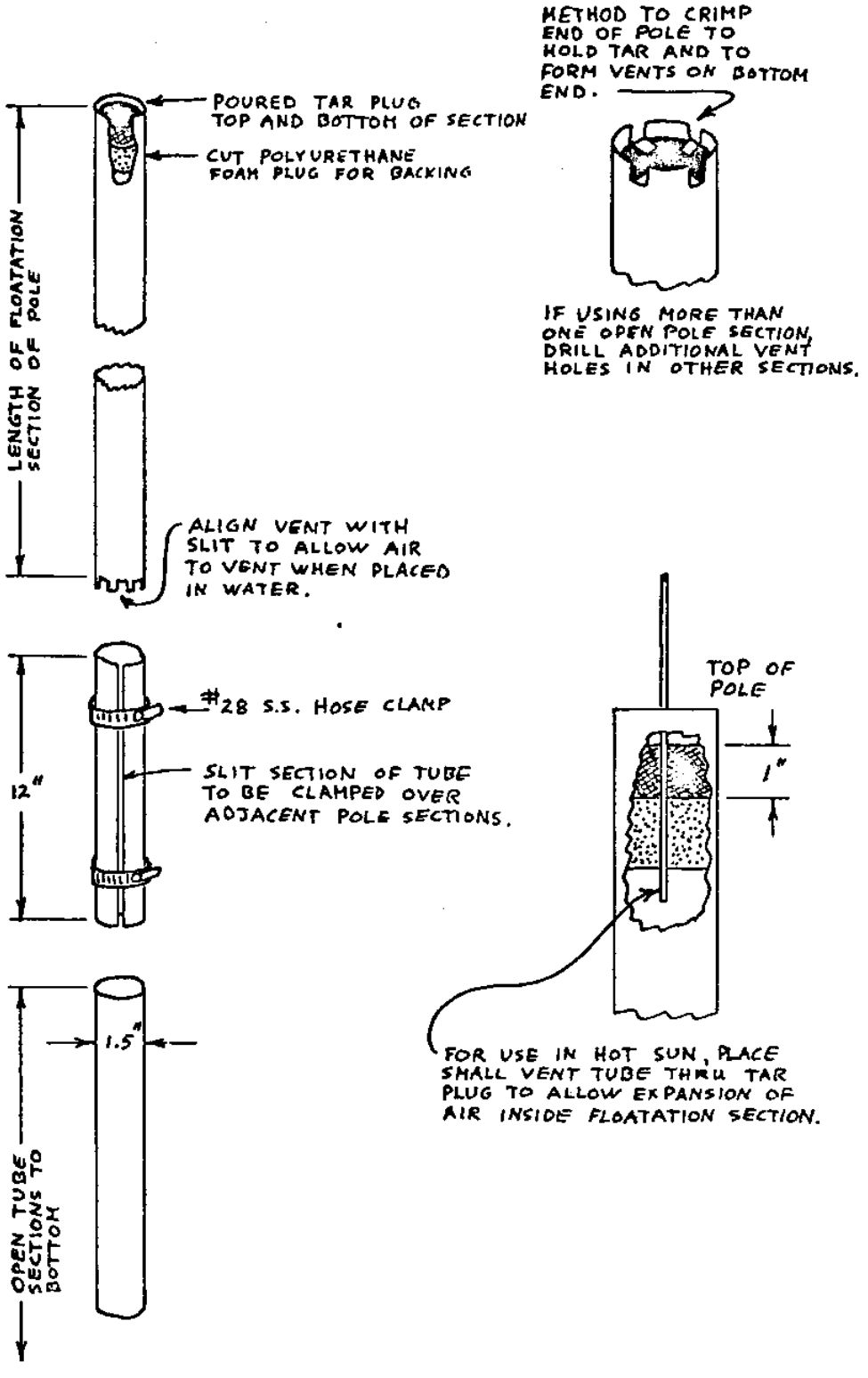

Fig. C.6--Method of joining pole sections and sealing the ends of the buoyant section.

splices will be needed. Each splice consists of one foot of split tubing and two clamps.

Tubing; Aluminum alloy 2024-T3 (alternate 6061-T6)
1.500 x .035 inches, 12 ft lengths
density 0.100 lb/in^3 or 172.8 lb/ft^3
specific gravity 2.7

Clamps; Stainless steel, size 28 adjustable
specific gravity 7.75
weight each 0.054 lb

Sea water; salinity 30 °/oo
temp. 20° C.
density 1.021 gm/cc or 63.8 lb/ft^3 (U.S.H.O. Pub. 615)

The buoyancy of the air chamber per foot is,

$$\frac{\pi}{4}(\text{I.D.})^2 (1\text{ ft})(\rho_w) =$$

$$\frac{\pi}{4}(1.430)^2 (1\text{ ft})\left(\frac{\text{ft}^2}{144\text{ in}^2}\right)\left(63.8\ \frac{\text{lb}}{\text{ft}^3}\right) = \quad 0.712\ \text{lb/ft}$$

The weight of the tubing per foot is,

$$\pi\,(d_m)(t_{wall})(12\text{ in})(\rho_T) =$$

$$\pi\,(1.465)(0.035)(12.)(0.100) = \cdots\cdots\ 0.1935\ \text{lb/ft}$$

The weight of submerged tubing per foot is,

$$(\rho_T - \rho_w)\,\pi\,(d_m)(t_{wall})(1\text{ ft}) =$$

$$(172.8 - 63.8)\,\pi\,(1.465)(0.035)\left(\frac{\text{ft}^2}{144\text{ in}^2}\right)(1\text{ ft}) =$$

$$(109.0)\quad \pi\,\frac{(1.465)(0.035)}{144} = \cdots\cdots\ 0.1219\ \text{lb/ft}$$

For the miscellaneous hardware it is usually easier to weigh individual items than to calculate the volumes, so use this method,

$$(\rho_H - \rho_w)\,(\text{vol.}_H) =$$

$$\left(\frac{\rho_H - \rho_w}{\rho_w} \times \frac{\rho_w}{\rho_H}\right)(\rho_H \times \text{vol.}_H)$$

let $\rho_w = 1$ and $\rho_H / \rho_w = (\text{sp. gr.})_H$

$$\left(\frac{\text{sp. gr.} - 1}{\text{sp. gr}}\right)_H (\text{wt.}_H)$$

For the clamps used underwater, their weight is

$$\left(\frac{7.75 - 1}{7.75}\right)(0.054\ \text{lb/ea}) = \quad 0.047\ \text{lb/ea.}$$

Setting up the equation and solving for the length of the air chamber,

$$\left(0.712 \frac{lb}{ft}\right) D = \left(0.1935 \frac{lb}{ft}\right) 2\,ft + \left(0.1219 \frac{lb}{ft}\right)(40' + 3') + \left(0.047 \frac{lb}{ea}\right) 6\,ea$$

$$0.712\ D = 0.387 + 5.24 + 0.282$$

$$D = 8.30\ ft$$

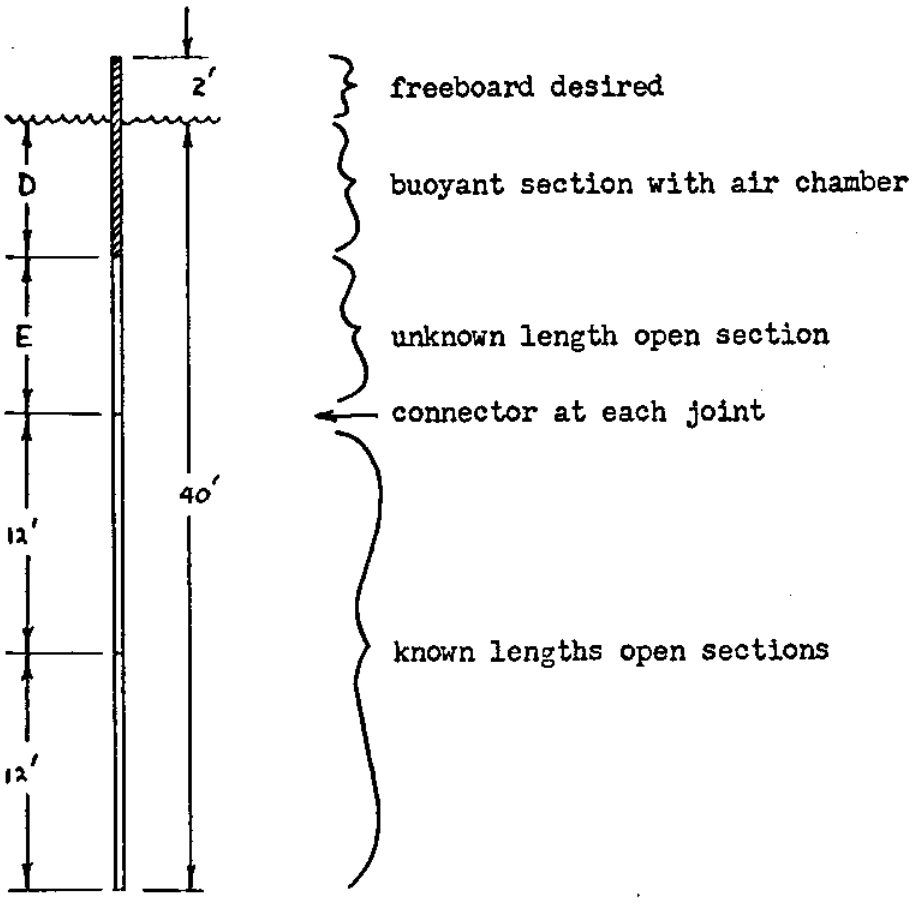

Therefore the length of the air chamber section is 8.30 + 2 = 10.30 ft and the open section E is 40 - 24 - 8.30 = 7.7 ft. The plugs used to close the air chamber may vary; the author used one inch of tar with a sp. gr. of 1.2 to seal the ends. These may be accounted for in the above calculations as hardware or the 1.4 inch loss of draft can be tolerated. Although the tar plugs are easy to pour and cheap, they tend to soften and are forced out by the expanding air when the

poles are heated by the Sun on a hot summer day. A small vent hole in the upper end of the air chamber would solve the problem and still not be large enough to allow water in. See figure C.6.

Open air bubble system

At times the depth of the water only warrants a pole that is less or not much longer than the stock length of the tubing as purchases. It is much easier in this case to plug only the upper end of the pole and drill a vent hole in the tube so as to entrain an air bubble just sufficient to buoy the pole at its required draft.

As an example, determine the position of a vent hole that will enable a pole to float with a draft of 10 ft and a freeboard of 2 feet. Only one tube of a standard 12 foot length is needed.

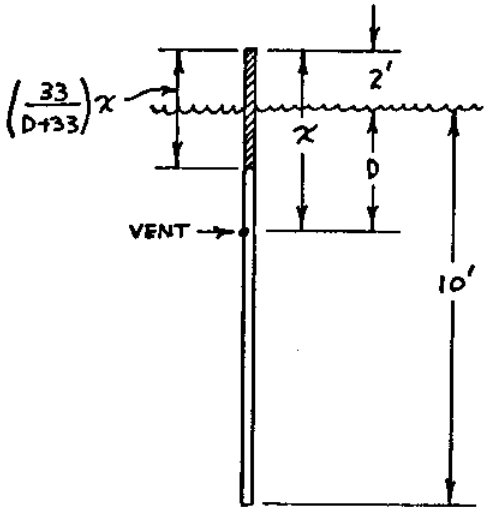

As before; [Upward force of buoyancy] = [Total force downward from pole]
The only difference is the air bubble starting with a length of x will compress to a length of $\left(\frac{33.2}{D+33.2}\right)x$ due to $\left(\frac{D+33.2}{33.2}\right)$ atmospheres of pressure on the bottom of the bubble.

$$\left[\left(\frac{33.2}{D+33.2}\right)x - 2'\right] 0.712 \frac{lb}{ft} = \left(0.1935 \frac{lb}{ft}\right) 2 \text{ ft} + \left(0.1219 \frac{lb}{ft}\right) 10 \text{ ft}$$

by definition $D = (x-2)$ ft

$$\left[\left(\frac{33.2\,x}{x-2+33.2}\right) - 2\right] 0.712 = 0.387 + 1.219$$

$$\frac{23.6\,x}{x+31.2} - 1.424 = 1.606$$

$$23.6x = (31.2+x)(1.606+1.424)$$

$$23.6x = 3.03x + 94.5$$

$$x = 4.6 \text{ ft}$$

Method of tracking the drifting poles

Conventional methods used in measuring the velocities of drifting poles are somewhat crude. The most common are: Using an anchored boat, a pole with a light string attached to it it allowed to drift with the current. The rate of paying out the string is measured and the direction of the drifting pole is observed. This method is not possible if more than one station is to be measured, and is also subject to handling errors as the string is paid out farther and farther. Transit triangulation is often used when a longer drift is desired. A single transit can be used if the observer tracks from a high enough position so as to be able to obtain both an alitiude and azimuth of the pole at various times. If enough height is not available, two transits must be used to triangulate time synchronized positions of the drifting pole. Each transit will require two people; one to record angles and time while communicating with the other transit, the second person to track a moving target on the cross hairs of the scope. To accurately follow more than a couple of poles, will require considerable skill and will be extremely fatiguing if done over a long period of time, such as a tidal cycle. Both the single and double transit methods are adaptable to night tracking by using a camera with time exposures.

The poles should be equipted with small high intensity stroboscopic lights. The triangulation is the same, except that it must be measured from the photographic plates.

None of the above methods were suitable for calibration of the GEK which was measuring the average velocity of the tides in a perpendicular direction to the Jamestown Bridge. Since the water depth varied quite widely across the passage, many drifting poles were required to give an accurate average velocity for the tidal currents. This made all the above methods practically impossible because many pole velocities would need to be recorded simultaneously, and the operation would need to continue for at least a half of a tidal cycle.

The method finally used proved accurate; all readings could be taken within five minutes and could be continued without much observer fatigue throughout the daylight hours. Since the range of the poles from the observer could be controlled, only one telescope was required. The problem of tracking a moving target with cross hairs was eliminated by using a reticle grid superimposed upon the field of view. A stopwatch was used to record a time of transit as the pole drifted across a known angle of view. The telescope could remain stationary since the field of view was much larger than that of a transit. A small boat would shuttle back and forth across the passage deploying and recovering the string of poles while they were tracked by the telescope on the share. A diagram of the system is shown in figure C.7.

Since the GEK recorded the velocity orthogonal to the vertical component of the Earth's magnetic field and the line of sight between the two electrodes, the calibration system should be designed to measure the same velocity vector. For this telescopic system when the sighting was kept very nearly parallel to the bridge, the observer recorded

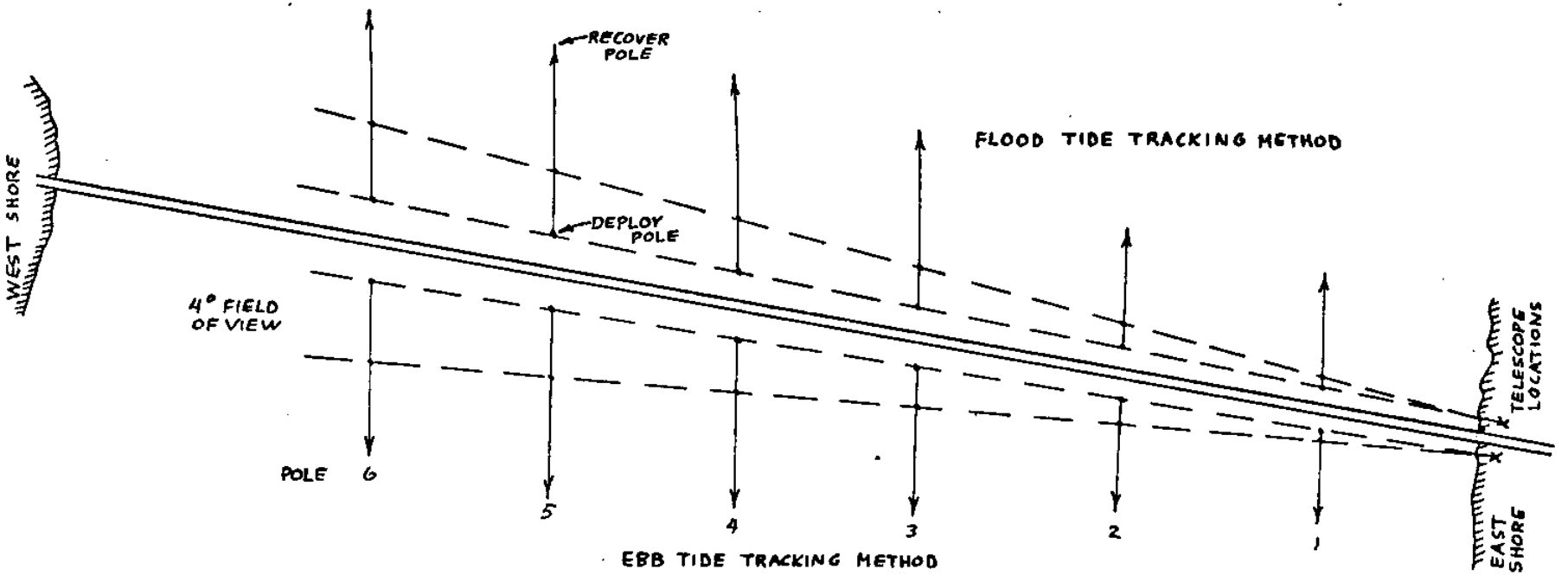

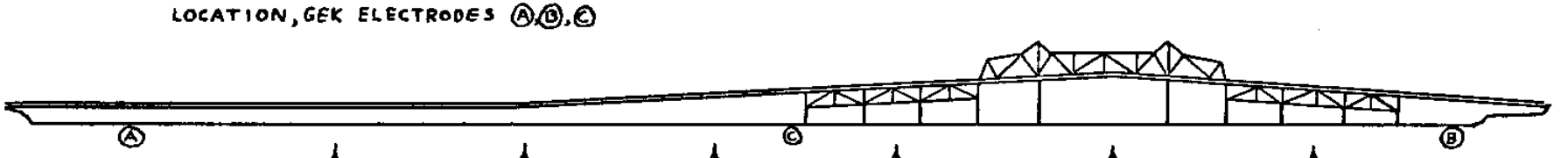

STATION	6	5	4	3	2	1
LOCATION BETWEEN PIER	38-37W	21-20W	11-10W	4-3W	1W-1E	3-4E
RANGE TO SCOPE EAST SHORE	5590'	4630'	3710'	2770'	1790'	810'
RANGE TO SCOPE WEST SHORE	1130'	2090'	3010'	3950'	4930'	5910'

Fig. C.7--Tracking diagram and sighting ranges for drifting poles.

($V \cos \theta$), where θ is the angular deviation from the perpendicular to the bridge. In this way the calibration system would measure only that component of the tidal flow that the GEK would record.

Visual acuity and telescopic magnification

Before continuing, some background should be prepared that will enable the reader to determine the feasibility of observing a small pole at a large distance.

A normal eye with 20/20 vision can recognize an upper case letter such as E, that has a height subtending 5 minutes of arc and each element subtending one minute of arc. Visual acuity is defined as the reciprocal of the angular size of the recognizable element; in the case of 20/20 vision, one minute equals a visual acuity of 1.0. This normal visual acuity of one minute is most often used in the design of optical instruments. (Smith, 1966, p. 105)

Vernier acuity is also important in tracking the poles. This is the ability to align two objects and for our purpose is the ability to align a cross hair on a pole. It is normally five to ten times the visual acuity, but it will be less for a moving target. It was found that the greatest optical error was caused by an individual's response time while operating the stopwatch.

The narrowest black line in front of a bright field that the eye can detect is from 1/2 to one second of arc. With a bright line on a dark field the size of the line is not as important as its brightness. This means that it is important to use a bright paint on the poles such as the fluorescent types that are brighter when activated by sunlight. Over the water red-orange, orange, yellow and yellow-green are best recognized.

It was found that while the shore observer could detect and follow the pole, it was difficult for the personnel in the boat to locate the poles for retrieval. The boat usually was rolling and heaving from its motion through waves; this made it difficult to distinguish the vertical pole among distant waves and reflections from the Sun. Small fluorescent pennants about 3 feet above the surface of the water helped solve this problem and also helped the shore telescope in tracking distant poles.

The Sun angle and glare off the water is very important in determining the direction of view for the telescope and while polaroid filters will reduce the glare on the water, the best visual perception is with the Sun behind the observer. If the operation is to last throughout the day, plans must be made to change the viewing direction if the glare develops later in the day.

The telescope used for the calibration of the GEK at the Jamestown Bridge was a binocular type which while producing less eye fatigue also made it easier to separate the pole from the background because of the stereo perception. A single telescope projects only a two dimensional image. A binocular telescope decreases the stereo perception by its magnification, if the objective lenses are the same ocular distance as the eyes. If the objective lenses are further separated the stereo perception can be increased to normal. The particular binoculars this author used could be used with 1/3 the normal stereo perception or with full stereo perception. The latter was possible because of a 27 inch separation of the objective lenses.

The ability to resolve the pole optically is both a function of the observer's visual acuity and the resolution of the optical system. The resolving limit for an optical system is a direct function of

wavelength and an inverse function of the aperture of the system. The focal length and therefore the magnification does not affect the resolution.

For ordinary visual instruments in the mid-optical portion of the electromagnetic spectrum, which includes telescopes and cameras, the limiting resolution as shown by Smith (1966, p.141) is

$$\alpha = \frac{140}{d} \text{ sec of arc}$$

where d is the clear aperture of the system. This resolution can be hindered by systems that include various optical aberrations, but most better instruments are designed to minimize these effects.

It shall now be shown how a telescope would be chosen for optical tracking of the poles in the West Passage. The maximum working distance at the Jamestown Bridge location is 6000 feet and the poles have a diameter of 1.5 inches.

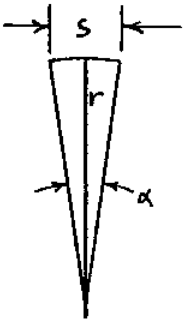

$$\tan\left(\frac{\alpha}{2}\right) = \frac{s}{2r}$$

for small angles $\tan\alpha \approx \alpha$ radians

$$\alpha \text{ rad.} = \frac{s}{r}$$

$$= \frac{1.5''}{6000 \text{ ft}} \times \frac{\text{ft}}{12''} \times 206{,}265 \frac{\text{sec arc}}{\text{rad.}}$$

$$= 4.3 \text{ sec of arc}$$

This is the angle that the system must resolve. To resolve this,

$$\alpha = \frac{140}{d \text{ mm}}$$

$$d \text{ mm} = \frac{140}{4.3} = 32.6 \text{ mm diameter}$$

The objective lens should be about 33 mm in diameter. Notice that the magnification of the lens system will not increase the resolving power but it will enable the human eye to "see" the resolving ability of the telescope. If the eye can resolve one minute of arc, the telescope will need a magnification of,

$$(M.P.)\alpha = 1 \text{ min. of arc}$$

$$(M.P.) = \frac{60 \text{ sec of arc}}{4.3 \text{ sec of arc}}$$

$$(M.P.) = 14 X$$

The telescope used had an aperture of 43 mm and a M.P. of 10X. Even though the visual image was not sharp, it was possible to recognize the drifting poles because of other visual perceptions besides acuity. These include color perception, motion perception, stereo perception and of course the small pennant enhanced the visual acuity. It is interesting to note that with the binocular telescope, with maximum separation of the objective lenses, the stereo perception alone would be capable of aligning two poles within 300 feet of each other at a distance of 6000 feet.

From other experiments, the 10X telescope was found to be limited to tracking at ranges not much greater than the 6000 feet. Greater ranges were greatly subject to weather, waves, Sun angle and the wind direction of the pennants.

The actual calculation of the pole velocities was determined from the relation,

$$(VEL.)\,fps = \frac{\text{range ft}}{1000 \text{ ft}} \times \frac{\text{mils}}{\text{sec}}$$

knots = 0.592 x fps

meters/sec = 0.3048 x fps

The ranges (Parsons et al., 1938) were pre-set by fastening markers on the bridge at the stations shown in figure C.7. When other areas are to be studied, the ranges will have to be pre-set with buoy markers or with triangulation from pre-set angles on a second telescope or transit. The reticle grid screen used is shown in figure C.8. It is calibrated in mils since the telescope used was a WW I artillery battery command telescope, marked with the following specifications.

B.C. Telescope
Model of 1915, A1
Field 4° - 15' Power 10
B.& L. Opt. Co. 1918 R.G.C.
3895

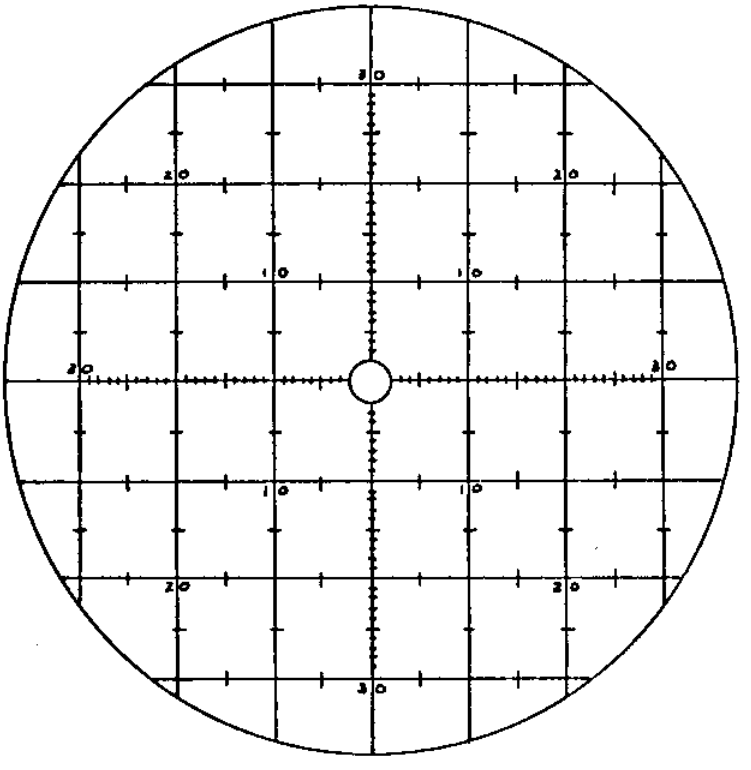

Fig. C.8--Reticle grid screen for telescope.

Notes for an efficient operation

(a) When the operation is to last for a tidal cycle, all personnel should be prepared to remain on station for the full time or a suitable relief available. This includes a sufficient supply of fuel for the boat, lunches and extra equipment in case of repairs. Extra pole sections should be available on board the boat. Radio communications should be available that are reliable. Voice communication may be possible at times.

(b) If the poles are affected by the wind, wind velocities

must be recorded over the water.

(c) It is usually easier for the poles to be deployed as the boat goes away from the tracking shore. In this way the boat will not obscure the poles and they can be tracked as soon as they are steady. The poles have a small mass and the air in the vented tubing cushions them as they enter the water so they may be heaved over board very rapidly.

(d) Provisions for changing tracking positions should be planned if as in the case of the Jamestown Bridge, the Sun glare is a problem later in the day.

(e) The visual tracking should be quick so as to obtain all pole velocities in a small time span. The angular mils subtended by the poles should be in general, great enough so as to take 10 seconds. This helps eliminate the reflex error while using the stopwatch. Obviously the field of view of the telescope and the current velocities will modify the time available.

Wind drag on the poles

As mentioned before, the local wind conditions will have an effect on the velocity of the poles. The amount each pole is influenced will be determined by the freeboard of the pole and if the pole carries a pennant for better visibility. The effect of the wind was checked by rough experiments which were not performed as carefully as hindsight would have dictated; although in general they show the advantage of keeping the freeboard of the poles as small as possible and relying on the pennants for visual tracking. Since the experimental results were not as accurate as desired, the final pole data for the GEK calibration was corrected using a theoretical drag coefficient.

All the data was originally corrected with both the experimental and theoretical drag. By examining all the uncorrected and corrected velocity profiles it was decided that the wind did not have enough effect on various lengths of poles to affect their relative horizontal velocity distribution across the passage. It also did not seem to change the band of scatter of the data. The absolute velocity of the poles was very much affected by the wind and this is why correction for the wind must be made.

During the calibration of the GEK on June 17, two different combinations of poles were observed. The first with a short and long pole was to determine the effect of the wind on the poles. The second with two short poles, one of which did not have its pennant attached. This was to determine the effect of the wind on the pennant.

Wind drag on the short and the long pole

The best data run was taken at 1155 hrs DST with the regular 48 foot pole at station 2, plus a 12 foot pole and a float-drogue placed as close as possible to the 48 foot pole. Both poles had pennants attached to them. The diagram of figure C.9 shows the relative positions at the start and finish of the run. The separation of the poles and float at the finish was due to the combined effect of the wind and the vertical variation of the tidal velocity. The final separation of the short and long pole was 50 feet. The float (see appendix A) had a drogue at 6 feet depth and was of such a design that resulted in the observed velocity of the float being about 7/8 of the water velocity at the depth of the drogue. Therefore the excess drift of the float over the long pole can be used as an indication of the excess surface current which would have affected the short pole.

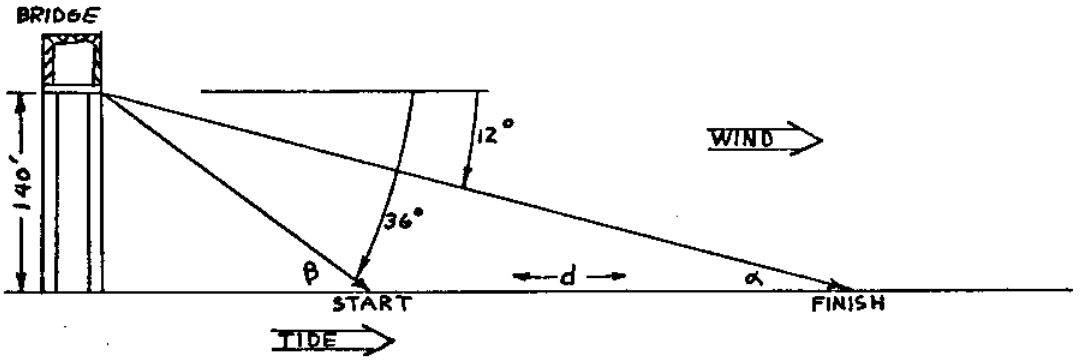

$$d = 140' (\cot \alpha - \cot \beta)$$
$$= 465'$$

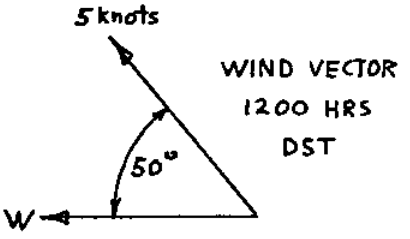

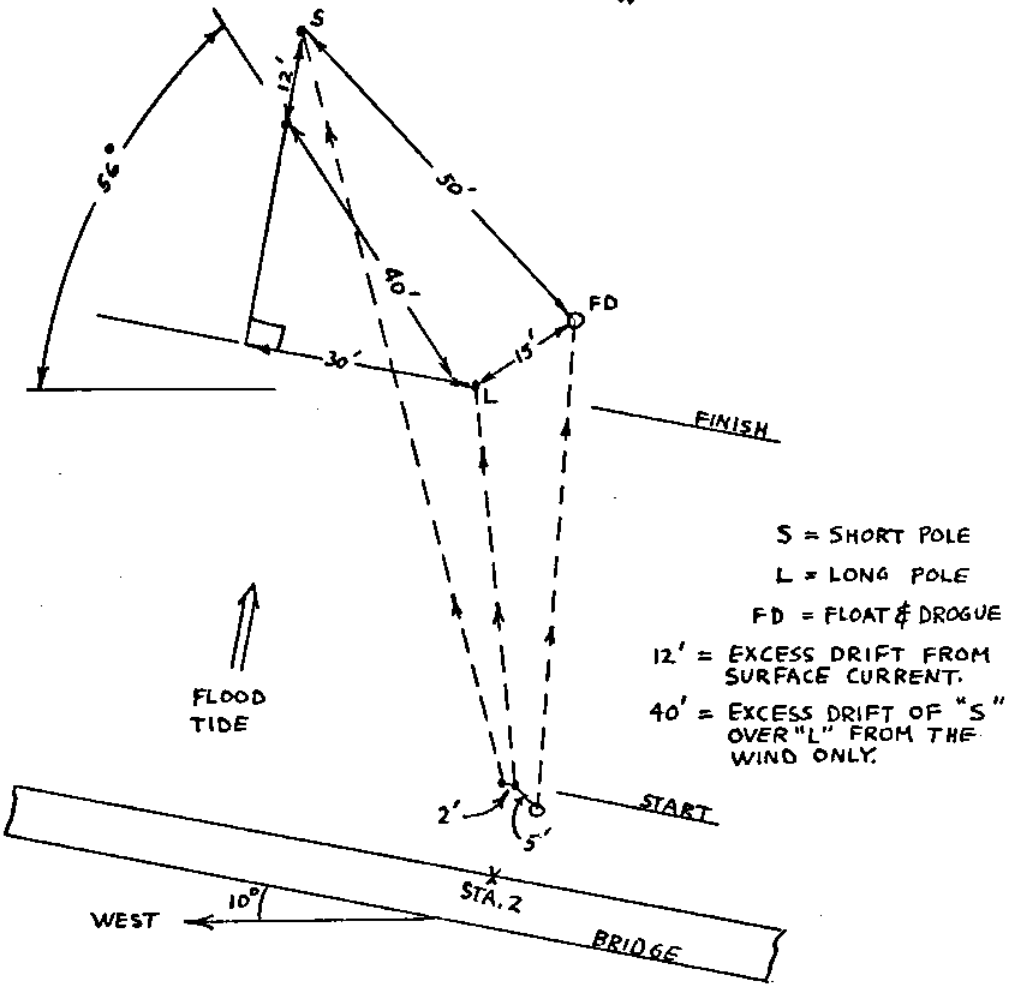

Fig. C.9--Relative positions of poles and drogue in determining the C_d for the wind on the poles.

From the vector diagram this is about 12 feet. Subtracting the 12 feet from the 50 feet (vectorially) leaves about 40 feet for the excess drift of the short pole over the long pole due to the wind. The resultant drift vector is in close agreement with the actual wind vector as recorded at Quonset Point.

From the telescope data at 1155 hrs pole no. 2 had a velocity of 0.597 knots = 1.008 fps. The time of drifting was 465 ft/1.008 fps = 465 sec. Since the 12 foot pole went 40 ft farther than the 48 foot pole, its velocity was 40 ft/465 sec = 0.086 fps faster than the 48 foot pole.

By definition the drag in both the water and air is,

$$D = \frac{1}{2} \rho V^2 C_d S$$

To analyse the data it is assumed that the drag from the wind is the same for both poles because the windspeed was around 10 fps and the difference in velocity between the two poles was only 0.086 fps.

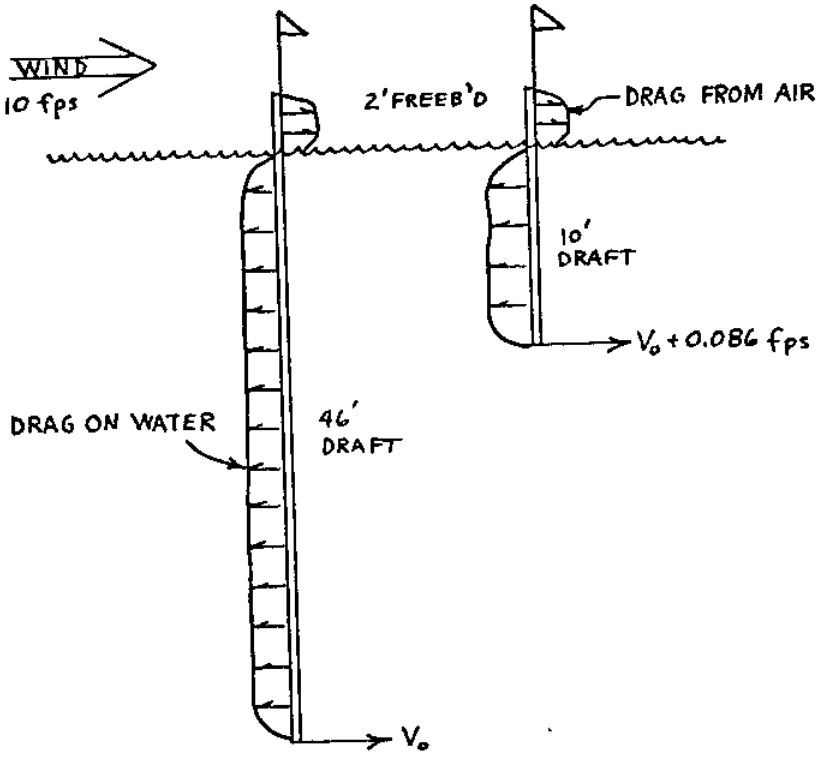

At the equilibrium velocity V_o, the drag on the pole from the air is equal to the resisting drag of the water.

Therefore, $\frac{1}{2} \rho V_o^2 C_{dL} S_L = \frac{1}{2} \rho (V_o + 0.086)^2 C_{dS} S_s$

water drag long pole = water drag short pole

where, $C_{dS} = 1.0$ for $V \approx 0.2$

$C_{dL} = 1.1$ for $V \approx 0.1$

$S_s = 1.5'' \times 10$ ft

$S_L = 1.5'' \times 46$ ft

$$V_o^2 (1.1)(46) = \left[V_o^2 + 2 (0.086) V_o + 0.086^2 \right](10)$$

Solving for V_o

$$V_o = 0.0687 \text{ fps}$$

The velocity of the short pole is

$$V_o + 0.086 = 0.154 \text{ fps}$$

The drag of the short pole on the water is,

$$D = \frac{1}{2} \rho_w V_w^2 C_{dS} S_s$$
$$= 0.995 (.154)^2 (1.0) \left(\frac{1.5}{12} \times 10\right)$$
$$= 0.0296 \text{ lbf}$$

The wind velocity acting on the poles was approximately 5 knots = 8.5 fps. The C_d for the 2 ft of pole and pennant in the wind was,

$$D = \frac{1}{2} \rho_a V_a^2 C_d S$$

where, $\frac{1}{2} \rho_a V_a^2 = \frac{V^2}{840}$

$S = 1.5'' \times 2$ ft

$V = 8.5$ fps

$D = 0.0296$ lbf

Therefore,

$$C_d = \frac{0.0296 (840)}{(8.5)^2 \left(2' \times \frac{1.5}{12}\right)} = 1.36$$

Which seems slightly large.

Checking the Reynolds number for the wind on the pole,

$$R_e = \frac{Vd}{\nu}$$
$$= \frac{8.5 (1.5/12)}{1.56 \times 10^{-4} \text{ ft}^2/\text{sec}}$$
$$= 6.8 \times 10^3$$

Examining figure C.1 for theoretical drag coefficients, C_d is found equal to 1.0. Since the pole exposed to the wind has a finite length and a L/d = 16/1, it is seen in figure C.2 that C_d might be slightly lower, equal to 0.9.

Wind drag on the pennant

It is possible that the C_d of 1.36 is due partially to the drag of the pennant. In this experiment two identical 12 ft poles, except that one carried a pennant, were allowed to drift together. The pole with the pennant gained about 25 ft on the non-pennant pole over a travel distance of 1200 ft. The velocity of the pennant pole (no. 4 pole) was 1.447 fps at 1230 hrs DST when the test was run. The wind velocity was about 6 knots. The time of drifting was 1200 ft/ 1.447 fps = 830 sec. The drift rate for the no. 4 pole was 25 ft/ 830 sec = 0.0302 fps greater than the non-pennant pole.

This corresponds to an excess underwater drag on the pole of,

$$\Delta D = \frac{1}{2} \rho (\Delta V)^2 C_d S$$
$$= 0.995 (0.0302)^2 (1.0) \left(\frac{1.5}{12} \times 10\right)$$
$$= 0.00113 \text{ lbf}$$

Since this drag must have been produced by the wind on the pennant,

$$D_{wind} = \frac{1}{2} \rho V^2 C_{d_\square} A$$

where, $\frac{1}{2} \rho V^2 = \frac{V^2}{840}$

$V = 6 \text{ kts} = 10.1 \text{ fps}$

$A = 0.167 \text{ ft}^2$ pennant area

$D = 0.00113 \text{ lbf}$

Therefore,

$$C_{d_\square} = \frac{0.00113 \ (840)}{(10.1)^2 \ (0.167)} = 0.057$$

This drag coefficient is based not on frontal area but the circumscribed area of the pennant. The shape of the pennant was selected

because it has more rigidity and less flutter than a conventional square flag. The material was waterproof and fairly rigid.

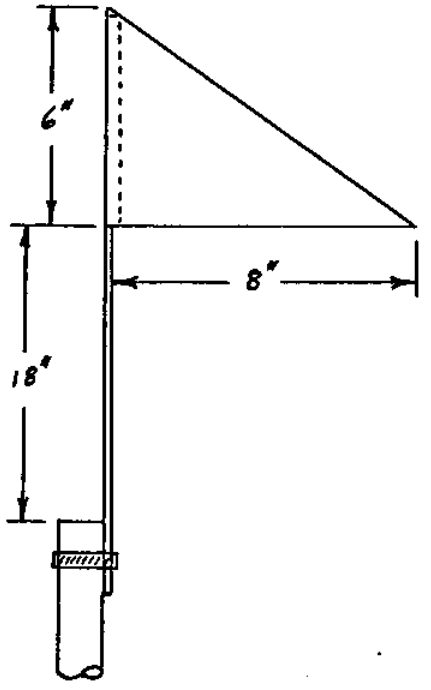

Combining the two experiments it is found that for a wind speed of 5.0 knots,

$$\text{drag 2 ft of pole} = \text{total drag} - \text{drag pennant}$$
$$= 0.0296 - 0.00113 \left(\frac{5\ kt^2}{6\ kt^2}\right)$$
$$= 0.0291 \text{ lbf}$$

Therefore the ratio of the drags is,

$$\frac{\text{drag 2 ft of pole}}{\text{drag pennant}} = \frac{.0291}{.000785} = \frac{37}{1}$$

This shows that the pennant drag is negligible and the large C_d of the pole must be due to other causes. Even if the C_d was 0.8 the ratio would be 22/1. This justifies the earlier statement that when adjusting the freeboard of the poles it would be best to have the smallest freeboard possible and rely on the pennant for tracking the poles.

Other causes of the large C_d of air on the pole

The most obvious error in calculating the C_d is in determining the true wind speed over the water. The wind was measured at Quonset Point four miles farther up the Bay and even though the wind was steady during the data runs, it has been shown that the velocity at the bridge is not exactly the same at Quonset Point. (see figure E.4) If the wind velocity was in error the C_d would vary as shown in figure C.10.

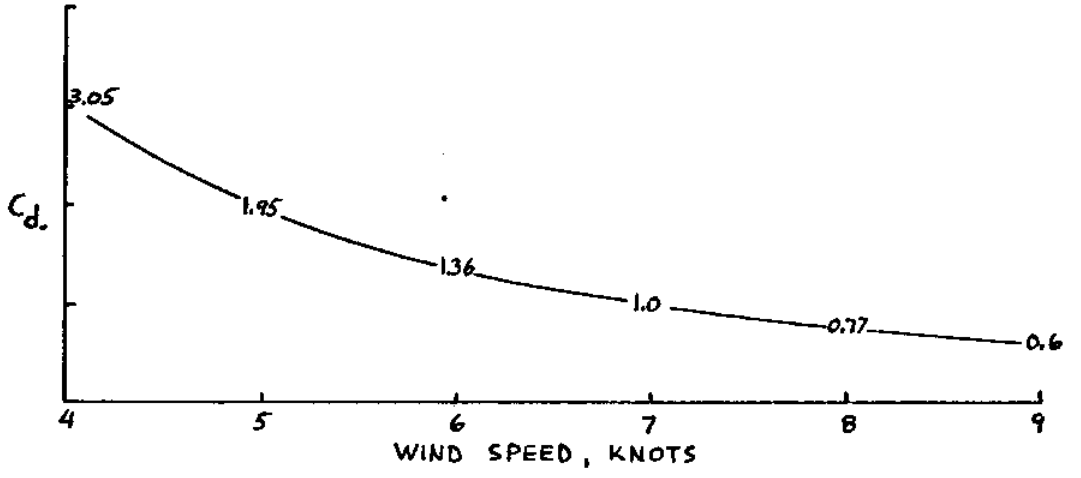

Fig. C.10--Variation of calculated C_d as a function of an error in the wind speed.

The cause could be from the actual water velocity profile and not the wind or instrumentation. Since the wind direction was similar to the tidal flow the wind may have induced a temporary surface current which in turn assisted in driving the poles forward. Teeson (1969) examined surface currents while studying the drift of oil slicks due to the wind. He found that they range from 2% to 5% of the wind velocity and for a 5 to 8 knot wind were around 2.3%. The depth of influence is very shallow, at times being only several centimeters. Yen and Wu (1969) assume that a typical surface current profile due

to wind stress to be,

$$V_w = v_s \left[1 - \left(1 - \frac{z}{h}\right)^{1/7} \right]$$

where, v_s is the surface current = wind vel. x 3%

To find the magnitude of the drag due to this surface current, let the wind velocity be 5 knots and the pole extend 3/4 of the way to the bottom of the channel. Ignore the drag effect from the wind on the pole above the water.

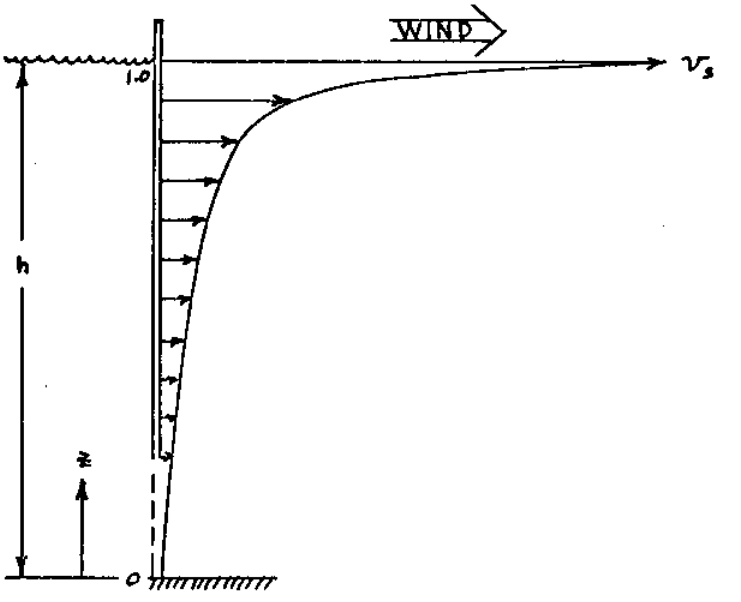

$$D_{water} = \frac{1}{2} \rho V_w^2 C_d S$$

$$\int_{.25}^{1.0} \text{drag}\ d\left(\frac{z}{h}\right) = \int_{.25}^{1.0} (0.995)\, V_w^2\, (1.0) \left(\frac{1.5}{12}\right) d\left(\frac{z}{h}\right)$$

$$= 0.1245 \int_{.25}^{1.0} V_w^2\ d\left(\frac{z}{h}\right)$$

$$= 0.1245 \int_{.25}^{1.0} (.225)^2 \left[1 - \left(1 - \frac{z}{h}\right)^{1/7}\right]^2 d\left(\frac{z}{h}\right)$$

$$= 0.1245 \int_{.25}^{1.0} (.225)^2 \left[1 - 2\left(1 - \frac{z}{h}\right)^{1/7} + \left(1 - \frac{z}{h}\right)^{2/7}\right] d\left(\frac{z}{h}\right)$$

integrating and solving,

drag = 0.000227 lb

This is much less than the drag on the pole due to the wind which is equal to 0.0296 lb. So it can safely be stated that the wind driven surface currents were negligible.

The wave action can not be considered because there were no waves at the time the experiments were run.

Wind correction factors for poles during the GEK calibration

Because of the uncertainty of the experimental C_d, it was decided that it would be best to assume that the C_d of the wind on the poles was a nominal 1.0 for the normal range of wind velocities. Putting this into a form suitable for use on the pole drift data,

At equilibrium

drag in air = drag in water

$$\tfrac{1}{2} \rho_a V_a^2 C_{d_a} S_a = \tfrac{1}{2} \rho_w V_w^2 C_{d_w} S_w$$

where, $\tfrac{1}{2} \rho_a V_a^2 = \dfrac{V_a^2}{840}$

$C_{d_a} = 1.0$

$S_a = \left(\frac{1.5}{12} \times 2\right)$ ft

$\tfrac{1}{2} \rho_w V_w^2 = 0.995 V_w^2$

$C_{d_w} = 1.0$

$S_w = \frac{1.5}{12} L = 0.125 L$

V_a = vel. of air past pole

V_w = vel. of water past pole

equating,

$$0.995\, V_w^2 = \frac{V_a^2}{840}\,\frac{(1.0)(2\text{ ft})\,\frac{1.5}{12}}{(1.0)(0.125)\,L}$$

$$V_w^2 = \frac{V_a^2}{L}\,(0.00238)$$

$$V_w = \frac{V_a}{\sqrt{L}}\,(0.049)$$

or if this function is put into the form of a graph,

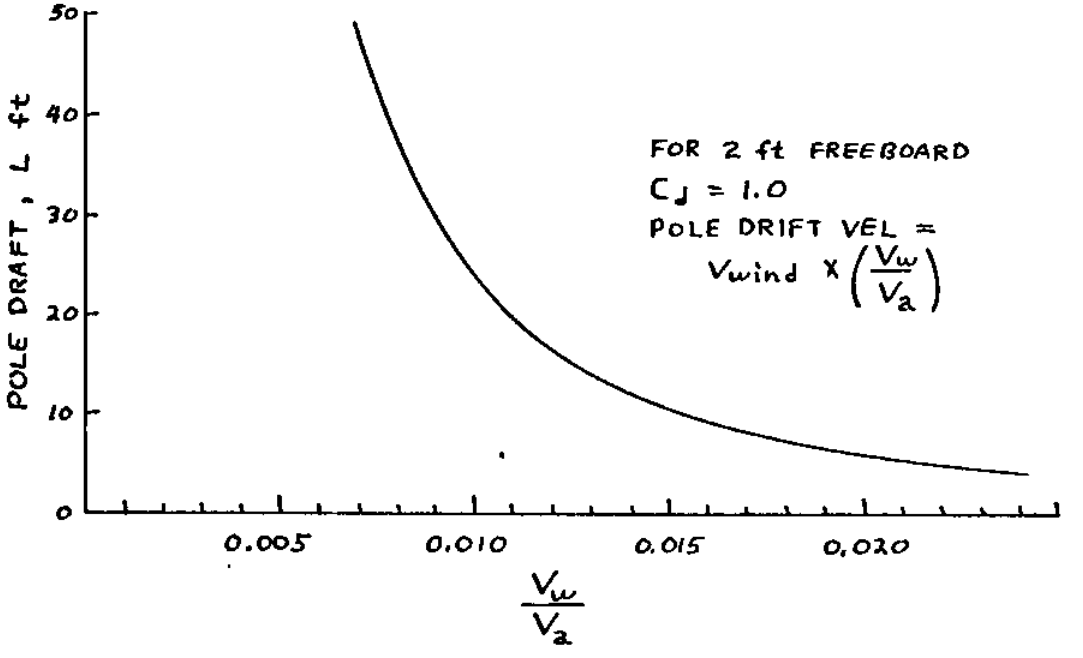

Fig.C.11--Pole drift velocity as a function of pole draft and the wind speed.

As can be seen for a wind of 10 knots on a pole with a 10 ft draft, the drift rate is 0.015 times 10 knots = 0.15 knots. If this occurs during a weak tidal velocity of 0.15 knots, the error is 100%. The importance of the wind correction can be easily seen

Using this graph, all the observed pole velocities in appendix E were corrected for the effect of the wind. The actual tidal velocity equals the observed pole velocity $\pm$ the wind drift. The wind drift was added or subtracted depending on the relative direction of the wind and the tide.

APPENDIX D

OPERATION OF THE GEK INSTRUMENTATION

The GEK recorder instrument box is basically a high input impedance DC voltmeter. The circuitry uses a DC operational amplifier with an input impedance of 10^{12} ohms to amplify the input signal by a factor of 100 so that it may be recorded permanently on a Rustrak model 288 strip chart recorder.

Rustrak recorder

The recorder uses pressure sensitive recorder paper and with a paper speed of 1 inch per hour will last for 31 days. Other paper speeds are available by changing gear trains in the drive mechanism. The slowest speed is 1/8 inch per hour and the fastest is 60 inches per hour. The speed used most of the time on the GEK in the West Passage was 1/2 inch per hour. The recorder is powered by a 12 volt DC power supply.

Scale ranges

The instrument has a scale adjustment that enables the recorder to be scaled from a maximum sensitivity of 0 to 6 mv full scale, to a minimum sensitivity of 0 to 100 mv full scale. If the input signal is negative the input wires can be reversed or the bias adjustment used. Terminals A and C are the normally positive imputs and B and D are the negative input terminals. If the bias adjustment is used,it can either raise or depress the zero position on the meter by up to 78 mv.

This bias is very stable and is suitable for long term use. The Recorder has a meter movement accuracy of ± 2% full scale. These features were needed to allow for the ground potential of approximately 70 mv and still enable the tidal signal to cover the full range of the chart paper.

Power supply

The power for the instrument consists of batteries for self-contained use, or if 110 vac is available, an internal rectifier converts to DC. Two power supplies A and B provide current to three voltage regulators all set at 12 volts output. They will regulate 12 volts as long as the input voltage is between 15.5 volts and 28 volts. The voltage regulators supply current to the amplifier, recorder drive motor and the switching relays. The internal batteries consist of two sets of three 6 volt lantern batteries. The external battery pack has two sets of four 6 volt lantern batteries for longer life. Normally the internal batteries are used during the time the external batteries are being replaced. The external power may also be 110 volts AC which is converted to about 23 volts DC. The nominal current drain from power supply A is 20 ma and 8 ma for power supply B. (The Rustrak takes 12 ma.) Greater battery life can be obtained if they are alternated between sets so as to equalize the use. The internal batteries will last for about a week and the external batteries will last for 3 to 4 weeks. The power supply voltages should be monitored periodically.

The test source uses two alkaline batteries, type E93. These were chosen because of their excellent shelf life and suitable operation in varying temperatures. The maximum current drain is 0.3 ma. Their life is greater than one year.

The bias circuit uses two mercury batteries, type E233N. These were chosen because of their extremely stable output voltages. Since the current drain is only 80 microamps the voltage depression is very slight and they can be used in freezing temperatures. There useful life is also greater than one year.

The clock timer is powered by a single alkaline battery the same as the test source and draws intermittent pulses of less than 1 ma. The battery will last for longer than a year, and can be used in freezing temperatures.

CAUTION

All batteries should be removed from the instruments when not being used for a period of greater than several months. Any time the lantern batteries are low in voltage they should be removed because of their tendency to leak.

Switching circuits

There are four inputs that can be measured in any combination of pairs. Normally these are brought into the instrument box through a moisture proof connector in the front of the box, but an alternate way is at the ELECTRODE OUTPUT terminals on the top panel. These pairs may be selected manually by switches or pairs AB and CD may be selected automatically, alternating every half hour. The chart paper does not drive at a constant speed and varies slightly with the temperature and the amount of chart paper on the spool. The automatic selector circuit provides accurate time marks during automatic sequencing and if an electrode pair is selected manually, hour marks can be put on the paper automatically by the hour mark relay. Both the hour marks and the automatic selector are controlled by an external timer that is plugged into the front of the instrument box. The clock is a cheap movement and

is somewhat temperature dependent, but at a stable temperature is accurate to within a minute a week. The clock may be adjusted for accuracy and the minute hand can be moved to set the time. Care must be taken not to bend the contact whiskers when entering the case. These close the relay circuits when the minute hand passes over them. The whiskers and the underside of the minute hand should be lightly cleaned every couple of months when operating.

Operating procedures

NOTE

Perform parts 1 - 3 only during the initial installation of the GEK or when trouble-shooting for problems.

Figure D.1 shows the various components of the GEK instrumentation and how they are hooked up. Refer to figure D.2 for the operating panel on the GEK recorder instrument.

1. Before the wires from the electrodes are installed they should be checked for continuity and if possible, the insulation should be soaked with salt water and a megger test performed. This should read greater than 200 M ohms.

2. After the electrode wires are installed to the electrode sites they should be capped with a waterproof connector and a megger test to ground performed from the Mecca connectors. Satisfactory values will depend on the type of wire used. The wires on the Jamestown Bridge, which crossed the passage above the water, were meggered with the electrodes removed and waterproof Mecca caps installed and placed back into the water with the electrode moorings. Typical values with a 500 vdc megger were in the range of 10 M to 60 M ohms depending

on the weather. Normally two readings are taken, one after 30 seconds of cranking and another after 60 seconds. The second value should be slightly greater than the first one because of the normal capacitance in the system. Definite breaks in the wire would read greater than 200 M ohms.

CAUTION

Do not megger or apply any voltage to the electrodes themselves or to the instrumentation.

3. The electrodes are installed in the water. Before connecting them with the recorder the output should be checked for excessive potentials from ground currents or from a shorted electrode. If one of the electrodes is shorted in the water, approximately 1.1 volts will be generated between the ground and the other operating electrode. When using a three electrode system, like that in the West Passage, comparison between pairs will indicate which electrode is shorted. If redundant pairs are used, as in the East Passage, the side with the bad electrode can also be easily determined.

The electrodes used have a resistance of 680 ohms each. This was determined by measuring the current drawn from electrode output terminals A-B by an ammeter during a known GEK signal.

4. If no excessive potentials are present the Mecca connectors are joined and the extension cable is plugged into the GEK recorder at ELECTRODES. If a three electrode system is being used, the fourth mecca must be plugged with an insulated blank plug to prevent moisture from condensing and causing a resistance path to ground for the electrode system. The high input resistance of the amplifier necessitates extreme precautions to prevent current leakage from the electrodes.

5. Power for the GEK recorder is obtained from any one of three methods; internal batteries, external batteries or external 115 vac. With the POWER SOURCE switch on INTERNAL, power is supplied from a 18 volt internal battery pack. With the POWER SOURCE switch on EXTERNAL, either the 24 volt battery pack may be plugged into the BATTERIES connector or a special extension cord plugged into the 115 VAC connector. Both connectors are on the front of the recorder box.

CAUTION

The external batteries and external 115 volts must not be connected at the same time.

The power supply voltages are checked at the READ VOLTAGE terminals and the batteries should be replaced if they are less than 15.5 volts on either A or B terminals.

6. Position ELECTRODE SELECTOR switches to the desired pair of electrodes, i.e. one switch to A and another to D reads the potential between electrodes A-D. For the potentials between A-C or B-D only one switch needs to be operated. Any unused switches must be OFF.

To add hour marks to the chart the clock timer is plugged into the AUTO TIMER connector. Position switches to MANUAL SELECTOR ON and HR MARK RELAY after the desired electrode pair is selected as above.

To operate on automatic switching between electrode pairs,using the clock timer, position switches to AUTO AB CD SELECTOR ON and AUTO SELECTOR RELAY. In this mode <u>all</u> ELECTRODE SELECTOR switches must be in the OFF position. If only three electrodes are being used, one being common to the others, connect a jumper wire from the unused electrode to the common electrode at the ELECTRODES OUTPUT terminals.

7. To calibrate the chart paper the following switch positions are set: TEST ON, TEST POLARITY to POS, BIAS to OFF. All three adjustment pots should be set to zero and the FILTER CONSTANT to .05 value. Set AMP ON, the recorder should indicate zero, if not adjust the needle zero under the plastic Rustrak name plate. Adjust TEST ADJ to a value mid-scale of the desired scale range. The ten-turn pot reads 0 to 100 mv in 0.1 mv divisions. The TEST POLARITY switch can be used to duplicate either a positive or a negative incoming signal. Positive is when electrode signals A and C are positive with respect to the B and D signals.

Set the SCALE ADJ pot so that the desired mid-scale reading is indicated on the chart paper. Run the TEST ADJ pot up and down to check various values. It is best to operate the recorder, (set REC ON) and read the chart paper since it is more accurate than observing the meter needle.

> The calibration of the test signal is done by reading the TEST ADJ signal at the AMPLIFIER INPUT terminals with a high impedance low range voltmeter. If it does not read the indicated value on the TEST ADJ pot, adjust the CAL trim pot so it does. Once set it rarely needs adjustment except in cases where extreme accuracy is needed at the far ends of the TEST ADJ pot.

8. To raise or depress the meter zero position on the chart paper use the BIAS switch. To raise the zero position set the TEST ADJ to zero, set the BIAS switch to POS and use the BIAS ADJ to move the zero to the desired position. To depress the zero set

the BIAS switch to NEG. In this case the zero position will be off scale on the bottom, therefore use a positive TEST ADJ value and depress it an equivalent amount. Notice that depressing the zero is equivalent to moving the scale range up: an example, 0 - 10 mv is moved up to 50 - 60 mv.

9. The FILTER CONSTANT switch controls the frequency response of the amplifier. There are three settings; 0.05 second, 0.5 second and 5.0 seconds. Three times the filter constant is the time for a step signal to change to 95% of its final value on the chart. A frequency response diagram is shown in figure J.2 of appendix J.

The 5.0 second value is usually used while recording the GEK signal and the 0.05 second value is usually used for adjusting and checking test signals. The writing speed of the Rustrak is one strike every 2 seconds, this limits the frequency response that can be recorded.

10. The AMPLIFIER INPUT and OUTPUT terminals are for checking the amplifier circuit and reading the output of the test signal during the calibration of the test signal. The gain is approximately 100. The amplifier can also be used for other uses through these terminals.

11. Inside the instrument box is silica gel desiccant and a humidity indicator located behind the front door. The humidity should be kept below 50% relative humidity.

12. To load and unload the chart recorder, refer to the Rustrak manual. If the chart paper tears at the sprocket holes, the takeup spool needs to be lubricated at the fiber slip clutch. On this Rustrak two 4 mil poly washers served as lubrication and solved the problem.

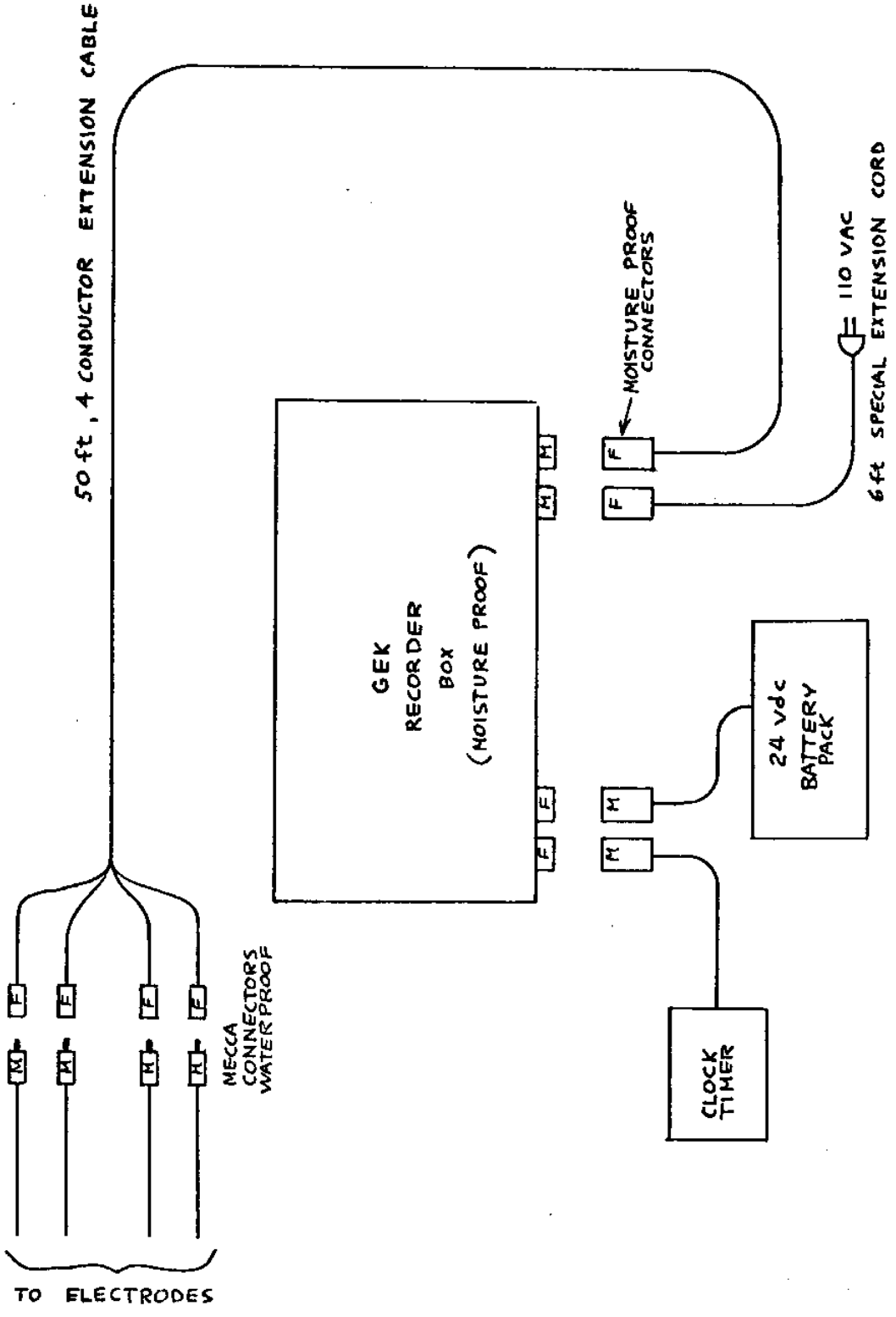

Fig. D.1--Schematic diagram for typical instrumentation.

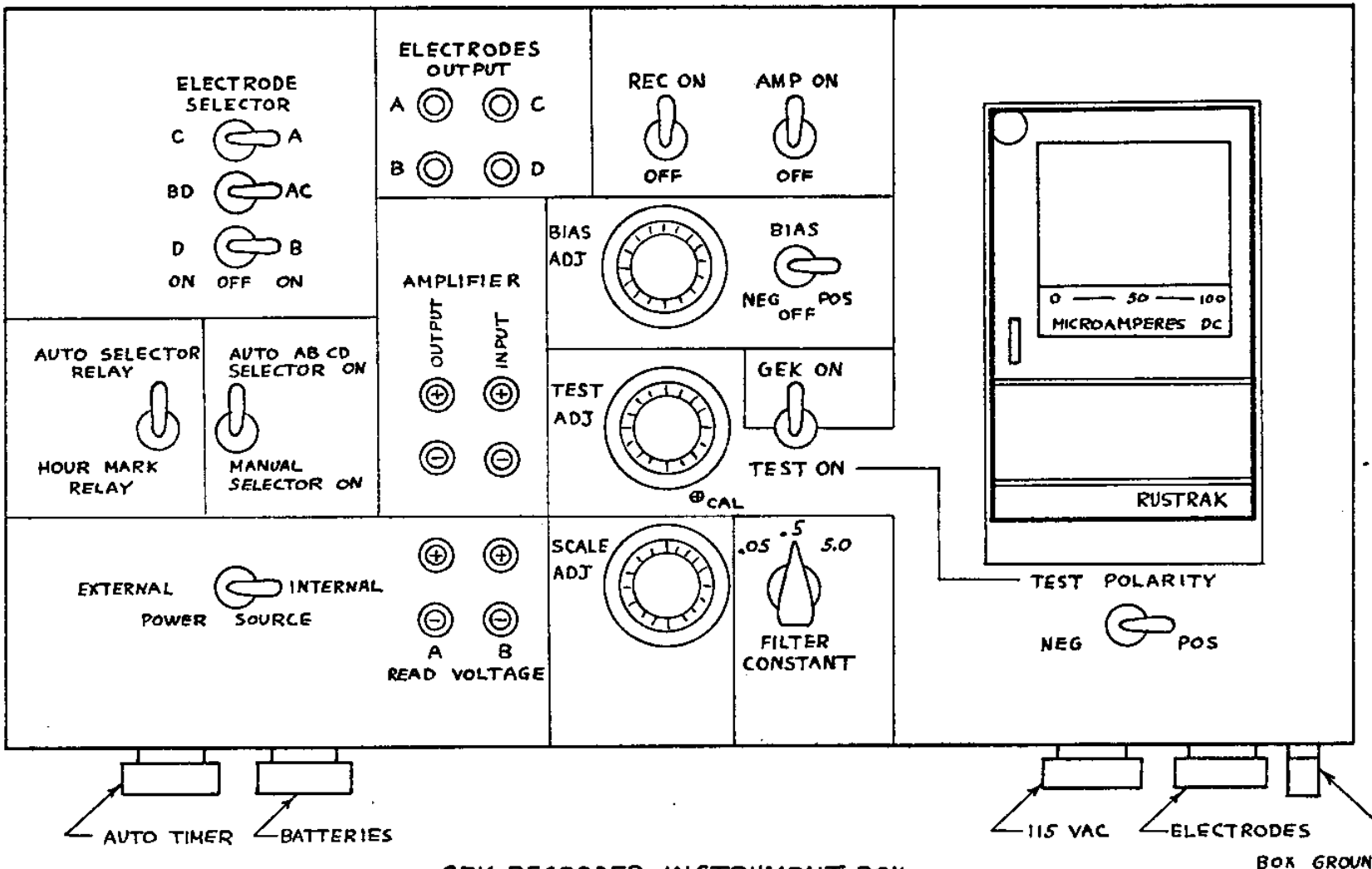

GEK RECORDER INSTRUMENT BOX

Figure D.2

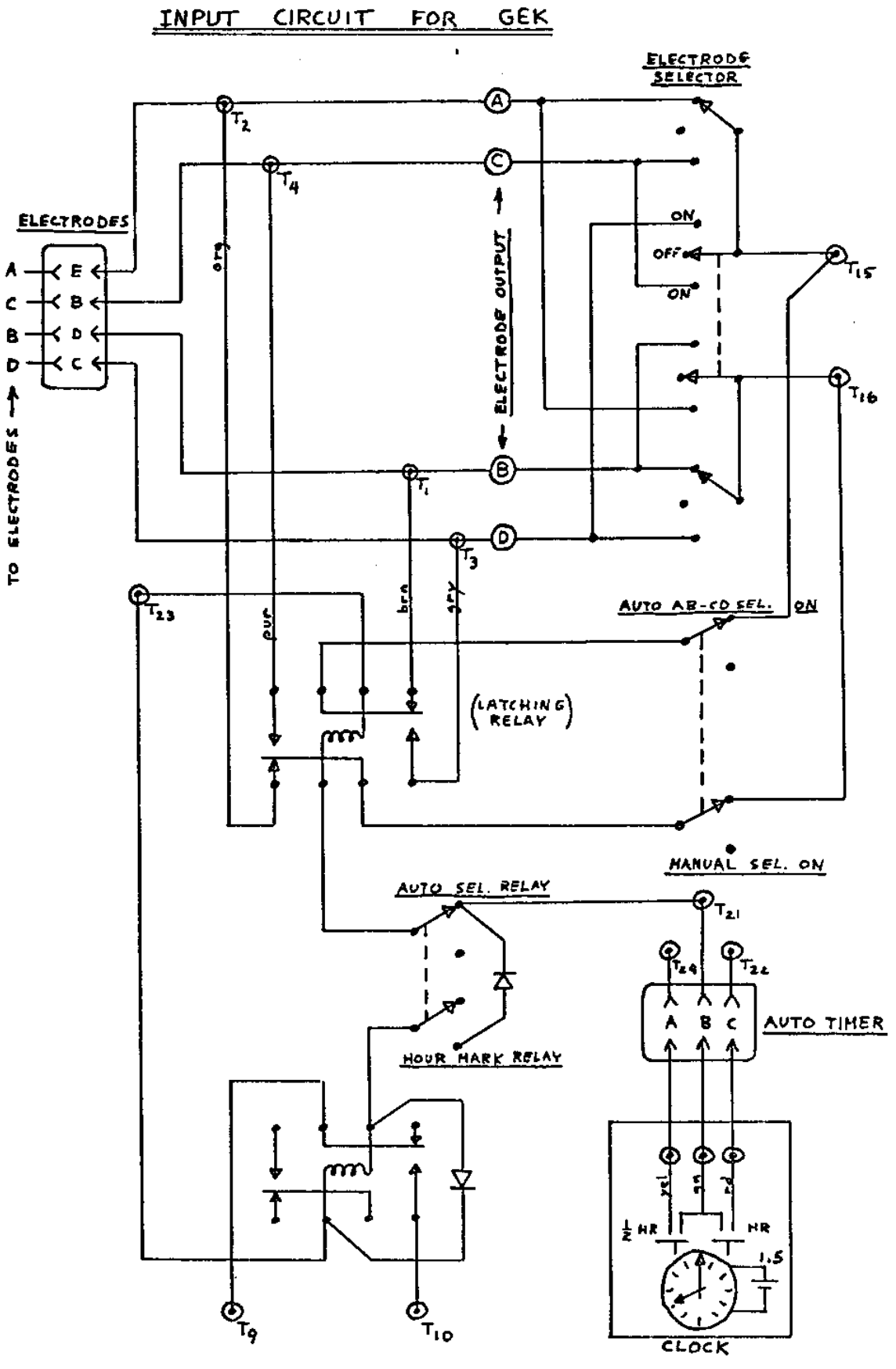
INPUT CIRCUIT FOR GEK
ELECTRODE SELECTOR
ELECTRODES
A
C
B
D
E
B
D
C
TO ELECTRODES
ELECTRODE OUTPUT
ON
OFF
ON
T2
T4
T1
T3
T15
T16
T23
AUTO AB-CD SEL. ON
(LATCHING RELAY)
MANUAL SEL. ON
AUTO SEL. RELAY
T21
T24
T22
A B C
AUTO TIMER
HOUR MARK RELAY
½ HR
HR
1.5
CLOCK
T9
T10

Figure D.3

AMPLIFIER CIRCUIT FOR GEK

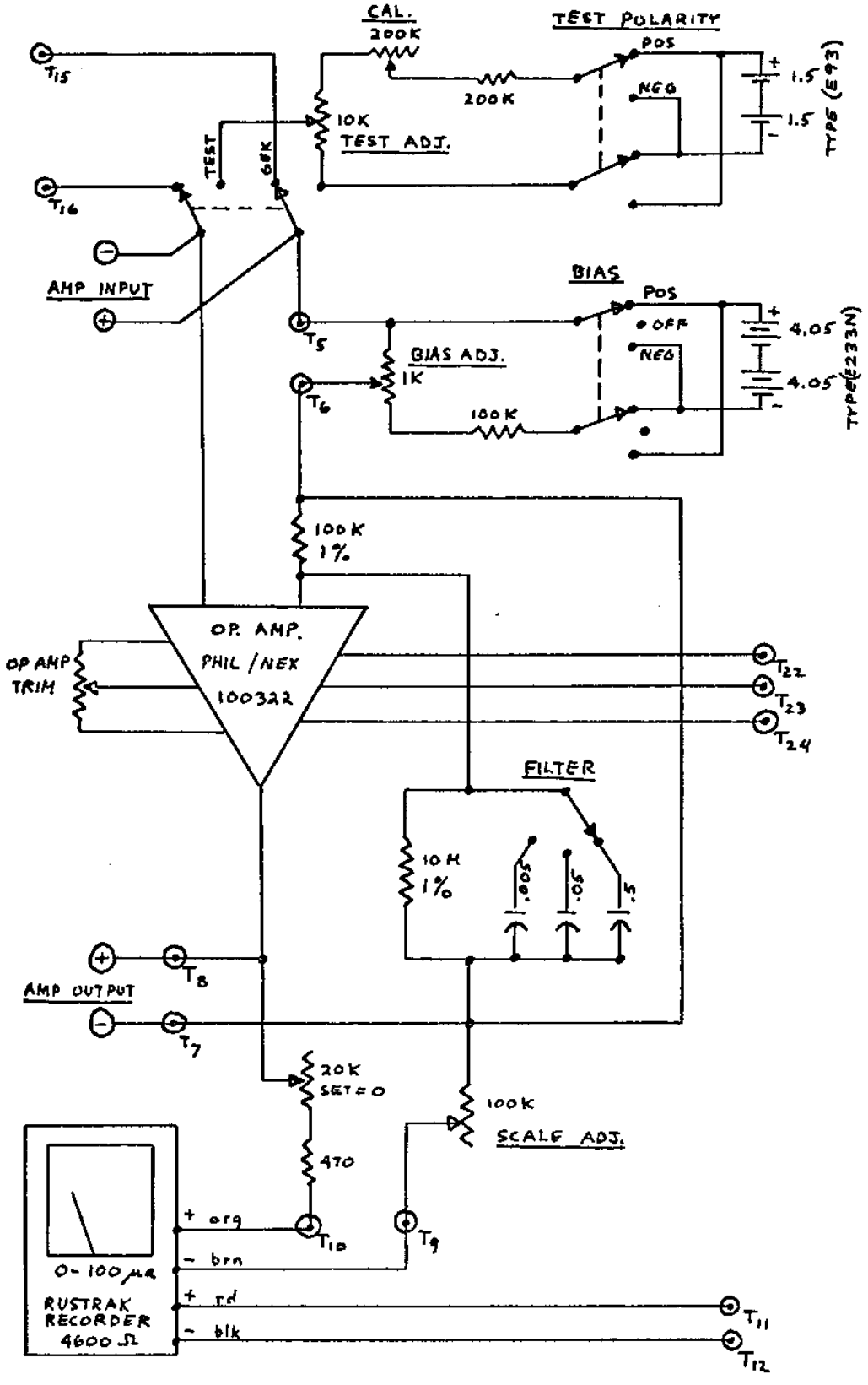

Figure D.4

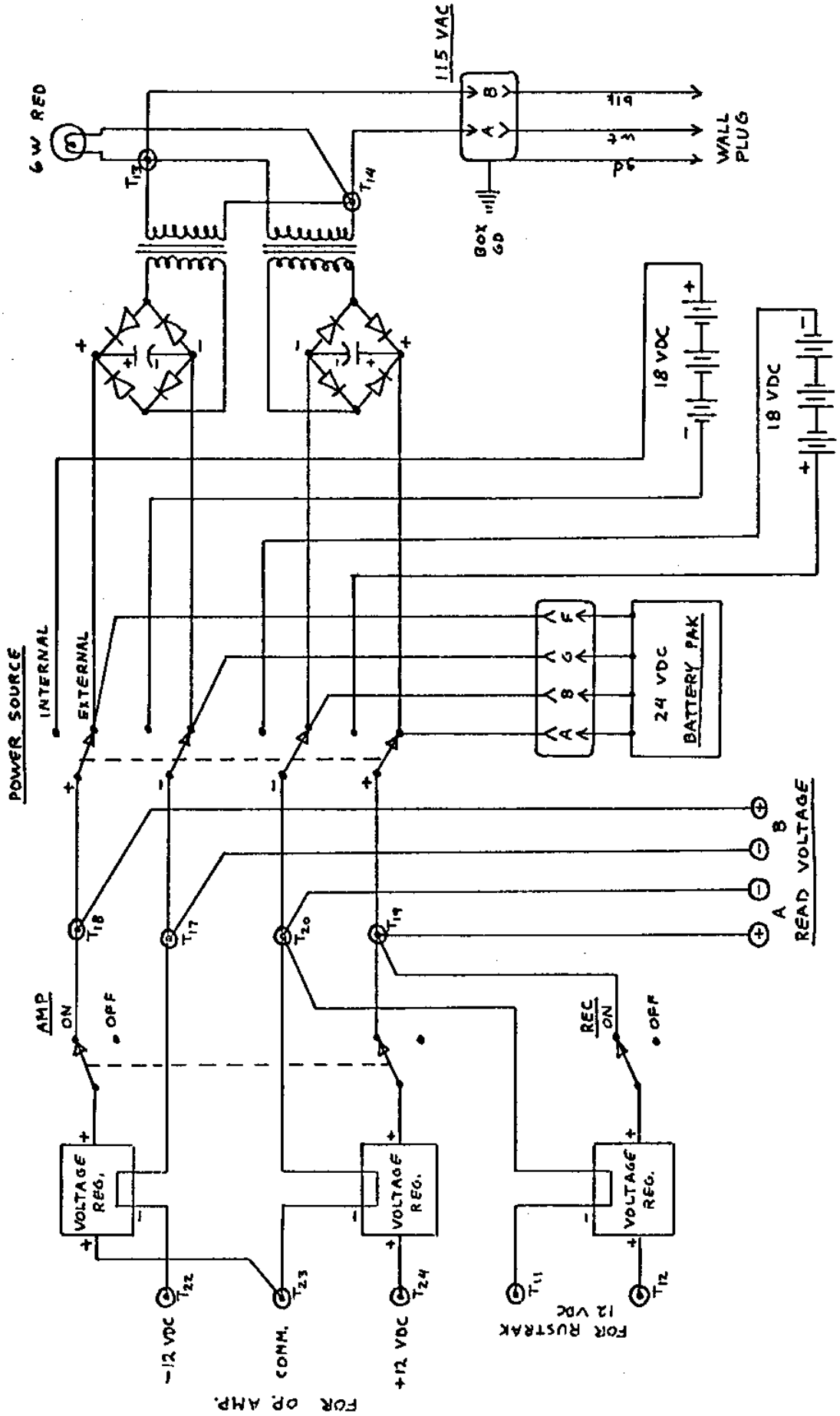

POWER SUPPLY CIRCUIT FOR GEK

Figure D.5

APPENDIX E

CALIBRATION OF THE GEK

The exact mathematical solution to the electrical potential produced by a tidal current flowing through an estuary is not possible to solve analytically. The best approach available is an empirical method; in which the GEK is installed and the solution to $\int \phi_{AB}\, dt$ is determined by comparison with the actual tidal currents in the area being measured by the GEK. The accuracy of this method depends upon the accuracy of being able to measure the true water velocity in the channel as a function of time and the accuracy of the potential electrical field in reflecting the water velocity. The accuracy of the physical measuring of the tides is discussed in appendix C, and the GEK theory and its limitations is discussed in appendix H. This discussion will describe the reduction and comparison of the observational data and the GEK recorded data, and the method used to calibrate the GEK system.

The West Passage under the Jamestown Bridge was an unfortunate location for the GEK but was unavoidable because of the unavailability of suitable submarine cable. It was ideal for installation, service and the visual observation of the tides, but it was difficult to measure average velocities because the channel depth varied drastically, as can be seen in figure B.1 of the West Passage. Since these velocities varied both vertically and horizontally across the passage, a large number of calibration measurements were required for an accurate

representation. To eliminate taking measurements of the vertical profile, it was decided that a vertical drifting pole would approximate the average profile to an accuracy suitable for calibration of the GEK. Six of these poles were distributed across the passage and their drift was observed as the tides flowed in and out of the Bay. The poles were designed to float with 2 feet of their length above water and with the end as close to the bottom as possible without dragging on the bottom during low tide or on a shoal. Figure E.1 shows the transverse profile of the passage and the respective positions of the poles and their lengths. Two bottom profiles are shown, one just north of the bridge and one just south of the bridge. The profiles were obtained using a recording fathometer over the areas that the pole drift was measured. Different sides of the bridge were used for ebb and flood measurements.

The fact that the tidal height varied about four feet at the time the calibration was performed required an extra four feet clearance between the bottom of the channel and the poles. This plus not having an accurate transverse profile of the passage when the poles were built, caused the poles to be shorter than they should have been. The poles therefore only integrated the water velocity over 70% to 90% of the water column, depending on the location and tidal height. This was a hinderance in the current measurements and its effect can be seen later.

In the fall of 1970 and the spring of 1971 a study was undertaken of vertical current profiles using a vertical array of Savonius current meters in the West Passage just north of the area included on the map of figure B.1. The results were published as the Rome Point Circulation Study (1971). Four current meters (one of which malfunctioned) were placed in a water column of 42 feet at mid channel. Figures E.2 and

E.3 show some of the results. For vertical profiles during neap tides, figure E.2 shows that there can be periods of extreme variation in the tidal velocities from the surface to the bottom. If figure E.3 is examined, which shows the vertical profiles approaching spring tides, it can be seen that as the tidal currents get stronger the vertical variation becomes less pronounced. Narragansett Bay sometimes experiences a double flood phenomenon because of its physical characteristics, and it appears that the greatest vertical variations occur during the first flood. These velocity profiles show that at times there are bottom currents that are quite different from the upper currents. This is the reason for concern that the drifting poles did not reach closer to the bottom of the channel.

The method of operation was as follows. A sighting binocular telescope was set up on one shore with a line of view parallel to the bridge. The poles were launched on the north side of the bridge during flood and on the south side of the bridge during ebb tide. Six poles were placed under their respective stations on the bridge as fast as possible by a boat going across the channel. With the telescope, the angular velocity of each pole was observed as it drifted away from the bridge. Since the range of each pole was known, the angular velocity was converted to knots. This was continued throughout the tidal cycle, or as long as desired, by recovering the poles and repeating the operation. Each set of poles was observed in a time span of less than five minutes. For a more detailed explanation and description of this method, see appendix C.

This method was used on June 17, 1971 and on July 8, 1971 which were respectively a neap and a spring tide period of the month. Both days had similar weather conditions; summer days, with the temperature

in the 70's. The wind speed was recorded at the Quonset N.A.S. fleet weather station and is shown in figure E.4. Since the distance from the Quonset Point station is several miles, a portable windmeter was used on July 8 in the boat that deployed the poles. These wind speeds are also shown in figure E.4 for comparison. The velocities of the poles were affected by the wind and the final data has been corrected for this effect. Appendix C discusses what comparisons were made and the method used to adjust for the local wind.

The final velocities of the poles are recorded in figures E.5 and E.6. It appears that the data has a large scatter, but if the velocities for each station are plotted, trends are observed. Referring to figures E.7, E.8, E.9 and E.10, the velocities are greater in the center of the passage and lesser on the sides of the passage as would be expected. Slack water occurs at different times and occurs sooner for the poles in the shallower water depth. The deviation of individual velocities are the greatest for poles in the shallow half of the passage, but these velocities may be more accurate than they appear because when the velocities are averaged for the shallow half and deep half of the passage, as shown in figures E.11 and E.12, the deviation from a smooth curve is not as great. Also when all the stations are averaged, as in figures E.14 and E.15, the deviation is less than that for each half of the passage. This indicates that the mass transport is a smooth function since the tidal forcing functions are gradual. As smaller and smaller sections of water are examined, the local topographic features are seen altering the velocities. This could be considered as an effect of the inertial mass of the water in the Bay and as a conservation of continuity through the passage.

Going back to figures E.11 and E.12 showing the average

velocities for each half of the passage, it is seen that the velocities on the shallow, or west, side lead those for the deep side. Lamb (1932) describes a similar phenomenon in tidal estuaries where the bottom currents lead the surface currents. This can be seen in the vertical velocity profiles in figures E.2 and E.3. In both cases the phenomenon can be explained by the fact that the inertia of the moving water causes it to remain in motion until acted upon by outside forces. The whole water column is acted upon by the tidal forcing function while the bottom water is influenced by an additional force due to the bottom friction. Using figure C.4 for visualization, the effect of the friction is to slow down the bottom currents and allow them to reverse sooner. The phase lead of the GEK velocities with respect to the pole velocities, that are shown later, can be explained by this phenomenon.

The original recordings for the GEK on June 17 and July 8 are shown in figure E.13. To find the electrode null at slack water, it is difficult to use the average slack time as indicated by the drifting poles because the poles did not reach deep enough to be influenced by the tidal currents near the bottom of the passage. It has been shown that they can be appreciably different from those toward the surface. The only solution is to use a "best guess" as to when the bottom currents were similar to the upper currents and use these velocities and times to compare the GEK with the velocities of the poles. Examining figures E.2 and E.3, it is seen that during the flood period the velocities in the vertical column of water are equal at a time about 1/3 through the flood cycle, as defined by the upper current meter. For the ebb period the water velocities are in phase but not equal at maximum ebb. Using these relationships for a known equality

in both the flood and ebb period, the GEK velocity was proportioned into flood and ebb by the same ratio as the average pole velocities at these times. The calculations are shown in table E.1. The results are,

Date	Slack potential		Scale factor	
	total span	deep half	total span	deep half
6-17-71	68.5 mv	64.5 mv	10.65 mv/kt	6.4 mv/kt
7-8-71	73.5 mv	68.5 mv		

Using the original GEK records, the potential difference between each trace and its slack is measured and converted by its respective scale factor to velocity in knots. The results are plotted in figures E.14 and E.16 for June 17 and in figures E.15 and E.17 for July 8.

Both pairs of curves exhibit a phase difference which is more pronounced in the deeper channel, and also more pronounced on July 8 than on June 17. This phase lead of the GEK velocities can be explained by the effect of friction on the water neared the bottom. The GEK represents an average water velocity from the surface to the bottom and the poles represent the middle and upper currents. If the bottom currents tend to lead the upper and middle currents, it follows that the GEK will lead the pole velocities. The amount of phase difference should only be treated as a qualitative trend because as seen in figures E.2 and E.3 that even adjacent tidal cycles can differ drastically.

Potentials were taken during the GEK calibration on July 8 between electrodes A-C which spanned the shallow half of the passage. This data was analysed to determine if the sum of the potentials across the deep and shallow sections of the passage were equal to the total

Table E.1

	Calibration for total passage		Calibration for deep half of passage	
	Avg. vel. of poles 1 thru 6	GEK potential	Avg. vel. of poles 1 thru 3	GEK potential
July 8, 1971				
Ebbing tide, 1100 hrs	1.24 kt	60.2 mv	1.30 kt	60.2 mv
Flooding tide, 1530 hrs	0.73 kt	81.2 mv	0.65 kt	72.7 mv
difference	1.97 kt	21.0 mv	1.95 kt	12.5 mv
Scale factor	21.0/1.97 = 10.65 mv/kt		12.5/1.95 = 6.4 mv/kt	
Potential between ebb and slack at 1100 hrs	10.65 mv/kt x 1.24 kt = 13.3mv		6.4 mv/kt x 1.30 kt = 8.3 mv	
Potential between flood and slack at 1530 hrs	10.65 mv/kt x 0.73 kt = 7.8 mv		6.4 mv/kt x 0.65 kt = 4.2 mv	
Slack potential	60.2 + 13.3 = 73.5 mv		60.2 + 8.3 = 68.5 mv	
June 17, 1971				
Flooding tide, 1130 hrs	0.48 kt	73.6 mv	0.45 kt	67.4 mv
Using same scale factor as on July 8	10.65 mv/kt		6.4 mv/kt	
Potential between flood and slack at 1130 hrs	10.65 mv/kt x 0.48 = 5.1 mv		6.4 mv/kt x 0.45 kt = 2.9 mv	
Slack potential	73.6 - 5.1 = 68.5 mv		67.4 - 2.9 = 64.5 mv	

potential across the passage. If this were true, at any time t

$$(\phi_{AB} - \phi_{CB})_t = (\phi_{AC})_t$$

Since ϕ consists of the potential generated by the tide and the constant potential at slack tide, it is also true that

$$(\phi_{AB} - 73.5\ mv)_t - (\phi_{CB} - 68.5\ mv)_t = (\phi_{AC} - x)_t$$

Solving for x, the slack potential between electrodes A-C, when all the tidal potentials are zero,

$$x = 73.5 - 68.5 = 5.0\ mv$$

Checking this by examining n data points for ϕ_{AC} in figure E.13 it was found that

$$\frac{\sum_1^n (\phi_{AB} - 73.5)_t - (\phi_{CB} - 68.5)_t - (\phi_{AC} - 5.0)_t}{n} = -3.03\ mv$$

and not zero as would be expected.

Therefore the slack potential is not 5.0 but probably 5.0 + 3.03 = 8.0 mv. The excess difference of 3.0 mv is not explainable and during other experiments it was found that ϕ_{AC} as measured at the east end of the bridge was not equal to ϕ_{AC} as measured at the west end. This also is not explainable.

Using a slack potential of 8.0 mv, the electrodes A-C are calibrated in the same way as the others.

Table E.2

Calibration for shallow half of the passage		
	Avg. vel. of poles 4 thru 6	GEK potential
July 8, 1971		
Flooding tide, 1545 hrs	0.85 kts	3.8 mv
Scale factor	3.8 mv/0.85 kts = 4.47 mv/kts	
Slack potential	8.0 mv	

The results are shown in figure E.18, with both the continuous GEK record $(\phi_{AB} - \phi_{CB}) - 5.0$ and the individual data points $\phi_{AC} - 8.0$, against the average velocities for poles 4 through 6. These curves show that the sum of the potentials across each half of the passage equals the total potential across the passage minus a constant offset voltage and that they compare well with the actual tidal current.

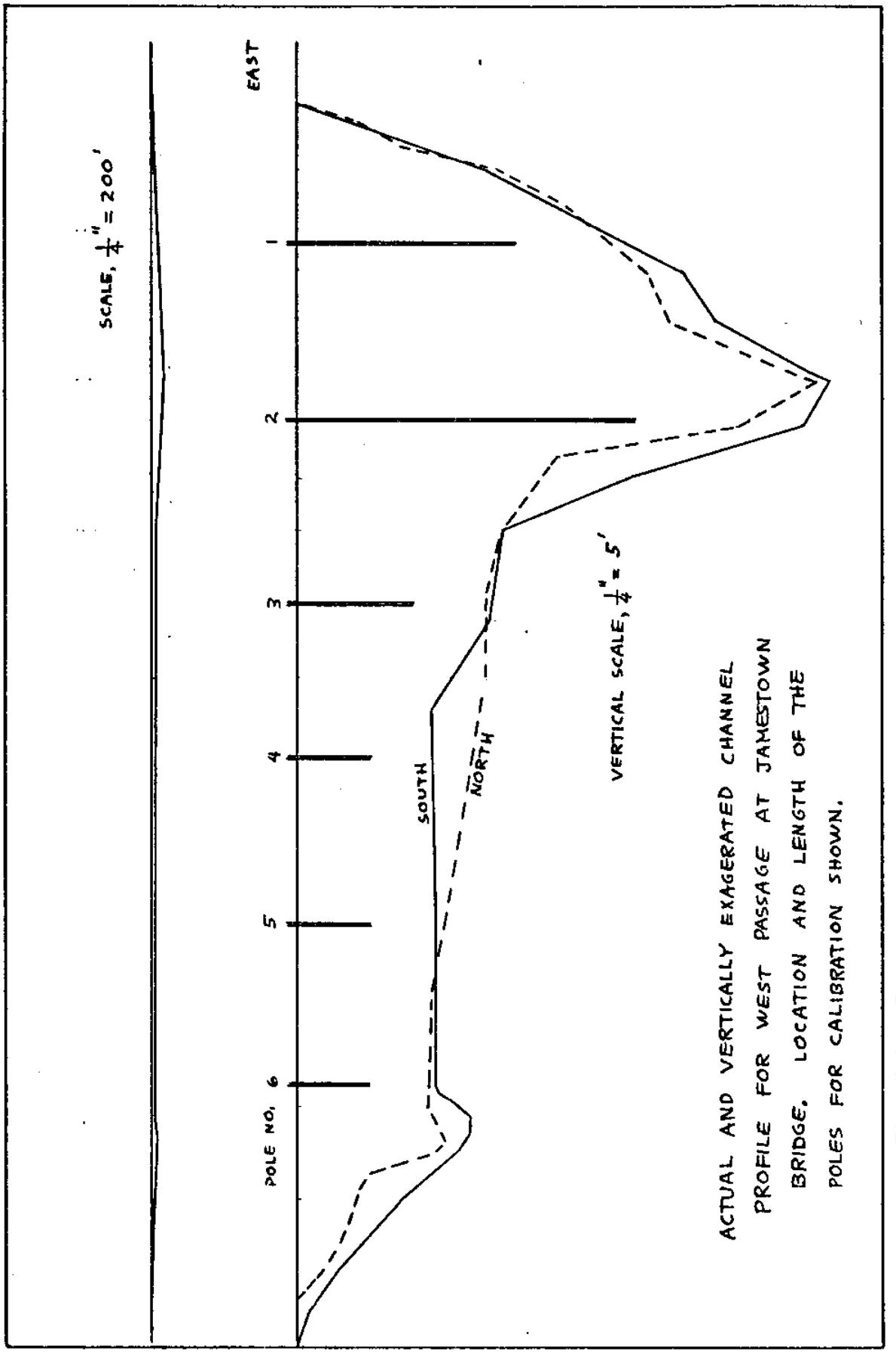

Fig. E.1-- Transverse profile of West Passage under Jamestown Bridge.

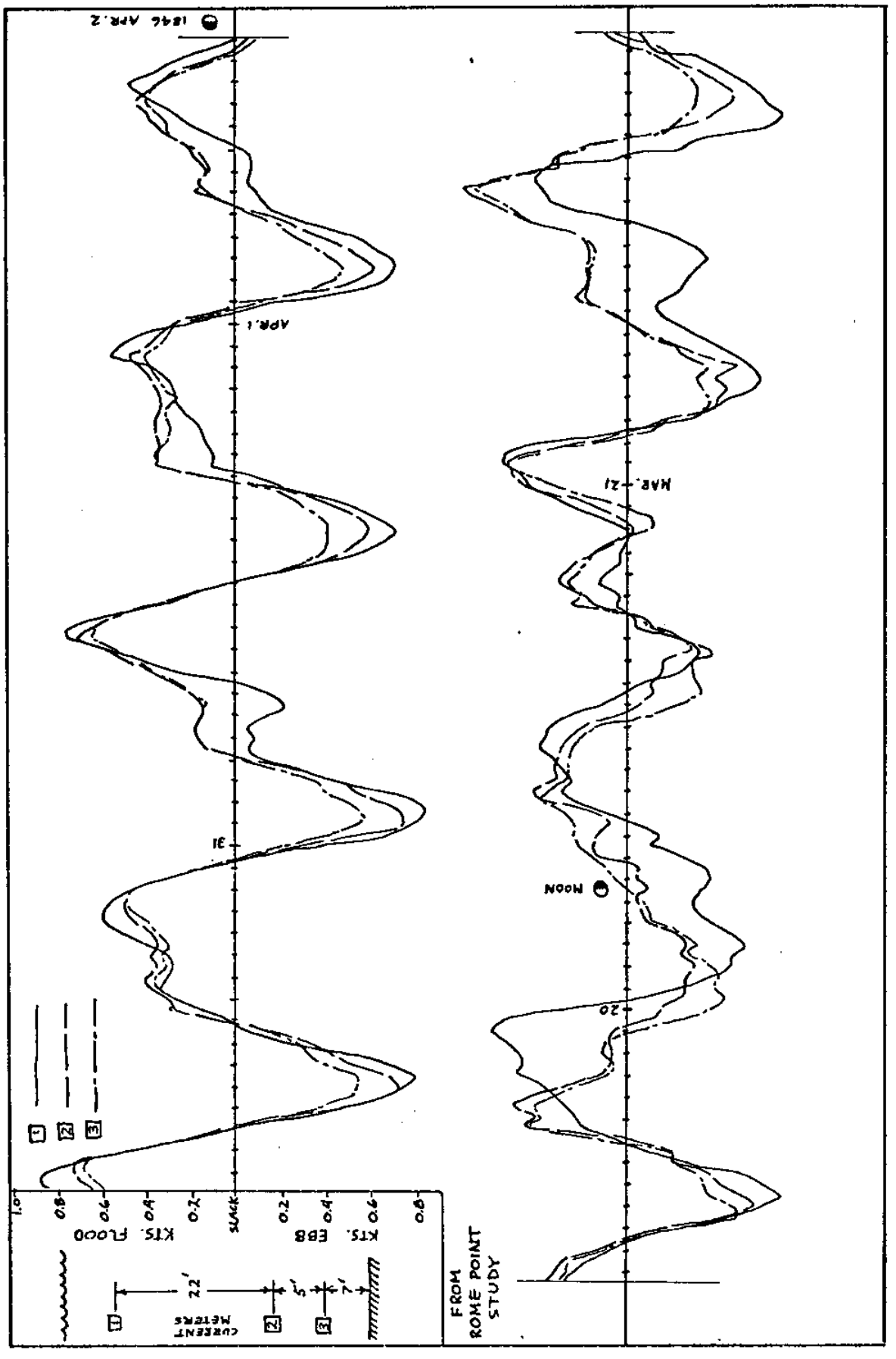

Fig. E.2--Vertical profile of tidal velocities during a period of neap tides.

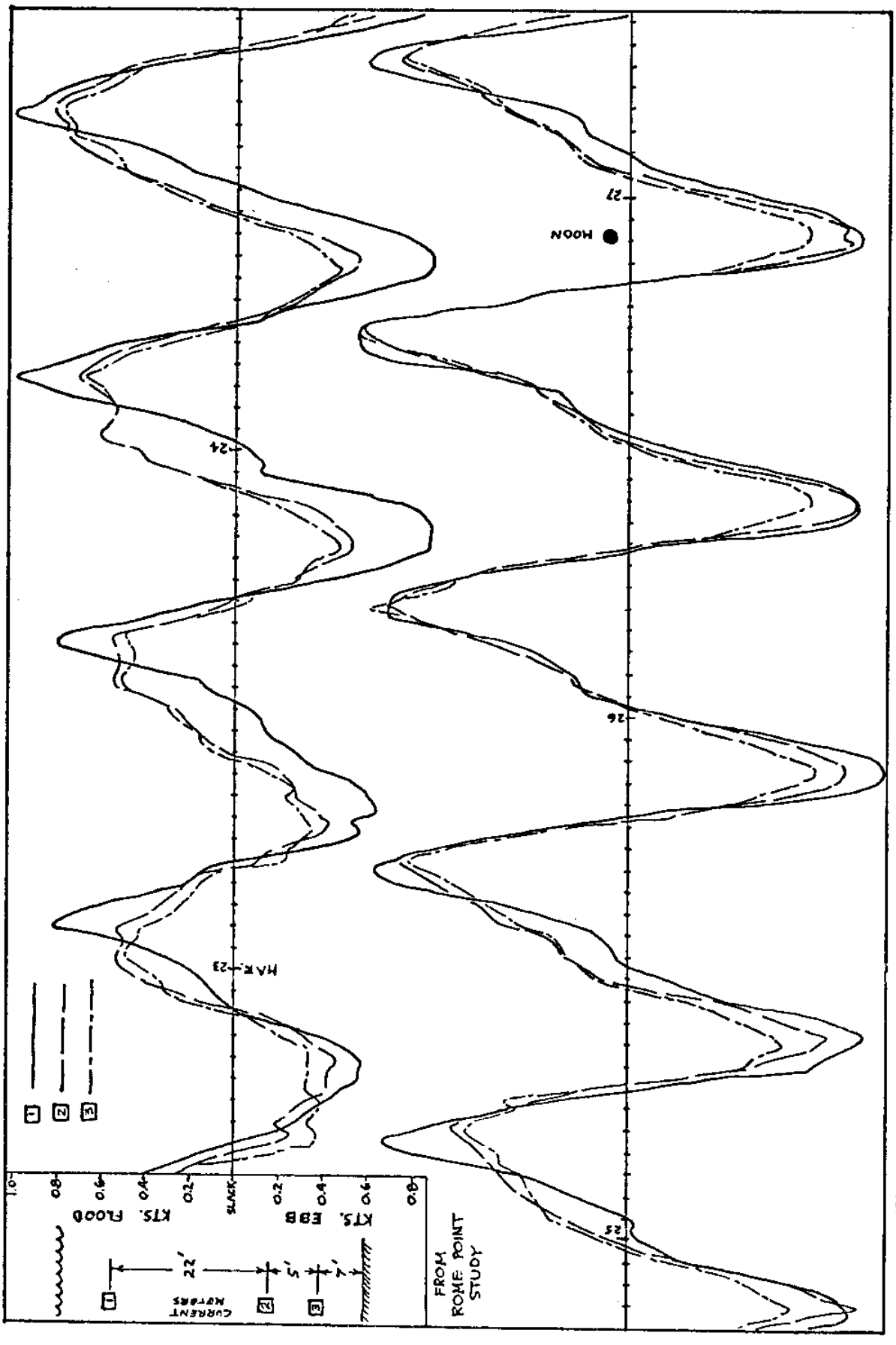

Fig. E.3--Vertical profile of tidal velocities during a period of approaching spring tides.

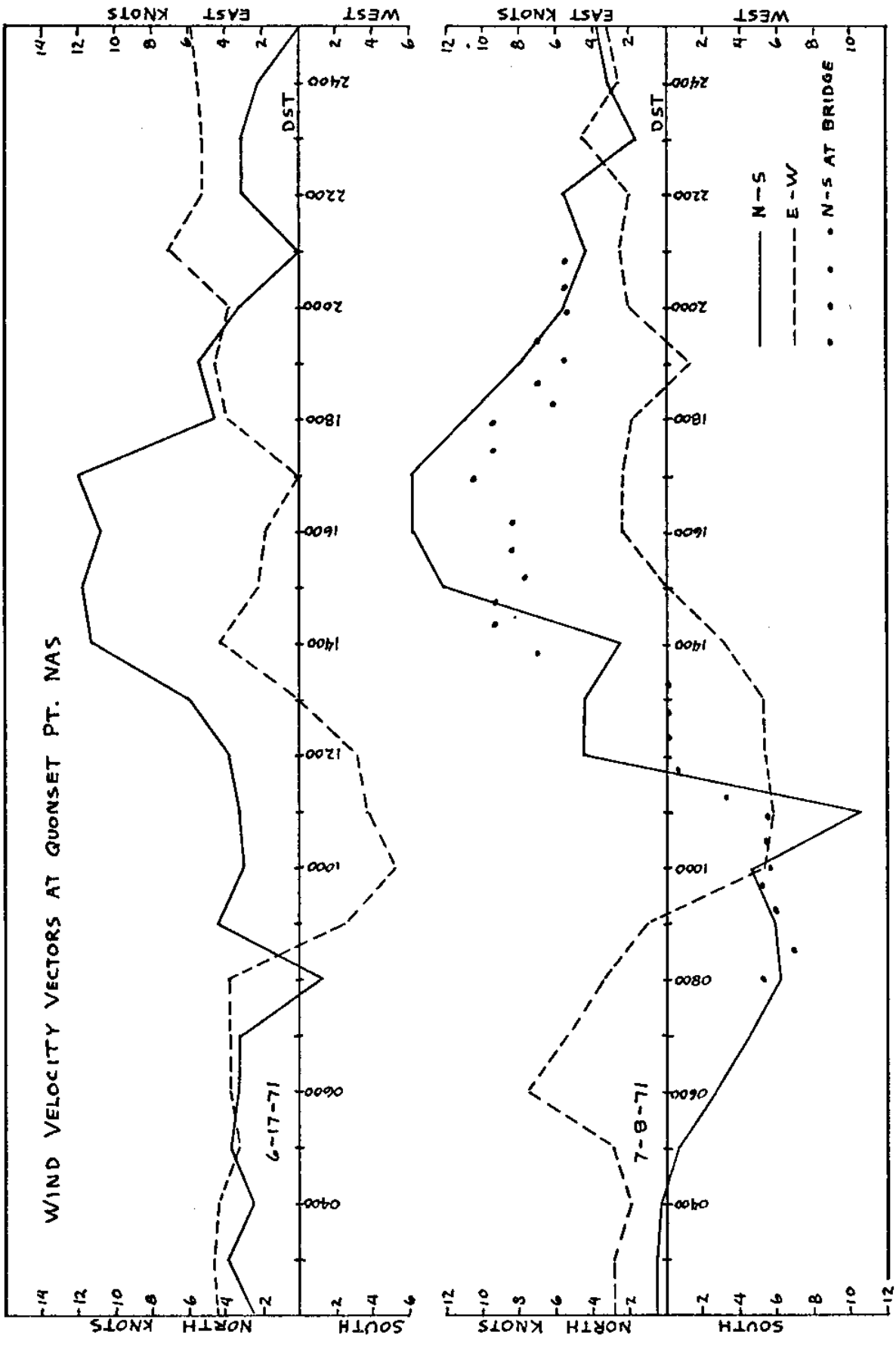

Fig. E.4--Wind velocity vectors at Quonset Point N.A.S.

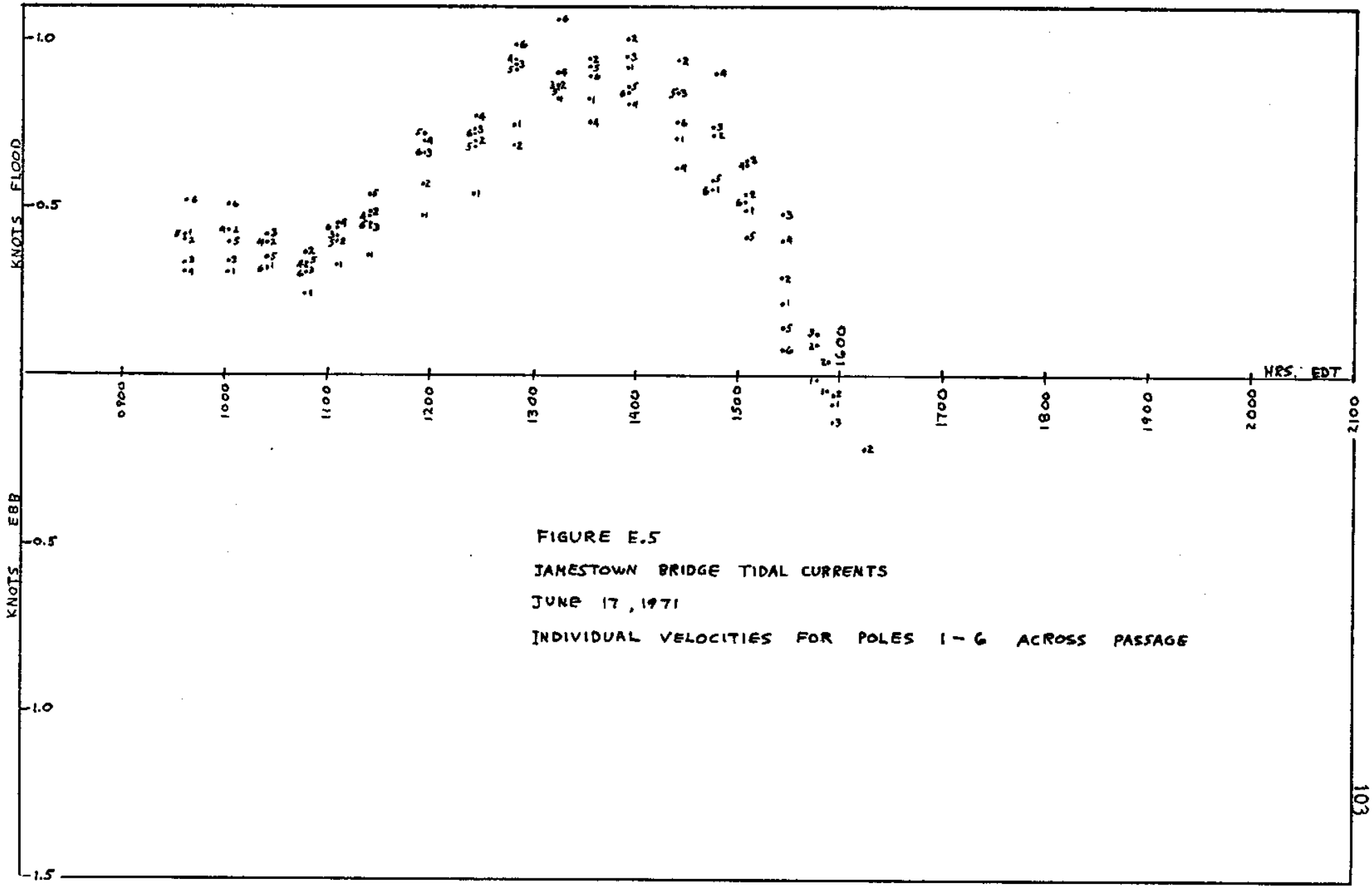

FIGURE E.5

JAMESTOWN BRIDGE TIDAL CURRENTS

JUNE 17, 1971

INDIVIDUAL VELOCITIES FOR POLES 1 – 6 ACROSS PASSAGE

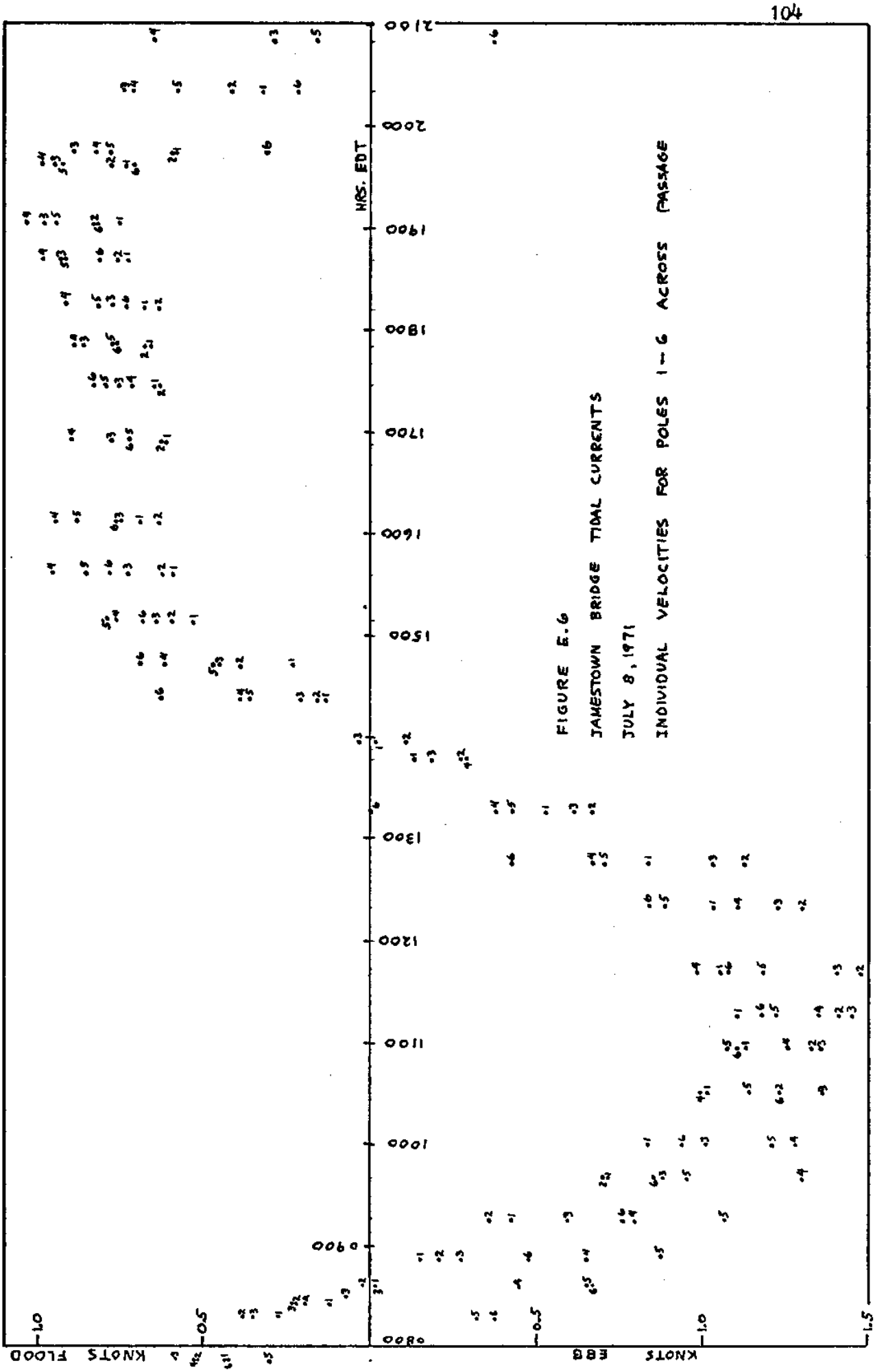

FIGURE E.6

JAMESTOWN BRIDGE TIDAL CURRENTS

JULY 8, 1971

INDIVIDUAL VELOCITIES FOR POLES 1 - 6 ACROSS PASSAGE

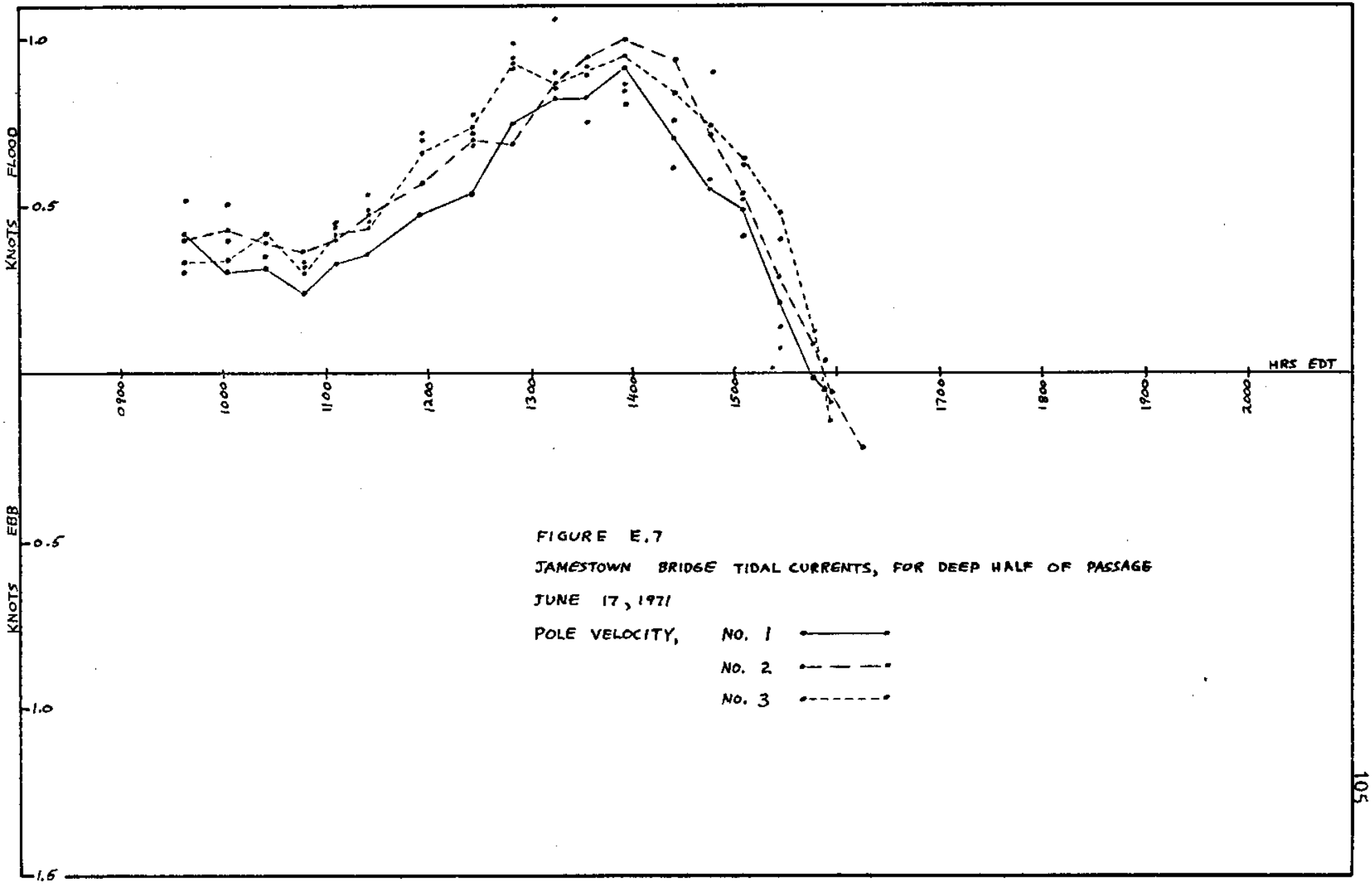

FIGURE E.7

JAMESTOWN BRIDGE TIDAL CURRENTS, FOR DEEP HALF OF PASSAGE

JUNE 17, 1971

POLE VELOCITY, No. 1 ——•——

No. 2 •— — —•

No. 3 •-------•

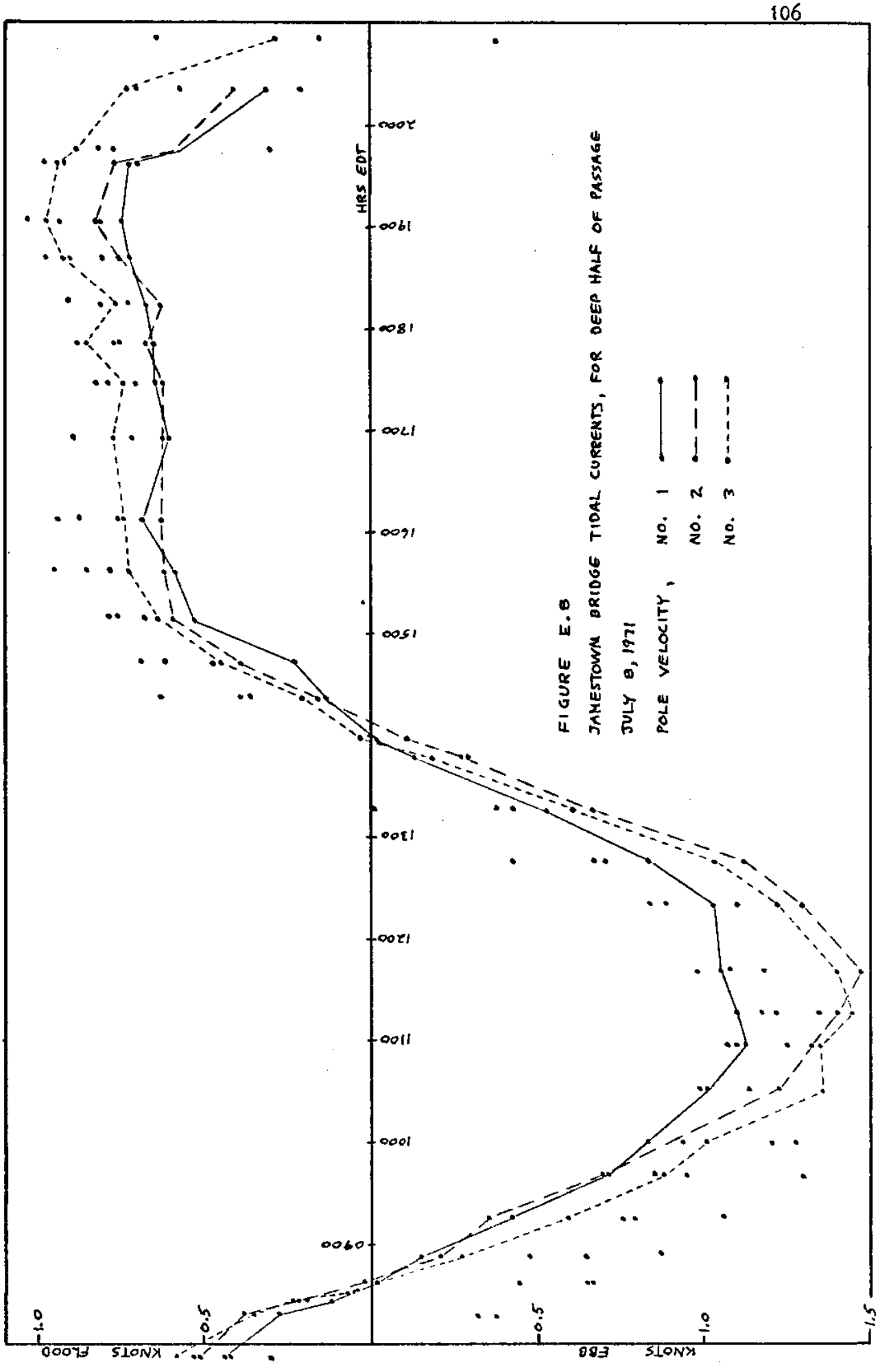
HRS EDT
0900
1000
1100
1200
1300
1400
1500
1600
1700
1800
1900
2000
KNOTS FLOOD
KNOTS EBB
0.5
1.0
1.5
FIGURE E.8
JAMESTOWN BRIDGE TIDAL CURRENTS, FOR DEEP HALF OF PASSAGE
JULY 8, 1971
POLE VELOCITY, NO. 1
NO. 2
NO. 3

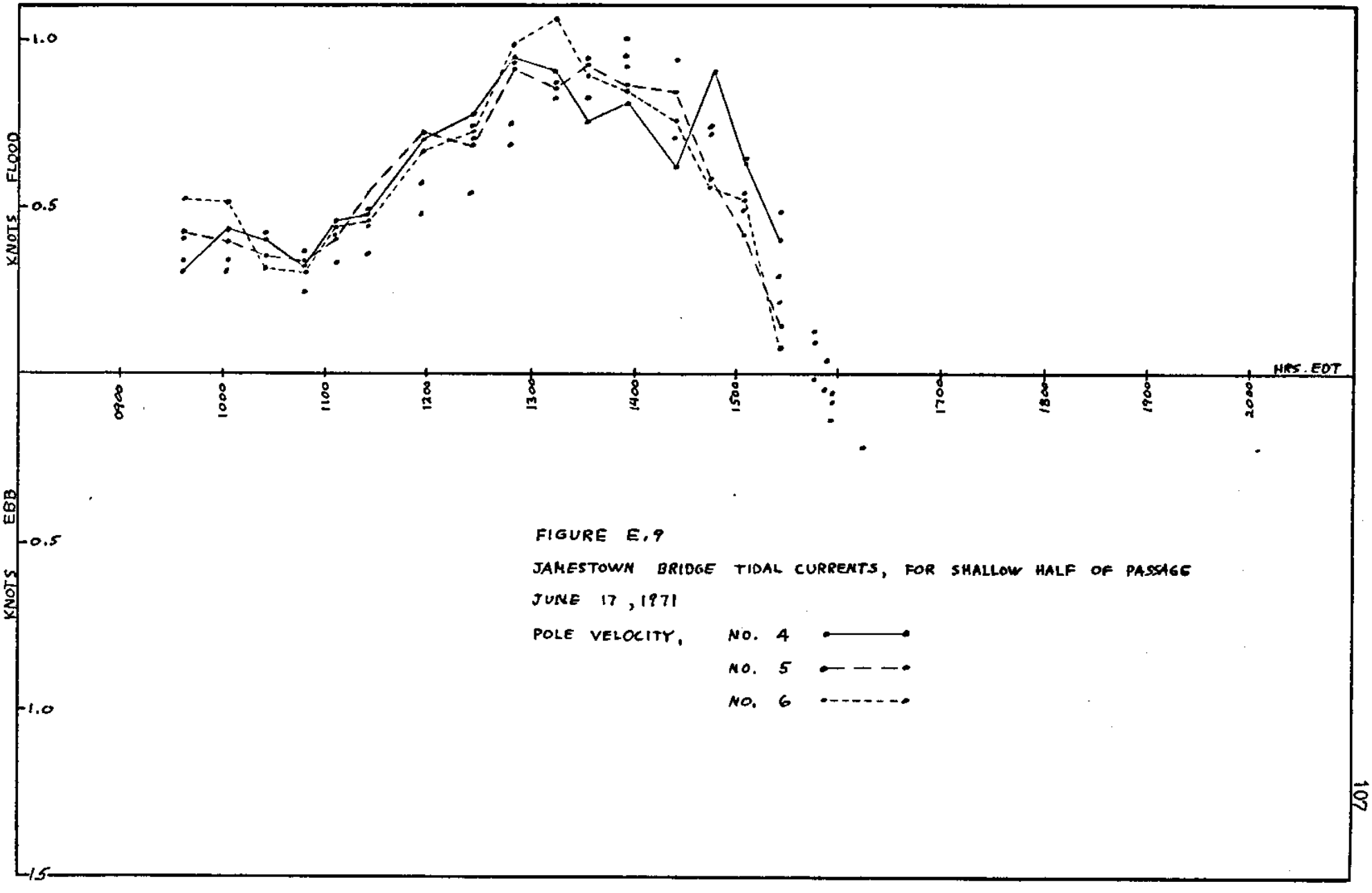

FIGURE E.9

JAMESTOWN BRIDGE TIDAL CURRENTS, FOR SHALLOW HALF OF PASSAGE

JUNE 17, 1971

POLE VELOCITY, NO. 4 ——•——

NO. 5 •— — —•

NO. 6 •-------•

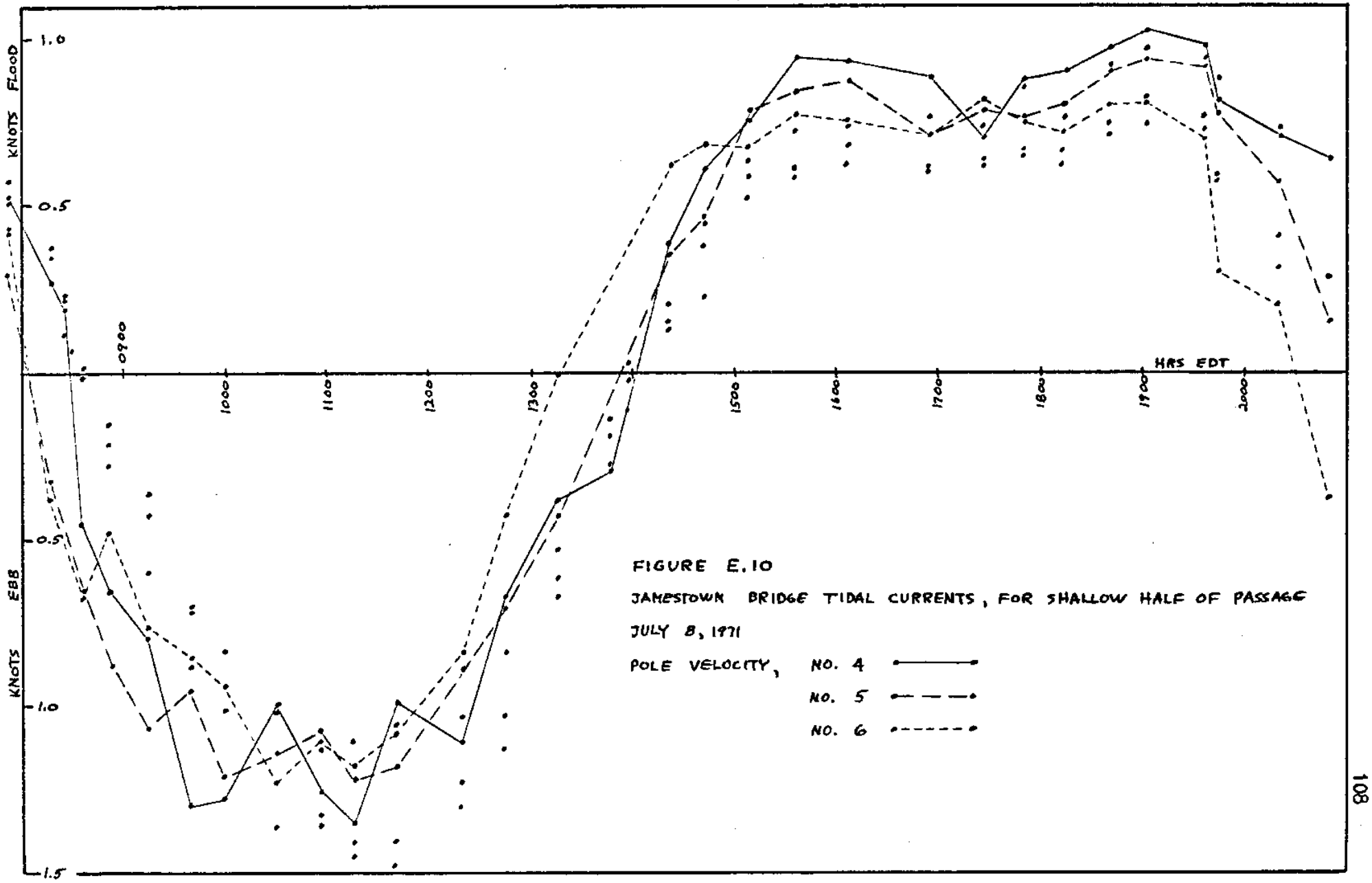

FIGURE E.10

JAMESTOWN BRIDGE TIDAL CURRENTS, FOR SHALLOW HALF OF PASSAGE

JULY 8, 1971

POLE VELOCITY, NO. 4 ——•——

NO. 5 —•— —•—

NO. 6 •------•

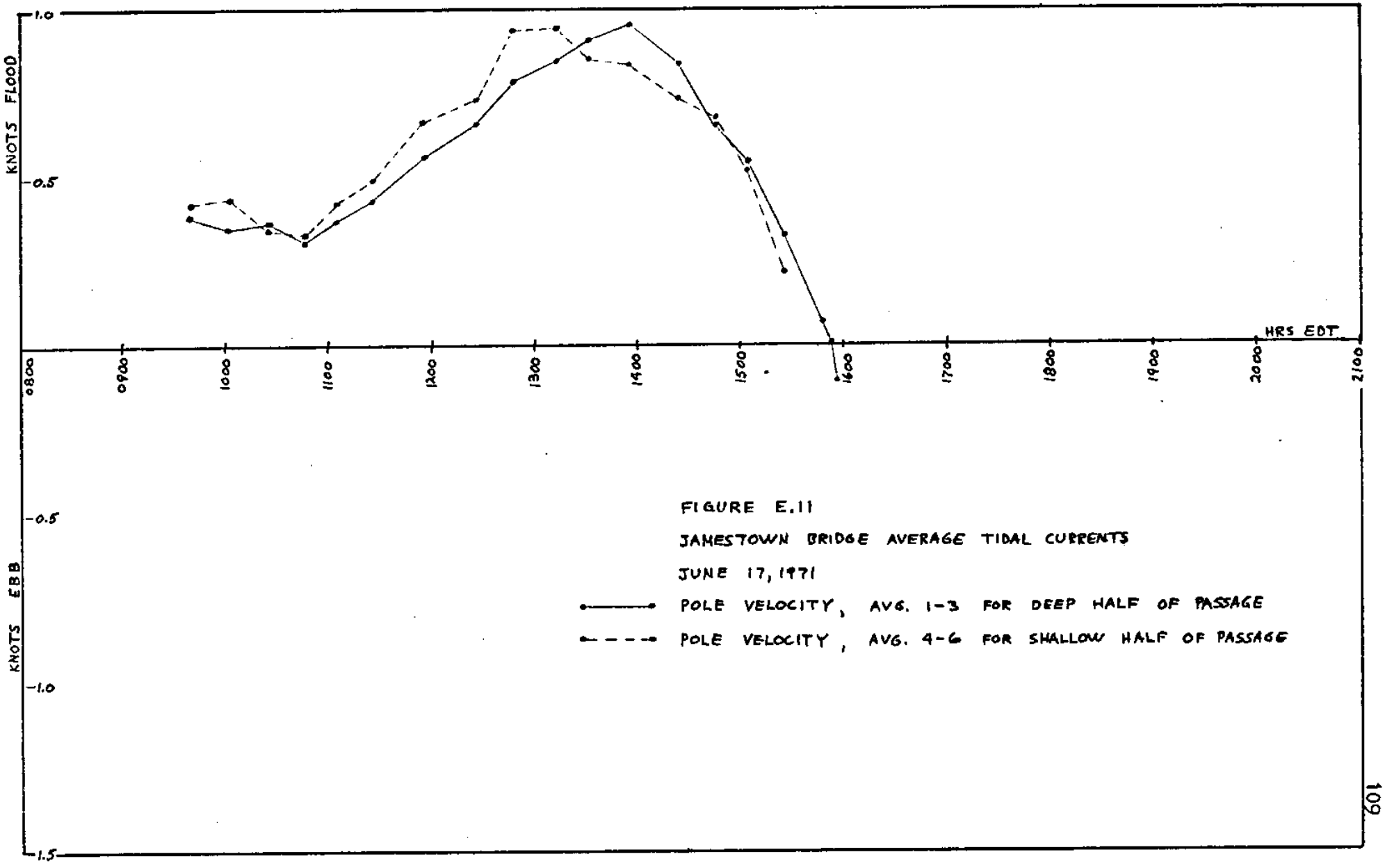

FIGURE E.11

JAMESTOWN BRIDGE AVERAGE TIDAL CURRENTS

JUNE 17, 1971

——•—— POLE VELOCITY, AVG. 1-3 FOR DEEP HALF OF PASSAGE

—•— •— POLE VELOCITY, AVG. 4-6 FOR SHALLOW HALF OF PASSAGE

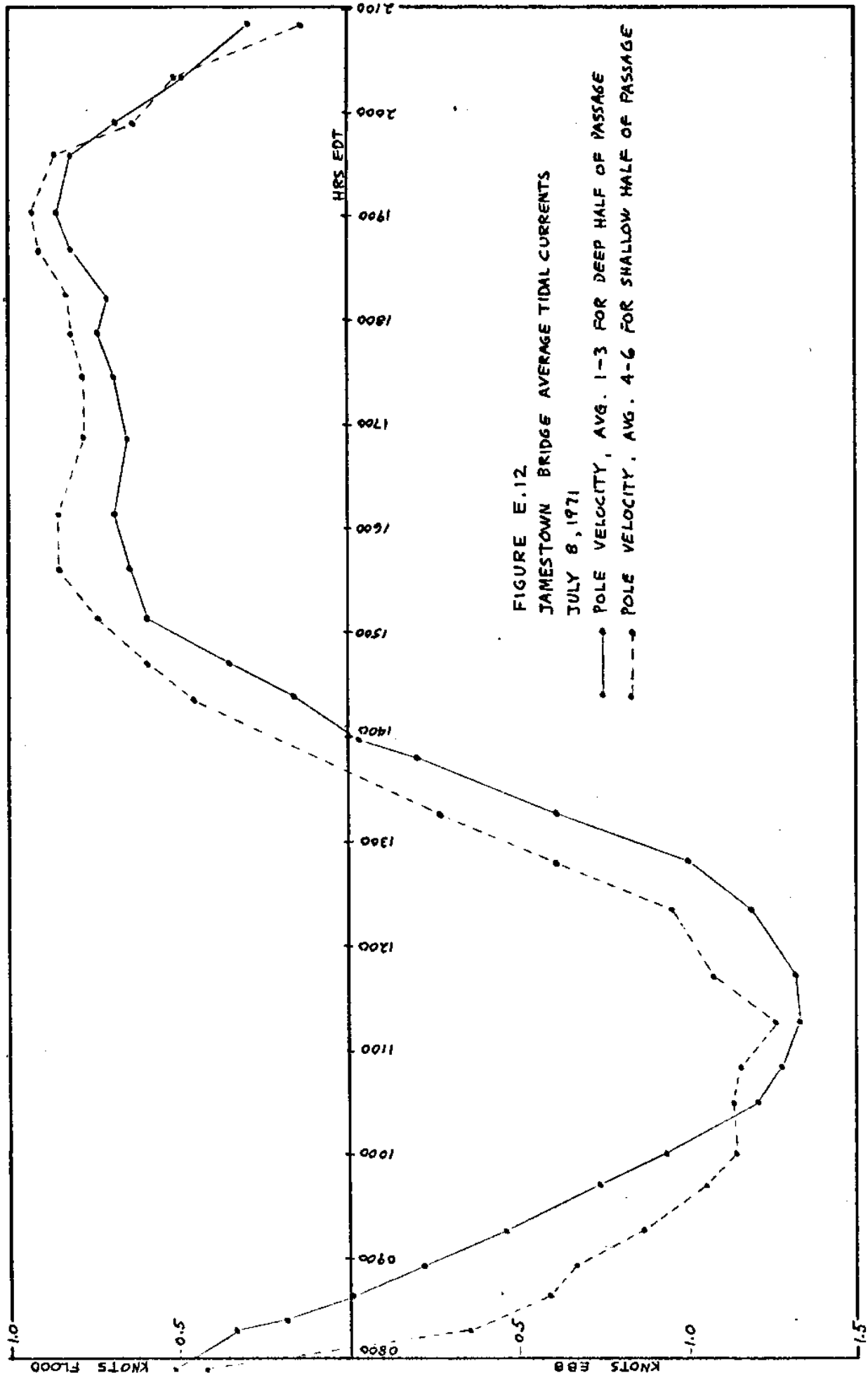
HRS EDT
0800
0900
1000
1100
1200
1300
1400
1500
1600
1700
1800
1900
2000
2100
KNOTS FLOOD
1.0
0.5
KNOTS EBB
0.5
1.0
1.5
FIGURE E.12
JAMESTOWN BRIDGE AVERAGE TIDAL CURRENTS
JULY 8, 1971
POLE VELOCITY, AVG. 1-3 FOR DEEP HALF OF PASSAGE
POLE VELOCITY, AVG. 4-6 FOR SHALLOW HALF OF PASSAGE

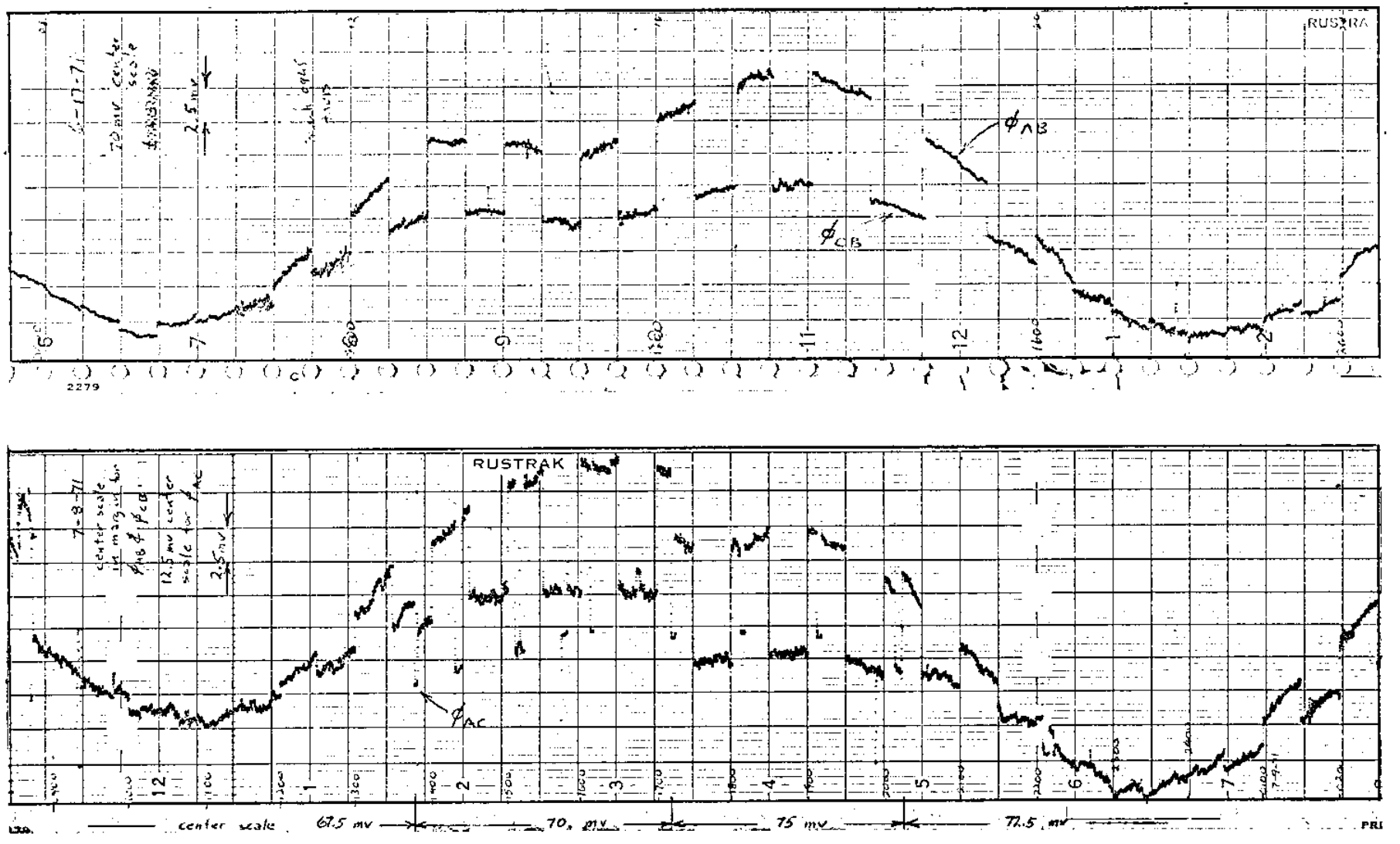

Fig. E.13--Original GEK recordings of potentials on June 17, 1971 and July 8, 1971.

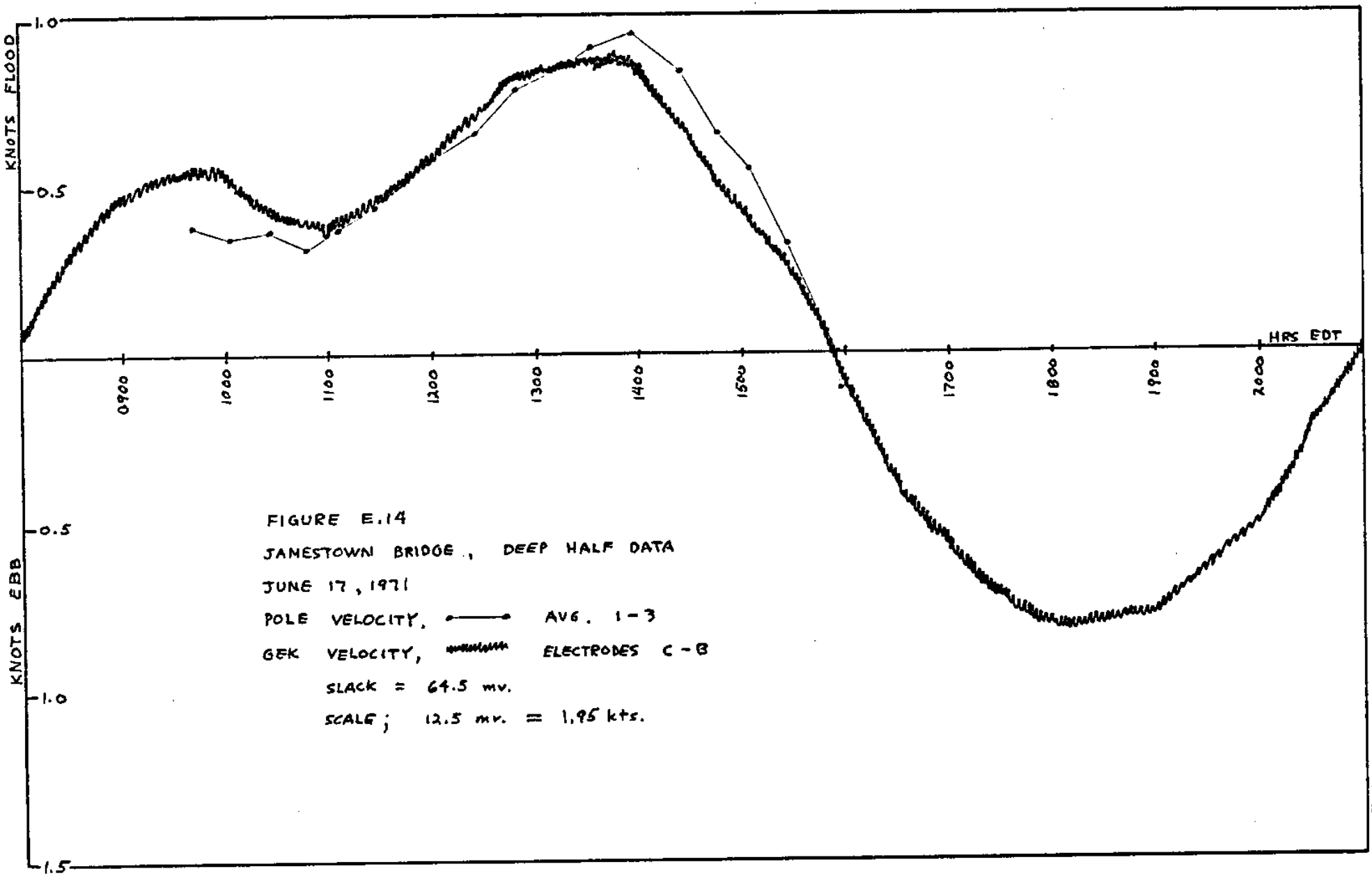

FIGURE E.14

JAMESTOWN BRIDGE, DEEP HALF DATA

JUNE 17, 1971

POLE VELOCITY, ——— AVG. 1-3

GEK VELOCITY, ~~~~~ ELECTRODES C-B

SLACK = 64.5 mv.

SCALE; 12.5 mv. = 1.95 kts.

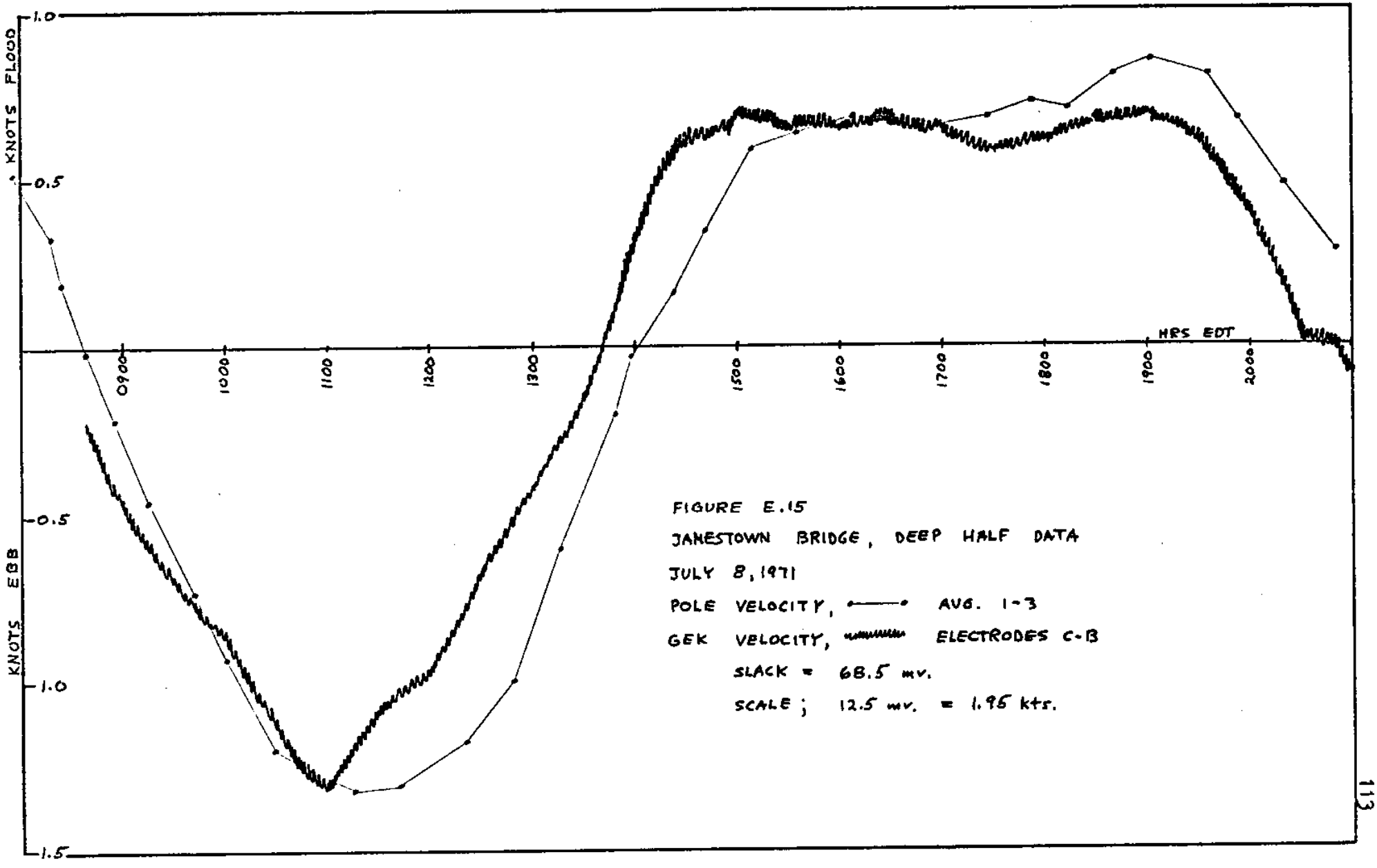

FIGURE E.15

JAMESTOWN BRIDGE, DEEP HALF DATA

JULY 8, 1971

POLE VELOCITY, •——• AVG. 1-3

GEK VELOCITY, ~~~~~ ELECTRODES C-B

SLACK = 68.5 mv.

SCALE; 12.5 mv. = 1.95 kts.

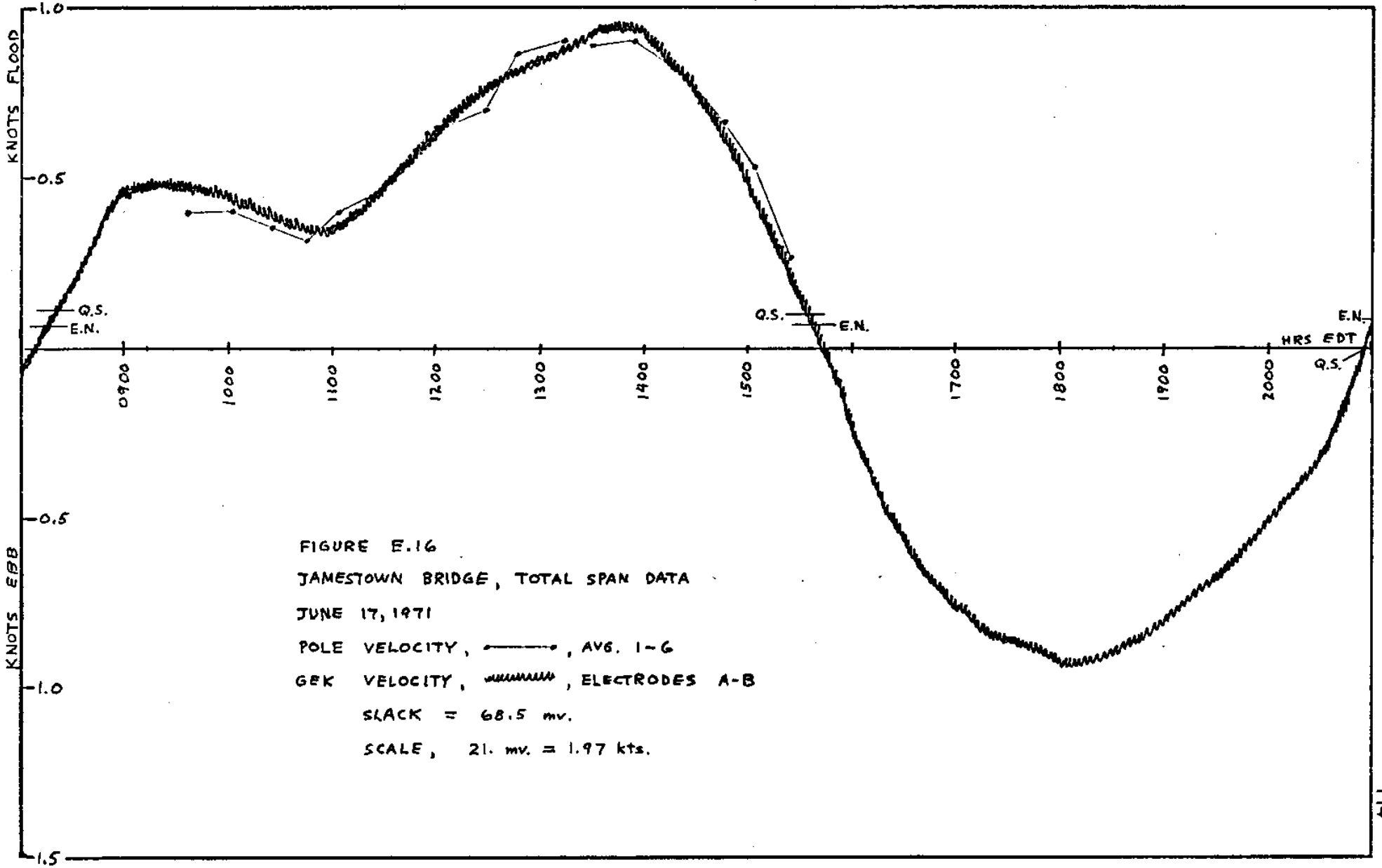

FIGURE E.16

JAMESTOWN BRIDGE, TOTAL SPAN DATA

JUNE 17, 1971

POLE VELOCITY, ———•———, AVG. 1-6

GEK VELOCITY, ~~~~~~~~, ELECTRODES A-B

SLACK = 68.5 mv.

SCALE, 21. mv. = 1.97 kts.

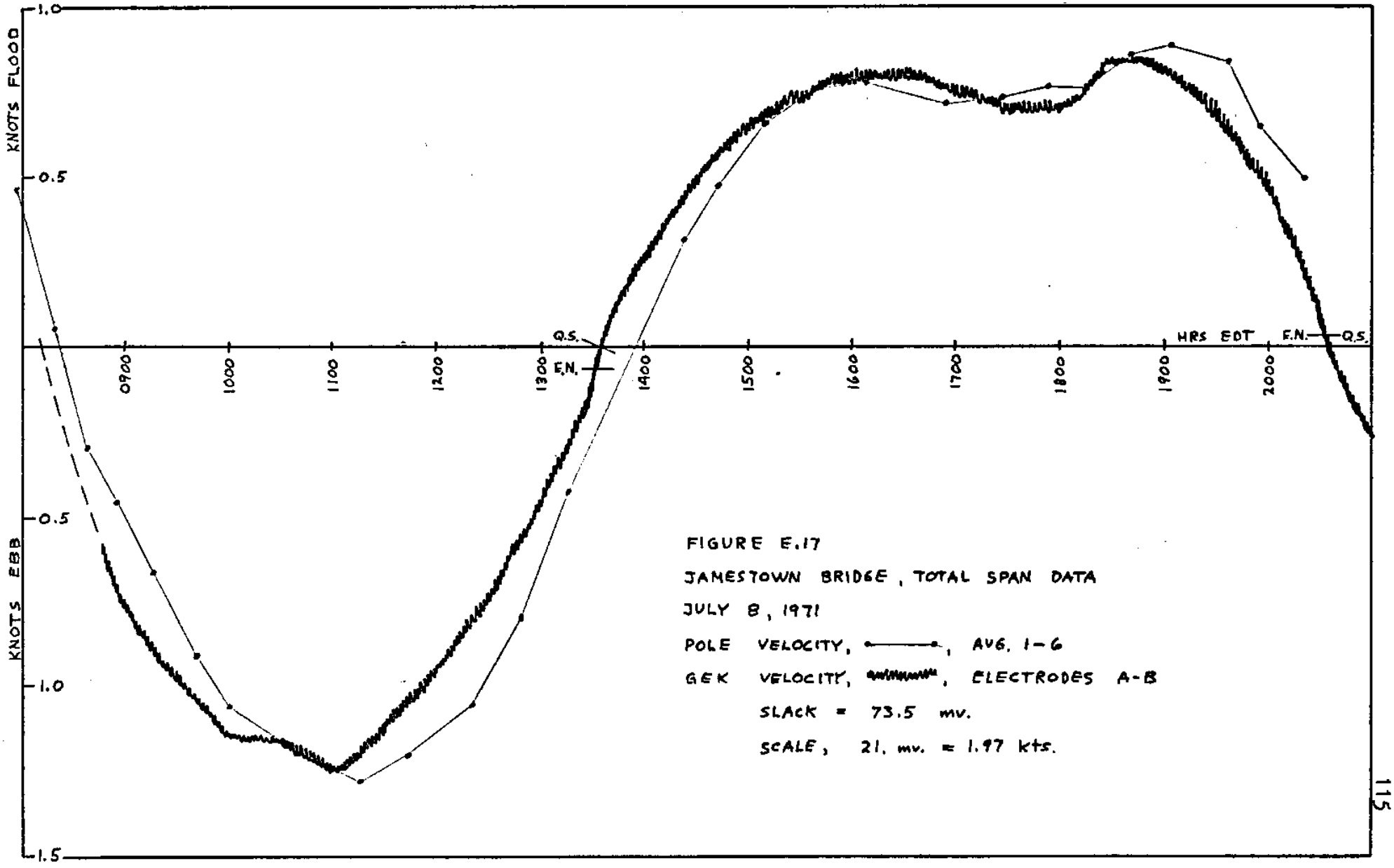

FIGURE E.17

JAMESTOWN BRIDGE, TOTAL SPAN DATA

JULY 8, 1971

POLE VELOCITY, ———, AVG. 1-6

GEK VELOCITY, ~~~~~, ELECTRODES A-B

SLACK = 73.5 mv.

SCALE, 21. mv. = 1.97 kts.

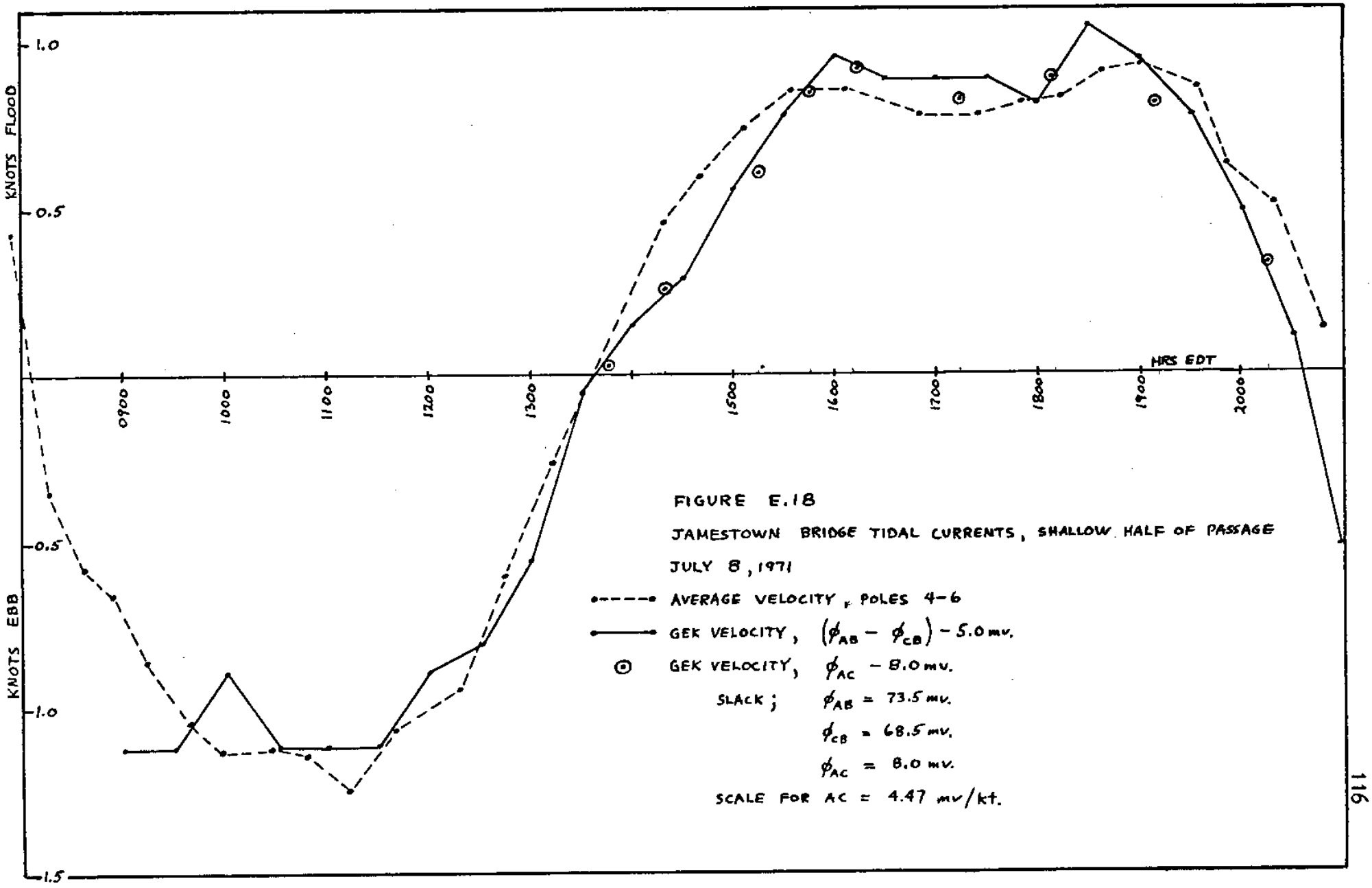

FIGURE E.18

JAMESTOWN BRIDGE TIDAL CURRENTS, SHALLOW HALF OF PASSAGE

JULY 8, 1971

AVERAGE VELOCITY, POLES 4-6

GEK VELOCITY, $(\phi_{AB} - \phi_{CB}) - 5.0$ mv.

GEK VELOCITY, $\phi_{AC} - 8.0$ mv.

SLACK; $\phi_{AB} = 73.5$ mv.

$\phi_{CB} = 68.5$ mv.

$\phi_{AC} = 8.0$ mv.

SCALE FOR AC = 4.47 mv/kt.

APPENDIX F

QUASI-SLACK ANALYSIS AND SIGNAL DRIFT

The GEK measures the total potential across the West Passage, which includes not only that produced by the motion of the tides but that produced by other extraneous electrical signals. If the GEK is to be calibrated the potential at slack tide must be known because this serves as a base line for the calibration. If this base line or slack potential is constant the GEK will remain permanently calibrated. If the extraneous electrical signal level is not constant the slack potential will vary and the calibration will not be permanent.

When the GEK was calibrated by observing drifting poles, it was found that the slack potential was not constant. Therefore, even though the relative scale factor of millivolts per knots was determined, a partial calibration of slack water is required each time the GEK is to be used. To perform this day after day would be costly in time and manpower, ultimately defeating the task of producing an economical instrumentation system.

Therefore, a quasi-slack was devised to assist in the analysis of the GEK record. The quasi-slack is defined as the potential of a base line drawn through adjacent flood and ebb tidal periods, as recorded on the GEK, which divides the cycle into equal areas. For the quasi-slack to be equal to the actual slack, the amount of water flooding through the GEK would equal the amount of water ebbing through the GEK. This is not necessarily the situation because the tidal velocities do vary in both amplitude and duration.

Planimeter method to find the quasi-slack

Using a polar planimeter, each two adjacent tidal flows were integrated over the GEK record in a figure-eight pattern. If a proper quasi-slack position was chosen, the planimeter indicated zero area, since the clockwise and counterclockwise integration of the planimeter cancel each other.

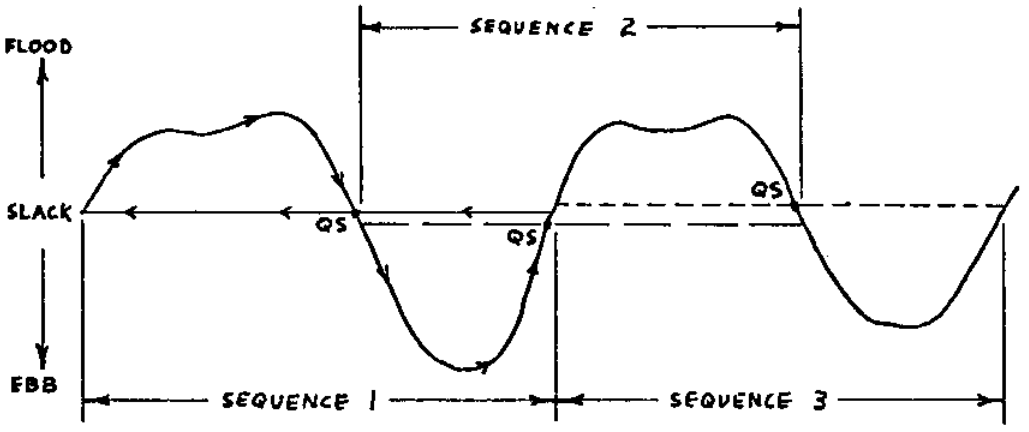

By going through each two adjacent tidal flows and determining a quasi-slack potential for each, a record of the variation was found and is shown in figure F.1. Figure F.1 shows that there was considerable change in the quasi-slack potential. In early May the mean value was about 72 mv while toward early December the mean was about 74 mv. This offset of 2 mv potential is approximately equal to 0.2 knots which will produce a tidal increase of 0.8 feet, averaged over the entire Bay, for each tidal cycle of 12.5 hours. Obviously not a probable situation if the tidal range is only around 4 feet. Therefore, it is concluded that there may be a long term drift with short term variations imposed upon it.

To determine if the quasi-slack method of analysing the

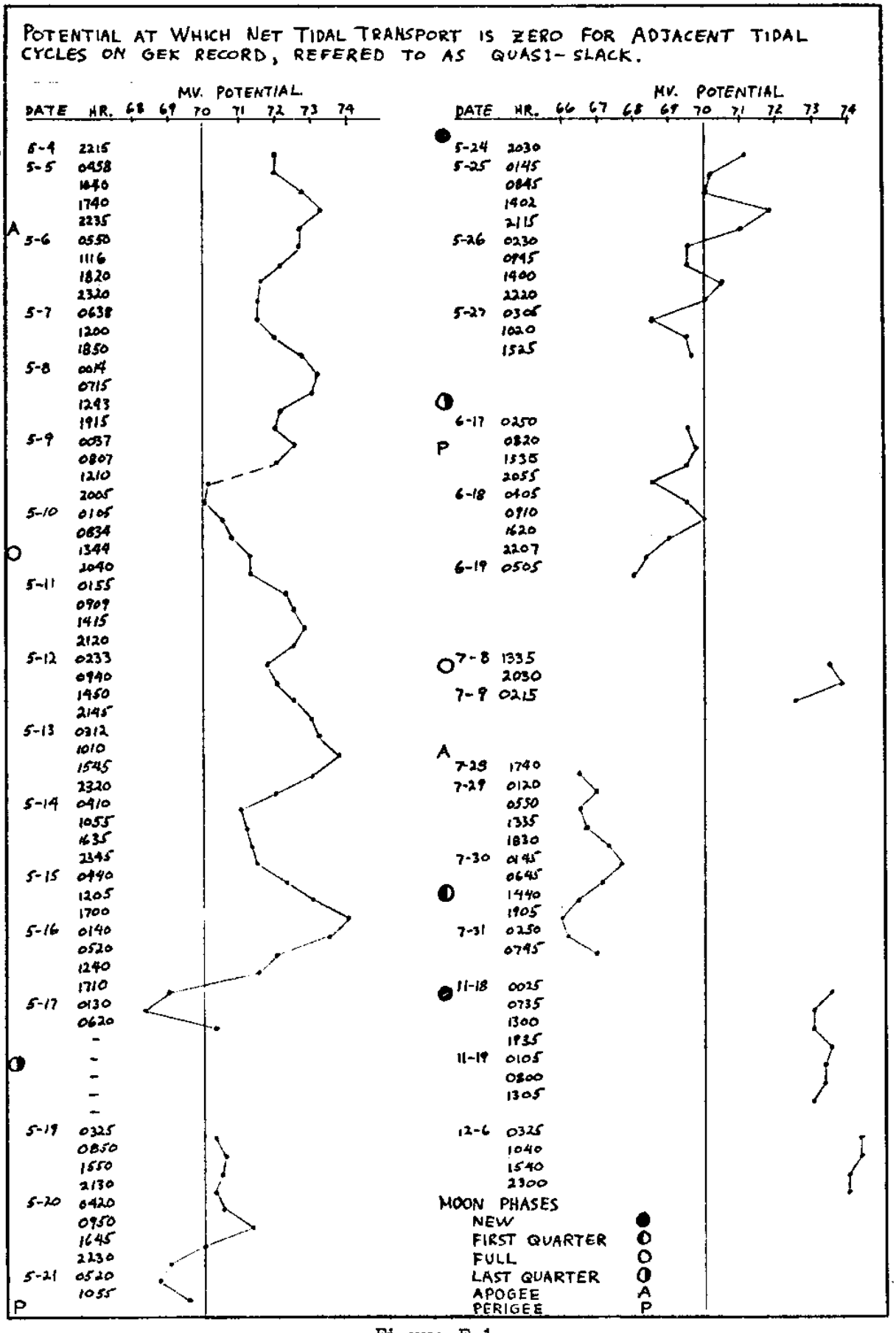
POTENTIAL AT WHICH NET TIDAL TRANSPORT IS ZERO FOR ADJACENT TIDAL CYCLES ON GEK RECORD, REFERED TO AS QUASI-SLACK.
MV. POTENTIAL
DATE HR. 68 69 70 71 72 73 74
5-4 2215
5-5 0458
1840
1740
2235
A
5-6 0550
1116
1820
2320
5-7 0638
1200
1850
5-8 0014
0715
1243
1915
5-9 0037
0807
1210
2005
5-10 0105
0834
1349
2040
5-11 0155
0909
1415
2120
5-12 0233
0940
1450
2145
5-13 0312
1010
1545
2320
5-14 0910
1055
1635
2345
5-15 0940
1205
1700
5-16 0140
0520
1240
1710
5-17 0130
0620
-
-
-
-
-
5-19 0325
0850
1550
2130
5-20 0420
0950
1645
2230
5-21 0520
1055
P
MV. POTENTIAL
DATE HR. 66 67 68 69 70 71 72 73 74
5-24 2030
5-25 0145
0845
1402
2115
5-26 0230
0945
1400
2220
5-27 0305
1020
1525
6-17 0250
P 0820
1535
2055
6-18 0405
0910
1620
2207
6-19 0505
7-8 1335
2030
7-9 0215
A
7-28 1740
7-29 0120
0550
1335
1830
7-30 0145
0645
1440
1905
7-31 0250
0745
11-18 0025
0735
1300
1935
11-19 0105
0800
1305
12-6 0325
1040
1540
2300
MOON PHASES
NEW
FIRST QUARTER
FULL
LAST QUARTER
APOGEE A
PERIGEE P

Figure F.1

GEK records is useful, these causes of drift will need to be examined and identified. If the short term variations can be recognized or shown negligible on the GEK record, the resultant signal should give an indication of the long term variations. If these are either tolerable or predictable, some degree of accuracy can be attached to the permanent calibration of the GEK. If this is not possible, the degree of accuracy of the quasi-slack analysis can be stated. The final object is to extract as much information from the GEK signal that is possible, and to determine methods of improving future GEK installations.

Short term quasi-slack variations

Electrode electrochemical changes

Electrode electrochemical variations are produced when the electrode pairs are not emmersed in similar environments. The two electrodes are essentially potential batteries only needing some unbalance in their environments to develop their own electric potential. The electrodes are as identical in physical and chemical composition as manufacturing permits, so this leaves us the salinity, temperature and pressure environments to examine. The pressure effect is negligible since the electrode itself is a solid and the depth differences are only 2 feet for the electrodes on the ends of the bridge and 20 feet for the center electrode. The salinity and temperature of the water does vary and can produce an extremely high percentage of error in the GEK, but it must be noted that the potential thus generated will not be a permanent one but will vary as the water conditions vary during each flood and ebb. This makes it extremely difficult to relate to the daily tides unless the electrodes are buffered against the ambient water or additional instrumentation is installed to record the temp-

erature and salinity. This problem was not completely solved in this GEK installation. Although the salinity changes were buffered, the electrodes were susceptible to temperature variations which were in the range of 2^{o} C (equivalent to 1 mv potential). For more information, see appendix I for the experimentation performed on this problem. For the present discussion it is assumed that the temperature differences between the electrodes are not predictable and therefore no corrections can be made for them for this GEK.

Wind effects

The wind should be expected to influence the flow of water into and out of the Bay. At a windspeed of between 4 and 6 m/sec (7.8 to 12.5 knots) gravity waves are generated (Ippen, 1966,p.136) and the wind shear stress, proportional to the velocity squared, over the water causes a movement of the water. Chosing 12 knots for the critical speed and assuming that a wind direction $\pm 40^{o}$ north and $\pm 40^{o}$ south will influence the transport of water into and out of the Bay, a representative wind factor was devised. This is calculated by taking hourly wind velocities 12 knots and greater, squaring and summing them during six hour intervals. The daily slacks divide the day into four approximate equal segments. Since the local winds conform to a predicable pattern throughout the day during the summer, the six hour intervals selected were;

0100 to 0600 hrs	night
0700 to 1200	morning
1300 to 1800	afternoon
1900 to 2400	evening

All these values are plotted in figure F.2 for intervals that corresponded to the approximate GEK quasi-slack times. Comparison

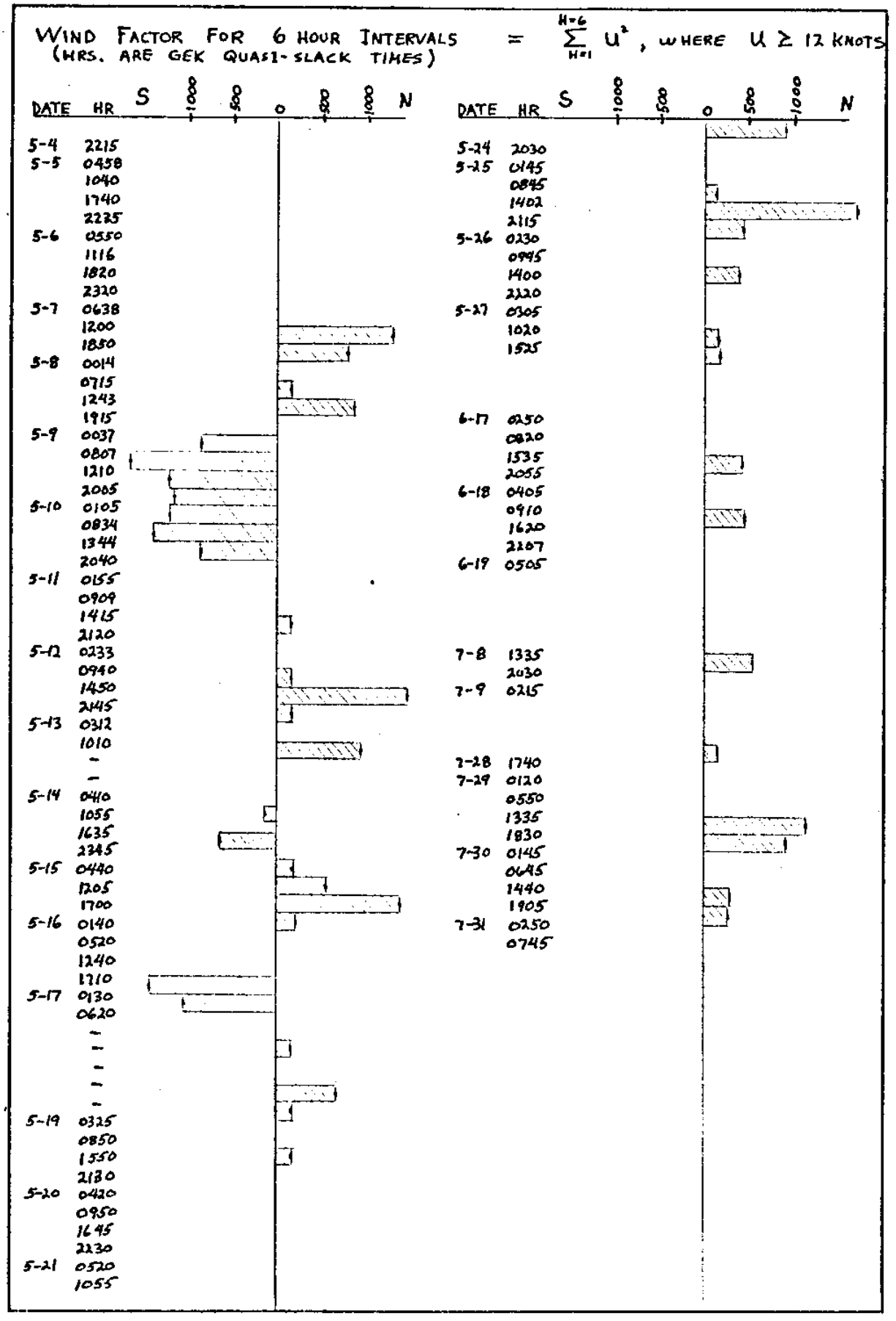
WIND FACTOR FOR 6 HOUR INTERVALS = $\sum_{H=1}^{H=6} U^2$, WHERE $U \geq 12$ KNOTS
(HRS. ARE GEK QUASI-SLACK TIMES)
DATE HR
S 1000 500 0 500 1000 N
5-4 2215
5-5 0458
1040
1740
2235
5-6 0550
1116
1820
2320
5-7 0638
1200
1850
5-8 0014
0715
1243
1915
5-9 0037
0807
1210
2005
5-10 0105
0834
1344
2040
5-11 0155
0909
1415
2120
5-12 0233
0940
1450
2145
5-13 0312
1010
–
–
5-14 0440
1055
1635
2345
5-15 0440
1205
1700
5-16 0140
0520
1240
1710
5-17 0130
0620
–
–
–
–
–
5-19 0325
0850
1550
2180
5-20 0420
0950
1645
2230
5-21 0520
1055
DATE HR
S 1000 500 0 500 1000 N
5-24 2030
5-25 0145
0845
1402
2115
5-26 0230
0995
1400
2220
5-27 0305
1020
1525
6-17 0250
0820
1535
2055
6-18 0405
0910
1620
2207
6-19 0505
7-8 1335
2030
7-9 0215
7-28 1740
7-29 0120
0550
1335
1830
7-30 0145
0645
1440
1905
7-31 0250
0745

Figure F.2

between wind north and south and the short term quasi-slack variations can be made by flipping corresponding pages. It is quite apparent that almost everytime the wind is above 12 knots, it is reflected by the quasi-slack potential increasing or decreasing. It should be understood that this is only a qualitative analysis and does not give enough data to predict the wind effect of transport.

River runoff

River runoff from rain would tend to increase the ebb flow and would cause the quasi-slack to move downward in potential. Hicks (1959) gives approximately 88 cfs as the runoff in the West Passage. For a tidal flow of 4.5×10^9 ft^3/ half cycle (later determined),

$$88 \frac{ft^3}{sec} \times 6 \text{ hrs} = 1.9 \times 10^6 \ ft^3 / \text{half cycle}$$

and this is only

$$\frac{1.9 \times 10^6}{4.5 \times 10^9} \times 100 = 0.04\ \%$$

This enables rain water to be neglected even if it constitutes up to 10 times the predicted amount and shows that it probably will not be detectable on a GEK.

The lunar and solar tidal components

As mentioned previously, the water into and out of the Bay is not equal from day to day and this mainly dependent on the lunar and solar tidal forces. To calculate these forces and the resultant tidal flow in West Passage would be difficult, and for the accuracy required in this analysis it will be sufficient to observe the direct effect of the tidal currents and to deduce the tidal flows that produced them.

The direct effect of the tidal currents is to change the tidal

height in the Bay. By convention the quasi-slack is determined every half-tidal cycle and can be considered representative of an excess or deficit in the mass transport into the Bay during that time interval. Over a long time interval this net transport is zero (neglecting river runoff) since the mean water level is considered constant in the Bay. This net transport which is proportional to the integral of the water velocity through the passages, is reflected in the tide height records in the Bay. Likewise, the velocity is proportional to the time differential of the tide height. This relation is used to extract the effect of the tidal forces from the quasi-slack values.

A graphic example is shown in figure F.3. Using a sinusoidal representation for the tide, curve (a) shows a velocity curve as it would be recorded on the GEK. It has been integrated over every tidal cycle to find the quasi-slack points every half cycle. Curve (b) shows a trace of the quasi-slack points. Curve (c) shows a trace of the tidal height that corresponds to curve (a). The average tide heights are indicated every half cycle and a trace of them is shown in curve (d). If the $\Delta h/\Delta t$ of curve (d) is plotted, curve (e) is obtained. Multiplying curve (e) by a conversion constant (an arbitrary $k = 1/2$ for this example only) and subtracting from the quasi-slack curve (b), results in curve (f) which is zero for the total time interval. What has been done is to extract the tidal forces (plus any wind effect) from the quasi-slack values. If there was any extraneous drift in the original curve (a) it would show up (on a sample frequency of about 6 hours) when the resultant curve (f) was plotted.

The only record of tide height on a continuous basis was that from the Quonset Point Naval Air Station in Narragansett Bay. Only the maximum and minimum tide heights are used so the time lag of the

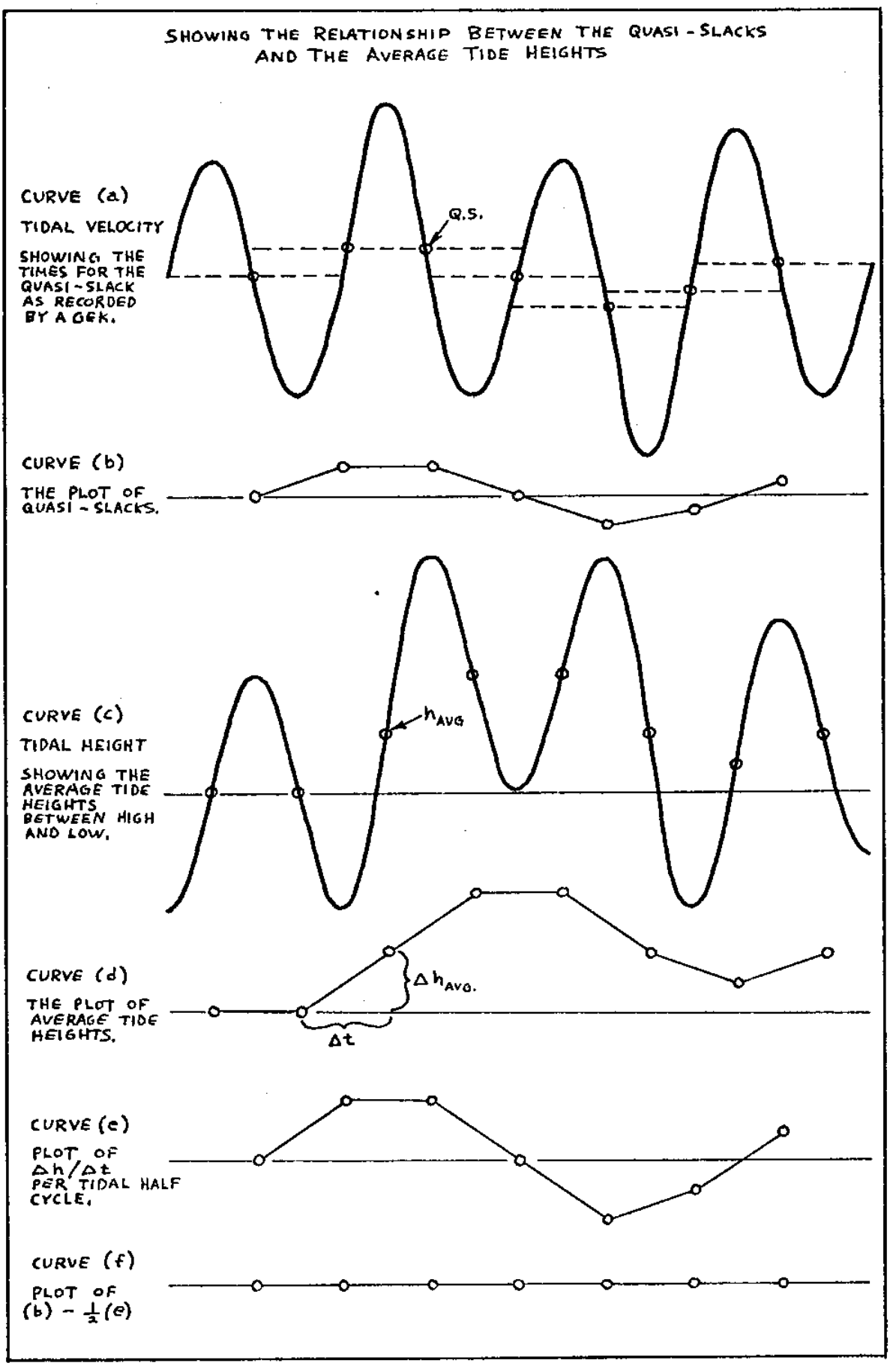
SHOWING THE RELATIONSHIP BETWEEN THE QUASI-SLACKS AND THE AVERAGE TIDE HEIGHTS
CURVE (a)
TIDAL VELOCITY
SHOWING THE TIMES FOR THE QUASI-SLACK AS RECORDED BY A GEK.
Q.S.
CURVE (b)
THE PLOT OF QUASI-SLACKS.
CURVE (c)
TIDAL HEIGHT
SHOWING THE AVERAGE TIDE HEIGHTS BETWEEN HIGH AND LOW.
h_{AVG}
CURVE (d)
THE PLOT OF AVERAGE TIDE HEIGHTS.
$\Delta h_{AVG.}$
Δt
CURVE (e)
PLOT OF $\Delta h/\Delta t$ PER TIDAL HALF CYCLE.
CURVE (f)
PLOT OF (b) - $\frac{1}{2}$(e)

Figure F.3

tides up the Bay are of no concern. The fact that the station is about half the distance up the Bay helps to make it a fair average. From the tide records the average tide height was obtained and is plotted in figure F.4. It is the average height of the adjacent high and low waters and is adjusted to the mean low water level at Quonset Point. Since the quasi-slacks are determined by integrating over an interval of a whole tidal cycle (even though they are plotted every half cycle), the $\Delta h/\Delta t$ in figure F.5 is plotted at twice the change in average tide height per half cycle from figure F.4. This figure shows the diurnal quality of the tidal cycle as opposed to the semi-diurnal which is usually seen in examining the tide charts for the Bay.

The next step is to determine the constant that will convert the tidal height change per cycle to Δ mv of quasi-slack so that figure F.5 can be subtracted from figure F.1. Theoretically, considering West Passage only, a 1.0 mv offset in slack potential that lasts for one tidal cycle will change the Bay water level by,

$$\frac{(180{,}000\ ft^2)(1.689\ ft/sec\text{-}kt)(12.5\ hrs/cycle)(3600\ sec/hr)}{(110\ mi^2)(5280\ ft/mi)^2(10.65\ mv/kt)} = 0.42\ \frac{ft}{mv\text{-}cycle}$$

where, 180,000 ft^2 = cross section of west passage at GEK at mean water level.
110 $miles^2$ = area of Narr. Bay excluding Sakonnet River and below the Jamestown Bridge.
10.65 mv/kt = calibration scale factor, see appendix E.

The problem arises that the Bay has essentially two openings (neglecting the Sakonnet River narrows) to the ocean and that no way was provided for observing what percentage of the water in the Bay passes through the West Passage. One way to determine this percentage is to compare tidal transport as measured by integration of the GEK calibration curves in figures E.16 and E.17, and compare them with their respective tidal changes as recorded at Quonset.

AVERAGE TIDE HEIGHT AT QUONSET N.A.S. FROM [(HIGH TIDE + LOW TIDE) ÷ 2] - 3.5'

DATE	HR.	AVERAGE TIDE HEIGHT, FT. (2.5 – 3.0 – 3.5)
5-4	2215	
5-5	0458	
	1040	
	1740	
	2235	
5-6	0550	
	1116	
	1820	
	2320	
5-7	0638	
	1200	
	1850	
5-8	0014	
	0715	
	1243	
	1915	
5-9	0037	
	0807	
	1210	
	2005	
5-10	0105	
	0834	
	1344	
	2040	
5-11	0155	
	0909	
	1415	
	2120	
5-12	0233	
	0940	
	1460	
	2145	
5-13	0312	
	1010	
	1545	
	2320	
5-14	0410	
	1055	
	1635	
	2345	
5-15	0440	
	1205	
	1700	
5-16	0140	
	0520	
	1240	
	1710	
5-17	0130	
	0620	
	–	
	–	
	–	
	–	
	–	
5-19	0325	
	0850	
	1550	
	2130	
5-20	0420	
	0950	
	1645	
	2230	
5-21	0520	
	1055	

DATE	HR.	AVERAGE TIDE HEIGHT, FT. (2.5 – 3.0 – 3.5)
5-24	2030	
5-25	0145	
	0845	
	1402	
	2115	
5-26	0230	
	0945	
	1400	
	2220	
5-27	0305	
	1020	
	1525	
6-17	0250	
	0820	
	1535	
	2055	
6-18	0405	
	0910	
	1620	
	2207	
6-19	0505	
7-8	1335	
	2030	
7-9	0215	
7-28	1740	
7-29	0120	
	0550	
	1335	
	1830	
7-30	0145	
	0645	
	1440	
	1905	
7-31	0250	
	0745	

TIDE HEIGHT REFERED TO MLW.

Figure F.4

EXCESS TIDAL FLOOD OR EBB TO CAUSE THE FLUCTUATION OF THE AVERAGE TIDE HEIGHT AT QUONSET POINT.

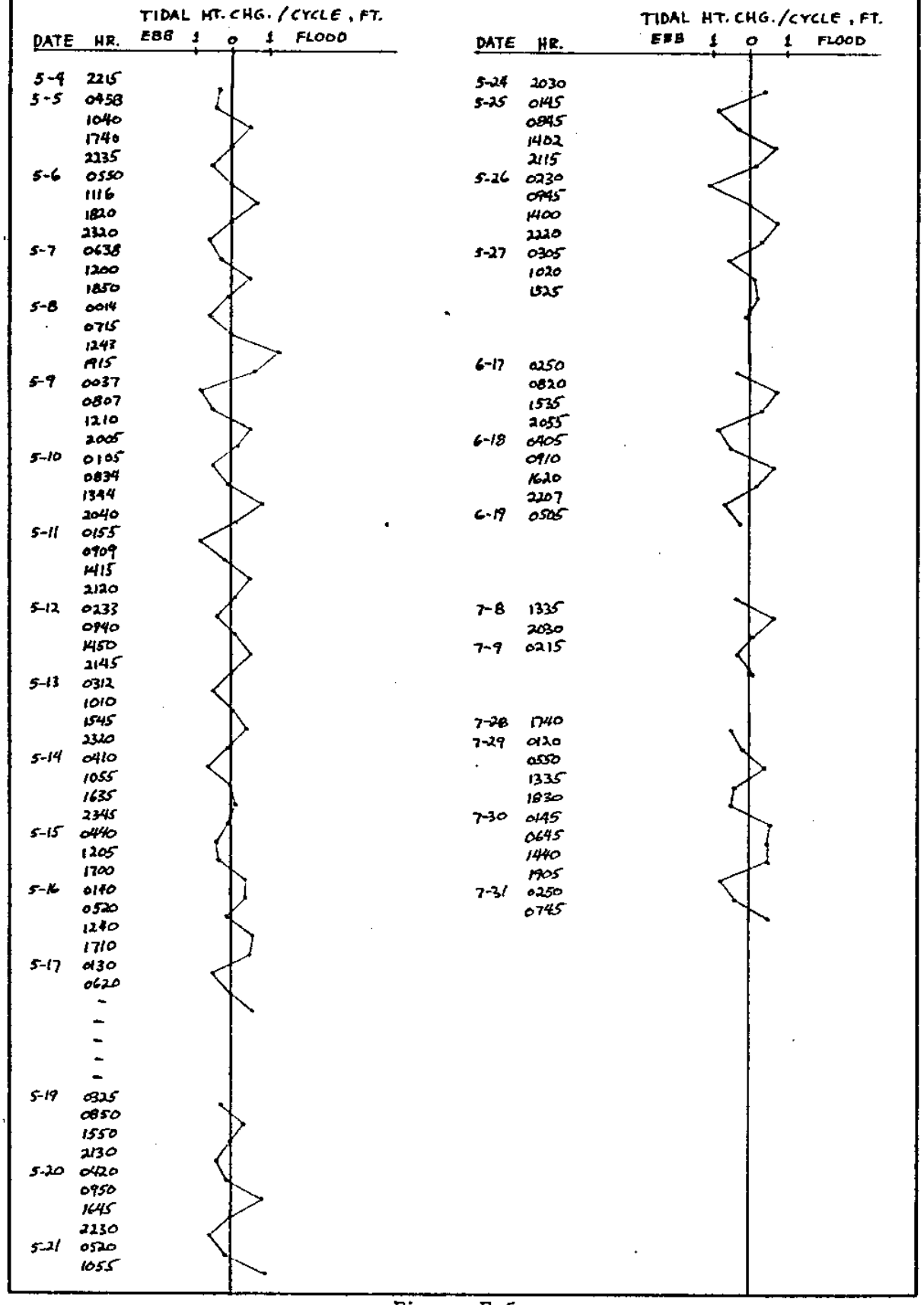

Figure F.5

Using a planimeter on the two curves the following transports were calculated from the following relationship,

$$Q = (180{,}000\ ft^2)(1.689\ ft/sec\text{-}kt) \int_{t_1}^{t_2} V\, dt$$

June 17, 1971

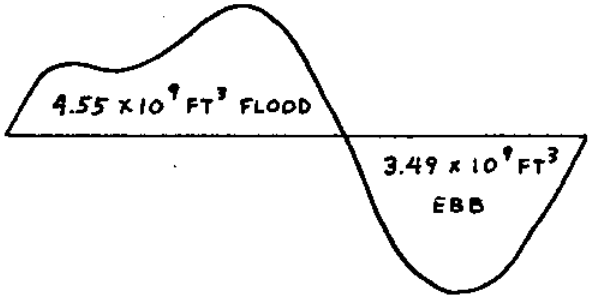

excess flood = $1.06 \times 10^9\ ft^3$

July 8, 1971

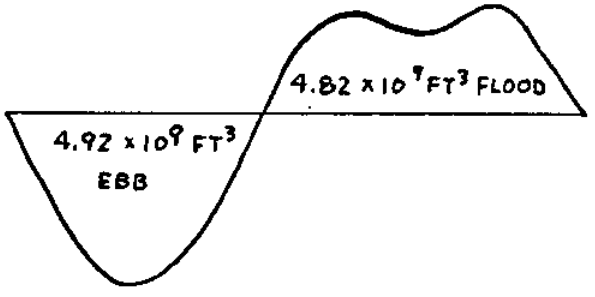

excess ebb = $0.1 \times 10^9\ ft^3$

The calculated level change in the Bay due to water passing only through the West Passage is,

$$\Delta h, ft = \frac{transport, ft^3}{110\ miles^2\ (5280\ ft/mi)^2}$$

Solving for Δh for each flood and ebb half cycle, and tabulating the values with the observed tide changes, as recorded at Quonset Point, gives table F.1.

Table F.1

Percentage of tide flowing through West Passage

Date	Transport ft^3	Tidal level change, ft		Percentage thru GEK
		Calc.	Observed	
6-17-71	4.55×10^9 flood	1.48	4.1	36%
	3.49×10^9 ebb	1.14	3.8	30%
7-8-71	4.92×10^9 ebb	1.60	3.65	44%
	4.82×10^9 flood	1.57	4.3	36.5%

The accuracy of measuring the observed level change from chart paper is ± 0.05 ft, or equivalent to 0.05 ft/3.65 ft = $\pm$ 1.5%. The planimeter is accurate to about $\pm$ 1% when integrating the GEK records. Therefore, assuming the basic method is valid, the best accuracy that could be expected is about 2%.

To obtain a conversion factor it will be assumed that an average of 37% of the water passes through the West Passage.

$$0.42 \frac{ft}{mv\text{-}cycle} \times \frac{1}{37\%} = 1.1 \frac{ft}{mv\text{-}cycle}$$

To check this value against the GEK result on other days a different approach is used. On four separate intervals of at least two full days, the tidal height change per cycle is plotted against the GEK quasi-slack potential, i.e. figure F.5 against figure R.1. This is shown in four graphs on figure F.6. Each graph starts at S and proceeds from slack to slack to the end of that interval, F. A line of 1.1 ft/mv-cycle is included for comparison to the flood and ebb lines between slacks. From these graphs trends can be observed. If there was no drift all lines would pass through zero at the same

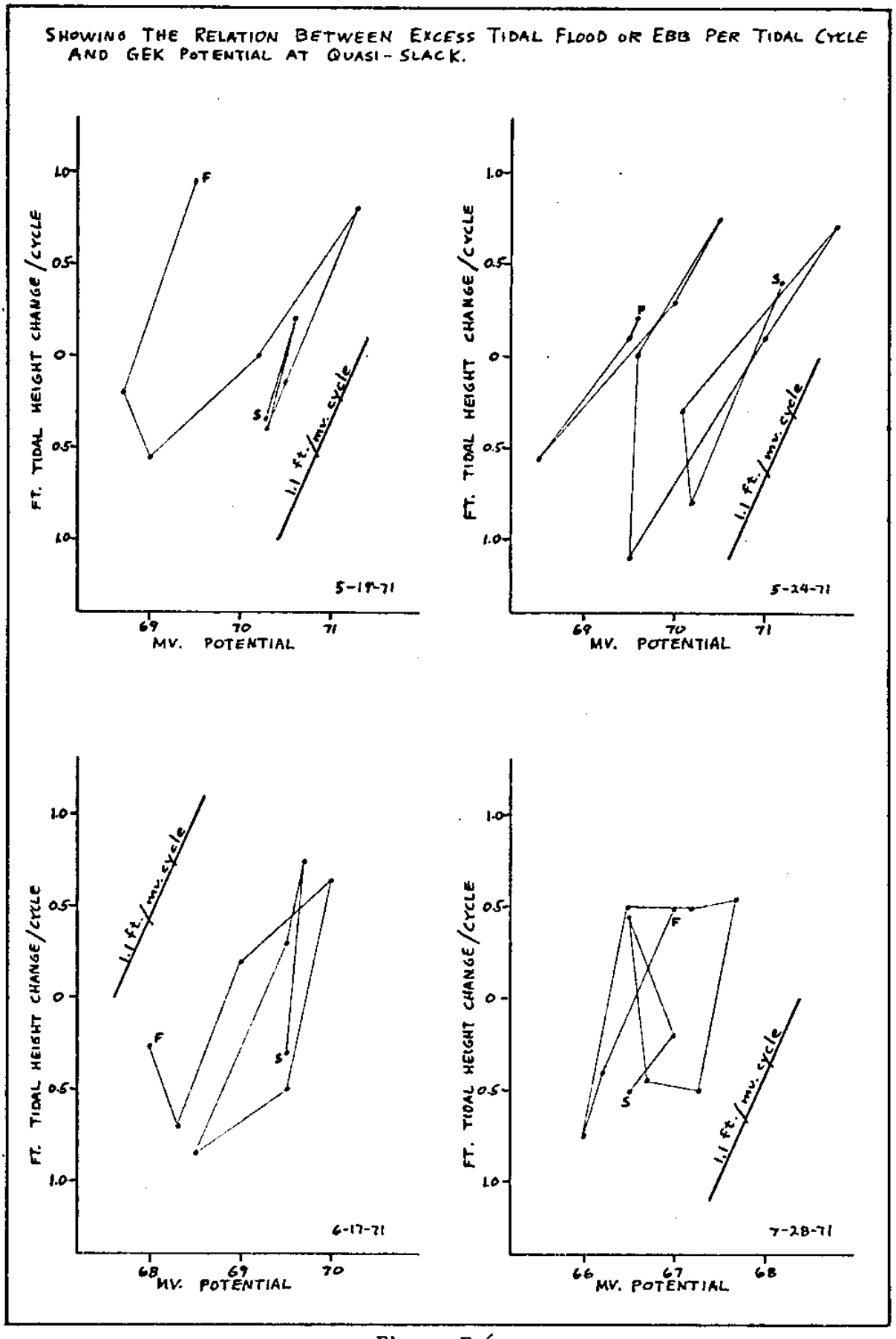
SHOWING THE RELATION BETWEEN EXCESS TIDAL FLOOD OR EBB PER TIDAL CYCLE AND GEK POTENTIAL AT QUASI-SLACK.
FT. TIDAL HEIGHT CHANGE/CYCLE
MV. POTENTIAL
1.1 ft./mv. cycle
5-19-71
5-24-71
6-17-71
7-28-71
F
S

Figure F.6

potential, and the slope of the line would show the difference in total flow through East and West Passage. An example of obvious drift is between the 6th and the 7th slack on the graph for 5-24-71. It is seen that the slopes are in general around 1.1 ft/mv-cycle.

Using the value of 1.1 ft/cycle equals 1 mv quasi-slack potential change, figure F.5 is subtracted from figure F.1 to obtain figure F.7 which is the quasi-slack potential minus the lunar and solar tidal components (and the wind effects). This is the resultant electrode null and its drift throughout the days the GEK was operating. It is seen in figure F.7 that there is still considerable fluctuation.

Water circulating around Conanicut Island

If because of the shape of the Bay or because of the direction of strong winds, water is moved around Conanicut Island, the flood and ebb through West Passage will not be the same. This was mentioned in reference to the slope of the lines in figure F.6. This could cause some of the fluctuation of the quasi-slack but to detect this it would require an accurate means of determining day to day flow through East Passage and possible through the Sakonnet River narrows. This was not done and is an important reason to include GEK instruments in these areas if further data is taken in the future.

Magnetic field changes

The effect of fluctuations in the Earth's magnetic field are examined in appendix J. Long term magnetic drift only affects the amplitude of the GEK output and is only 0.03% per year. The only fluctuations that would affect reading the quasi-slack potentials are magnetic storms. Large ones such as in figure J.8 of appendix J make it difficult to find the quasi-slack when using a planimeter.

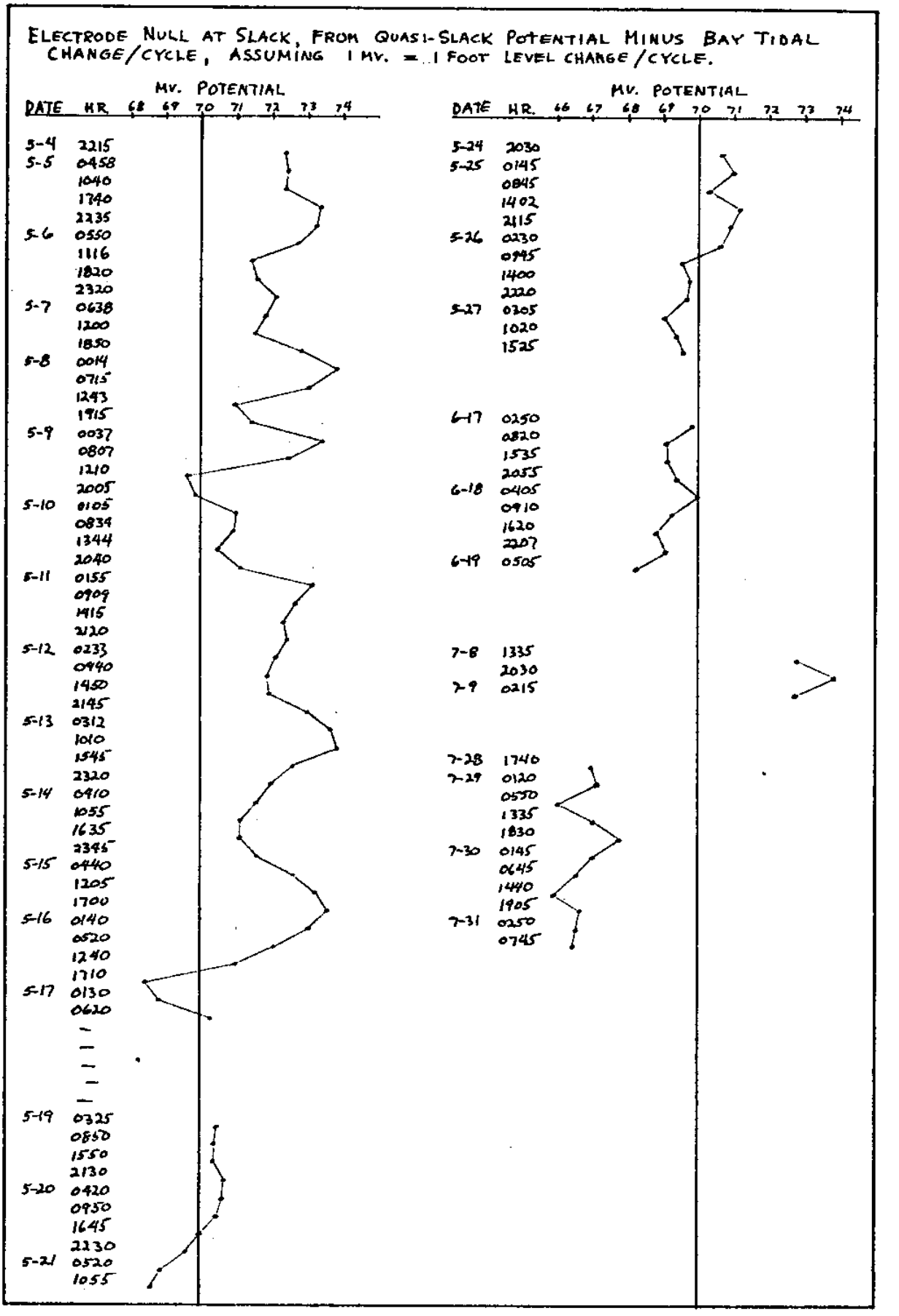
ELECTRODE NULL AT SLACK, FROM QUASI-SLACK POTENTIAL MINUS BAY TIDAL CHANGE/CYCLE, ASSUMING 1 MV. = 1 FOOT LEVEL CHANGE/CYCLE.
MV. POTENTIAL
DATE HR. 68 69 70 71 72 73 74
5-4 2215
5-5 0458
1040
1740
2235
5-6 0550
1116
1820
2320
5-7 0638
1200
1850
5-8 0014
0715
1243
1915
5-9 0037
0807
1210
2005
5-10 0105
0834
1344
2040
5-11 0155
0909
1415
2120
5-12 0233
0940
1450
2145
5-13 0312
1010
1545
2320
5-14 0410
1055
1635
2345
5-15 0440
1205
1700
5-16 0140
0520
1240
1710
5-17 0130
0620
5-19 0325
0850
1550
2130
5-20 0420
0950
1645
2230
5-21 0520
1055
MV. POTENTIAL
DATE HR. 66 67 68 69 70 71 72 73 74
5-24 2030
5-25 0145
0845
1402
2115
5-26 0230
0945
1400
2220
5-27 0305
1020
1525
6-17 0250
0820
1535
2055
6-18 0405
0910
1620
2207
6-19 0505
7-8 1335
2030
7-9 0215
7-28 1740
7-29 0120
0550
1335
1830
7-30 0145
0645
1440
1905
7-31 0250
0745

Figure F.7

It appears that during magnetic storms the signal was erratic enough to question any quasi-slack potentials obtained during that time. These times are shown in figure F.8.

Intervals of an unsteady signal having a period of 30 minutes to one hour also seem to be an occasional problem. They appear similar to magnetic interference but do not seem to be related when compared to the corresponding magnetic record.

Long term quasi-slack variations

Miscellaneous electrical problems

Definite breaks in the wires and shorts to ground were easily detectable on the GEK since a short to ground would produce about 1.1 volts and a break would make the recorder go off scale in either direction. Many times there appeared a discrete signal jump that would not go off scale, but deflect by a couple of millivolts, which might, but not always return to a normal value sometime later. Several of these are shown GEK recordings in figure F.9. The effect they have on the quasi-slack is shown in figure F.8 where their magnitude and polarity correspond with the change in quasi-slack potentials.

These were a serious problem in the operation of the GEK and may be related to minor resistance leakage in the instrument and wires. It was not possible to relate any specific signal jump to a particular cause, but in general they seemed to become more frequent later in the season and during times of rain and fog. At times the underwater connectors seemed to be moist when opened and the wires that were laid over the bridge developed breaks in the insulation from chaffing. Vandalism, malicious or otherwise, was also a problem and it is possible that all the damage to the wires was never found. The method of stringing the wire made it difficult to inspect it visually.

SHOWING EVENTS THAT MAY CONTRIBUTE TO THE FLUCTUATION OF THE ELECTRODE NULL AT SLACK.

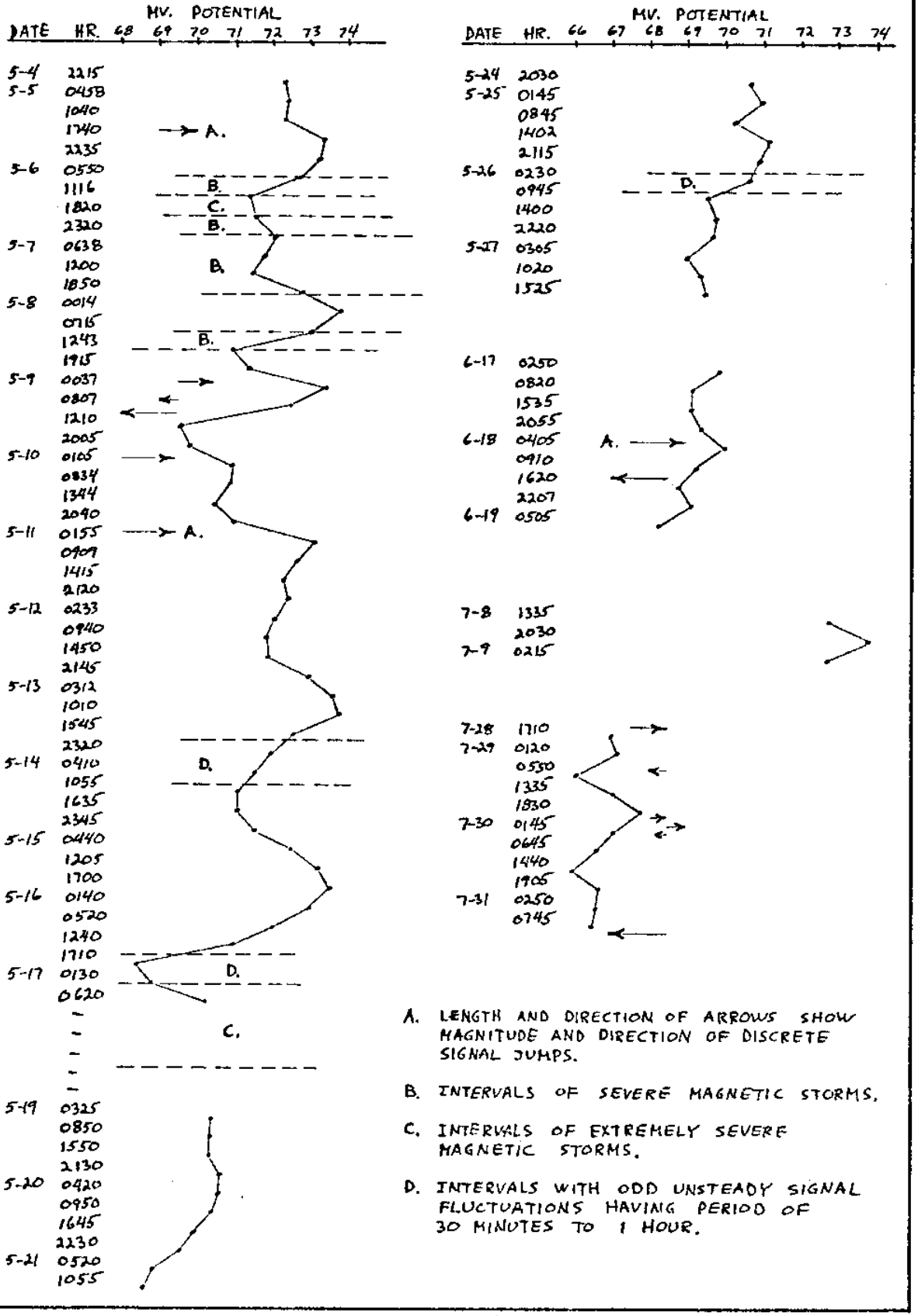

A. LENGTH AND DIRECTION OF ARROWS SHOW MAGNITUDE AND DIRECTION OF DISCRETE SIGNAL JUMPS.

B. INTERVALS OF SEVERE MAGNETIC STORMS.

C. INTERVALS OF EXTREMELY SEVERE MAGNETIC STORMS.

D. INTERVALS WITH ODD UNSTEADY SIGNAL FLUCTUATIONS HAVING PERIOD OF 30 MINUTES TO 1 HOUR.

Figure F.8

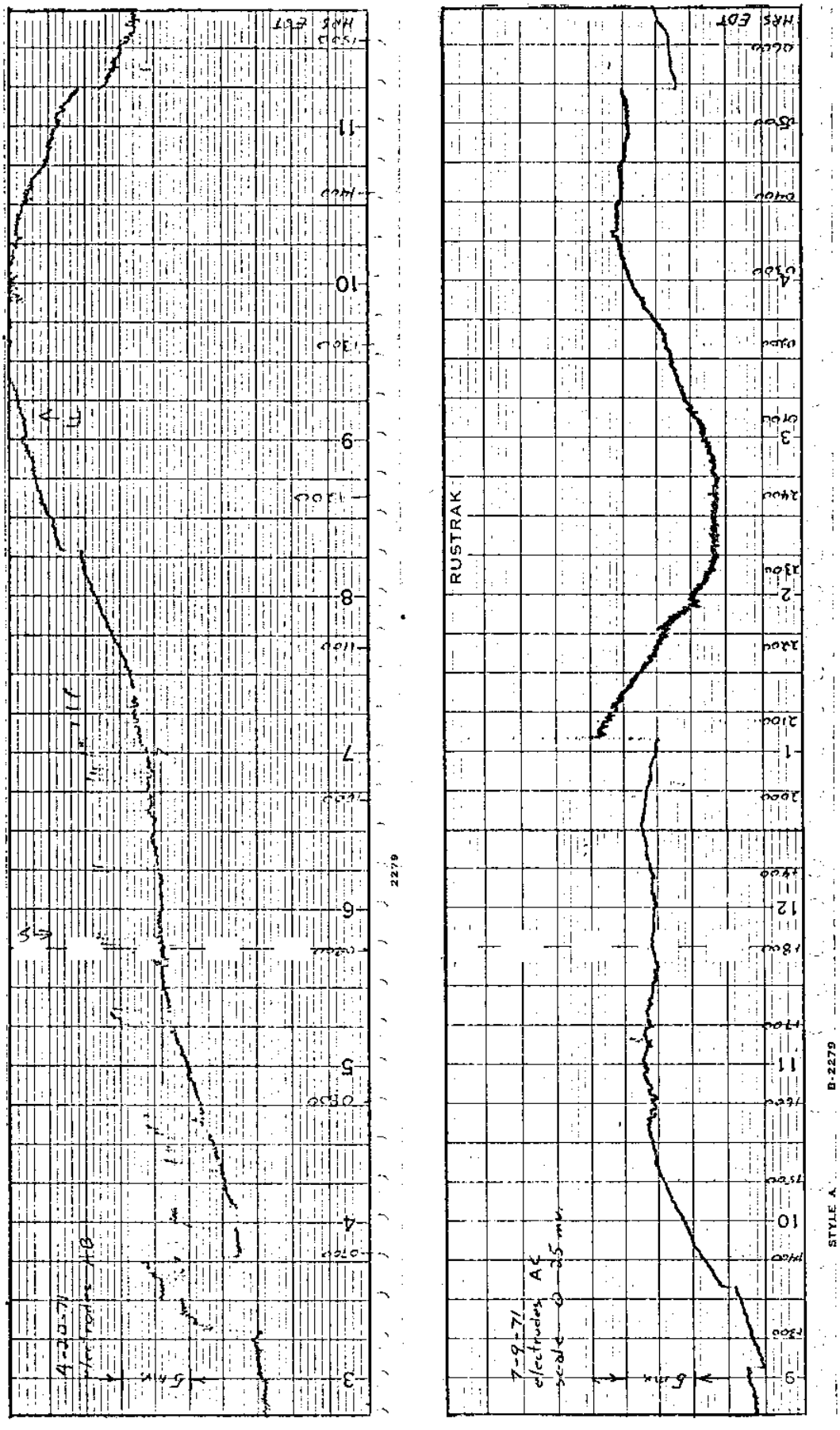

Figure F.9--Two types of electrical disturbances that were not explained.

Instrument and electrode drift

Instrument drift was small enough to be unobservable in the laboratory. The GEK operated on batteries all the time it was recording in the West Passage. Since the electrode switching relay will not switch when the batteries drop below 15.5 volts, and the amplifier will still operate at this voltage, it is obvious on the GEK record when the battery voltage becomes low. The bias battery could cause the recorder to drift but the mercury batteries are very stable and the current drain is only 80 microamps. The recorder was checked at least every other day and a bias check was made, no drift was observed. The temperature sensitivity of the recorder was checked with just the bias on and a shorted (zero) input, by moving the instrument from room temperature to below freezing and back to room temperature. The results are shown in figure F.10 and were reversible.

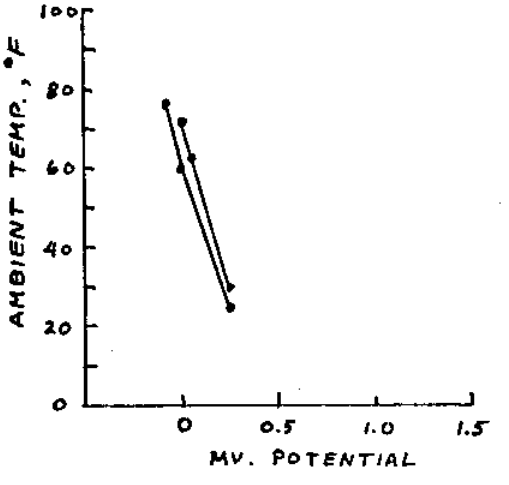

Fig. F.10--Temperature sensitivity of the GEK recorder.

This shows that for temperature drops down to freezing, the error will be only around 0.3 mv and can be neglected because in a

normal day the temperature will not vary more than about 20° F, or equivalent to an error of 0.15 mv.

The drift of the offset potential of the electrode pairs was a difficult value to measure on location beacuse it required first taking one electrode up and transporting it across the bridge. Then the other electrode was removed from the water and both of them were attached to a paired jumper and placed back into the water. The recorder, being portable, was brought 450 feet down to the shoreline and the readings were taken. This whole operation including reinstalling everything would take at least one hour. Needless to say, the electrodes were disturbed from their environment. The few times this was done indicated that the offset potential was approximately zero each time, but the only times that it was checked was when severe noise or step changes occurred on the record. There were many times when the electrodes were shorted to ground and many times when they were subjected to the ground potential because of operation slips, connector failures, wire failures or vandals. So it is difficult to determine what the actual offset voltage was between the electrodes, but it would not be too inaccurate to state that any drift was slow and would tend to go toward zero when the system was operating properly.

The long term drift of the electrodes and the bias was checked under laboratory conditions and it is shown in figure F.11. The electrodes were the ones deployed in the passage; A on the west side, B on the east side. The test was run after the bias batteries were used for one year and the electrodes had been in the Bay about 10 months. It shows that the drift rate stabilizes quite fast once it reaches its normal value. The reason for the initial - 4 mv offset was not determined.

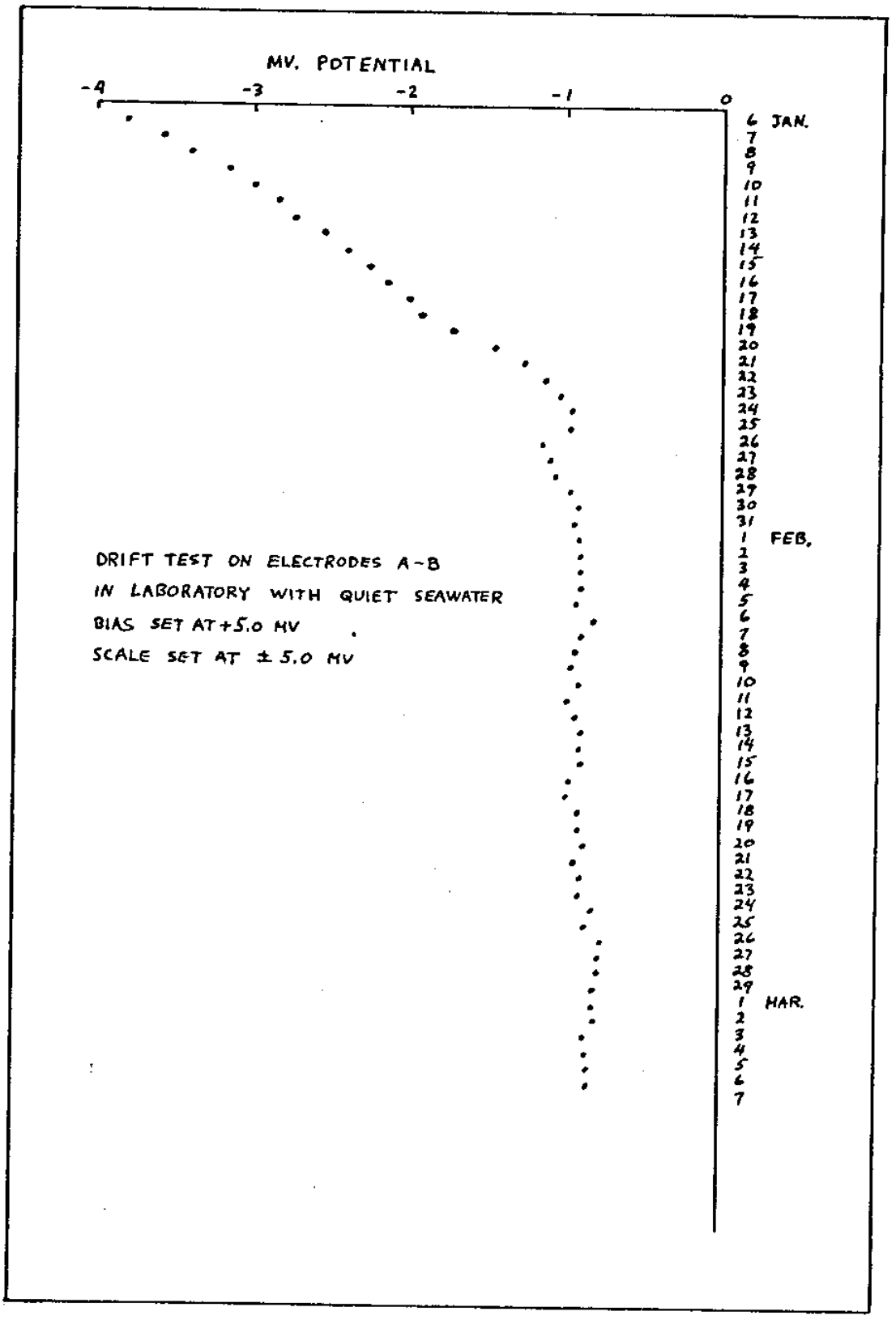

Fig. F.11--Drift test on electrodes A-B in laboratory.

Telluric potentials

Related to the long term magnetic variations are the earth currents (telluric currents) which are not only natural, but manmade in some cases. In the particular location at the Jamestown Bridge, large ground potentials exist and the effect they have on the GEK is to offset the tidal potentials by a DC value of approximately 70 mv. Since the transformers for the bridge lights were only 460 feet from the east electrode, any electrical leakage from the transformers might be contributing to the ground potential.

To examine the nature of the earth currents, two similar ground rods were driven into the earth, one about 100 feet up on the west shore, the other inside the GEK instrument cage about 420 feet up on the east shore of the passage. These recorded the ground potential across the passage for a period of 10 minutes every hour. After one week, the probes stabilized and a noticable drift stopped. From measurements with ammeters and an oscilliscope it was found that the ground potential was much larger than that recorded by the GEK electrodes. About 500 mv potential was present so a voltage divider, shown in fig. F.12, was used to enable approximately 70 mv of the signal to be read on the recorder scale. An automatic switching circuit enabled alternate reading of the GEK electrodes and the ground potential.

This was a simple way to obtain a comparison, but suffers from the fact that any variation in the 500 mv ground potential was reduced to approximately 14% of its original value when recorded. (The final ratio was 1: 7.64.) Even so, two conclusions were observable. Figure F.13 shows the variation in ground potential for a period of 12 days. It shows that the earth currents are definitely subject to the tides

and that any long term change would be better observed on the GEK recordings themselves.

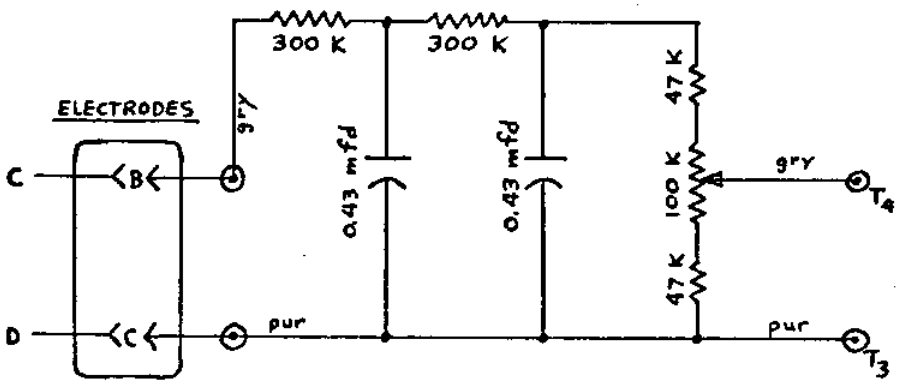

Fig. F.12--Voltage divider to enable the ground potential to be recorded on the GEK recorder.

Figure F.14 shows a comparison of actual potentials between the GEK and ground probes using hourly values. The magnitude of variation is similar as would be expected, both being produced by the tidal velocity, but there is a noticeable phase difference. Even though the readability of the ground probes limit its accuracy in figure F.14 to about 1.5 mv while the GEK is readable to 0.2 mv, the phase lead of the ground probes seems valid.

This shows that the telluric potential, either as a long term drift or short term fluctuation, is a very difficult quantity to determine and may be almost impossible to predict. Included in this difficulty is the fact that a DC signal is found when only AC power is in the locality. The GEK recorder at several times recorded a steady signal. This appeared when the installation was first operated and was due to the bridge road lights being on. This appeared as a steady DC signal and sometimes with a slow drift. The needle on the recorder

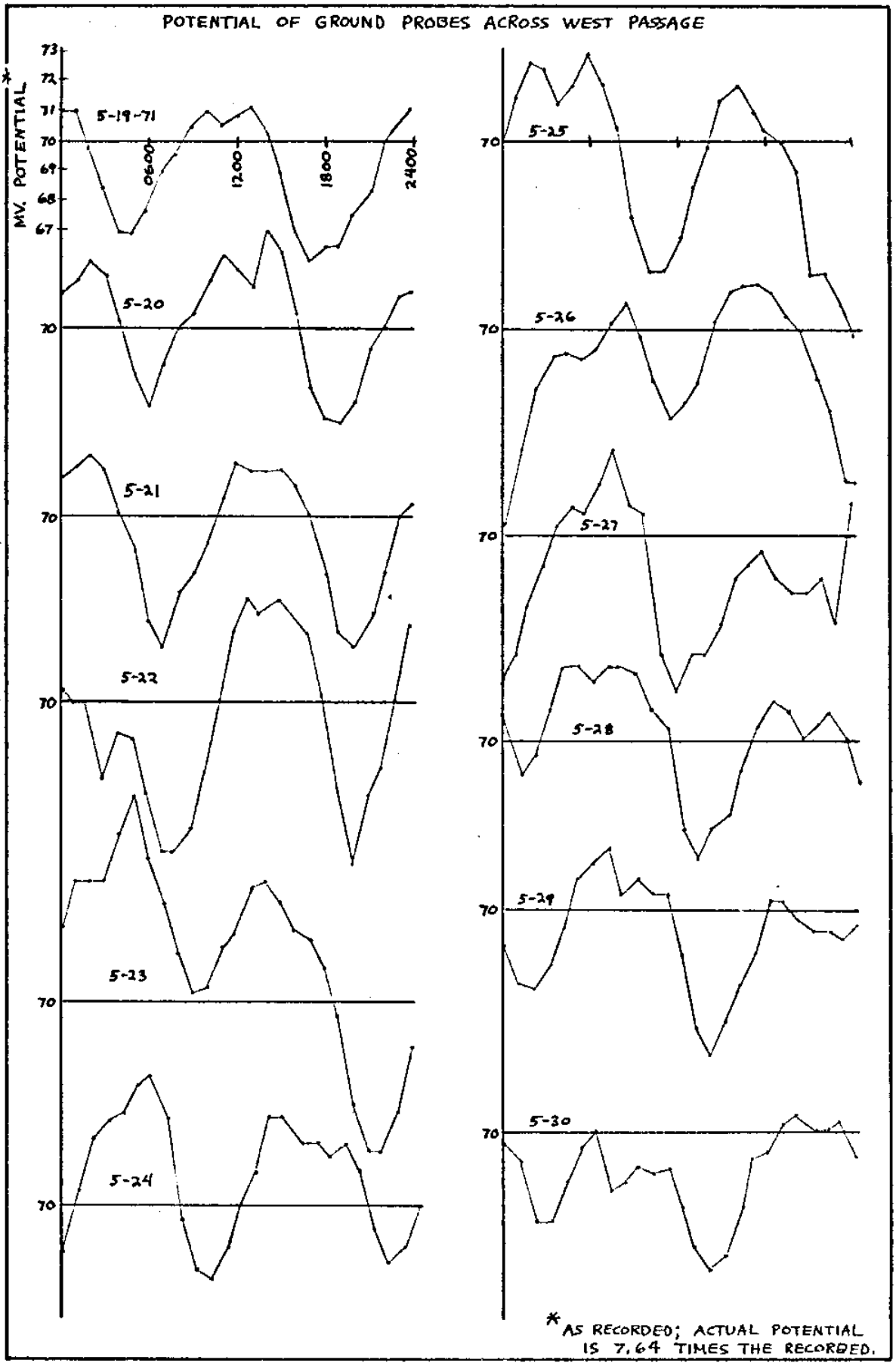
POTENTIAL OF GROUND PROBES ACROSS WEST PASSAGE
MV. POTENTIAL *
73
72
71
70
69
68
67
5-19-71
0600
1200
1800
2400
5-20
5-21
5-22
5-23
5-24
5-25
5-26
5-27
5-28
5-29
5-30
* AS RECORDED; ACTUAL POTENTIAL IS 7.64 TIMES THE RECORDED.

Figure F.13

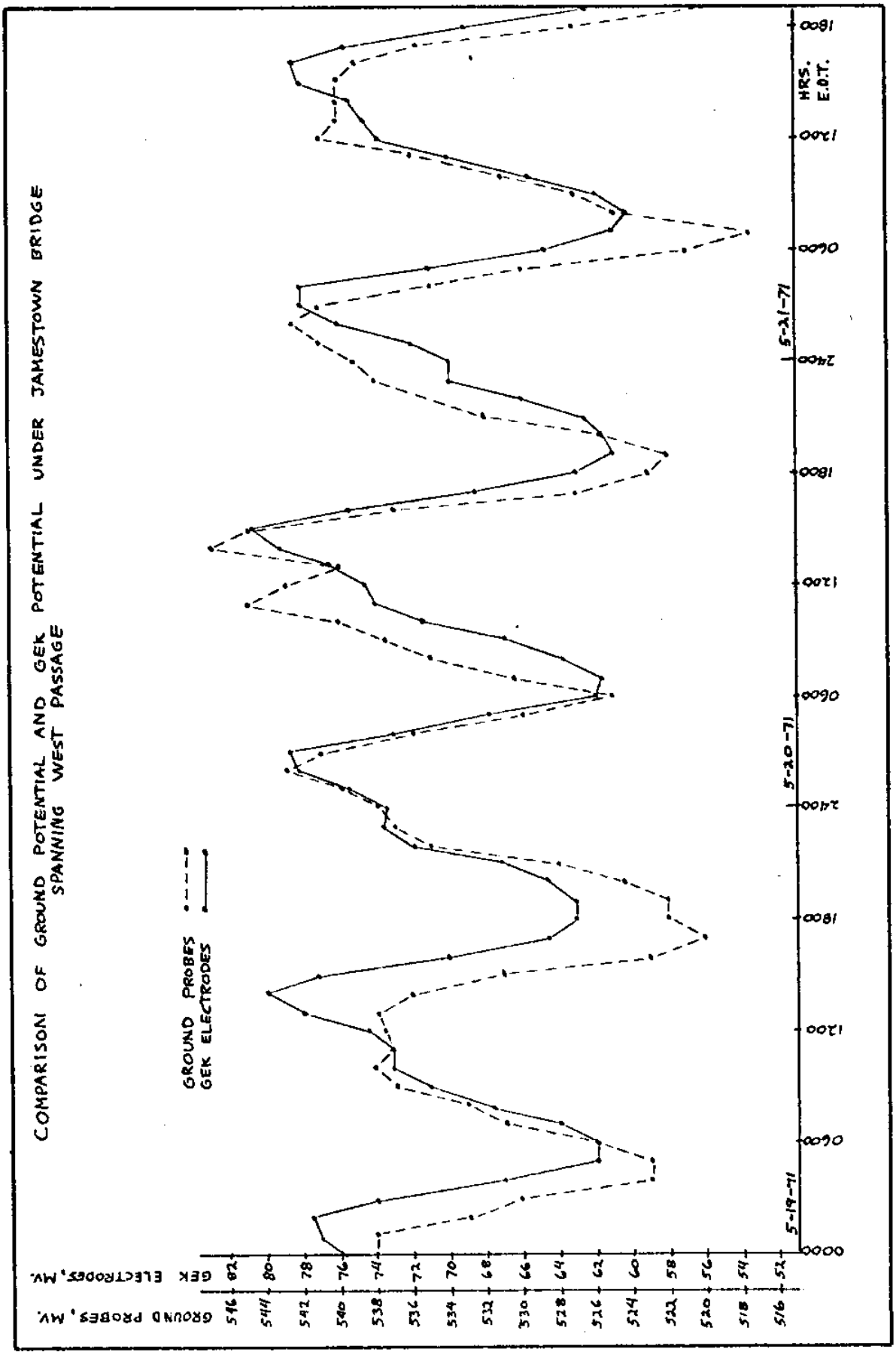
COMPARISON OF GROUND POTENTIAL AND GEK POTENTIAL UNDER JAMESTOWN BRIDGE
SPANNING WEST PASSAGE
GROUND PROBES
GEK ELECTRODES
GROUND PROBES, MV.
GEK ELECTRODES, MV.
HRS. E.D.T.
5-19-71
5-20-71
5-21-71

Figure F.14

during this time would vibrate so as to appear a blur. An example of this is shown in figure F.15. The phenomenon was removed when a filter with a longer time constant was inserted in the amplifier feedback. The needle was then steady and no change was observable when the lights would go on or off.

It was also found that it was possible to eliminate the phenomenon by removing a coil of excess input cable that was stored on top of the instrumentation case. It was later stored about 12 feet away from the case and in a direction away from the bridge lighting power transformers. These transformers which supply power to the lights on the bridge were only 15 feet from the GEK instrumentation and were unavoidable. The fact that the GEK instrumentation could produce a DC signal from the induced potential of an AC magnetic field increases the difficulty in determining the true telluric potential.

The signal from the GEK electrodes was checked for various AC signals that might be present. The check was made with an oscilliscope during the daytime and the results are shown below. The causes of these signals were never determined.

Peak frequencies	DC signal volts	AC signal volts
1.38 M Hz	+ .09	± .15
125. K Hz	+ .09	± .15
17.5 K Hz	+ .07	± .12
60. Hz	nil	nil

Unaccounted drift and quasi-slack accuracy

After having examined the quasi-slack variations and accounted for as much as possible with the information available, figure F.8

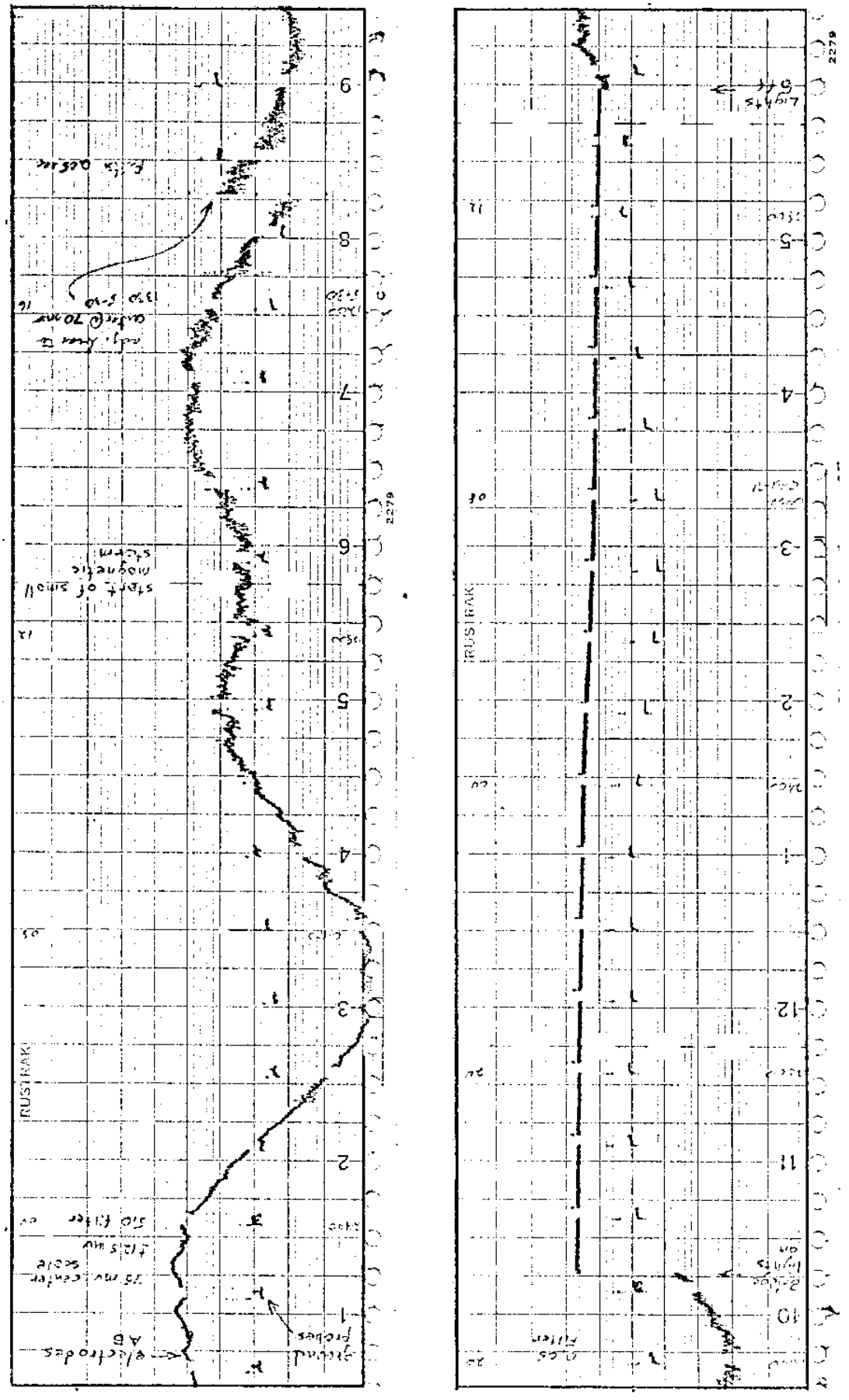

Figure F.15--Effect of bridge lights on CEK recording.

shows the final unaccounted drift of the electrode null at slack tide. The fact that inherent electrode drift is very slow, leaves the possibility of telluric potential variations and thermal variations between the electrodes as the cause of the unaccounted drift. The telluric potentials are not able to be observed except by observation of the GEK signal itself and will always be a problem that must be examined at each GEK site. The difference in temperature between electrodes is a problem that could have been solved easily by placing the electrodes deeper in the water and insulating them against sudden temperature changes.

This uncertainty in the electrode null at slack makes it necessary to do a partial calibration each time an accurate slack potential is needed. Upon examination of the actual slack from the calibration, the quasi-slack from figure F.1 and the electrode null from figure F.7, during the two days the GEK was calibrated, an approximate error can be obtained if either is used in lieu of the actual slack. Table F.2 shows the results. The quasi-slack and electrode null points are shown on figures E.16 and E.17 for comparison. From table F.2 it is seen that although the computed electrode null obtained from figure F.7 seems to have a more consistent error, both systems have errors in the range of 10% of the actual tidal velocities.

To look at the overall problem of measuring tidal mass transport, it is seen that although the gross tidal transport may be measured to an accuracy of 10% of the total flow, the net transport is much more difficult to measure. If net transport is defined as the excess tidal flow over a full tidal cycle, it is observed from the GEK data that this could be around 10% of the gross tidal flow. (This value can be found if a rough comparison is made between the full

Table F.2

Velocity error if the quasi-slack or electrode null is used in lieu of the actual slack

Date	Quasi-slack time	mv potential		Difference	
		Actual slack	Quasi-slack	mv	knots
6-17-71	0820	68.5	69.7	- 1.2	- 0.112
	1535		69.5	- 1.0	- 0.094
	2055		68.5	0	0
			Electrode null		
	0820		69.2	- 0.7	- 0.066
	1535		69.2	- 0.7	- 0.066
	2055		69.4	- 0.9	- 0.085
			Quasi-slack		
7-8-71	0810 ?	73.5	NA		
	1335		73.5	0	0
	2030		73.8	- 0.3	- 0.028
			Electrode null		
	0810 ?		NA		
	1335		72.8	+ 0.7	+ 0.066
	2030		73.8	- 0.3	- 0.028

tidal range and the average tide height change in figure F.4 from slack to slack.) In this case a 10% accuracy in net transport would necessitate determining the actual average slack potential to 1%. With the variables involved it would be an improbable task. Consider the temperature variation between the electrodes; to achieve this accuracy would mean regulating or knowing the temperature

difference to within 0.2° C. Consider the difficulty in observing the horizontal and vertical profiles of the tidal velocity during the calibration of the GEK. If during ideal conditions the GEK measured the average water velocity within 1%, it is shown in figure H.2 that the average mass velocity might still be in error by 5%.

With the above considerations, the results using the quasi-slack method of finding the electrode null can be expected to have an error of 10% if the electrodes are compensated for temperature differences. If the electrodes are not compensated (or insulated) as was the situation in this installation, the error could be as much as 20% at times.

APPENDIX G

COMPARISON WITH PREDICTED TIDES

With the limited data obtained from the GEK and the analysis by using the quasi-slack, the accuracy of the predicted slack times, predicted maximum ebb times and the predicted maximum flood and ebb velocities will be examined.

The predicted values of the tides were obtained from the U.S. Coast Guard Tide Tables and the Tidal Current Tables (1971). The predicted slack times were determined for two areas. From the tidal current tables the nearest substation is the area west of Dutch Island in the West Passage. This is close enough to the Jamestown Bridge so there should be no difference in the slack times. The other is the predicted high and low water times at the Newport Harbor in the East Passage. This was used because of a general belief that these high and low water times give actual slack times at the Jamestown Bridge with less orror.

The comparison of GEK quasi-slack times against the predicted times is shown in figures G.1 and G.2. Two results are obvious; the scatter in the data and the average value is displaced so as to have the predicted slack later than the GEK slack. The figures show that the predicted times are at times quite far from the actual slack, and in general the low tide times are more inaccurate than the high tide times. These quasi-slack times are probably accurate to within 15 minutes of the actual slack times. This is seen from examining the

calibration chart on figures E.16 and E.17. An error of 1 mv (15% error in tidal transport) in the quasi-slack potential only produces an error of 10 minutes in the slack time because of the fast deceleration and acceleration of the velocities through the slack times. The local belief that the Newport high and low tides are the better values appears true, but not by much and the data scatter is not much less.

The predicted time of maximum ebb is compared in figure G.3 This time is easy to obtain from the GEK and is not dependent on the electrode null. The times obtained from the GEK can only be accurate to the nearest 5 or 10 minutes because of the rounded shape of the velocity curve. For similar reasons the maximum flood velocity is very hard to locate; sometimes there are two separate maximum flood velocities and sometimes the maximum flood holds for several hours as in the GEK records on July 8,1917. For this reason it is not possible to compare the flood velocities. Figure G.3 shows a large scatter of values, along with the actual time being later for the predicted maximum ebbs. It is seen that in these three cases the predicted times may be in error by an hour or more from their actual times.

Morse (1957) tried to calibrate a GEK by using the predicted velocities and comparing them against their respective potentials as recorded by the GEK. This method was tried for the West Passage GEK and the results are presented in figures G.4 and G.5. In both cases the scale factors were determined from the ratio of mv potential about the quasi-slack and the predicted velocities in the area west of Dutch Island. It is easily seen on the map of West Passage in figure B.1, the velocities will not be the same at Dutch Island as those at the bridge because the bottom profiles are different and therefore exhibit a

different cross section to the tidal flow. So it is expected that the GEK velocities differ by some proportionality from those at Dutch Island. In figure G.4 it is seen that the flood and ebb scale factors are quite different most of the time. There seens to be a patterm, but not a readily predictable one. In figure G.5 the same data is grouped on a non-time scale. The scale factor obtained from the drifting pole calibration is shown in this figure as a line with a 10.65 mv/kt slope. The line A-A bisects the ebb and flood data, and shows that the higher predicted velocities tend to be flood tides while the lower predicted velocities tend to be ebb tides. This is just the opposite of the tides at the bridge where the ebb velocities tend to be greater than the flood velocities. This could be due to the predicted tidal velocities being wrong or they could be due to the channel geometry in the area of Dutch Island. The data points being displaced to the right would indicate that the tidal currents are greater in the channel west of Dutch Island than those under the bridge. The error band on the GEK quasi-slack potential could be as much as 2 mv.

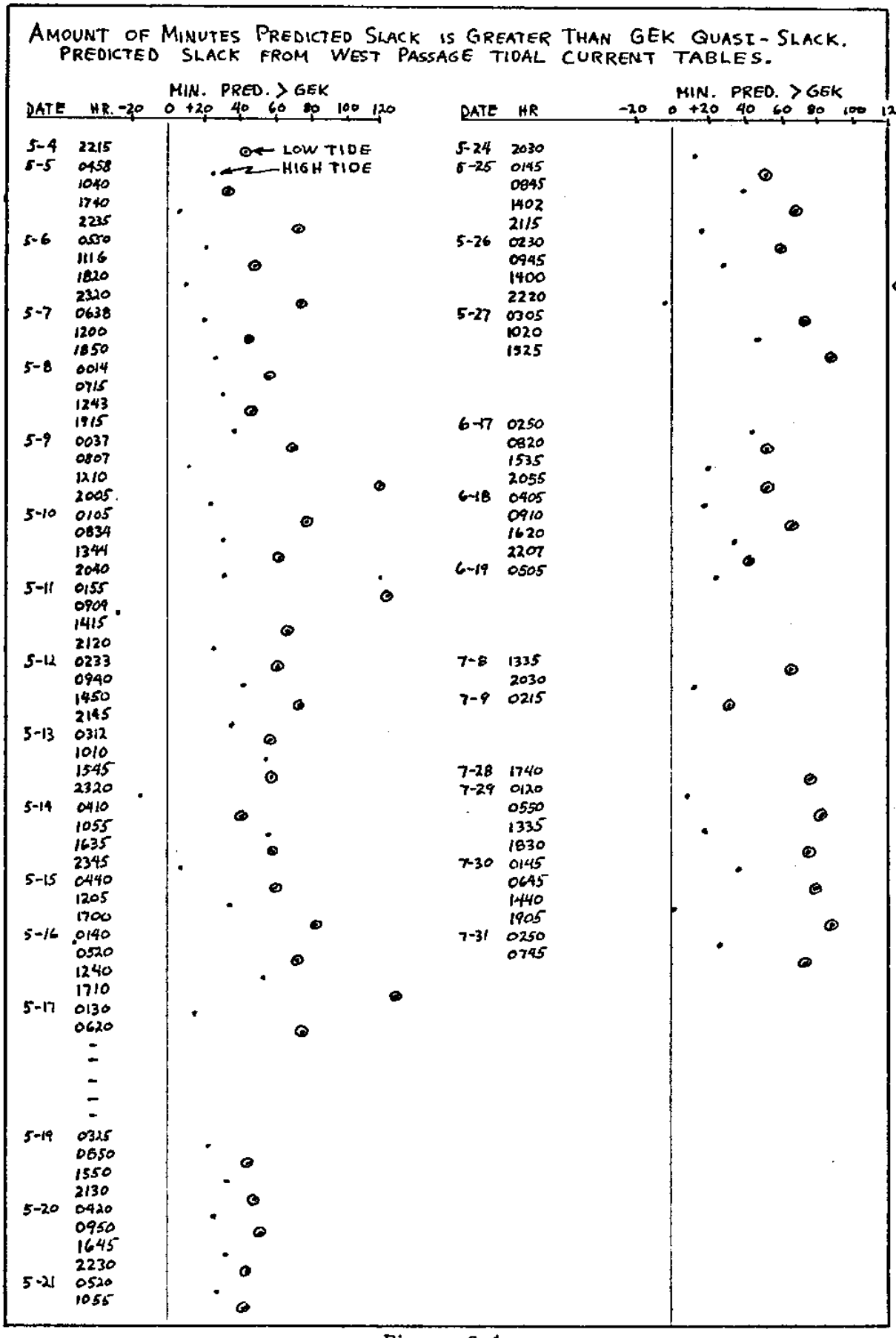
AMOUNT OF MINUTES PREDICTED SLACK IS GREATER THAN GEK QUASI-SLACK.
PREDICTED SLACK FROM WEST PASSAGE TIDAL CURRENT TABLES.
DATE HR. -20 0 +20 40 60 80 100 120
MIN. PRED. > GEK
LOW TIDE
HIGH TIDE
5-4 2215
5-5 0458
1040
1740
2235
5-6 0530
1116
1820
2320
5-7 0638
1200
1850
5-8 0014
0715
1243
1915
5-9 0037
0807
1210
2005
5-10 0105
0834
1341
2040
5-11 0155
0909
1415
2120
5-12 0233
0940
1450
2145
5-13 0312
1010
1545
2320
5-14 0410
1055
1635
2345
5-15 0490
1205
1700
5-16 0140
0520
1240
1710
5-17 0130
0620
5-19 0325
0650
1550
2130
5-20 0420
0950
1645
2230
5-21 0520
1055
DATE HR
-20 0 +20 40 60 80 100 120
MIN. PRED. > GEK
5-24 2030
5-25 0145
0845
1402
2115
5-26 0230
0945
1400
2220
5-27 0305
1020
1925
6-17 0250
0820
1535
2055
6-18 0405
0910
1620
2207
6-19 0505
7-8 1335
2030
7-9 0215
7-28 1740
7-29 0120
0550
1335
1830
7-30 0145
0645
1440
1905
7-31 0250
0745

Figure C.1

AMOUNT OF MINUTES PREDICTED SLACK IS GREATER THAN GEK QUASI-SLACK.
PREDICTED SLACK FROM NEWPORT HIGH-LOW TIDAL HEIGHT TABLES.

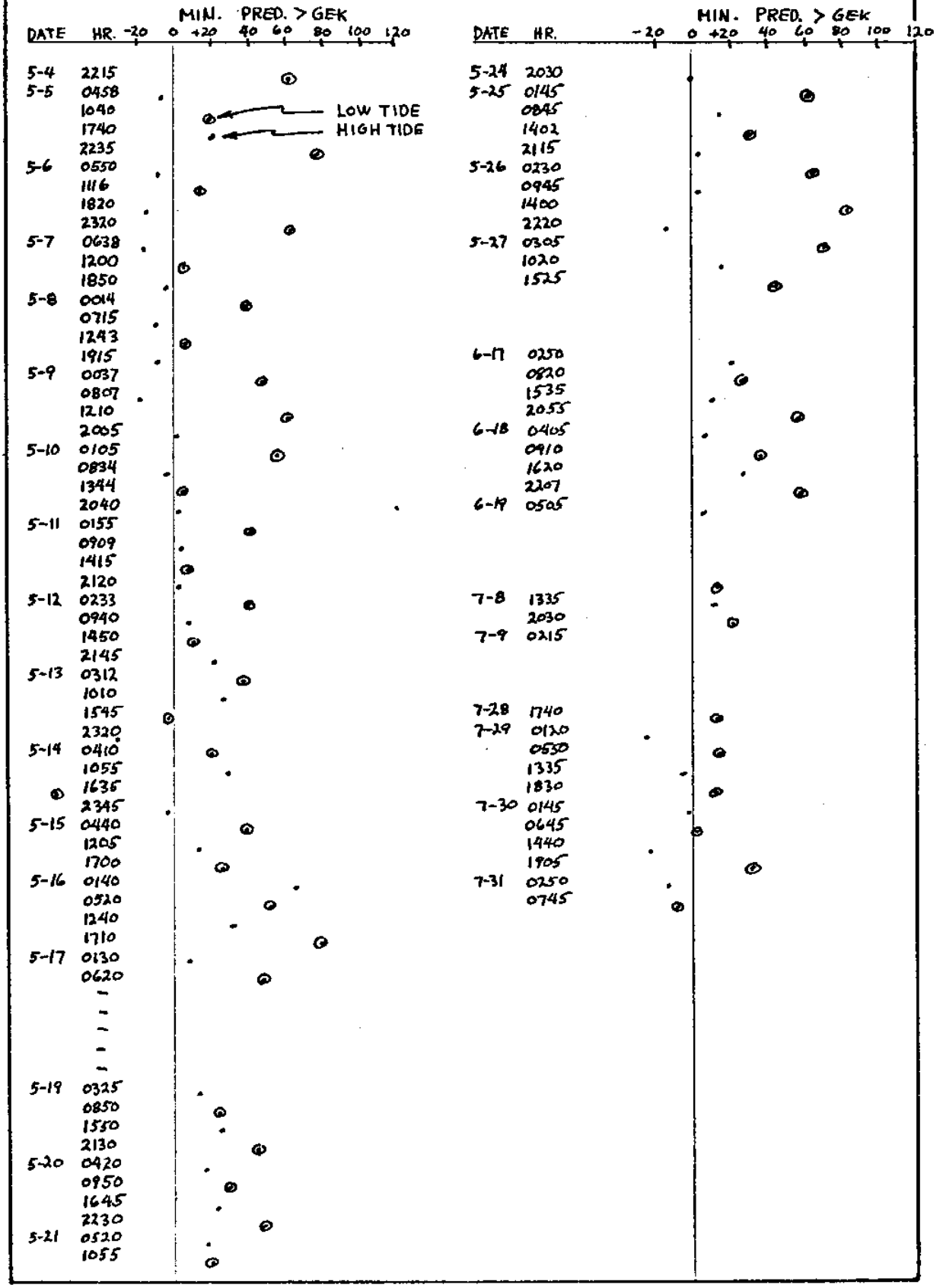

Figure G.2

AMOUNT OF MINUTES PREDICTED MAX. EBB IS GREATER THAN GEK MAX. EBB. PREDICTED EBB FROM WEST PASSAGE TIDAL CURRENT TABLES.

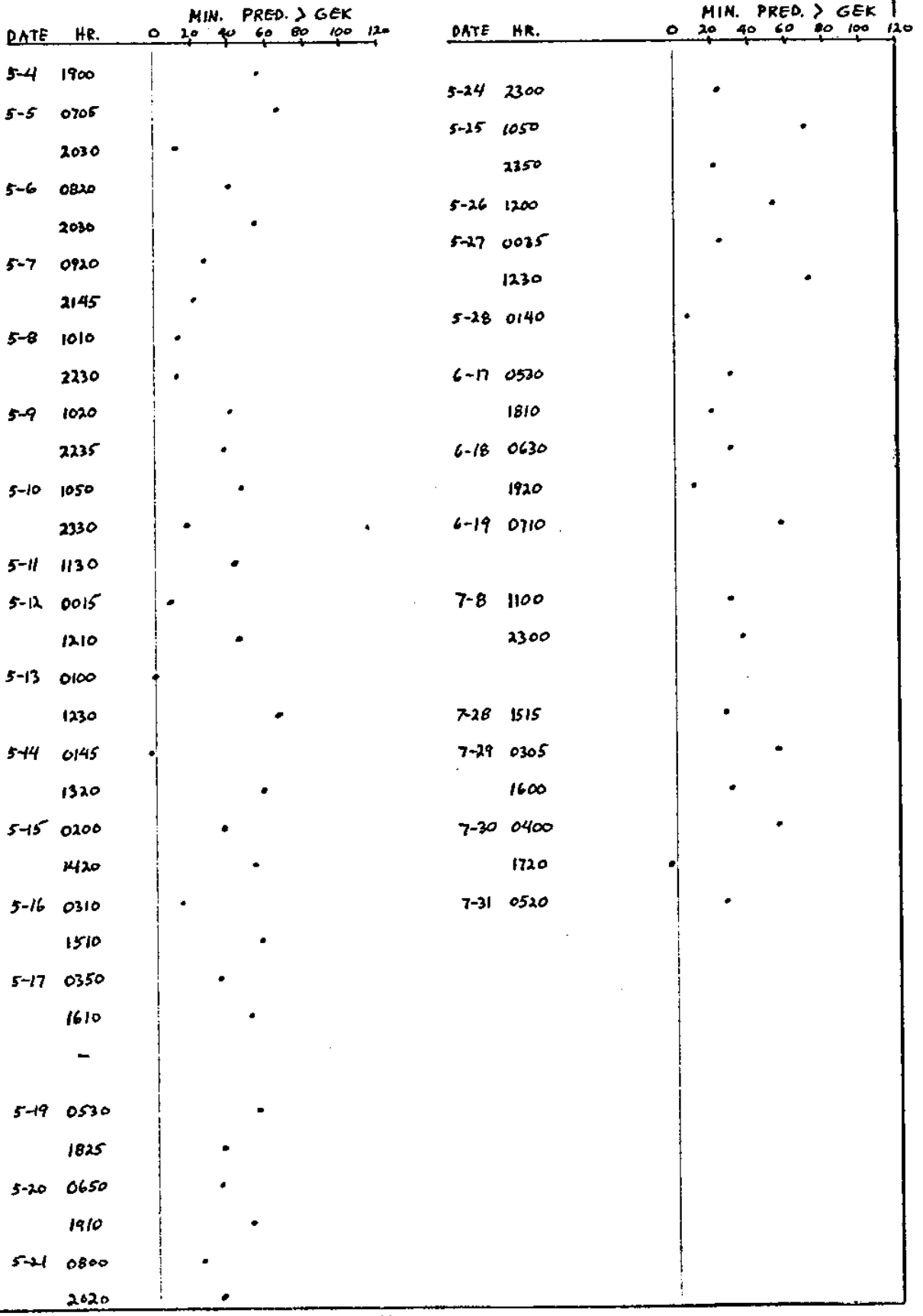

Figure G.3

SCALE FACTORS; FROM GEK POTENTIALS ABOUT QUASI-SLACK AND PREDICTED VELOCITIES IN WEST PASSAGE FROM CURRENT TABLES.

DATE	HR.	mv./kt. 3 4 5 6 7 8 9 10
5-4	2215	EBB
5-5	0468	FLOOD
	1040	
	1740	
	2235	
5-6	0550	
	1116	
	1820	
	2320	
5-7	0638	
	1200	
	1850	
5-8	0014	
	0715	
	1243	
	1915	
5-9	0037	
	0807	
	1210	
	2005	
5-10	0105	
	0824	
	1344	
	2040	
5-11	0155	
	0909	
	1415	
	2120	
5-12	0233	
	0940	
	1450	
	2145	
5-13	0312	
	1010	
	1545	
	2320	
5-14	0410	
	1065	
	1635	
	2346	
5-15	0440	
	1205	
	1700	
5-16	0140	
	0520	
	1240	
	1710	
5-17	0130	
	0620	
	–	
	–	
	–	
	–	
	–	
5-19	0325	
	0850	
	1550	
	2130	
5-20	0420	
	0950	
	1645	
	2230	
5-21	0520	
	1055	

DATE	HR.	mv/kt. 3 4 5 6 7 8 9 10
5-24	2030	
5-25	0145	
	0845	
	1402	
	2115	
5-26	0230	
	0945	
	1400	
	2220	
5-27	0305	
	1020	
	1525	
6-17	0250	
	0820	
	1535	
	2055	
6-18	0405	
	0910	
	1620	
	2207	
6-19	0505	
7-8	1335	
	2030	
7-9	0215	
7-28	1740	
7-29	0120	
	0550	
	1335	
	1830	
7-30	0145	
	0645	
	1440	
	1905	
7-31	0250	
	0745	

Figure G.4

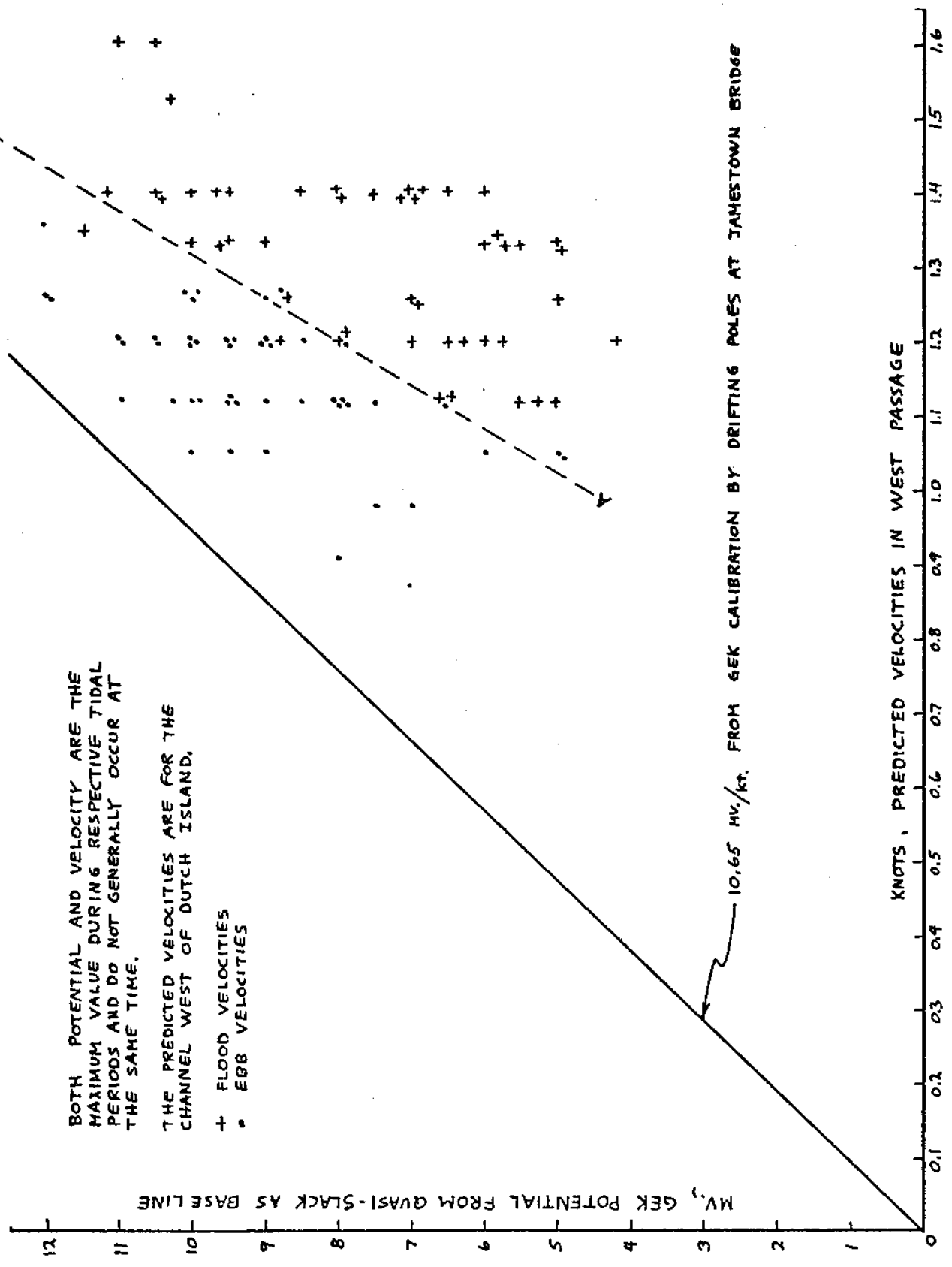

Fig. G.5--Scale factors of figure G.4 plotted on a non-time scale and compared with GEK calibration by drifting poles.

APPENDIX H

ANALYTICAL CALCULATIONS OF POTENTIAL ACROSS WEST PASSAGE

The electromotive force induced by a moving conductor in a magnetic field is equal to,

$$E = (\bar{V} \times \bar{B}) \cdot \bar{L}$$

where, E = emf in volts
$\bar{V}$ = velocity of the conductor in m/sec
$\bar{B}$ = magnetic flux in weber/m^2
$\bar{L}$ = length of conductor in meters

The Earth's vertical magnetizing force H_z at Narragansett Bay is 0.54 oersteds (cgs units), as shown on the U.S. Hydrographic Chart No. 1702. This produced a flux density of,

$$B_z = \mu_o H_z = (1)(0.54) = 0.54 \text{ gauss}$$

where μ_o is the relative permeability of 1 in cgs units.

It is unfortunate that so many systems of units are in use and that many geophysicists interchange the units gauss with oersteds. If the MKS system that is more common to engineering was used, $\mu_o = 4\pi \times 10^{-7}$ and units of flux density would not equal units of field intensity. It is also unfortunate that the tidal velocities are always referred to in knots, and of course all distances are in feet on land. Accepting such difficulties as a normal event, a "nautical" MKS system will be used.

Finding the electromotive force for the GEK across the passage

$$E = (V\bar{j} \times B\bar{k}) \cdot L\bar{i}$$

$$E = B_z L_x V \cos\theta$$

The electrical current direction through the water is

$$\bar{I} = \bar{V} \times \bar{B}$$

$$= V\bar{j} \times B\bar{k}$$

$$= (VB)\bar{i}$$

This shows that the west side of the channel is positive for a flooding tide and negative for an ebbing tide.

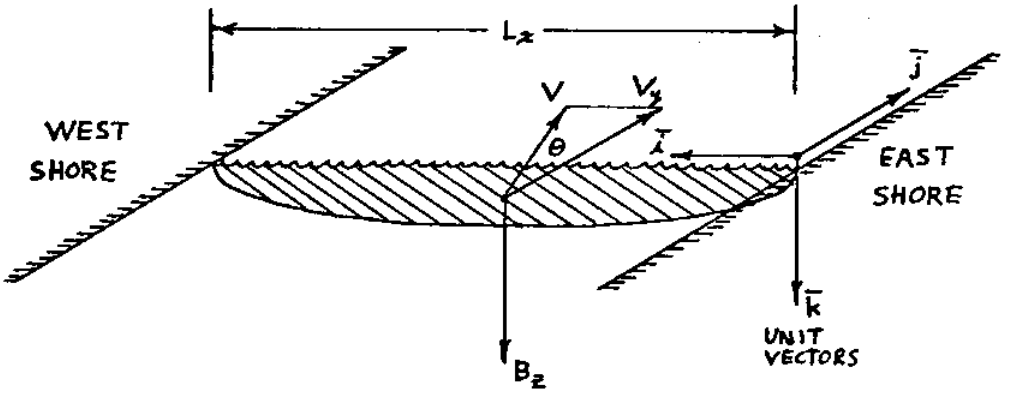

The unit vector i is parallel to the bridge.

$$E = B_z (L_x V_y)$$

$$E = \left(0.54 \text{ gauss} \times 10^{-4} \frac{\text{weber}}{\text{m}^2\text{-gauss}}\right)\left(6400 \text{ ft} \times 0.3048 \frac{\text{m}}{\text{ft}}\right)\left(1 \text{ kt} \times 0.5148 \frac{\text{m}}{\text{sec-kt}}\right)$$

$$E = 0.0541 \text{ volt}$$

$$\frac{E}{\text{knot}} = 54.1 \frac{\text{mv}}{\text{kt}}$$

The actual potential difference ϕ_{AB} across the total channel was 10.65 mv/kt.

Effect of a conducting channel bottom

It is assumed that the loss of potential is due to a conducting channel bottom. To analyse this, a solution will be presented based on an analysis by Longuet-Higgins et al. (1954). Assume that the water velocity is parallel and uniform, the magnetic field H is uniform, the resistivity of the water and channel bottom are uniform and the section of water moving has a width much greater than the depth. The moving seawater induces a horizontal emf in the channel that causes an electrical current to flow across the channel and

return through the sea bottom. This is shown in the sketch below.

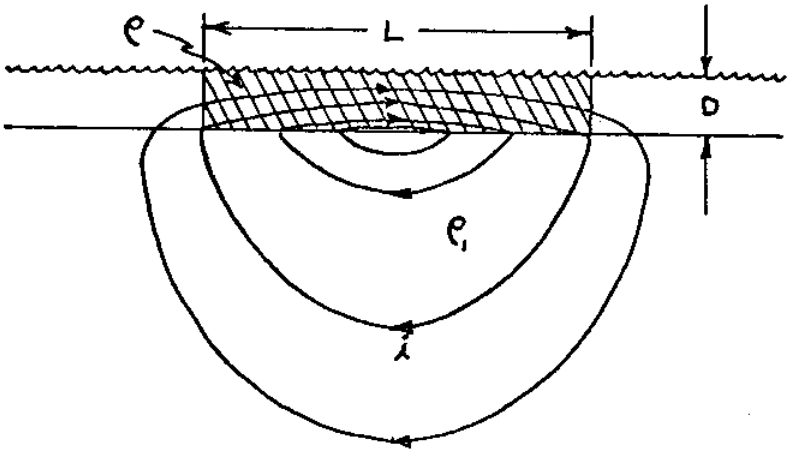

This is analogous to the electrical circuit,

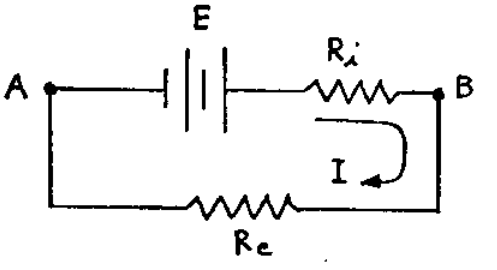

The total current flowing around the circuit is

$$I = \frac{E}{R_\lambda + R_e}$$

and the potential between terminals A and B is

$$\phi_{AB} = I R_e = \frac{E}{1 + R_\lambda / R_e}$$

By analogy the potential across the channel is

$$\phi_{AB} = \frac{E}{1 + \left(\frac{\rho}{D} \frac{D^*}{\rho_1} \right)}$$

with the internal resistance $R_i = \frac{\rho L}{A} \propto \frac{\rho L}{D}$

and the external resistance $R_e = \frac{\rho_1 L}{A^*} \propto \frac{\rho_1 L}{D^*}$

where, D = depth of the channel
D* = effective depth of penetration for the field
A = area of channel as a conductor, proportional to D since channel length is infinite
ρ = resistivity of the water
ρ_1 = resistivity of the channel bottom

So it is seen that the conductivity of the channel bottom depends upon the ratio R_i/R_e. If this ratio is very small the conductivity of the bottom has little effect; if it is very large the potential is effectively shorted out; and when it is in the range of unity the potential gradient is dependent on the channel bottom conductivity.

Effect of a vertical variation of velocity

If the width L of the channel is large compared to its depth D, the direction of the induced emf from H_z will be mainly horizontal and Longuet-Higgins et al. (1954) have shown that the potential gradient is the same as if the water moved with its mean velocity. An electrical circuit analogy can be made where the internal resistance is replaced by a number of electric cells E with resistances R_i, all in parallel across terminals A and B.

Effect of a horizontal variation of velocity

The magnetic field H_x and a velocity that is a function of x will produce an emf of magnitude $B_x D V_x$ in a vertical direction. This will contribute to the current density at any point in the water by the factor,

$$B_x D \left(\frac{dV}{dx}\right)$$

So the relative magnitude of the current densities between the two components is

$$B_x D_z \frac{dV}{dx} \quad : \quad B_z L_x \frac{dV}{dy}$$

Because of the angle of the Jamestown Bridge to the magnetic declination, the $B_x = 0.17 \sin 28^\circ$. The length of the bridge is 6400 ft and the average depth is 28 ft. Hence, the ratio is

$$\frac{B_x D_z \frac{dV}{dx}}{B_z L_x \frac{dV}{dy}} = \frac{0.17 \cos 28^\circ (28) \frac{dV}{dx}}{0.54 \quad (6400) \frac{dV}{dy}} = 0.000\,64 \frac{V_x}{V_y}$$

Therefore for this GEK there will be little contribution to the horizontal current density or to the horizontal potential gradient.

Elliptical channel analysis

Longuet-Higgins et al. (1954) gives the potential for the interior of an elliptical stream as

$$\phi = \frac{E}{1 + \frac{\varrho L}{\varrho_1 2D}}$$

where, L = major axis of ellipse
2D = minor axis of ellipse

This solution is used often when other researchers have needed a theoretical potential produced by an ocean current or tidal estuary. This has been done because it is almost impossible to derive an analytical solution for an exact equation that would describe the variable conditions found in nature. When the ellipse is shallow the equation gives a fairly accurate approximation and it does give a basis of comparison for different situations.

If we compare the elliptical solution with the solution shown for the conducting channel bottom it can be seen that the equivalent depth of penetration of the potential field into the sediment is equal to 1/2 L for the elliptical channel bottom.

A useful term is the "k" factor which can be considered a measure of the GEK installation efficiency and is defined as,

$$k = \frac{\phi_{AB}}{E}$$

which will approximate one if the external resistance R_e is infinite. [This factor is the reciprocal of the "k" defined and used by von Arx (1950).] In the West Passage GEK,

$$k = \frac{10.65}{54.1} = 0.1965$$

To examine the effect of the conducting channel bottom on the loss of signal, the elliptical solution will be used with a modification. The external resistivity consists of different layers of sediment over a bedrock base plus a steel bridge over the passage. To allow for this, let

$$k = \frac{1}{1 + R_i/R_e}$$

and since all the external resistances are in parallel,

$$\frac{1}{R_e} = \frac{1}{R_1} + \frac{1}{R_2} + \frac{1}{R_3} + \cdots$$

the "k" factor will be

$$k = \frac{1}{1 + \frac{R_i}{R_1} + \frac{R_i}{R_2} + \frac{R_i}{R_3} + \cdots}$$

The best available data on the channel bed from Hersey et al. (1961) and Parsons et al. (1938) is reproduced in figure H.1. Bedrock was not reached in the test borings near the west shore, but seismic profiles, 4000 feet north of the bridge, by Birch and Dietz (1962) indicate bedrock at a depth of 100 to 150 feet. This bedrock is composed of metamorphic and granitic rock which has an electrical resistivity from 10^5 ohm-cm for bed-shale to 10^7 ohm-cm for granite. The unconsolidated sediments above the bedrock consist of sands,

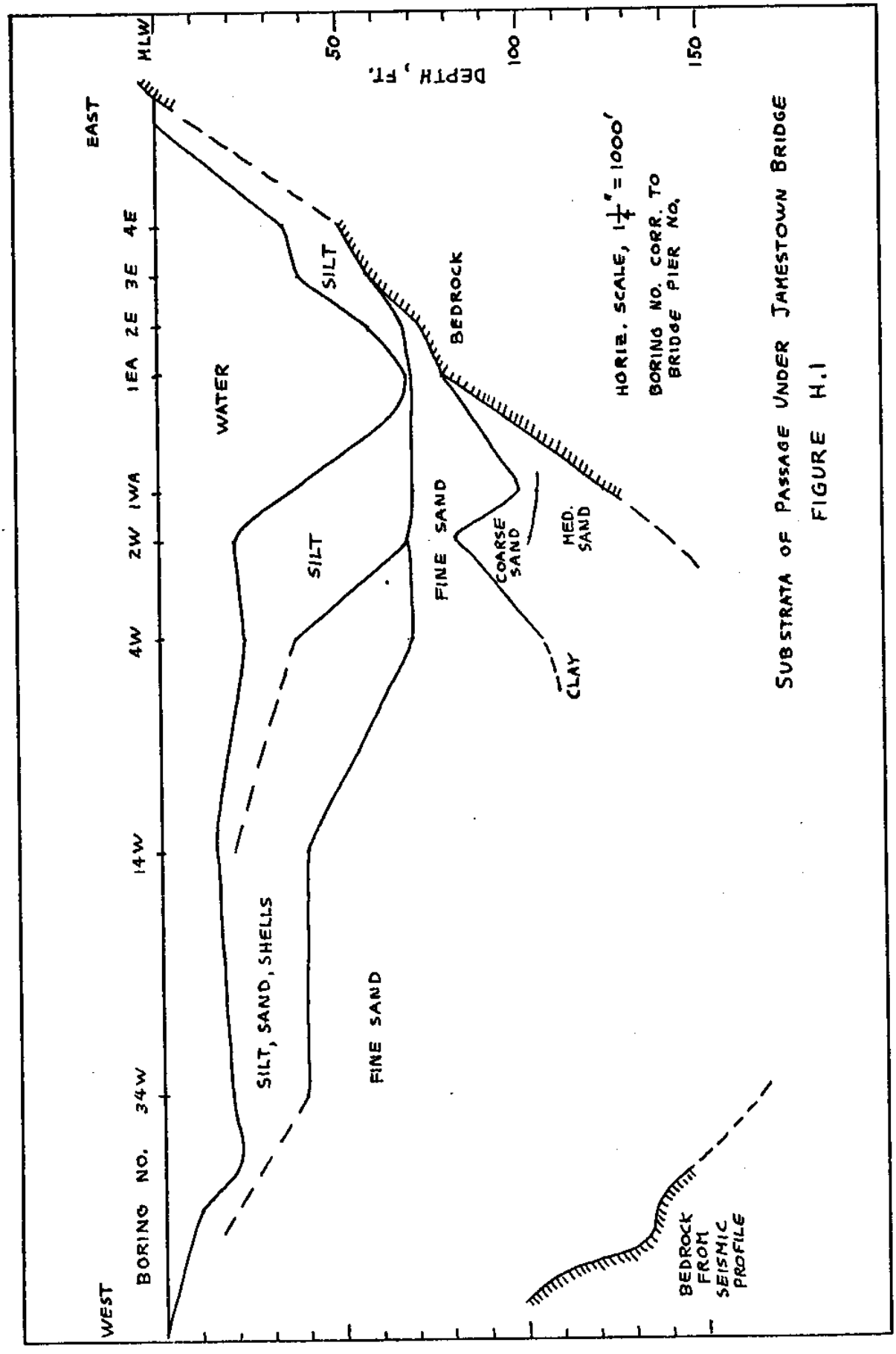

SUBSTRATA OF PASSAGE UNDER JAMESTOWN BRIDGE

FIGURE H.1

soft broken rock, gravel, clay and silt. These have a resistivity from 2 x 10^4 ohm-cm for blue clay to 10^5 ohm-cm for gravel and moist sand. (Hodgman, ed., 1959, p. 2600) The upper layers consist of silty sand and shells which probably are saturated with seawater giving them a resistivity on the order of 10^2 to 10^3 ohm-cm. The layer of silt and sand on the immediate bottom of the channel is around 80 to 120 ohm-cm, (Williams, 1970).

The bridge, although not directly grounded to earth, has many indirect electrical contacts with it because it is a steel bridge with reinforced concrete abutments and piers. The resistivity of such steel is around 20 micro ohm-cm.

For an approximate solution the situation will be treated as an elliptical function where D_e is the depth of the equivalent ellipse and D* is the effective depth of penetration of the potential field which may not be equal to 1/2 L.

$$K = \frac{1}{1 + \frac{\rho D^*}{\rho_1 D_e}}$$

The sketch below shows the situation.

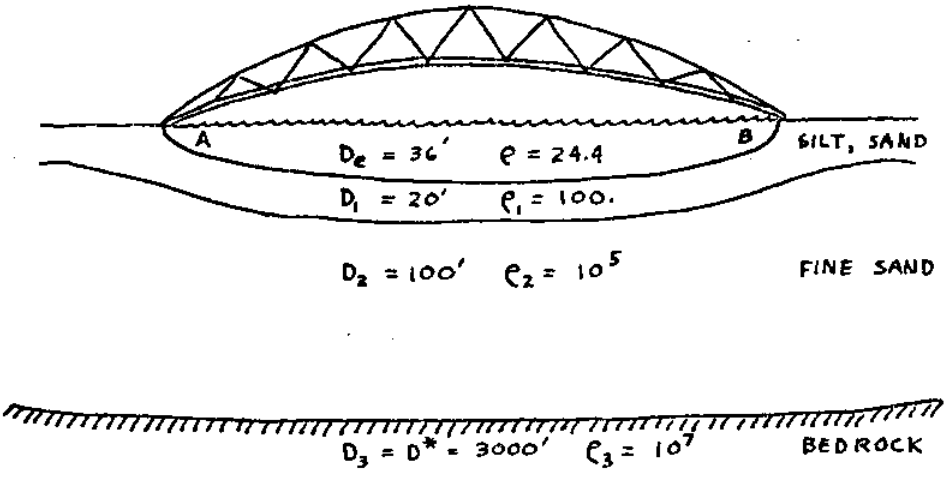

where, L_b = 6400 ft, length of bridge
A_b = cross section of steel bridge
$\rho_b = 20 \times 10^{-6}$ ohm-cm, bridge resistivity

$$D_e = \frac{4}{\pi}\left(\frac{180{,}000\ ft^2}{3200\ ft}\right) = 35.8\ ft$$

Combining the resistivities

$$K = \frac{1}{1 + \frac{R_i}{R_e}}$$

$$K = \frac{1}{1 + \frac{\rho}{D}\frac{D_1}{\rho_1} + \frac{\rho}{D}\frac{D_2}{\rho_2} + \frac{\rho}{D}\frac{D_3}{\rho_3} + \frac{\rho}{D}\frac{A_b}{\rho_b L_b}}$$

$$K = \frac{1}{1 + \frac{24.4}{35.8}\left(\frac{20}{100}\right) + \frac{24.4}{35.8}\left(\frac{100}{10^5}\right) + \frac{24.4}{35.8}\left(\frac{3000}{10^7}\right) + \frac{24.4}{35.8}\left(\frac{A_b}{20 \times 10^{-6} \times 6400}\right)}$$

$$K = \frac{1}{1 + 0.133 + 0.00068 + 0.000203 + 5.3\,A_b}$$

It is shown that effect of the resistivity of the fine sand and bedrock is so great as to allow only a negligible amount of the electric field to pass through the channel bottom deeper than 20 feet. Since the depth of the different sediments is known to a fair degree of accuracy, it can be stated that even if the resistivity is inaccurate to an order of magnitude, this will not effect the factor "k" very much. This means that the electrical field that the GEK measured was being shunted by the upper sediment of silt, sand and by the bridge.

Eliminating the ineffective lower layers of the sediment and the bedrock, the approximate cross sectional area of the steel bridge is found to be

$$K = 0.1965 = \frac{1}{1 + 0.133 + 5.3\,A_b}$$

$$1.133 + 5.3\,A_b = \frac{1}{0.1965}$$

$$A_b = \frac{5.09 - 1.133}{5.3}$$

$$A_b = 0.75\ ft^2$$

This is a reasonable value if the approximate nature of the situation is considered. To find what the GEK might record if the bridge was not present,

$$\phi_{AB} = \frac{54.1 \text{ mv/kt}}{1 + 0.133} = 47.7 \frac{\text{mv}}{\text{kt}}$$

Which shows the drastic effect of the bridge on the GEK signal strength. Supposing that the original estimate of the resistivity of the sediment above the bedrock was entirely wrong and the conductivity of the bridge was negligible. Solving for the resistivity of the sediment with k still equal to 0.1965.

$$0.1965 = \frac{1}{1 + \frac{\rho}{D_e}\left(\frac{100}{\rho_1}\right)}$$

$$0.1965 = \frac{1}{1 + \frac{24.4}{35.8}\left(\frac{100}{\rho_1}\right)}$$

$$0.1965 = \frac{1}{1 + \frac{68.3}{\rho_1}}$$

$$0.1965 + \frac{13.4}{\rho_1} = 1$$

$$\rho_1 = 16.7 \text{ ohm-cm}$$

This is less than that of the water. It is known from Williams (1970) that even under the best conditions, ρ_1 will never be better than 100 ohm-cm. If ρ_1 of the sediment is let equal to 100 ohm-cm it is seen from the above equation that the depth of the sediment would need to be 6 times 100 feet, or a total sediment depth of 600 feet. This is clearly impossible and it must be concluded that the loss of signal is probably due to a large degree to the steel bridge.

From the passage profile in figure H.1 it is apparent that the

resistivity is probably different across the passage and that the channel bottom is not perfectly elliptical. This is verified by the following results.

	Between electrodes	$\left(\frac{\phi}{V}\right)\frac{mv}{knot}$	Electrode distance	$\left(\frac{\phi}{LV}\right)\frac{mv}{kt\text{-}km}$
Total span	A-B	10.65	6400 ft	5.45
Deep half	C-B	6.4	3000 ft	7.06
Shallow half	A-C	4.47	3400 ft	4.31

If the resistance through the sea water is relatively constant with respect to the estimate of the sediment resistivity and if B_z is constant, the variation of (ϕ/LV) is due to differences in sediment resistivity.

$$\frac{\phi}{LV} = \frac{B_z}{1 + R_i/R_e} \propto \frac{R_e}{R_e + \text{constant}}$$

The results show that the shallow half of the channel is more conductive than the deep half. It is not worthwhile to solve for an equivalent sediment resistivity because an accurate resistivity of the steel bridge and exactly how it is grounded to earth are not known.

Effect of a change in the resistivity of the water

It is seen in figure I.1 of appendix I that the resistivity of the water varies from day to day. The calibration of the GEK is dependent upon

$$K = \frac{\phi_{AB}}{E} = \frac{1}{1 + R_i/R_e}$$

which is a function of the external resistivity and the resistivity of the tidal water. The external resistivity remains fairly constant because of the permanent nature of the bridge and sediment, and the fact that the diffusion of the salt water into the sediment is slow.

Since the resistivity of the water can vary as the temperatures and salinity of the tidal water vary through the day and from day to day, this effect should be examined.

Let $$k = \frac{1}{1 + \frac{x}{a}} = \frac{a}{a + x}$$

where, $x = R_1 = \rho / D$

$$a = R_e = \frac{R_1 R_b}{R_1 + R_b}$$

For a differential change in k with respect to ρ

$$dk = \frac{-a}{(a + x)^2} dx$$

For a resistivity change $\Delta\rho$ of 1 ohm-cm with

$R_1 = \rho_1 / D_1$ (as before)

$R_b = \frac{\rho_b L_b}{A_b}$ (as before)

$$R_e = \frac{\left(\frac{100}{20}\right)\left(\frac{20 \times 10^{-6} \times 6400}{0.75}\right)}{\left(\frac{100}{20}\right) + \left(\frac{20 \times 10^{-6} \times 6400}{0.75}\right)} = 0.165$$

$$dk = \frac{-R_e}{(R_e + R_i)^2}\left(\frac{1\ \Omega\ cm}{35.8\ ft}\right) = -0.0065$$

The percentage change where $k = 0.1965$ is

$$\frac{dk}{k} \times 100 = \frac{-0.0065}{0.1965} \times 100 = -3.3\%$$

which is small. From figure I.1 the largest variation in ρ was 1 ohm-cm on 6-28-71 between 0915 and 1445 hours. So it can be seen that even though this potential error is small it could contribute to the inaccuracy of the GEK.

Tidal mass transport

Excluding other problems for a moment, the GEK ideally measures the horizontally and vertically averaged velocity of the water through

the passage at any specific time. Therefore in previous calculations of the tidal transport, the integrated average velocity has been used to calculate the average mass transport. To show that this is not necessarily true an extreme example will be shown. If in the diagram below, the water in sections 1, 2, and 3 is flooding at one knot and the water in sections 4, 5 and 6 is ebbing at one knot, the average velocity is zero but the average transport is actually flooding.

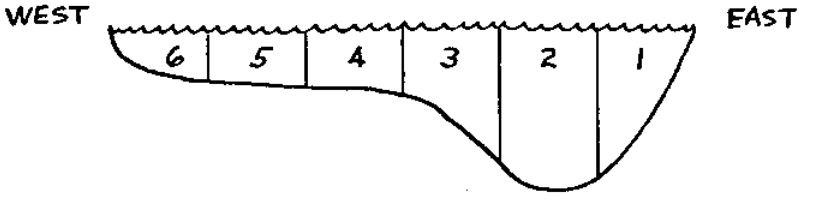

The tidal transport is to an approximation of 6 sections,

$$Q = \int (A_1V_1 + A_2V_2 + A_3V_3 + A_4V_4 + A_5V_5 + A_6V_6)\, dt$$

and would be more accurate as smaller sections are used.

Therefore if $Q = A \int V^* \, dt$

where, $V^* = \sum_{n=1}^{6} \frac{A_n V_n}{A}$ and n is the section and pole number.

This velocity curve for the poles, as recorded on July 8, 1971, is shown in figure H.2 as the dashed line.

If as in the calibration of the GEK

$$Q = A \int V_m \, dt$$

where, V_m is just the simple arithmetic mean of all the poles the velocity curve for the poles, as recorded on July 8, 1971, is shown as the solid line in fugure H.2. The results show that the difference between the two methods is small and for the accuracy of this GEK study, the mass transport can be derived from the simple

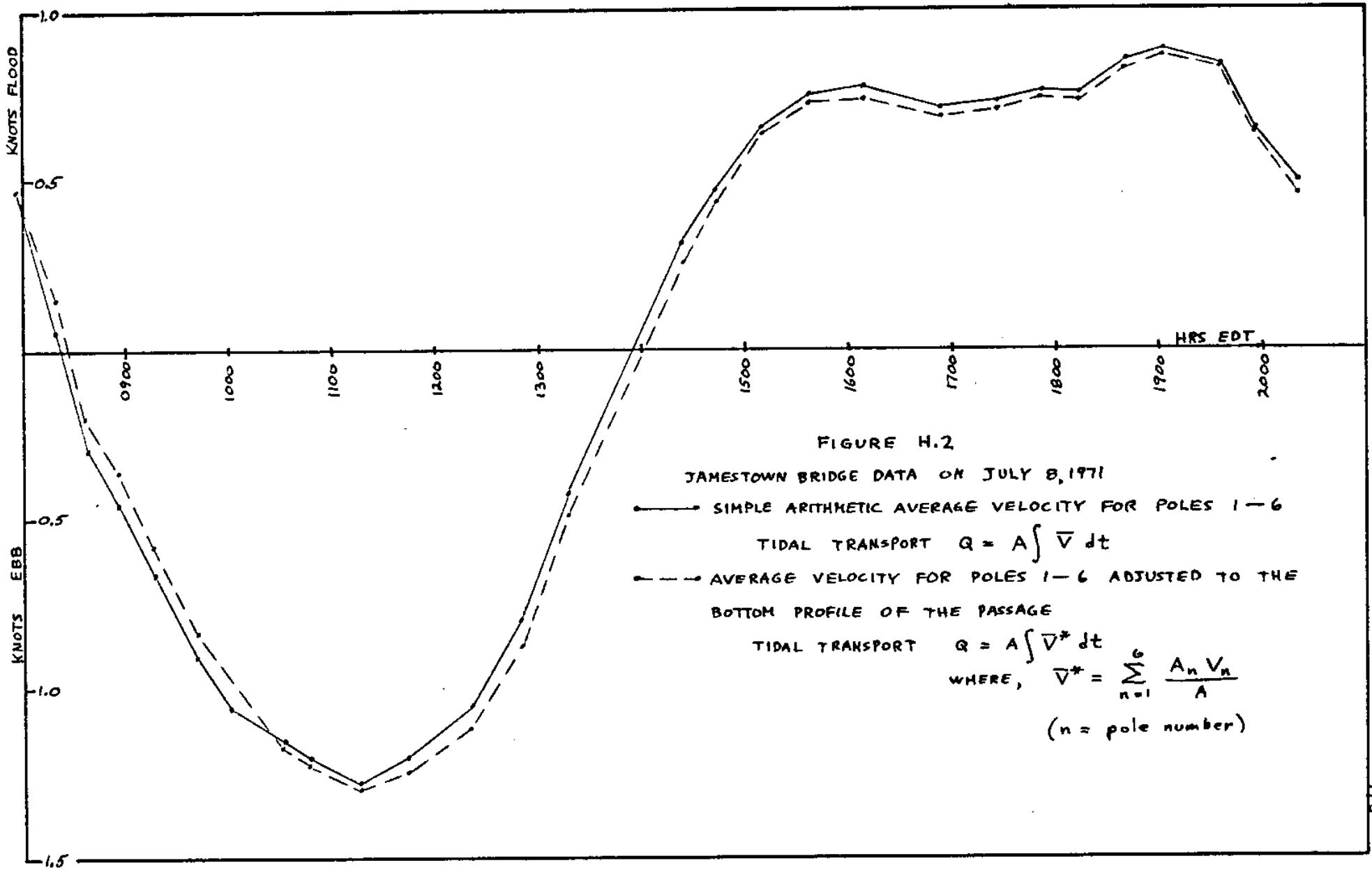

FIGURE H.2

JAMESTOWN BRIDGE DATA ON JULY 8, 1971

——— SIMPLE ARITHMETIC AVERAGE VELOCITY FOR POLES 1 — 6

TIDAL TRANSPORT $Q = A\int \bar{V}\, dt$

– – – AVERAGE VELOCITY FOR POLES 1 — 6 ADJUSTED TO THE BOTTOM PROFILE OF THE PASSAGE

TIDAL TRANSPORT $Q = A\int \bar{V}^*\, dt$

WHERE, $\bar{V}^* = \sum_{n=1}^{6} \frac{A_n V_n}{A}$

(n = pole number)

arithmetic average of the individual velocities of the poles through the passage.

Using this average velocity the calibration factor for the tidal mass transport can be obtained.

$$\frac{dQ}{dt} = A V_m$$

$$= L D_m V_m$$

$$= \frac{L D_m E}{B_z L} \qquad \text{where} \quad E = B_z L V_m$$

$$= \frac{D_m E}{B_z}$$

$$= \frac{D_m}{B_z k} \phi_{AB} \qquad \text{where} \quad E = \frac{\phi_{AB}}{k}$$

Therefore

$$\frac{d\left(\frac{Q}{\phi_{AB}}\right)}{dt} = \frac{D_m}{B_z k}$$

and for West Passage

$$\frac{d\left(\frac{Q}{\phi_{AB}}\right)}{dt} = \frac{(28 \text{ ft} \times 0.3048 \text{ m/ft})}{(0.54 \times 10^{-4})(0.1965)} \times 10^3 \frac{\text{mv}}{\text{volt}}$$

$$= 807. \frac{m^3}{\text{mv-sec}} \quad \text{or} \quad 28{,}500 \frac{ft^3}{\text{mv-sec}}$$

Table H.1 compares this and other results for West Passage with other GEK installations.

Table H.1

Comparison of various GEK installations

Reference	Location	mv/kt-km		$k = \phi/E$	$\frac{m^3}{mv\text{-}sec}$
		Theoretical[1]	Measured		
Wertheim 1954	Florida Straits	29.2	--	0.95[2]	--
Olsson 1955	Cook Strait N.Z.	26.0	--	0.94[2]	--
Morse 1958	Mosquito Pass	27.5	--[3]	--	--[3]
	Wescot Channel	26.0	15.4[3]	0.56[5]	169.[4]
	Deception Pass	27.5	22.4[4]	0.82[5]	565.[4]
Bloom 1964	Bering Strait	--	3.80[6]	0.137	4850.
Hughes 1969	Irish Sea				
	cable 001	--	--	0.57	1950.
	cable 002	--	--	--	1470.
	cable 003	--	--	0.46	4780.
Klein 1970	Marsdiep	--	--	0.2	2800.
	Borndiep Netherlands	--	--	0.2	800.
Krabach 1972	West Passage Narr. Bay	--	5.45	0.1965	807.

[1]Based on elliptical channel.

[2]Calc. from $k = \frac{1}{1 + \left(\frac{\rho L}{\rho_1 2D}\right)}$

[3]An average of several values.

[4]Calibrated by use of predicted velocities.

[5]Bedrock channel, signal loss from other sources.

[6]From the slope of calibration curve for 1956-58 installation.

APPENDIX I

ELECTRODE SELECTION AND ELECTROCHEMICAL ERRORS

Electrode selection

In order for the GEK to measure the electrical potential generated by the moving water, a good electrical contact is needed between the wires and the seawater. This will be a metal to electrolyte junction which inherently produces an electrical potential of its own. Since the opposing metal to electrolyte junction also produced a similar potential, these potentials tend to cancel each other out. If bare copperwires were used, the corrosion of the copper would produce polarization of the copper and the resulting potentials would be large and erratic enough to mask out the GEK signal. To minimize these effects, the only contact with the seawater is through non-polarizing silver-silver chloride electrodes. These are not the only types of contacts used; von Arx (1950) mentions the possible use of calomel electrodes, although he prefers the silver-silver chloride electrodes. Olsson (1955) used copper-copper sulphate electrodes in porous pots in damp ground for his land GEK installation. Sanford (personal communication, 1971) used existing electrical ground systems across Vineyard Sound. The University of Miami, Florida (personal communication, 1971) plans to use pure lead plates buried in the sediment for a GEK installation. In selecting the electrodes or type of electrical contact to be used, consideration must be given to the total potential the GEK will measure and the resulting current density on

the electrode surfaces, the environment the electrodes will be placed in, the availibility of the electrodes and of course the stability and thermodynamic properties of the electrodes.

The electrodes used in the West Passage were the silver-silver chloride electrodes which are suitable for use in seawater because of their common Cl^- ions, their insolubility and chemical durability, their physical durability and capability of operating in any orientation.

Several problems still must be examined with this electrode system. First is the problem of matching the electrodes electrically. Most electrodes are hand manufactured and this creates small unpredictable physical and chemical dissimilarities between electrode pairs. This is observed as an "offset" potential when two electrodes are placed in the same environment. This should be lower than 1 mv, but it is more important that it be a constant value and not drift, both in a steady state and in dynamic situations. Many researchers are trying to produce an Ag-AgCl electrode with greater stability, sensitivity and reproducibility. Ives and Janz (1961) report four kinds of electrode construction that are being examined: (a) electrolytic, the electrolytic deposition of both the silver and silver halide; (b) thermal, the decomposition in a furnace of a paste of silver oxide, silver halate and water to form a silver-silver halide compound; (c) thermal-electrolytic, the electrolytic formation of the silver halide on a thermally reduced silver oxide paste; (d) miscellaneous, such as the use of precipitated silver halide on silver. The electrodes used in the GEK are of the thermal construction and manufactured by Ocean Research Equipment, Inc. for use in their towed GEK system (Ocean Research Equipment, Inc., 1965). The other electrodes examined,

but not used in the West Passage GEK, were constructed at Woods Hole Oceanographic Insititute. They were constructed by the thermal method of von Arx (1962) except the firing was modified as recommended by Sanford (1967). The general method of matching electrodes is to manufacture several electrodes and then match them in pairs for the lowest potential difference and the greatest electrical stability.

The second problem is that of electrode polarization which alters the measured potential of an electrode and depends upon the magnitude of the external current and its direction. These are commonly called activation polarization and concentration polarization. Both reduce the available potential from an electrode as the external current between the electrodes is increased. Since this may not occur at both electrodes at the same rate, an unbalance in potential can result. This polarization can not be entirely eliminated because any working instrument for measuring emf must draw some current from the electrodes, but the polarization can be made negligible by using an exceptionally high impedance measuring circuit for the GEK. The amplifier circuit for the West Passage GEK employed a DC operational amplifier circuit with 10^{12} ohms input impedance. While this draws negligible current from the electrodes, it must be realized that any circuitry before the amplifier could have extraneous conductive paths to the ground via switches, electrical insulation or even damaged input wires. These were in general reduced to minimal values so polarization was not a problem in this GEK installation.

The third problem is that the electrodes are spaced far apart in the passage and may be in different environments and therefore subjected to water of differing salinity and temperature. When two identical electrodes are in contact with differing salt concentrations and also

when they are at different temperatures, electrochemical and electrothermal potentials are generated between the electrodes. This requires trying to locate the electrodes in areas that are subject to the minimum variation in salinity and temperature as the tide floods and ebbs through the passage. The next requirement is to try and buffer the metal-electrolyte junction from transients in water properties. The final effect this problem has on the GEK signal is due to both the magnitude of the electrochemical-thermal potential and the time response between the environmental change and the electrode change. The actual location for placing electrodes probably will be more determined by wanting to monitor a specific channel than by trying to match a channel to electrode requirements. Buffering the electrodes from the environment is discussed below. The salinity and temperature variations as the tide floods and ebbs are the two most important variables that must be understood and accounted for when the electrodes are installed across the tidal estuary.

Salinity variations

The silver-silver chloride electrodes form an electrical path to each other through a liquid junction. This can cause an electrical potential that is additive to any "offset" potential already existing from physical differences in the electrodes themselves. The additional signal due to the liquid junction is shown by Ives and Janz (1961) to be,

$$Ag\,|\,AgCl\,|\,NaCl, m_1\,\vdots\,NaCl, m_2\,|\,AgCl\,|\,Ag$$

where the vertical dotted line indicates the liquid-liquid junction. This is called a "concentration cell with transport" where the natural cell reaction is to transfer sodium chloride ions from the higher to the lower concentration. As long as the diffusion in this kind of cell

is slow and does not essentially alter the concentrations of the solutions, and the boundary zone is formed by natural interdiffusion of the two electrolytic solutions, the emf of the liquid junction can be described as,

$$E = \frac{-2RT}{F} \int_{m_1}^{m_2} t_{Na^+} \; d(\ln a_{Na^+})$$

The activity a_{Na^+} is equal to the molarity of the Na^+ multiplied by a correction factor, called the activity coefficient, which varies as a function of concentration and temperature. The transport number t_{Na^+} of the ion varies with concentration across the diffusion zone. Experimentally Sanford (1967) obtained a salinity coefficient of - 0.532 mv per °/oo with the von Arx type electrode for a salinity $S_1 = 37°/oo$ and $S_2 = 29.6°/oo$. He assumes through experimental justification that seawater behaves similar to NaCl of equal ionic strength and from this determines a salinity coefficient of potential of

$$\mathcal{E}_s = - \frac{61.18\,T}{S} \quad \mu v / °/oo$$

The dependence of $\mathcal{E}_s$ on temperature is then,

$$\frac{\partial \mathcal{E}_s}{\partial T} = - 2 \; \mu v / °/oo / °C.$$

for average seawater. Von Arx (1950) gives an average value of - 0.69 mv per °/oo for a salinity range of 26 to 36°/oo. The time constant for his cell was approximately 20 minutes. This is the response time for the cell to reach 63% of its final value. After 2 and 3 time constants the cell will reach 86% and 95%, respectively, of its final value.

Although this salinity coefficient is important, it is as necessary to know the time constant of the electrode. If the time constant of the electrode system in the estuary can be made longer than the tidal period, and the salinity differential between the two electrodes

is not great, the GEK signal will not be affected enough to warrant a correction. This is very desirable because if the GEK system does require the salinity differential to be monitored, it greatly reduces the economy and increases the complexity of the system.

A plot of several salinity differentials between the east and west shores is shown in figure I.1 on a typical tidal cycle. While not a complete study, it does indicate that the salinity differential might be in the range of 0.5 to 1.0°/oo.

To find the time constant for the electrodes, a sample of saltwater was collected from the mouth of the Bay and both electrodes were allowed to stabilize in it. A second jar of this seawater, which had been diluted to 7/8 concentration with freshwater, was connected with a salt bridge to the first jar. The salt bridge consisted of a 1/8 inch polyethylene tube, one foot long, filled with seawater and plugged at the ends with polyester fiber batten. This helped control the osmotic pressure which tended to transfer water from one jar to the other and change the concentrations of the solutions. After the two electrodes were stable in the seawater, electrode A was transfered to the 7/8 seawater jar and the transient emf was recorded on the GEK recorder. After the transient stabilized, the electrode A was placed back into the normal seawater. The test was then repeated using the electrode B. This test was done using both the bare von Arx type electrodes and the commercial electrodes from ORE, Inc. The electrodes from ORE, Inc. were inserted in plastic tubes filled with 2 inches of fiberglass insulation to simulate the actual installation in the West Passage. This increased the ion diffusion time between the seawater and the Ag-AgCl electrodes, although the greater contribution was from the very fine packed glass fibers inside the Lucite electrode housing.

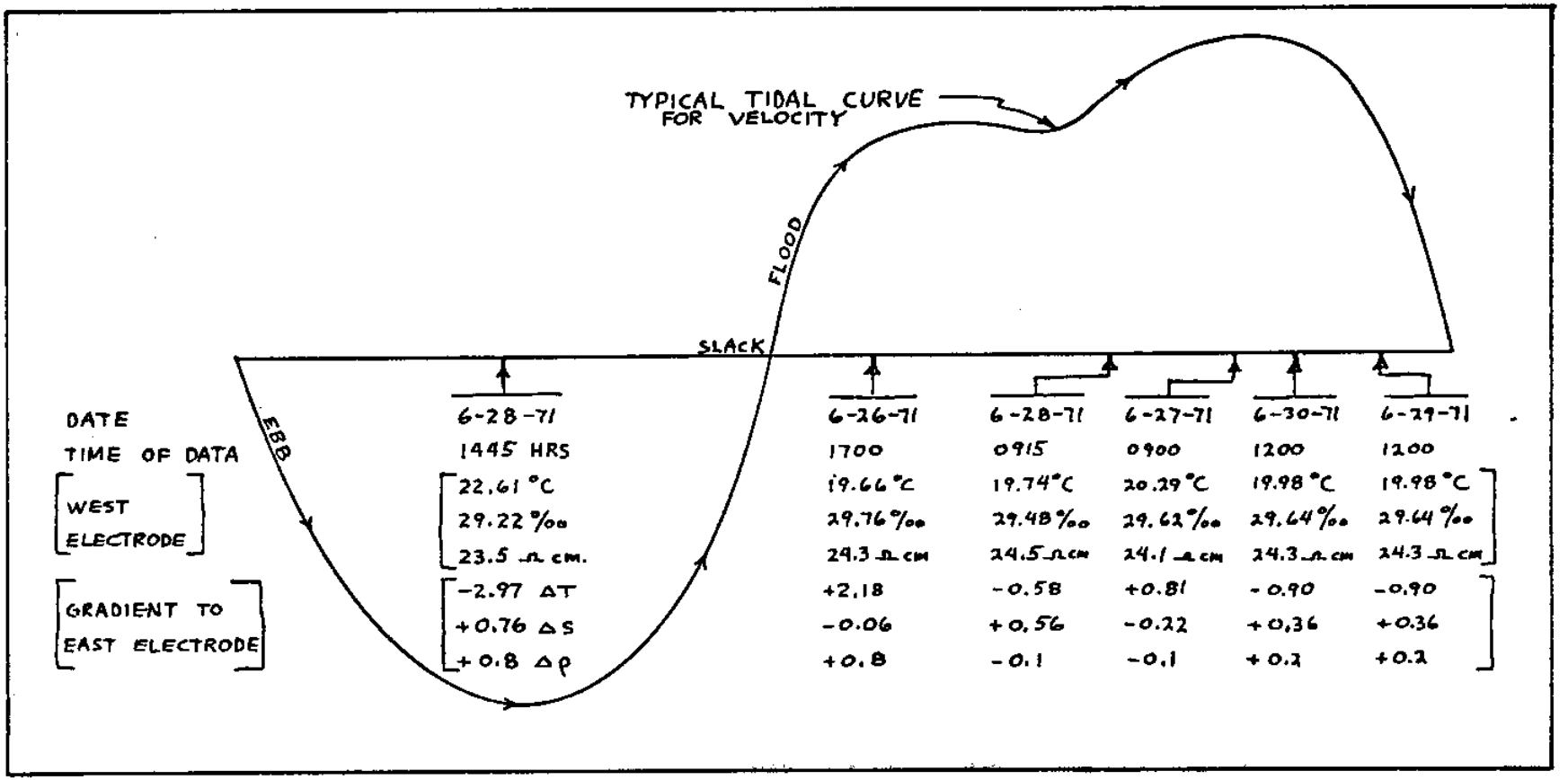

Fig. I.1--Temperature, salinity, resistivity and their gradients across the West Passage taken at the GEK electrodes.

The results for both electrode types are shown in figures I.2 and I.3. For the bare electrodes the time constant is around 30 minutes for the first transient. Notice that the transient response was not as great as the electrodes were moved back and forth between the different concentrations. This is probably due to the entrapment of ion concentrations on the surface of the electrodes. The initial response produced a salinity coefficient of 0.7 mv per °/oo. The packed electrode test was run for 24 hours and the final value was back to zero mv, probably due to a slight drift. This shows that the ion diffusion time was small enough to be negligible for this GEK installation. If the diffusion time is to be limited even more, the electrodes may be encased in chemically pure and similar seawater environments and allowing electrical conductance to the extermal seawater only through a microporous membrane or glass plug.

Temperature variations

The Ag-AgCl electrode system also responds to a temperature differential between the electrodes. This temperature coefficient of potential is also dependent upon the temperature and concentration of the seawater. Sanford (1967) experimentally derives a formula of,

$$\mathcal{E}_T = 315. + 3.5\,\Delta T \quad \mu v/^\circ C$$

for a salinity of 37°/oo at 22° C. The dependence of $\mathcal{E}_T$ on salinity was determined experimentally to be

$$\frac{\partial \mathcal{E}_T}{\partial S} = -2.5 \quad \mu v/^\circ C/^\circ/_{oo}$$

Von Arx (1950) gives a value of - 0.59 mv per ° C for a range of 0 to 30° C for the temperature coefficient. Although the magnitude of the potential is essential, it is also necessary to know the time constant for the system to respond to the temperature differential.

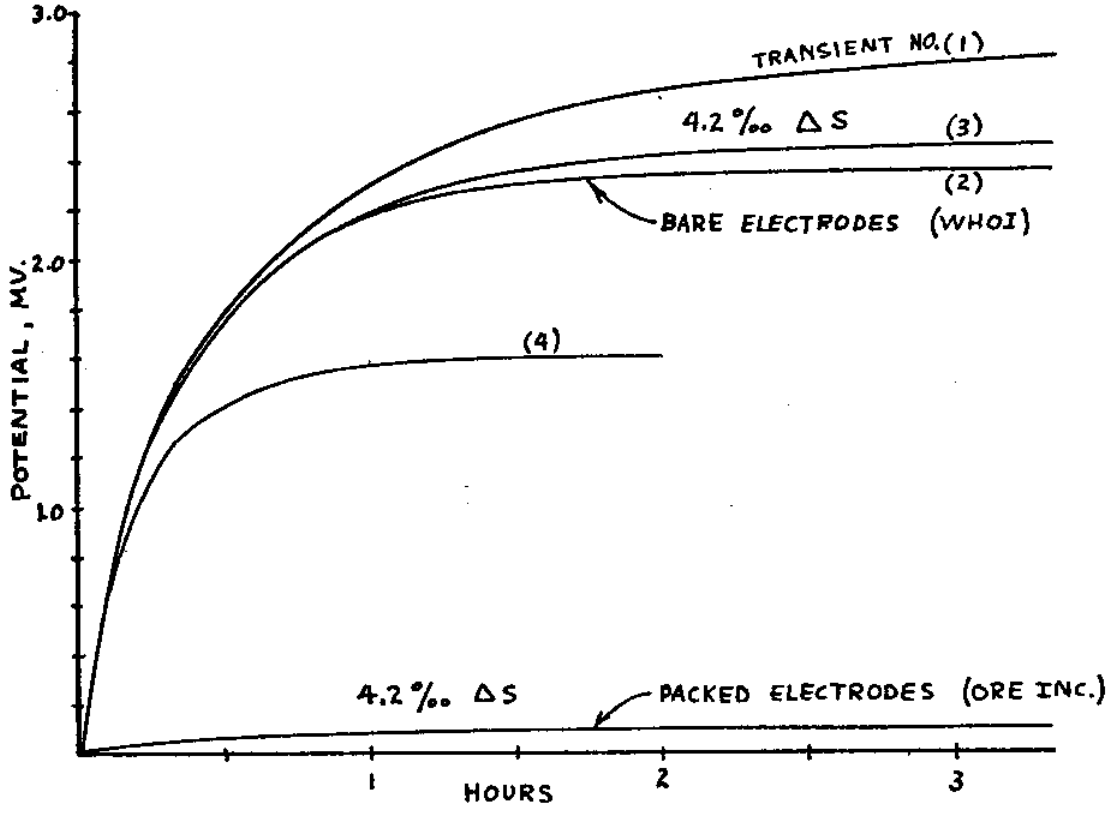

Fig. I.2--Response of Ag-AgCl electrodes to a salinity gradient, potential as a function of time.

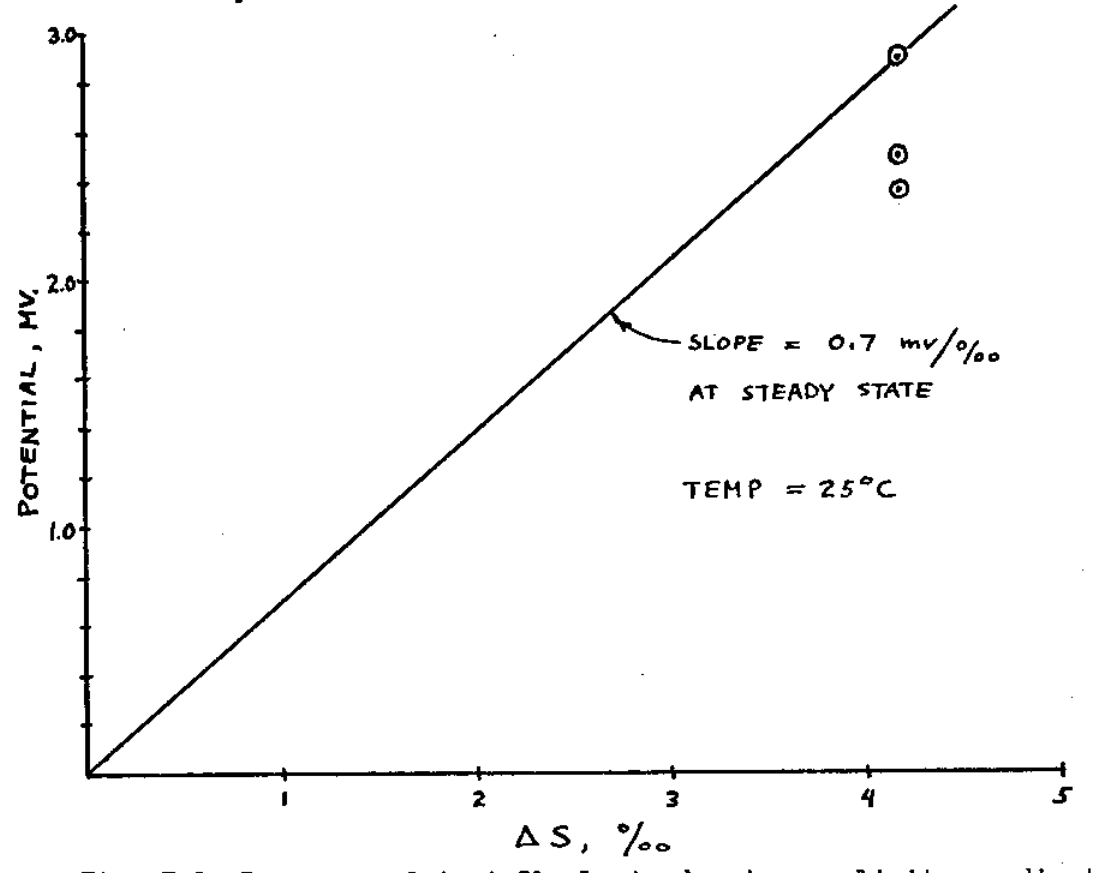

Fig. I.3--Response of Ag-AgCl electrodes to a salinity gradient, potential as a function of the salinity gradient.

The time constant of the system was determined by using a similar experimental procedure as that used for the salinity coefficient. The salinity was kept constant for the two jars of seawater while one was at ambient room temperature and the other was controlled by a calorimeter water bath. The calorimeter was capable of maintaining the bath temperature to within 0.1° C automatically. The two electrodes A and B were allowed to stabilize in the jar at room temperature. When the temperature differential was established in the calorimeter jar, electrode A was placed in the calorimeter and the emf transient was recorded on the GEK recorder. Then B electrode was also placed in the calorimeter jar and the transient observed. This was done for both the von Arx electrodes and the commercial ORE, Inc. electrodes. The results are shown in figures I.4 and I.5. The bare electrodes responded instantaneously. The ORE electrodes show essentially the response the actual electrode installation in the West Passage had. This is because the styrofoam blocks that the electrodes were imbeded in were only designed to protect the electrodes against physical damage and external contamination from marine life, not thermal insulation. From this it is concluded that the temperature variations in the water could have affected the GEK potential. Figure I.1 gives some typical values across the passage at the electrode locations. The temperature differential is quite varied in this section of the passage and since the temperature was not recorded throughout the calibration of the GEK, no correction can be made. Recommendations for future GEK installations that are in an estuary would include either a temperature monitoring of the electrodes and/or enclosing the electrodes in a vacuum insulator to increase the time constant of the electrode response to temperature transients during the

tidal cycle. If the insulator was the only means used, the average temperature variation between the two electrodes would have to be constant. This could probably be achieved if the electrode locations were similar in depth and hydrography. The east and west ends of the Jamestown Bridge are the antithesis of this requirement.

Effect on the West Passage GEK

With a temperature differential across the passage the warmer electrode will be positive with respect to the colder one, and for a salinity differential the electrode in the lesser salinity will be positive with respect to the one in the greater salinity. Since the warmer water in an estuary is associated with the less saline water, these potential errors will add together. From the salinity test it was found that the diffusion time was long enough to make a salinity correction unnecessary. From figure I.1 it is seen that the temperature differential could be around $\pm 2^{\circ}$ C. This will cause an error of $\pm$ 0.64 mv to the actual potential generated by the tidal currents. For a scale factor of 10.65 mv/knot on the GEK, this corresponds to about $\pm$ 0.06 knots or a total of about 10% error.

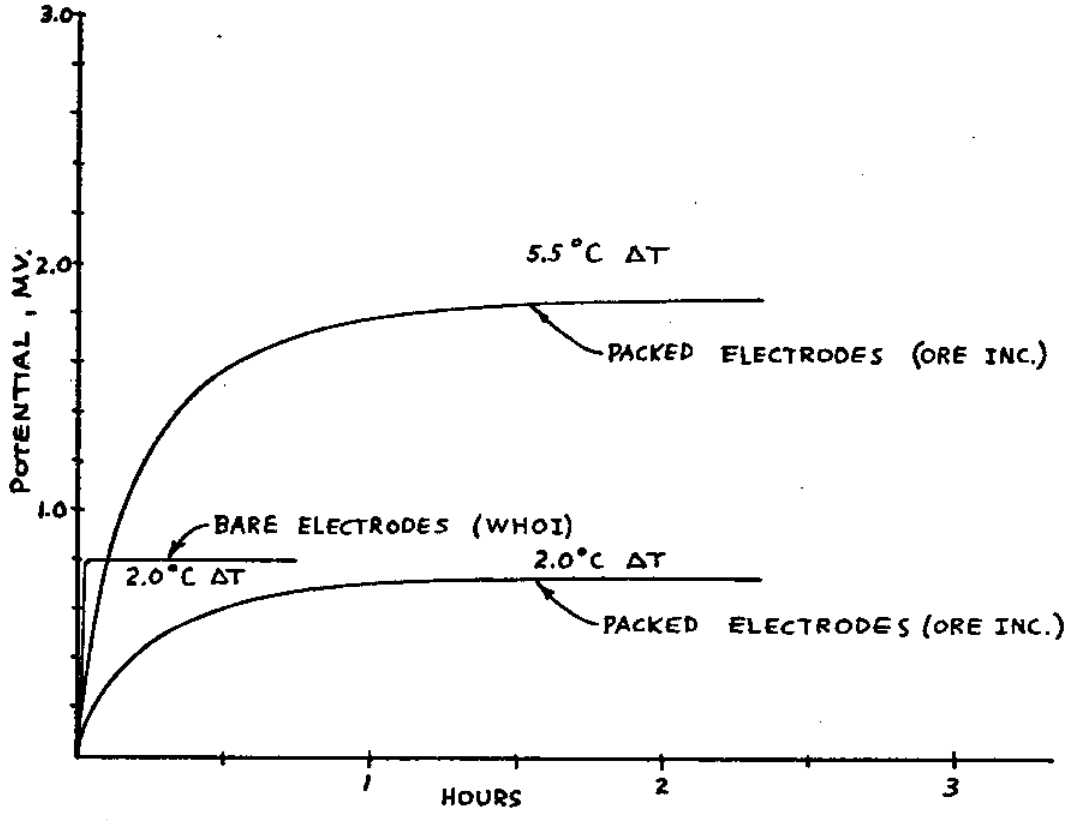

Fig. I.4--Response of Ag-AgCl electrodes to a temperature gradient, potential as a function of time.

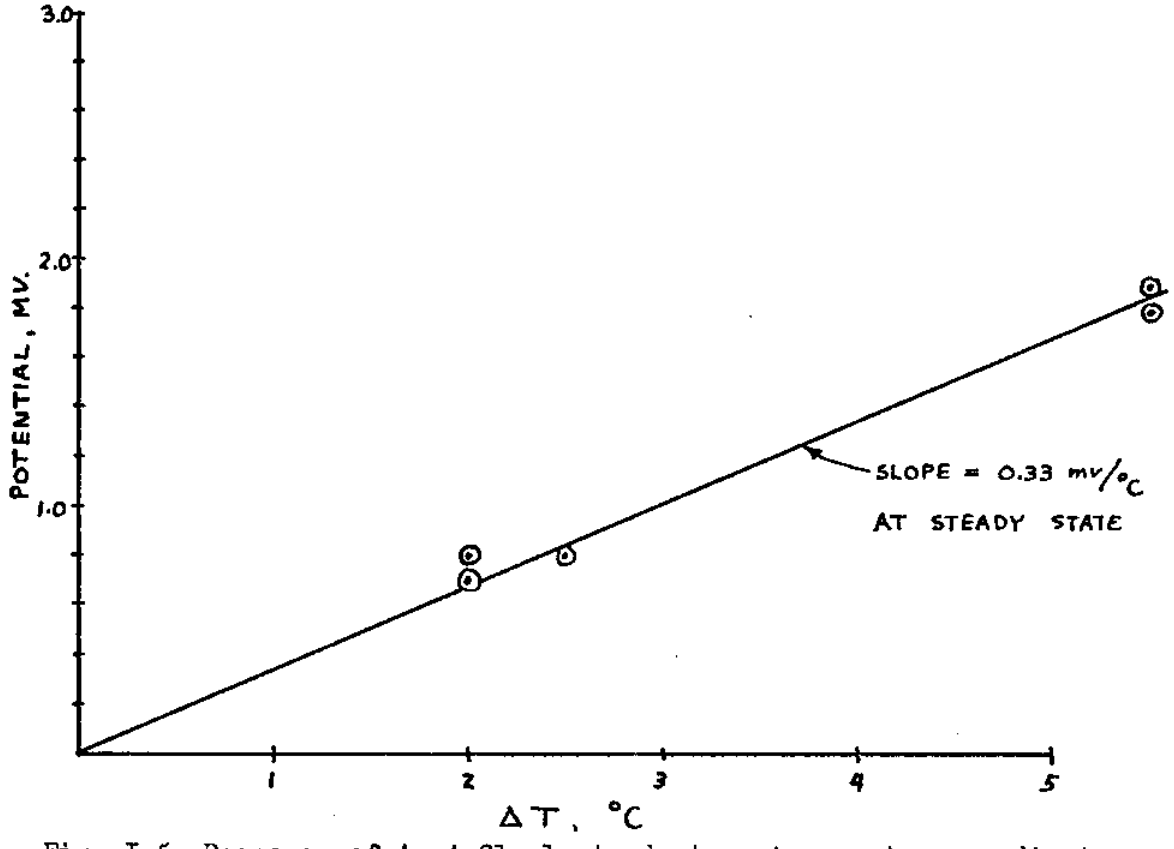

Fig. I.5--Response of Ag-AgCl electrode to a temperature gradient, potential as a function of the temperature gradient.

APPENDIX J

GEOMAGNETIC DISTURBANCES

In the calculation of electrical potential and in the calibrations of the potential with actual tidal currents, the magnetic field has been assumed relatively constant. This is not entirely true and the degree of variation of the magnetic field should be examined.

The Earth's magnetic field has many variations associated with it. In this discussion they will be examined in two broad catagories; short term variations and long term variations. The short term variations, or transients, with a time period on the order of the GEK recorder would show up as signal noise and tend to blur the record trace. The long term variations with a period of the order of a tidal cycle to a month would tend to make any calibration of the GEK during one time of the year invalid for another time of the year.

Short term magnetic variations

These are the most easily compared because they can be visually matched with disturbances on the GEK recordings. The GEK detects the magnetic variations the same way the Earth's magnetic field is measured by the flux gate variograph. A voltage is induced in a coil that is proportional to the number of turns of wire around a core, the cross sectional area of the magnetic field enclosed, the effective permeability of the core material and the time derivative of the magnetic field passing along the axis of the coil. With everything constant except the magnetic field, the voltage is proportional to the time

Micropulsations

If a line is plotted on figure J.1 that corresponds to a 0.3 mv deflection on the recorder (γ/sec = 10/1) it is seen that the GEK in general should not be affected by the bulk of the geomagnetic micropulses. But when the data from the GEK and data from the nearest geomagnetic observatory at Weston, Massachusetts were examined, visual correlation was found in many cases. Figures J.3 and J.4 show a definite correlation between irregular micropulses and transient noise on the GEK. Not only do the groups of pulses match with the corresponding ones on the GEK, but the individual spikes in each group correspond. These records were during a time of exceptionally low magnetic activity. The only correlation apparent was for the shorter period micropulses, the longer transients with a 20 - 30 minute period on the GEK did not compare with geomagnetic activity. The upper tracing in figures J.3 and J.4 are records of the total magnetic field obtained from a rubidium vapor magnetometer.

Upon examining the micropulses more carefully in figure J.4 at 0545 hours U.T., the transient on the GEK consists of six cycles which is the same number there is on the total field record. The transient of six cycles on the total field record have an average amplitude of 0.5γ with a total period of 85 seconds. This transient is plotted on figure J.1 as point (T) and corresponds with the spectrum.

By further examination the field rate of change for the second spike at 0545 is found to be 1.5 in 30 seconds = 0.05 γ/sec. In southern New England the ratio of the horizontal to the total magnetic field is $\frac{17,000\ \gamma}{57,000\ \gamma}$.

rate of change of the magnetic field. While most are induction coils several meters in diameter, one has been built to enclose 67 km^2. These are very sensitive detection devices that measure high frequency magnetic variations (micropulsations) well.

In this case the GEK forms an induction loop that consists of the wire passing over the bridge and the conducting water underneath the bridge. To calculate the response, this GEK installation has an air gap under the bridge that will be approximated.

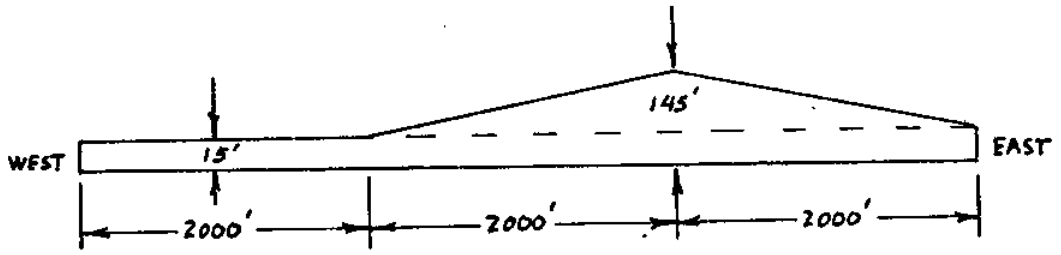

$$\text{The area} = \left(15 \times 6000 + \frac{130 \times 4000}{2}\right) 0.093\ m^2/ft^2$$

$$= (350{,}000\ ft^2)\ 0.093$$

$$= 32{,}000\ m^2$$

The induced voltage is,

$$E = N \frac{d\phi}{dt}$$

where, N = one conducting loop
ϕ = magnetic flux, which is the flux density, B x the cross-sectional area, A

The magnetic flux density B (gauss) = μ_oH(oersteds)

where, μ_o = 1 in the cgs system

Geophysicists use the unit gamma γ which is equal to 10^{-5} oersteds. Converting to the MKS system of units and expressing the voltage produced by a transient of 1γ/sec in the magnetic field,

$$E = NA \frac{dB}{dt}$$

$$= (1)\ (32{,}000\ m^2)\ \frac{d}{dt}\left(\frac{10^{-5}\ gauss/sec}{10^{4}\ gauss/weber/m^2}\right)$$

$$= 32{,}000\ (10^{-9})\ weber/sec$$

$$= 3.2 \times 10^{-5}\ volts$$

$$= 0.032\ mv\ /\ \gamma/sec$$

This compares with the sensitivity of the detector coil used at the Institute for Telecommunication Sciences and Aeronomy in Boulder, Colorado (Matsushita and Campbell, 1966, p.195) where they have 16,000 turns of wire on a two meter diameter coil.

$$E = 16{,}000\ (3.1\ m^2)\ 10^{-9}\ weber/sec-m^2$$

$$= 0.05\ mv\ /\ \gamma/sec$$

Figure J.1 shows a general representation of the geomagnetic spectrum (Ibid., p.823).

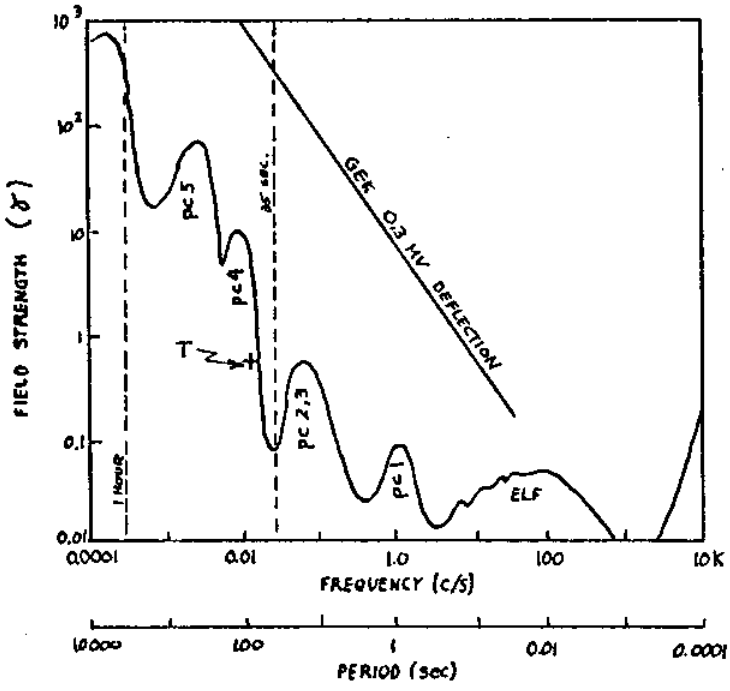

Fig. J.1--Electromagnetic spectrum of geomagnetic transients.

The vertical dotted lines show the frequency range that can be observed on the GEK. The recorder has a printing speed of one mark every 2 seconds and a paper movement of 1 inch per hour (or 1/2 inch per hour). Most GEK potentials were recorded with a 5 second time constant filter in the amplifier. Therefore the highest frequency observable would be about,

$$f_c = \frac{1}{2\pi RC}$$

$$= \frac{1}{2\pi\ (10^7\ \Omega)(0.5 \times 10^{-6}\ \text{farads})}$$

$$= 0.0286\ \text{cycles/sec}$$

or in terms of the lowest period, 35 seconds.

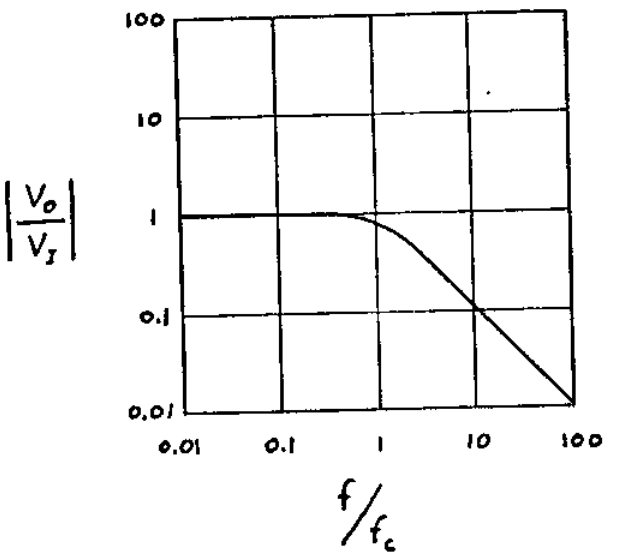

Fig. J.2--Frequency response of GEK amplifier on 5.0 sec time constant.

In observing these magnetic variations, the chart speed of 1 inch per hour will limit the resolution of the higher frequencies. The lowest frequencies are those that are not obscured by the varying tidal potentials.

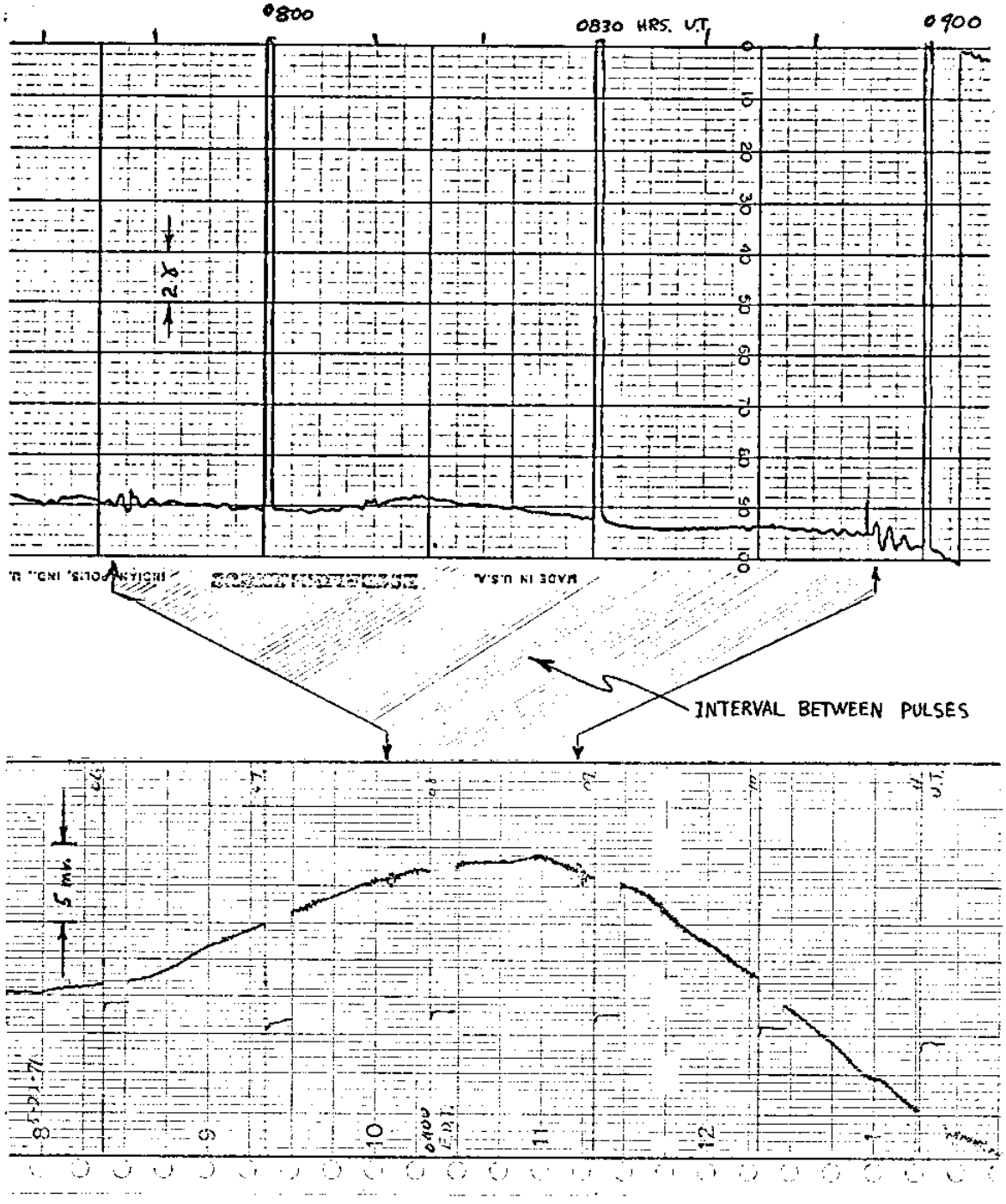

COMPARISON BETWEEN GEOMAGNETIC MICROPULSES AND PULSES ON THE GEK.
DATE : 5-22-71

Figure J.3

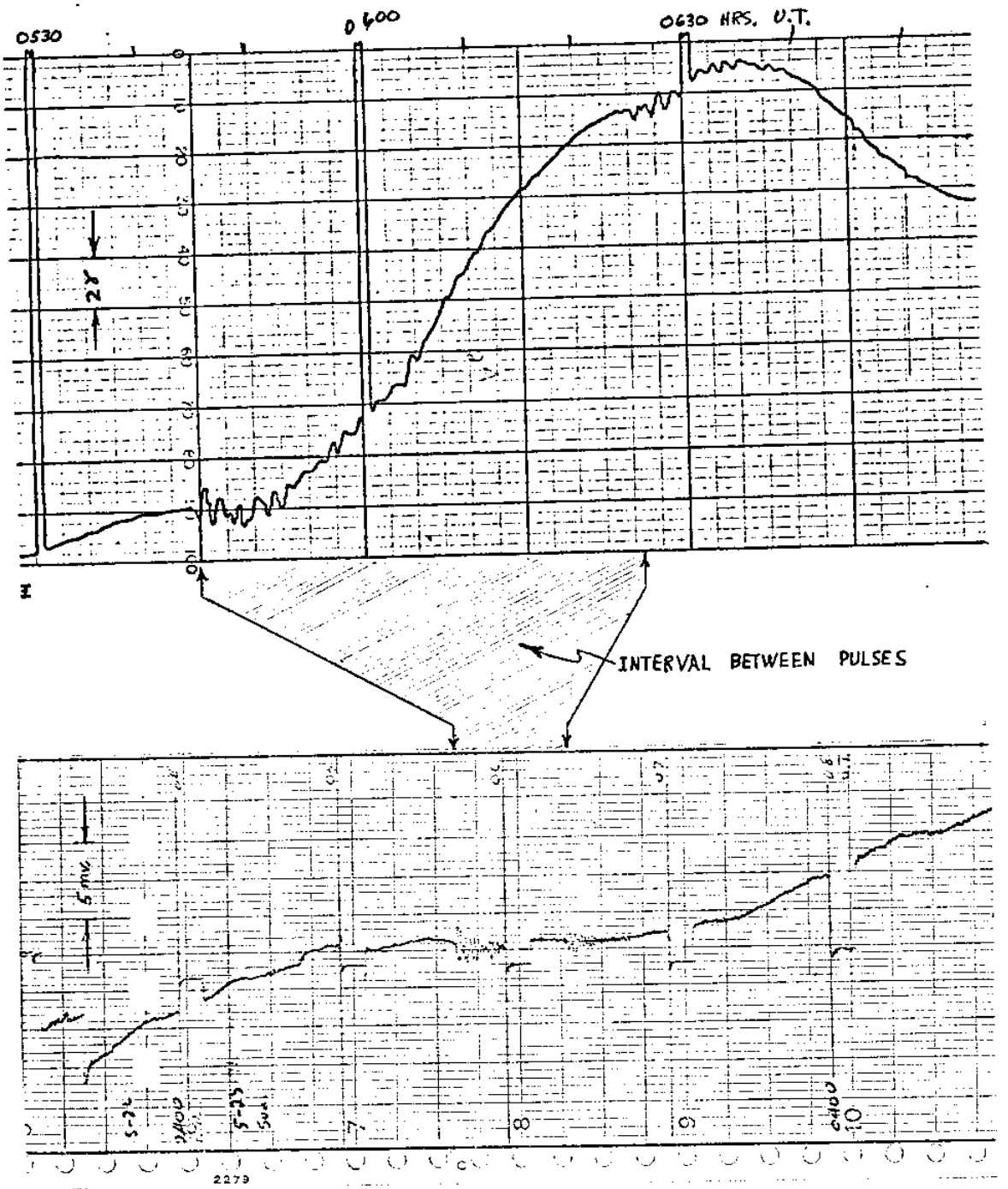

COMPARISON BETWEEN GEOMAGNETIC MICROPULSES AND PULSES ON THE GEK.
DATE: 5-23-71

Figure J.4

So the rate of change for the horizontal component is,

$$0.05 \frac{\gamma}{sec} \times \frac{17,000}{57,000} = 0.015 \gamma/sec$$

Since the sensitivity of the GEK's induction loop is 0.032 mv/γ/sec , the theoretical potential induced by this pulse is

$$E = 0.032 \frac{mv}{\gamma/sec} \times 0.015 \gamma/sec = 0.00048 \text{ mv}$$

This is clearly below the level that should be detectable on the recorder. Examining the corresponding GEK pulse for 0545 hours, it is approximately 1.0 mv in amplitude. This is 2000 times that calculated. In operating the GEK, the primary concern is with the effect of magnetic transients and not so much with the direct cause. Therefore this discrepency was not examined with further detail.

Higher frequency electrical noise from thunder and electrical storms was not studied with the GEK on the 5.0 second filter, which was the normal operating mode. One time when a thunder storm was passing several miles away the GEK recorder was operating, but with the 0.05 second filter. The GEK record below shows this storm which was at a peak at 1000 hours and gone by 1130 hours.

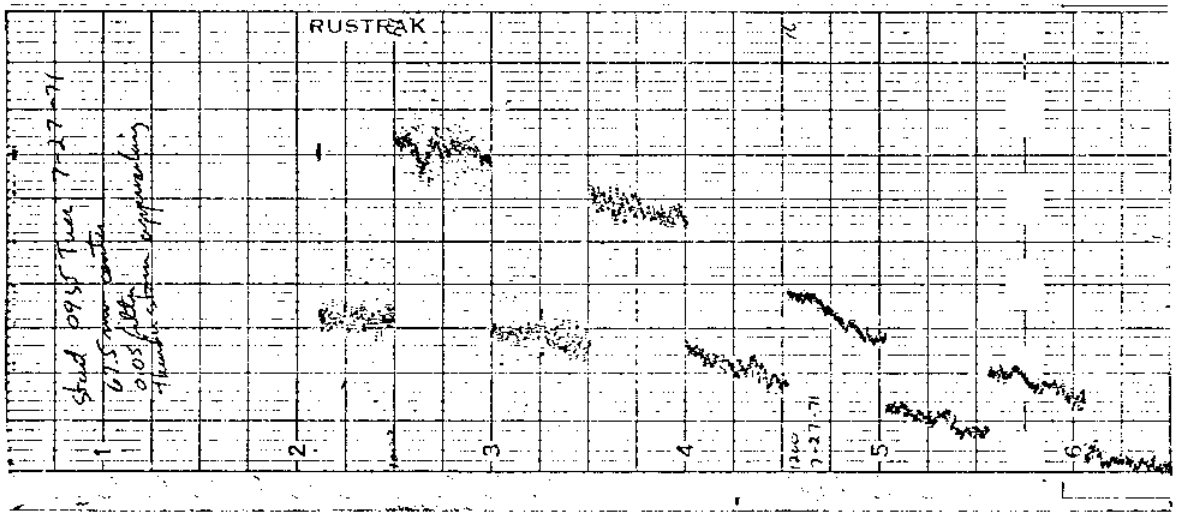

All other times when there was the chance of a thunder storm, the GEK recorder was disconnected from the wires on the bridge. This was a precautionary measure because it was not known what the effect would be if lightning struck the bridge.

Geomagnetic storms

More severe types of magnetic variations are the geomagnetic storms. These are relatively severe and long lasting disturbances with a more or less recognizable sudden start and lasting several days. Since they are disturbances originating from the Sun, they may reoccur in 27 day intervals. Fortunately ones severe enough to affect the GEK do not occur very often. Geomagnetic disturbances of these kinds occur with a wide range of intensities and are expressed in world-wide geomagnetic activity indices, K_p and A_p. To briefly define these; magnetometers at a number of stations throughout the world record a local 3-hourly K index, ranging from 0 to 9. This is a measure of the variation in the field strength over a 3-hour period; K = 0 indicates a quiet condition and K = 9 indicates very intense disturbances. The K indicies from these stations are combined to give the planetary index K_p. The index A_p is based on the amplitude variation of the field strength expressed in gammas. The 3-hourly values from individual stations are combined to give the planetary index a_p, and then these are averaged over a 24-hour period to obtain the A_p index.

To determine how these storms might appear as noise on the GEK recordings, the data from April 10 to May 31 was examined for all times when the GEK noise was greater than 10% of the maximum signal strength. This is approximately 1 mv and corresponds to about 0.1 knot tidal velocity. All these times are indicated on the K_p diagram of figure J.5

and on the corresponding days in the daily A_p listings of figure J.6 (Environmental Research Lab. prompt reports, 1971). It becomes apparent that the GEK probably is affected when K_p is greater than 5 and the A_p is greater than 20. To show a rough percentage of days that might be affected through a year, all A_p values greater than 20 are marked on figure J.6. Although this looks like a large percentage of the time, most times it will be possible to average the noise and obtain a suitable tidal velocity reading. Two examples of magnetic storms are shown in figures J.7 and J.8 with their corresponding fluxgate variometer charts. These show magnetic variations in the horizontal and vertical fields plus the declination variation. The K_p values are shown every 3 hours on the charts to show a comparison between K_p and the amount of effect on the GEK. Examining the GEK charts also shows that usually the quietest traces are during the night and early morning hours.

Long term magnetic variations

The basic equation that governs the GEK is, e = BLS, the output being proportional to the magnetic intensity. If a world map of secular variation of the vertical intensity is examined, it is found that the New England area has a change of about - 20γ/year. This is only

$$\frac{20\,\gamma}{54{,}000\,\gamma} \times 100 = 0.03\,\%$$

or .0003 x 10 mv = 0.003 mv change in the amplitude of the GEK signal. Clearly not enough to be noticed on the GEK for a very long time, if ever.

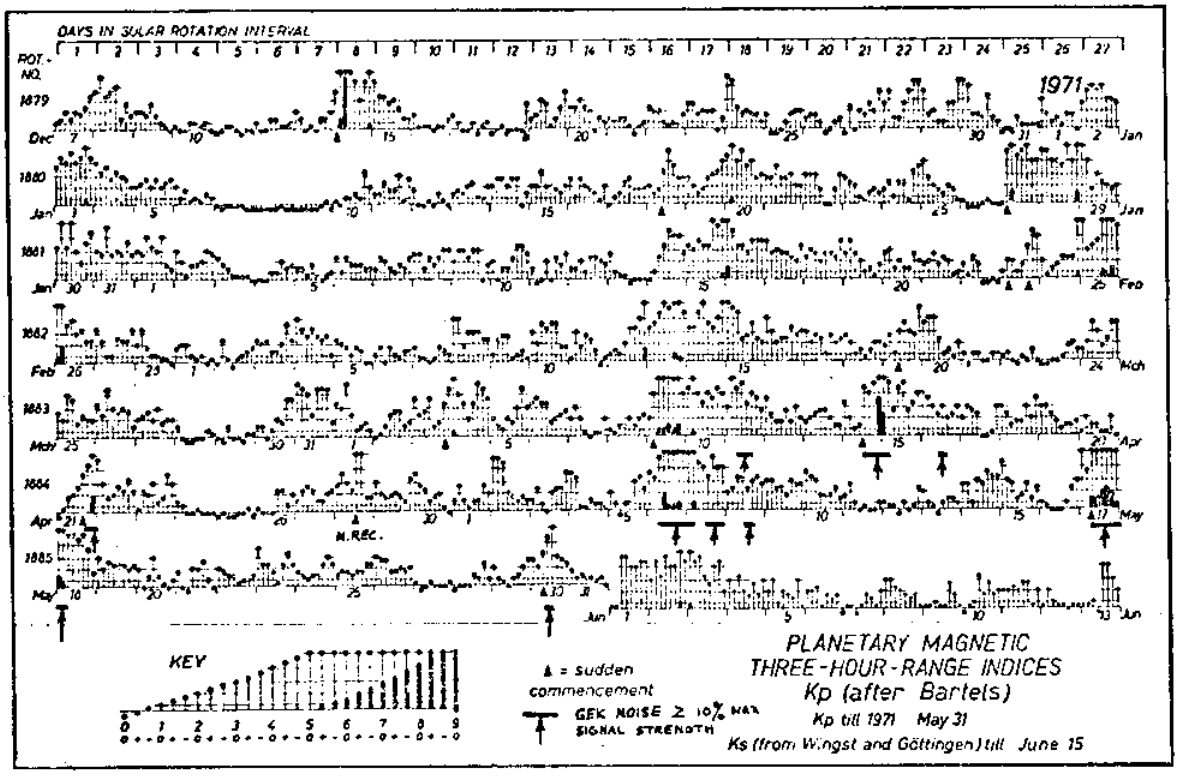

Fig. J.5--Geomagnetic Activity Indices, K_p.

DAY	1970 JUNE	JULY	AUG.	SEPT.	OCT.	NOV.	DEC.	1971 JAN.	FEB.	MAR.	APR.	MAY
1	(28)	10	4	[23]	10	2	1	6	16	4	12	7
2	9	11	6	18	9	4	4	19	9	4	7	17
3	11	[24]	4	15	14	8	4	[33]	4	9	16	8
4	8	[26]	4	11	[25]	7	5	16	4	14	[27]	8
5	6	16	3	8	9	9	8	9	4	5	11	8
6	3	15	8	5	6	12	8	4	6	4	14	[50]
7	9	5	12	6	4	[58]	8	1	6	4	6	[36]
8	13	10	[26]	8	2	8	19	0	10	15	6	13
9	5	[87]	19	5	2	8	6	1	10	6	[53]	12
10	6	[34]	7	6	7	17	3	6	10	15	[30]	11
11	4	10	9	1	15	[20]	2	8	5	7	[27]	4
12	5	14	9	5	16	10	4	3	6	[20]	10	4
13	10	10	6	[24]	9	9	4	6	4	[39]	8	4
14	8	9	4	19	8	7	[65]	9	[16]	[29]	[39]	14
15	13	5	7	11	4	4	14	8	[29]	[22]	[36]	12
16	9	6	[21]	8	[37]	5	4	7	[28]	14	15	5
17	13	8	[15]	8	[34]	6	3	6	13	9	8	[73]
18	(27)	5	[36]	10	[39]	18	3	15	12	6	11	[39]
19	8	5	14	18	11	18	10	13	9	16	8	10
20	18	6	4	15	7	3	8	[29]	8	13	4	5
21	17	[30]	5	[23]	1	[30]	4	12	7	3	[22]	5
22	4	12	6	12	18	18	6	10	3	3	14	5
23	4	9	7	6	[29]	[21]	7	6	13	3	10	11
24	6	[26]	4	6	14	12	14	10	13	14	3	7
25	6	[92]	8	8	6	13	4	9	[43]	12	1	6
26	13	[21]	17	6	4	8	4	2	[31]	15	5	9
27	(35)	14	12	19	5	10	8	[37]	10	9	8	2
28	7	4	12	7	15	8	18	[39]	6	2	21	4
29	6	[45]	10	5	13	2	12	16		2	9	6
30	5	7	5	9	9	1	13	[26]		9	8	19
31		14	12		4		2	17		[26]		4

Fig. J.6--Daily Average Indices, A_p.

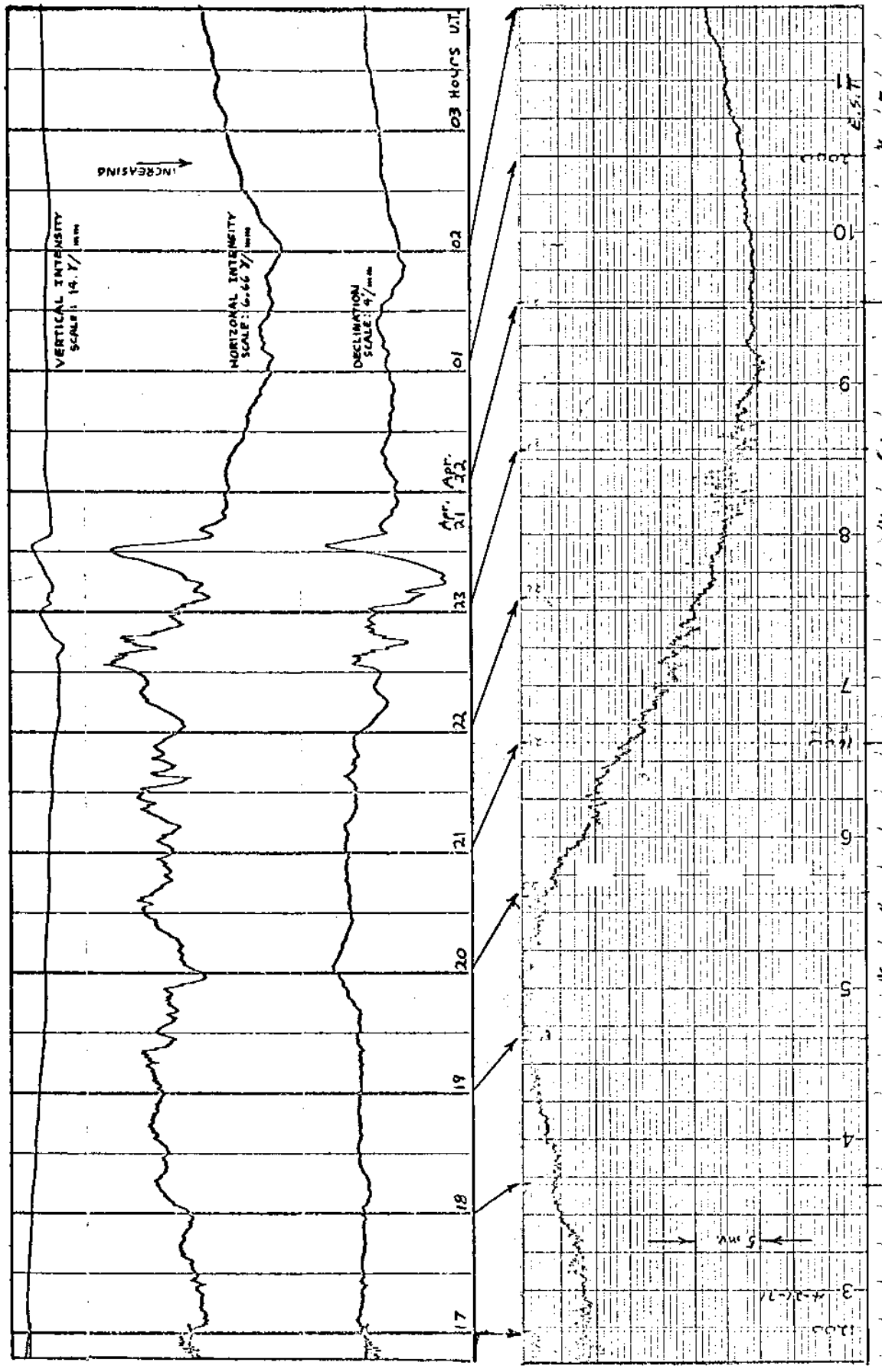

Fig. J.7--Comparison between small geomagnetic storm and noise on the GEK signal, Apr. 21, 1971.

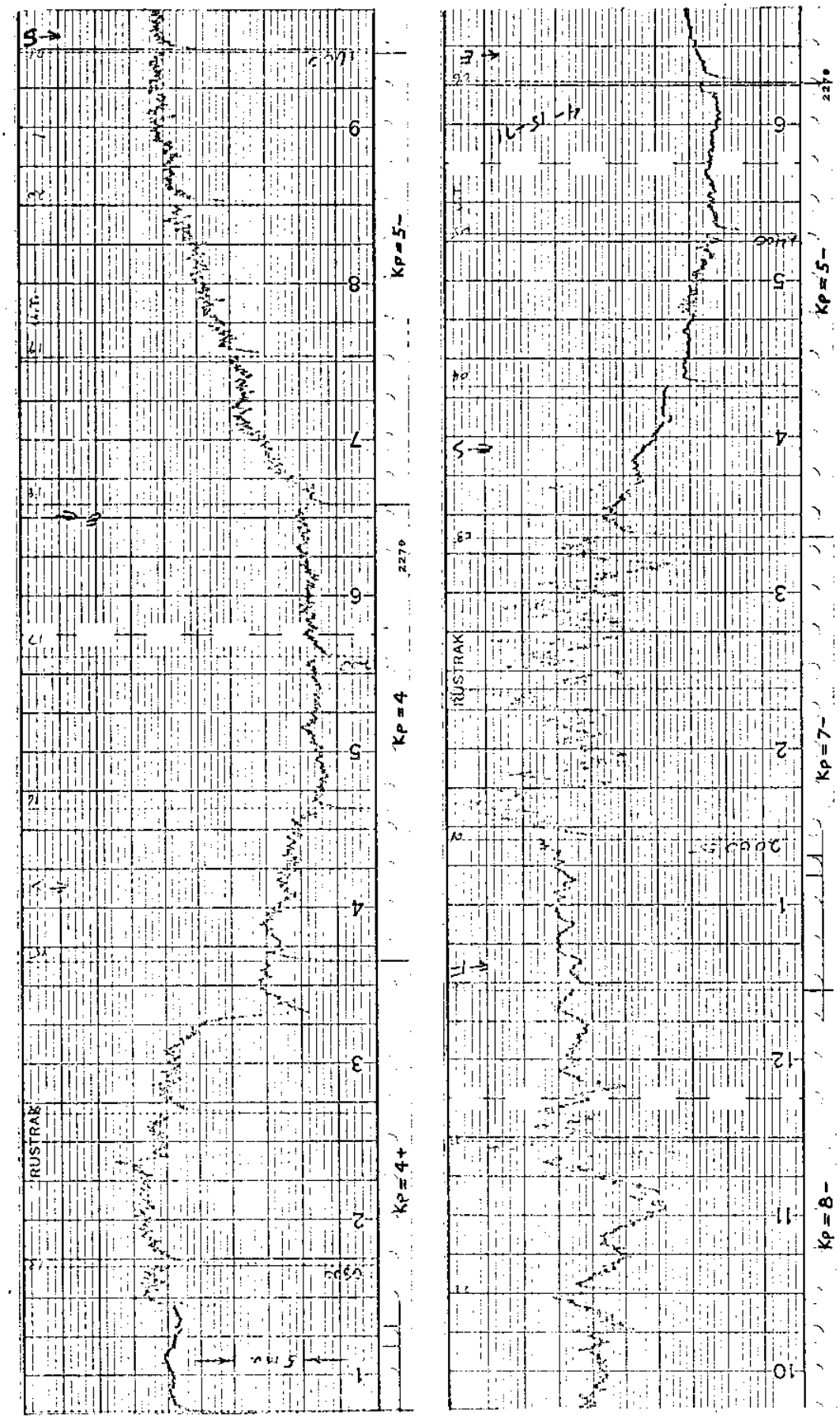

Fig. J.8--Example of severe geomagnetic storm as shown by noise on GEK signal, Apr. 14-15, 1971.

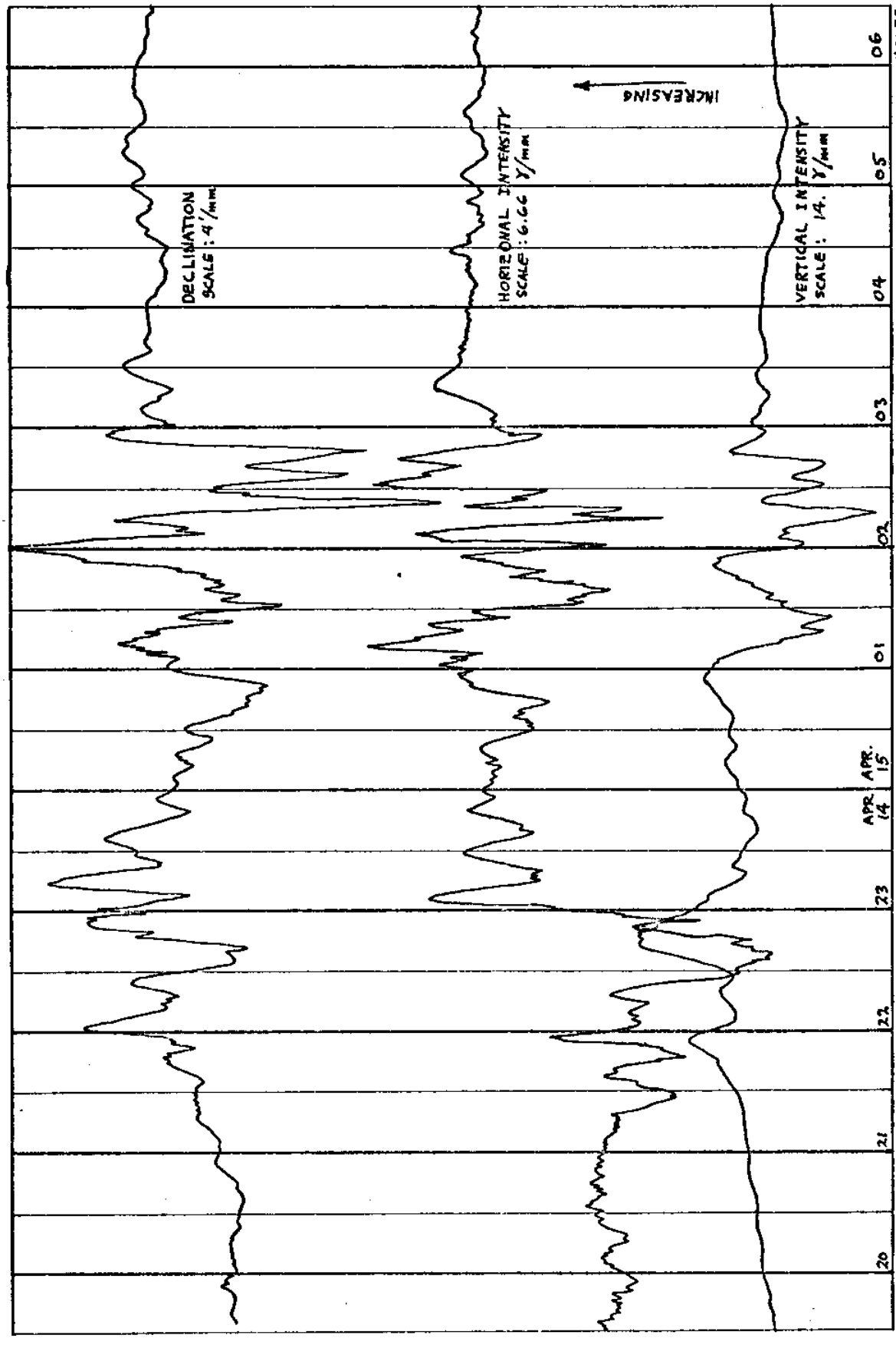

Fig. J.9--Example of severe geomagnetic storm as shown on flusgate variometer; to be compared with GEK signal on previous figure J.8.

REFERENCES

Binkerd, R.
1972. A New Application for Pole Floats.
Univ. of Rhode Island Dept. of Ocean Engineering, thesis

Birch, W. B., and Dietz, F. T.
1962. Seismic Refraction Investigations in Selected Areas of Narragansett Bay, Rhode Island. Jour. of Geophysical Research. vol. 67, no. 7, pp. 2813-2821.

Bloom, G. L.
1964. Water Transport and Temperature Measurements in the Eastern Bering Strait, 1953-1958. Jour. of Geophysical Research. vol. 69, no. 16, pp. 3335-3354.

Carrigan, A. L., ed.
1971. Geophysics and Space Data Bulletin. vol.VIII, no. 1, First quarter 1971. Space Physics Lab., Air Force Cambridge Research Lab., A.F. Systems Command, L.G. Hanscom Field, Mass.

Environmental Research Laboratories
Solar - Geophysical Data (prompt reports) July 1971. no. 323 part 1, data for June-May 1971. U.S. Dept of Commerce, NOAA, Environmental Data Service .

Faraday, M.
1832. Bakerian Lecture - Experimental Researches in Electricity. Phil. Trans. Royal Society of London, Part I, pp. 163-177.

Hersey, J. B.; Nalwalk, A. H.; and Fink, D. R.
1961. Seismic Reflection Study of the Geologic Structure Underlying Southern Narragansett Bay, Rhode Island. Ref. No. 61-19. Woods Hole Oceanographic Institute.

Hicks, S.D.
1959. The physical Oceanography of Narragansett Bay. Limnology and Oceanography. vol. 4, pp.316-327.

Hodgman, C.D., ed.
1959. Handbook of Chenistry and Physics. Cleveland, Ohio: Chemical Rubber Pub. Co.

Hoerner, S. F.
1965. Fluid - Dynamic Drag. Midland Park, New Jersey: By the Author, 148 Busteed Drive, 07432

Hughes, Peter
1969. Submarine Cable Measurements of Tidal Currents in the Irish Sea. Limnology and Oceanography. vol. 14, no. 2, pp. 269-278.

Hughes, W. F., and Brighton, J. A.
1967. Theory and Problems of Fluid Dynamics. New York: Schaum Publishing Co.

Ippen, A. T.
1966. Estuary and Coastline Hydrodynamics. New York: McGraw-Hill

Ives, D. J. G., and Janz, G. J. ed.
1961. Reference Electrodes, Theory and Practice. New York and London: Academic Press.

Klein, R. E.
1970. The measurement of Tidal Water Transport in Channels. Coastal Engineering Proceedings, vol. I, II, III. Sept. 13-18, 1970 at Washington, DC. Pub. by Amer. Soc. of Civil Engineers. pp. 1887-1901.

Lamb, Sir Horace
1932. Hydrodynamics, 6th ed. Cambridge University Press. (also pub. by Dover).

Longuet-Higgins, M.S.; Stern, M.E.; and Stommel, Henry
1954. The Electrical Field Induced by Ocean Currents and Waves, with Applications to the Method of Towed Electrodes. Papers in Physical Oceanography and Meteorology. vol. XIII, no. 1, Cambridge and Woods Hole, Mass.: MIT and WHOI. 37 pp.

Malkus, W. V. R., and Stern, M. E.
1952. Determination of Ocean Transports and Velocities by Electromagnetic Effects. Jour. of Marine Research. vol XI, no. 2, pp. 97-105.

Marine Research Inc.
1971. Prelininary data for report to the Narragansett Electric Co. Marion, Mass: unpublished data

Matsushita, S., and Campbell, W. H., ed.
1976. Physics of Geomagnetic Phenomena. Vol. I and II. New York: Academic Press.

Morse, R. M.
1957. The Measurement of Transports and Current Velocities in Tidal Streams by an Electromagnetic Method. Univ. of Washington, thesis. (also pub. as Univ. of Wash. Dept. of Ocean. Tech. Report 57, 1958)

Ocean Research Equipment, Inc.
1965. Report No. 05641. Instruction Manual O.R.E. Geomagnetic Electrokinetograph, Model 150. Falmouth, Mass.

Olsson, B.H.
1955. The Electrical Effects of Tidal Streams in Cook Strait, New Zeeland. Deep Sea Research. vol. 2, London: Pergamon Press Ltd. pp. 204-212.

Parsons, Klapp, Brinckerhoff and Douglas; Consulting Engineers
1938. Jamestown Bridge, General Plan and Elevation Borings. blueprint sheet no. 1, (from R.I. Highway Dept.)

Rome Point Circulation Study, Final Report
1971. July 31, 1971. Contract URI-98-20-7057 to Narragansett Electric Co. prepared at the Univ. of Rhode Island.

Sanford, T. B.
1967. Measurement and Interpretation of Motional Electric Fields in the Sea. Mass. Institute of Tech. Dept. of Geology and Geophysics, thesis.

Smith, W. J.
1966. Modern Optical Engineering. New York: McGraw-Hill

Teeson, D. H.
1969. The Movement of Oil Slicks at Sea: Preliminary Studies of Wind and Current Effects. Univ. of Rhode Island Dept. of Ocean Engineering, thesis.

Tidal Current Tables
1971. For Atlantic Coast of North America. U.S. Dept. of Commerce, Environmental Science Services Admin., Coast and Geodetic Survey. (Starting 1972,pub. by National Oceanic and Atmospheric Admin., National Ocean Survey, Rockville, Md.)

Tide Tables
1971. East Coast, North and South America. U.S. Dept. of Commerce, (Pub. same as Tidal Current Tables.)

U. S. Naval Hydrographic Office
1952. Tables for Sea Water Density, H. O. Pub. 615.

von Arx, W. S.
1950. An Electromagnetic Method for Measuring the Velocities of Ocean Currents from a Ship Under Way. Papers in Physical Oceanography and Meteorology. vol. XI, no. 3. Cambridge and Woods Hole, Mass.: MIT and WHOI. 62pp.

Wertheim, G. K.
1954. Studies of the Electric Potential Between Key West, Florida, and Havana, Cuba. Transactions, American Geophysical Union. vol. 35, no. 6, pp.872-882.

Williams, C. E.
1970. In-Situ Formation Factor Measurement at the Water-Sediment Interface. Unpub. report at the Univ. of Rhode Island. Presented at the INTEROCEAN '70 in Dusseldorf, Germany. Nov. 10-15, 1970.

Yen, C. L., and Wu, J.
1969. Some Factors Influencing Dispersion of Pollutants in Streams. Proceedings of the Annual North Eastern Regional Antipollution Conference. Univ. of Rhode Island, July. pp.16-21.

Young, F. B.; Gerrard, H.; and Jevons, W.
1920. On electrical Disturbances due to Tides and Waves. Phil. Magazine, Ser 6, vol. 40, pp. 149-159.